The Dissertation Committee for Adam Girard Gordon Certifies that this is the approved version of the following Dissertation:

The Lateral Preoptic Area Regulates the Ventral Tegmental Area and Drives Reinforcement and Complex Reward Behaviors

Committee:

Michela Marinelli, Supervisor

Hitoshi Morikawa

Michael Drew

John Mihic

Boris Zemelman

The Lateral Preoptic Area Regulates the Ventral Tegmental Area and Drives Reinforcement and Aversion

by

Adam Girard Gordon

Dissertation

Presented to the Faculty of the Graduate School of

The University of Texas at Austin

in Partial Fulfillment

of the Requirements

for the Degree of

Doctor of Philosophy

The University of Texas at Austin

December 2019

Dedication

To my wife, my family, my cats, and all the rats.

Acknowledgements

First, I would like to acknowledge my wife, Lydia Fennell-Gordon. I thank her for her endless patience as she edited my writing (which would be unintelligible without her), her thoughtful discussion of my work, and her support for me. Without her love and assistance I would not have produced the dissertation I present here nor would I be the scientists I am today.

I thank my advisor Micky Marinelli for her guidance and support throughout my training. Micky has honed my scientific skepticism and instilled an attention to detail and passion for rigor that will benefit me indefinitely. I cannot thank her enough for the time and energy she dedicated while training me to be the best scientist I can possibly be.

I thank my committee for their thoughtful advice throughout my PhD. multiple crucial ideas for experiments emerged from our committee meetings. Your support gave me the confidence to speak my mind and pursue my dreams.

I thank the members of the Waggoner center for providing the opportunity to share my research and receive constructive criticism. The questions and discussion following each talk provided me with insight I would not have received otherwise. In particular I thank Robert Messing and Hitoshi Morikawa for their intellectual guidance.

I thank all of my peers for their insights, conversation, and support along the way. In particular I would like to thank the following (in alphabetical order) Brian Bondy, Emma Brockway, Roberto Cofresi, Emily Grantham, Aaron Levi, Rajani Maiya, Nathan Nocera, Annie Park, Matt Pomrenze, and Anna Warden. Your friendship and wisdom was an immeasurable asset throughout graduate school.

I thank my lab mates for their blood, sweat, and tears as we slaved away to obtain the data I present in this dissertation or data yet to be presented. In particular, I would like to thank Stève Desaivre, Vorani Ramachandra, Lydia Gordon-Fennell, Adrian Guanawan, Kevin Sattler, and Jackie Nguyen. Without your help I would not have been able to collect the data that made up my PhD.

Finally, I would like to thank the following funding agencies that provided me with support that granted me the freedom necessary to complete my graduate work, the opportunity to attend conferences, and the ability to live a comfortable life in Austin: National Science Foundation Graduate Research Fellowship Program, Bruce Jones Fellowship, National Institute on Alcohol Abuse and Alcoholism Training Grant, Graduate Student Professional Development Award Travel Grant, and the Graduate Dean's Prestigious Fellowship Supplement.

Abstract

The Lateral Preoptic Area Regulates the Ventral Tegmental Area and Drives Reinforcement and Aversion

Adam Girard Gordon, Ph.D.

The University of Texas at Austin, 2019

Supervisor: Michela Marinelli

The lateral preoptic area (LPO) is an understudied brain region that is interconnected with reward centers of the brain, but the role it plays in modulating these reward centers and the behaviors these centers underlie is unknown. The LPO is positioned to regulate the activity of the ventral tegmental area (VTA) through a direct projection to VTA GABA and VTA dopamine neurons and through indirect connections via intermediary structures, including the lateral habenula and rostromedial tegmental nucleus, which potently regulate VTA dopamine neuron activity. Correlational studies find that LPO neurons are excited by both rewarding and aversive events, and neuronal activity in this structure is sensitive to fluctuations in cocaine levels throughout self-administration. However, the role of the LPO in these behaviors is unknown. Throughout this dissertation, I demonstrate that the LPO functionally regulates the activity of VTA dopamine and GABA neurons, drives both reinforcement and aversion, and increases activity in response to aversive events. Specifically, I found that stimulation of the LPO with bicuculline leads to inhibition of VTA GABA neurons and excitation of VTA dopamine neurons and precipitates cocaine and sucrose seeking behaviors. I also found that stimulation of the LPO with optogenetics

leads to inhibition of VTA GABA neurons and mixed effects on VTA dopamine neurons. In addition, stimulation of the LPO with optogenetics drives both reinforcement and aversion; it supports intracranial self-stimulation and drives real-time place aversion in the same subjects. However, I found that even though stimulation of the LPO does not drive place-preference *per se*, stimulation of the LPO is reinforcing in the real-time place preference procedure, because animals continue to obtain stimulation in the face of adversity. Finally, I found that, at the population level, the LPO increases its activity in response to aversive events and corresponding predictive cues, but not to rewarding events and corresponding predictive cues. Together, these results indicate that the LPO regulates the activity of VTA subpopulations, drives complex reward-related behaviors, and signals in response to aversive events, all of which argues that the LPO is a previously overlooked member of the brain reward circuit.

Table of Contents

List of Figures

List of Illustrations

Chapter 1: General introduction

1.1 Reward, Aversion, and Motivation

Motivational pathologies and consequences stemming from them are some of the leading causes of preventable death in the United States. Together, cocaine, tobacco, and alcohol use contributes to over 0.5 million deaths per year (Danaei et al., 2009). One common facet to these outcomes is reward and motivation, in which people continue to act in a way they know is harmful to their health. Individuals may be motivated to do things harmful to their health or may lack the motivation necessary to do things beneficial to their health, both of which can drive people to unhealthy outcomes. A better understanding of the ways in which the brain produces motivated behaviors may guide us towards more successful human interventions.

Drug abuse is a major problem throughout the world and is estimated to cost 20 million disability-adjusted life years annually (Louisa Degenhardt et al., 2013). At its core, addiction is a motivational pathology where people suffering from addiction are unable to cease using the drug despite a desire to (Kalivas and Volkow, 2005). One hallmark of drug addiction is relapse to drug taking (American Psychiatric Association. and American Psychiatric Association. DSM-5 Task Force., 2013). Relapse occurs when a drug user ceases consuming drugs, either volitionally or non-volitionally, and then resumes taking drugs. Relapse affects between 40-60% of people undergoing addiction treatment (McLellan et al., 2000). Another hallmark of addiction is continued use in face of adversity, which can be observed as drug users continue to take drugs in the face of mounting problems that stem from drug use. People suffering from addiction consume drugs even after drug use has produced devastating consequences.

Motivational pathologies, including drug addiction, are mediated in part by reward circuitry within the brain. Research has found many brain circuits that mediate these motivational pathologies (Volkow et al., 2008; Kenny, 2011b; a; Volkow et al., 2011), but there are many structures that remain unexplored. A greater understanding of how the brain generates reinforcement for rewards may grant us greater therapeutic interventions to prevent the development of motivational pathologies.

RODENT MODELS USED TO STUDY MOTIVATION AND VALENCE

Animal models are critical tools for studying human reward behavior because they allow experimenters to causally manipulate the brain and environmental contexts that contribute to the behaviors and experiences of interest. Throughout my dissertation, I will use multiple behavioral models to determine the rewarding, aversive, and motivational characteristics of particular neural systems. It is important to understand the specifics of these behavioral procedures in order to correctly interpret and relate results from these procedures. In the next few sections, I will outline some of the common rodent procedures used to model aspects of these behaviors, and in later sections, I will outline the neural systems that modulate behaviors within these procedures.

1.1.1 Classical Conditioning

Pavlovian conditioning, also known as classical conditioning, is a form of passive conditioning where subjects learn the association between conditioned stimuli and unconditioned stimuli. In this procedure, an experimenter will pair conditioned and unconditioned stimuli and then measure a response during the conditioned stimulus (Domjan, 2005). This procedure is useful for measuring responses in the absence of the unconditioned stimuli. For example, experimenters can measure the rewarding or aversive

qualities of an unconditioned stimulus using conditioned place preference, where an unconditioned stimulus is paired with a single side of a chamber (the conditioned stimulus) and then the animal's preference for the environment is measured in a subsequent test (Tzschentke, 2007). If an unconditioned stimulus is rewarding, then the animal will spend more time the conditioned side, while if the stimulus is aversive, then the animals will spend more time in the unconditioned side. A disadvantage of Pavlovian conditioning is that the experimenter cannot measure valence "online", and instead has to rely on measuring the valence with a memory test; the lack of conditioned response can reflect a lack of underlying valence of the unconditioned stimuli or a lack of learning between the conditioned stimulus and unconditioned stimulus. Another disadvantage to Pavlovian conditioning is that it does not directly test the reinforcing or motivational quality of stimuli directly. To directly test the reinforcing and motivational qualities, experimenters use operant conditioning procedures.

1.1.2 Operant Conditioning

Operant conditioning is a behavioral procedure used to study reward and motivation in which subjects can control stimuli through operating within their environment (Staddon and Cerutti, 2003). This distinguishes it from Pavlovian conditioning, which is inherently passive. Operant conditioning can be either positive, where subjects respond to obtain a rewarding unconditioned stimulus, or negative, where subjects respond to avoid an aversive unconditioned stimulus. In both cases, the operant outcome (delivery of a rewarding stimuli or removal of an aversive stimuli) leads to an increased likelihood of the preceding behavior (Keller and Schoenfeld, 1950). Prior to training, the behavioral action that has no intrinsic value to the subject but becomes imbued with value through repeated pairing with the unconditioned stimulus. In the context of reward and aversion,

experimenters can use positive and negative operant conditioning to assess the intrinsic properties of stimuli and neural systems.

Operant conditioning has numerous advantages that make it appealing to reward researchers, including its face and predictive validity. Face validity is how well an experimental model represents the real-world phenomenon it intends to model. In operant conditioning, subjects are directly self-administering rewards which is precisely what the phenomenon is intended to model in humans. Predictive validity pertains to a model's ability to predict results in the greater population. In the case of drug addiction, the majority of drugs that humans self-administer are drugs that rodents self-administer as well (O'Connor et al., 2011). Furthermore, environmental factors, such as stress, which increase drug use in humans also increase drug use in rodents (Logrip et al., 2012). The multiple sources of validity strongly support the use of operant conditioning in modeling human reward consumption.

1.1.2.1 Fixed-Ratio and Progressive-Ratio Operant Conditioning

Fixed-ratio self-administration is a form of operant conditioning that is used to model low- or moderate-cost consumption (Arnold and Roberts, 1997). A fixed-ratio schedule is a schedule of reinforcement in which each reward costs a set amount of responses (e.g. 5 responses per reward). With a low fixed-ratio schedule, subjects can obtain a stimulus without expending much time or energy in procuring it. This procedure is useful to determine if a stimulus is rewarding, which is determined based on operant response rates and response discrimination.

Progressive ratio is a form of operant conditioning that is used to model high-effort consumption (Arnold and Roberts, 1997). A progressive-ratio schedule is a schedule of reinforcement in which the cost for each reward increases with every reward delivery,

typically in a semi-logarithmic fashion (e.g. response per reward: 1, 4, 8, 10, 16, 20, etc.). In this procedure, researchers are interested not only in responding for reward, but also the maximal number of responses a subject is willing to make for a reward, known as "breakpoint." Progressive ratio more accurately models the excessive motivational effort humans are willing to make for rewards, such as drug rewards.

Progressive ratio responding more accurately measures the relative value of a stimulus compared to fixed-ratio responding. Under fixed-ratio schedules, changes in responding are difficult to interpret following many manipulations. For example, increases in the concentration of sucrose *reduces* the responding for sucrose reward on schedules with low response requirement (Cheeta et al., 1995). This may lead you to think that the rat perceives sucrose less rewarding at higher concentrations. However, it actually means that the rat simply no longer needs to administer as many times to obtain the desired amount of sucrose. Under progressive ratio, rats will *increase* responding for higher sucrose concentrations (Cheeta et al., 1995). This is because the rat assigns a higher value to higher concentrations of sucrose, thus the rat will work harder to obtain it. Together, fixed-ratio allows researchers to assess if a stimulus is rewarding and progressive ratio allows researchers to assess the relative value of stimuli.

1.1.2.2 Extinction and Reinstatement of Seeking

Extinction and reinstatement procedures are used to model precipitation of drug seeking in humans (Venniro et al., 2016). The procedures involve running animals through operant conditioning and then removing the unconditioned stimulus (i.e. the reward). This leads to a decrease in the number of responses that were previously reinforced (i.e. "extinction" of seeking). Following a reduction in responding, various events can be used to precipitate reinstatement of seeking, indicated by an increase in the number of responses.

The events that precipitate reinstatement of seeking can largely be separated into three distinct groups: 1) stressful events, such as foot shock or social defeat 2) re-exposure to the unconditioned stimuli, and 3) re-exposure to the conditioned stimuli (qualifier: this requires that the extinction procedure was conducted in the absence of the conditioned stimuli) (Venniro et al., 2016). In all three cases, the event produces an increase in the number of responses relative to extinguished responding, even though responses are not leading to unconditioned stimulus delivery.

Extinction and reinstatement are effective models for studying drug seeking prior to relapse in humans for the same reasons as stated above for self-administration. The behavioral procedure produces behavior that mirrors the human condition. The same three categories of events precipitate reinstatement of seeking behavior in both humans and rodents, and interventions that reduce reinstatement in humans also reduce reinstatement in rodents (Bossert et al., 2013). One important difference between the model and the human condition is that in the model, reinstatement is typically done under extinction conditions, where the subject is unable to obtain the unconditioned stimulus. This is done intentionally because it allows researchers to measure behavior without the effect of the unconditioned stimulus (e.g. cocaine effects). However, in the human condition, events may initially cause seeking of the unconditioned stimulus, but relapse by definition includes consumption of the unconditioned stimulus. Extinction and reinstatement procedures more accurately model the initial precipitation of seeking behavior than they model drug consumption following relapse.

1.1.2.3 Intracranial Self-Stimulation

Intracranial self-stimulation (ICSS) is a procedure used to determine the intrinsic reinforcing properties of neural circuits (Olds and Milner, 1954; Wise, 1996). The

procedure involves allowing subjects to operantly manipulate neuronal populations in similar conditions to self-administration procedures described above. Experimenters typically measure the response rate, which is the number of responses a subject performs for stimulation. Response rates are useful for determining if a brain region is capable of generating reinforcement. If stimulation is rewarding, subjects will acquire responding for it, and if brain stimulation is aversive, subjects will not. In fact, in the case of aversive brain stimulation, they may even acquire negative reinforcement, where they respond to pause the stimulation. Interestingly, stimulation of a particular brain region sometimes supports both positive and negative reinforcement (Wise, 1996). This phenomenon is presumed to be the result of stimulating both rewarding and aversive neuronal populations simultaneously; the positive or negative conditioning behavior emerges based on the procedure that is used. ICSS has allowed researchers to uncover many neuronal pathways throughout the brain that are reinforcing and also responsible for reinforcing natural reward behaviors.

Classically, ICSS involved self-stimulation via implanted electrical probes. A major caveat to electrical ICSS is that electrical stimulation drives depolarization of all membranes in the vicinity of the electrical probe, meaning that electrical stimulation activates both cell bodies and fibers of passage (Ranck, 1975). The advent of optogenetics allowed researchers to use genetically encoded light-sensitive channels to allow subjects to self-stimulate via activation of more defined neural populations. This stimulation method enables specific stimulation of genetically and projection defined subpopulations of neurons without stimulating fibers of passage.

1.1.2.4 Real-Time Place Testing

Real-time place testing (RTPT) is a method used to determine the valence of neural systems. Valence is the direction of subjective emotional states, where positive valence drives approach and negative valence drives avoidance (Tye, 2018; Berridge, 2019). In RTPT, subjects are placed into a multi-compartment apparatus (typically 2-4 compartments) in which one side is paired with a neuronal manipulation in real time. The subject can freely enter the paired compartment and receive stimulation that will continue until the subject exits the paired compartment. Optogenetics is almost exclusively employed for RTPT because it allows for the sub-second resolution of manipulations necessary to pair neural manipulations with a compartment in real-time. The standard metric that is used to determine the valence of a neuronal manipulation within RTPT is the amount of time in the optically paired compartment compared to the amount of time spent in the optically unpaired compartment(s). If the subject spends more time in the optically paired compartment, the neuronal manipulation has produced real-time place preference (RTPP), indicative of positive valence, while if the subject spends more time in the unpaired compartment(s), the neuronal manipulation has produced real-time place aversion (RTPA), indicative of negative valence.

RTPT offers some useful qualities compared to other procedures for measuring reward and aversion. RTPT measures the online valence of neuronal manipulations without the need to test for memory of the manipulation as required in traditional conditioned place-testing procedures. A lack of effect in traditional conditioned-place testing could be the result of a neutral stimulus or a stimulus that is unable to generate a memory sufficient to drive a conditioned response. This complication is resolved with RTPT due to its online nature: RTPT does not require memory formation to elucidate the valence of a manipulation. Additionally, RTPT can simultaneously test for rewarding properties

(Kravitz et al., 2012) and aversive properties (Stamatakis and Stuber, 2012) as the subject must choose a compartment to spend time in. This provides RTPT with an advantage over standard operant conditioning procedures, which are typically set up to measure either positive or negative reinforcement but not both simultaneously. During tests for positive and negative reinforcement, a lack of responding is difficult to interpret. For example, if an experimenter runs positive operant conditioning for a novel stimulus and the subjects do not respond, it is unclear if the stimulus is neutral or aversive. Furthermore, if a stimulus causes different effects across individuals, standard operant conditioning will be unable to accurately measure the diversity in responses. Overall, RTPT represents a relatively novel and useful procedure for measuring the online valence produced by manipulations of neural circuits.

1.2 Neural Circuits Underlying Motivation and Valence

In the previous section, I outlined several animal models used to measure motivation and valence properties of neuronal circuits. In this section, I will first outline three critical brain regions for generating motivation and valence, and then, I will discuss how these brain regions contribute to motivation and valence.

1.2.1 The Ventral Tegmental Area

1.2.1.1 VTA subpopulations

The VTA is a heterogeneous midbrain structure which contains a large population of dopamine neurons, smaller populations of GABA and glutamate neurons, and even smaller dual-expressing populations (Nair-Roberts et al., 2008; Barker et al., 2016; Root et al., 2016). For this dissertation, I will refer to VTA populations of dopamine, GABA, and glutamate as $VTA_{Dopamine}$, VTA_{GABA}, and $VTA_{Glutamate}$, respectively. Dopamine cells are

located throughout the VTA, and in all subnuclei of the VTA, dopamine is the largest subpopulation (Nair-Roberts et al., 2008). GABA neurons are also located throughout the VTA, and in all subnuclei of the VTA, GABA is the second largest subpopulation, encompassing approximately 35% of neurons (Nair-Roberts et al., 2008). Glutamate neurons represent a significantly smaller population of neurons in the VTA in comparison to dopamine and GABA (Yamaguchi et al., 2007; Ungless and Grace, 2012), encompassing approximately 2-3% of neurons (Nair-Roberts et al., 2008). These cells are denser in rostral and medial portions of the VTA and tapper off caudally and laterally (Yamaguchi et al., 2007; Yamaguchi et al., 2011; Root et al., 2016). In addition to the neurotransmitter populations outlined above, there are dual-expressing (e.g. dopamine / glutamate, GABA / glutamate) neurons throughout the VTA with a higher concentration medially than laterally (Root et al., 2014c; Zhang et al., 2015; Barker et al., 2016; Root et al., 2016). These dual-expressing populations send projections to the nucleus accumbens (Zhang et al., 2015) and lateral habenula and contain segregated "micro-domains" for intendent release of each neurotransmitter (Root et al., 2014c). The existence of dual-expressing populations is important to keep in mind when interpreting data following activation of different sub populations of VTA neurons because results can stem from regulating the intended subpopulation or can stem from a co-released neurotransmitter. In the remainder of this section, I will outline the major subpopulations of neurons within the VTA. Afterward, I will outline the connectivity of the VTA, the signaling patterns of the VTA, and finally discuss the causal role of VTA signaling in reward and motivated behavior.

Dopamine is a catecholamine neurotransmitter synthesized from dietary tyrosine using the following pathway: L-Tyrosine is converted to L-DOPA via tyrosine hydroxylase; L-DOPA is converted into dopamine via DOPA decarboxylase (Broadley,

2010). Tyrosine hydroxylase is the rate-limiting step of dopamine synthesis and is widely used as the definitive identifier of dopamine neurons.

Dopamine modulates neuronal activity through dopamine receptors. All dopamine receptors are seven-trans-membrane G protein-coupled receptors which produce effects through intracellular signaling cascades rather than directly altering membrane voltage. There are 5 subtypes of dopamine receptors that are broadly categorized into D1-like and D2-like receptors based on the receptors G protein coupling. In general, activation of D1-like receptors increases neuronal activity and activation of D2-like receptors decreases neuronal activity. D1-like receptors are coupled to G_s and include dopamine receptor subtypes D1 and D5. Activation of D1-like receptors leads to activation of adenylyl cyclase, which produces increases in cyclic adenosine 3',6'-cyclic monophosphate (cAMP), which then enhances activity of protein kinase A (Iversen, 2010). In general, activation of D1-like receptors positively modulates the post synaptic response to glutamate and thus enhance neuronal activity (Surmeier et al., 2007). D2-like receptors are coupled to $G_{i/o}$ and include dopamine receptor subtypes D2, D3, and D4. Activation of D2-like receptors leads to inhibition of adenylyl cyclase, which produces decreases in cAMP, which then decreases activity of protein kinase A (Iversen, 2010). In general, activation of D2-like receptors negatively modulate glutamatergic input and thus reduce neuronal activity (Surmeier et al., 2007).

GABA is the primary inhibitory neurotransmitter within the central nervous system. GABA is a small molecule synthesized from glutamate via glutamate decarboxylase (GAD). GABA cells are often identified by expression of GAD65 and/or GAD67 protein or mRNA. There are two primary classes of GABA receptors: GABA-A receptors, which are ionotropic chloride channels, and GABA-B receptors, which are $G_{i/o}$ coupled receptors (Hammond, 2015). For both classes of receptors, GABA binding

typically leads to a suppression of neuronal activity. However, depending on the chloride gradient and/or relative timing of GABA-A receptor activation and excitatory events, GABA-A receptors can have facilitatory or an event excitatory effect (Ben-Ari, 2002; Gulledge and Stuart, 2003). Even in light of these exceptions, GABA can generally be considered as a potent inhibitory neurotransmitter.

Glutamate is the primary excitatory neurotransmitter within the central nervous system. Glutamate is a small molecule synthesized from glutamine via glutaminase (Kandel, 2013). Glutamate cells are often identified by the expression of vesicular glutamate transporter (vGLUT), a necessary protein to package glutamate into vesicles for release. There are three subtypes of vGLUTs (VGLUT 1-3). VGLUT1 and VGLUT2 are expressed primarily in neuronal axons, while VGLUT3 can be found in both axons and somatodendritic regions (Fremeau et al., 2004). In general, VGLUT1 is found in cortical structures, VGLUT2 is found in subcortical structures, and VGLUT3 is found sparsely throughout the cortex and hippocampus. However, there are exceptions to this rule as VGLUT1 is found in the basal lateral amygdala and hippocampus, and VGLUT2 is found in layer 4 of the cortex. There are two classes of glutamate receptors: ionotropic and metabotropic. Ionotropic glutamate receptors include N-methyl-d-aspartate (NMDA) receptors, α-amino-3-hydroxyl-5-methyl-4-isoxazole-propionate (AMPA) receptors, and kainate receptors (Kandel, 2013). All ionotropic glutamate receptors are tetramers cation channels. In all cases, glutamate binding drives enhanced cation permeability which typically drives membrane depolarization. AMPA and kainate receptors are high speed ion channels that are permeable to sodium and potassium. On the other hand, NMDA receptors are slow speed ion channels that are permeable to sodium, potassium, and calcium. Metabotropic glutamate receptors (mGluRs) can be divided into two subclasses based on their associated G protein: group I mGluRs, which associate with G_q /G_{11}, and group II and

III mGluRs, which associate with $G_{i/o}$. In general, group I mGluRs act to increase neuronal activity and group II and III mGluRs decrease neuronal activity. However, there are exceptions including complex group I mGluR effects that are dependent on intracellular signaling (Niswender and Conn, 2010). Despite the examples to the contrary, glutamate can broadly be considered a fast-signaling excitatory neurotransmitter.

1.2.1.2 Projections to VTA Neurons

The VTA receives inputs from a broad range of limbic forebrain regions, including the hippocampus, extended amygdala, and midbrain regions (Watabe-Uchida et al., 2012; Beier et al., 2015; Faget et al., 2016). In addition, the VTA also receives inputs from secondary sensory areas (Comoli et al., 2003; Watabe-Uchida et al., 2012). By in large, the sub populations of the VTA each receive projections from a similar set of brain structures (Faget et al., 2016), but despite this, stimulation of brain regions will often produce biased effects on $VTA_{Dopamine}$ and VTA_{GABA} populations. For example, the lateral habenula sends glutamate projections to both $VTA_{Dopamine}$ and VTA_{GABA} neurons (Omelchenko et al., 2009), but stimulation of the lateral habenula with electricity (Christoph et al., 1986; Ji and Shepard, 2007; Brown and Shepard, 2016) and optogenetics (Lammel et al., 2012) stimulates VTA_{GABA} neurons and inhibits $VTA_{Dopamine}$ neurons. Knowing the neurotransmitter identity of inputs to the VTA is insufficient to determine the net effect of stimulation of the input. The lateral dorsal tegmentum and lateral habenula both send glutamatergic projections to the VTA, however the lateral dorsal tegmental input results in a net excitation of $VTA_{Dopamine}$ neurons and the lateral habenula input results in net inhibition of $VTA_{Dopamine}$ neurons. The diverse set of inputs to VTA neurons likely stems from the importance of the structure as a critical regulator of a diversity of motivated behaviors.

1.2.1.3 Projections of VTA Neurons

The VTA sends a divergent projection throughout the limbic forebrain (Matsuda et al., 2009; Russo and Nestler, 2013; Aransay et al., 2015; Barker et al., 2016). Previously, it was believed that the VTA output was exclusively dopaminergic, however, as mentioned above, more recent findings indicate that the VTA sends modest glutamatergic, GABAergic, and coexpressing projections to the nucleus accumbens and lateral habenula (Root et al., 2014b; Barker et al., 2016; Yoo et al., 2016). The vast majority of work studying the projections from the VTA have focused on the dopamine projection to the striatal complex. Dopamine neurons in the VTA and substantia nigra send projections to the striatum with extraordinarily large arborizations that can span as much as 0.45-5.7% of the striatum (Matsuda et al., 2009; Aransay et al., 2015). These massive projections allow dopamine neurons to modulate large regions of the limbic forebrain, which underlies the variety of functional roles of dopamine transmission.

Less is known about the connectivity of VTA_{GABA} and $VTA_{Glutamate}$ neurons compared with $VTA_{Dopamine}$ neurons. As stated above, VTA_{GABA} and $VTA_{Glutamate}$ send projections to distant targets including the striatum and habenula, but these populations also make local connections within the VTA (Omelchenko and Sesack, 2009; Dobi et al., 2010). Stimulation of VTA_{GABA} neurons inhibits $VTA_{Dopamine}$ neurons (Tan et al., 2012), and stimulation of $VTA_{Glutamate}$ neurons excites $VTA_{Dopamine}$ neurons (Wang et al., 2015). At this point, it is not clear if VTA_{GABA} and $VTA_{Glutamate}$ neurons that project to distant structures are the same neurons which make local connections, or if these represent unique populations of cells (Omelchenko and Sesack, 2009), but it is clear that VTA_{GABA} and $VTA_{Glutamate}$ neurons make local synapses to regulate $VTA_{Dopamine}$ firing.

1.2.1.4 Signaling patterns of VTA dopamine neurons

VTA neurons and striatal dopamine concentrations have sub-second time-locked signals to rewarding and aversive events, as well as predictive cues. During Pavlovian conditioning, $VTA_{Dopamine}$ neurons encode a reward prediction error (RPE) (Schultz, 1998; Cohen et al., 2012; Eshel et al., 2016). Within RPE, the difference between the predicted value and actual value is signaled, rather than the absolute value. Briefly, prior to conditioning, $VTA_{Dopamine}$ neurons do not respond to the conditioned stimulus, but they respond to rewarding unconditioned stimuli, such as sucrose. After training, $VTA_{Dopamine}$ neurons temporally shift their response from the unconditioned stimulus to the conditioned stimulus. In trained animals, differences from the expected reward are encoded as changes in firing. In theory, if the reward is as predicted by the conditioned stimulus, then $VTA_{Dopamine}$ cells will not change firing from baseline during the reward; if the reward is greater than predicted, then $VTA_{Dopamine}$ cells will increase firing from baseline during the reward; if a reward is less than predicted (or omitted) $VTA_{Dopamine}$ cells will decrease firing from baseline during the reward. In practice, a complete lack of response to the predicted unconditioned stimulus is not consistent across animal models and/or training procedures (Cohen et al., 2012).

In addition to sub-second signals, striatal dopamine concentrations have minute by minute signals that correlate with operant behavior. During operant conditioning for sucrose, dopamine concentration in the nucleus accumbens positively correlates with the number of lever presses subjects make, but not the number of sucrose pellets delivered (Sokolowski et al., 1998). In tasks with fluctuations in the reinforcement probability, subjects display low latencies to task engagement during periods of high probability of reinforcement and high latencies during periods of low probability. Minute by minute dopamine levels in the nucleus accumbens correlates strongly with task engagement, with

high levels of dopamine observed during periods of low latencies (high engagement) (Hamid et al., 2016; Mohebi et al., 2019). Minute to minute changes in dopamine seem to be related to a general motivational state rather than reinforcement learning.

$VTA_{Dopamine}$ cells fire in burst and tonic firing modes which produce sub-second and minute to minute changes in dopamine concentration, respectively (Grace, 1991). Further research has indicated that these modes of firing are not independent, as burst firing influences future tonic release rates (Lohani et al., 2018). To further complicate the relationship between $VTA_{Dopamine}$ neuron firing and dopamine release, recent research has demonstrated presynaptic regulation of dopamine release independent of firing of dopamine neurons. Berke et al. 2019 found that on a minute to minute basis, $VTA_{Dopamine}$ neuron firing did not correlate with dopamine levels in the striatum. These results imply that there may be presynaptic regulation of dopamine release in the striatum (Cachope et al., 2012; Threlfell et al., 2012), or dynamic release probabilities, which is in line with prior research (Lohani et al., 2018). Despite the complexity of the relationship between $VTA_{Dopamine}$ neuron firing and dopamine concentrations, there are clear causal relationships between both $VTA_{Dopamine}$ firing and dopamine concentrations with behavior.

1.2.1.5 The role of the VTA in behavior

Sub-second changes in dopamine levels in the striatum are casually related to reinforcement and motivation. RPE signaling patterns have been shown to be causally related to the expression of conditioning (Steinberg et al., 2013; Eshel et al., 2015; Chang et al., 2016). Stimulating $VTA_{Dopamine}$ neurons during reward omission, thereby mimicking a positive reward prediction error, increases seeking behavior (Steinberg et al., 2013), while inhibiting $VTA_{Dopamine}$ neurons, thereby mimicking a negative reward prediction error, decreases seeking behavior (Chang et al., 2016). In addition to Pavlovian

conditioning, sub-second manipulation of $VTA_{Dopamine}$ activity has been shown to be important for regulating consumption of rewards. Sub-second stimulation of the VTA drives time locked increases in responding for cocaine (Phillips et al., 2003), and optogenetic stimulation of $VTA_{Dopamine}$ neurons leads to reduced latency to task engagement (Hamid et al., 2016).

Minute by minute changes in dopamine in the striatum are also causally related to reinforcement and motivation in self-administration procedures. Reducing dopamine signaling by blocking dopamine receptors systemically and selectively in the nucleus accumbens leads to decreased progressive ratio breakpoint for cocaine (Hubner and Moreton, 1991; McGregor and Roberts, 1993). Furthermore, many studies have found that minute by minute changes in dopamine signaling alters reward seeking behavior. Pharmacological stimulation of dopamine release in the striatum and sustained increases in $VTA_{Dopamine}$ neuron activity drive seeking of natural and drug rewards (De Vries et al., 1999; Schmidt et al., 2006), while pharmacological blockade of dopamine receptors in the striatum and sustained reductions in $VTA_{Dopamine}$ neuron activity reduce precipitated reinstatement of seeking behavior (Anderson et al., 2003; Bachtell et al., 2005; Anderson et al., 2006; Marinelli et al., 2006; Xue et al., 2011). Take as a whole, the literature indicates that dopamine signals on multiple time frames, and these signals are critical modulators of reinforcement and motivation.

1.2.2 The Rostromedial Tegmental Nucleus

The rostromedial tegmental nucleus (RMTg) is a relatively recently discovered GABAergic region that extends caudally to the VTA (Perrotti et al., 2005; Jhou et al., 2009; Bourdy and Barrot, 2012). This structure is considered by some to be an inhibitory interneuron extension of the VTA and is also referred to as the “tail of the VTA.” The

structure was first described after finding an enhancement of ΔFosB staining in the RMTg following psychomotor stimulant administration (Perrotti et al., 2005). Further research has demonstrated that this structure is a potent inhibitor of $VTA_{Dopamine}$ neurons (Lecca et al., 2012; Bourdy et al., 2014). Recordings of the RMTg have revealed that RMTg neurons are stimulated by aversive events and inhibited by rewarding events. Additionally, lesioning the RMTg reduces $VTA_{Dopamine}$ pauses in neuron firing in response to aversive stimuli and reduces conditioned place aversion (Li et al., 2019). Inhibition of the RMTg during punishment also reduces the effectiveness of punishers (Vento et al., 2017). The RMTg receives a similar set of inputs as the VTA (Jhou et al., 2009), which mirrors the fact that VTA_{GABA} neurons receive similar inputs to $VTA_{Dopamine}$ neurons, further indicating the structure may be considered an inhibitory extension of the VTA. Overall, the literature clearly indicates that the RMTg is a potent inhibitor of $VTA_{Dopamine}$ neuron activity and is an important regulator of reward and aversive behavior.

1.2.3 The Lateral Habenula

The lateral habenula is a glutamatergic epithalamic structure that is a relay between the limbic forebrain and the midbrain cholinergic systems (Hikosaka et al., 2008). One feature that makes the lateral habenula unique is that the structure is primarily made up of glutamate neurons with only sparse GABA interneurons (Lecca et al., 2014). The lateral habenula receives large inputs from the lateral preoptic area (LPO), lateral hypothalamus, and the internal segment of the globus pallidum, and then sends outputs to the VTA and RMTg (Hikosaka et al., 2008). The lateral habenula projection to the VTA synapses onto both $VTA_{Dopamine}$ and VTA_{GABA} interneurons (Omelchenko et al., 2009), however the net effect of stimulation of the lateral habenula is stimulation of VTA_{GABA} neurons and inhibition of $VTA_{Dopamine}$ neurons (Christoph et al., 1986; Ji and Shepard, 2007; Lammel

et al., 2012; Brown and Shepard, 2016). The lateral habenula also inhibits $VTA_{Dopamine}$ neurons via the RMTg (Brown et al., 2017). The lateral habenula is believed to be an anti-reward center that upregulates activity in response to aversive events and to omissions of expected rewards (Matsumoto and Hikosaka, 2007). The lateral habenula is responsible for omission induced inhibition of $VTA_{Dopamine}$ neurons. Stimulation of the lateral habenula produces inhibition of $VTA_{Dopamine}$ neurons, lateral habenula neurons are activated prior to $VTA_{Dopamine}$ inhibition (Matsumoto and Hikosaka, 2007), and ablation of the lateral habenula diminishes omission induced inhibition of $VTA_{Dopamine}$ neurons (Tian and Uchida, 2015). The lateral habenula is not the only region that controls reductions in $VTA_{Dopamine}$ activity, as ablation of the lateral habenula does not block punishment induced reductions in $VTA_{Dopamine}$ activity (Tian and Uchida, 2015). In regards to reward and aversion, stimulation of the lateral habenula is aversive, supports negative reinforcement, and punishes future responding (Friedman et al., 2010; Lammel et al., 2012; Stamatakis and Stuber, 2012). Overall, the lateral habenula has emerged as an important regulator of $VTA_{Dopamine}$ neuron activity and reward behavior.

1.2.4 Neural mechanisms of Cocaine Reinforcement

Cocaine produces its effects through increasing brain concentrations of dopamine and norepinephrine by blocking the dopamine transporter (Kuhar et al., 1991; Koob et al., 2014). The dopamine transporter is present on dopamine terminals, where they actively reuptake dopamine from the synaptic cleft. Therefore, blocking the dopamine transporter prevents dopamine from being cleared from the cleft which indirectly increases dopamine concentrations extracellularly (Kuhar et al., 1991; Koob et al., 2014). In addition to modulating dopamine levels in the synapse, cocaine also modulates $VTA_{Dopamine}$ neuron firing. Cocaine administration decreases $VTA_{Dopamine}$ neuron firing in most neurons in

anesthetized rats but increases $VTA_{Dopamine}$ neuron firing in a subpopulation of neurons in awake rats (Olds and Milner, 1954; Wise, 1996), possibly through disinhibition (Steffensen et al., 2008; Bocklisch et al., 2013).

Cocaine reinforcement is primarily supported by increased dopamine concentrations in the nucleus accumbens. Rats will self-administer cocaine and amphetamine directly to the nucleus accumbens (Phillips et al., 1994; Ikemoto, 2003), and blockade of dopamine within the nucleus accumbens decreases motivation for cocaine, as indicated by a decrease in progressive-ratio responding (McGregor and Roberts, 1993). Pairing cocaine with conditioned stimuli imbues the conditioned stimuli with motivational value. As result, even after the reinforcer is removed, animals will continue to respond for cues previously paired with cocaine reward for many days. Following extinction of responding, exposure to cues previously paired with cocaine, administration of cocaine, and stressful events will precipitate reinstatement of seeking (Venniro et al., 2016). This effect is dependent on dopamine signaling, as blockade of dopamine reduces precipitated relapse (Anderson et al., 2003; Bachtell et al., 2005; Anderson et al., 2006; Xue et al., 2011), and stimulation of dopamine release itself precipitates relapse (Mahler et al., 2019). Taken as a whole, the literature clearly indicates that dopamine is a critical regulator of cocaine self-administration and seeking behavior.

1.2.5 Neural mechanisms of Sucrose Reinforcement

Sucrose is an innately rewarding, unconditioned stimulus in many mammals. Neonates of a variety of mammals, including humans, non-human primates, rats, and mice, exhibit a reward response to sucrose consumption without any prior training, as indicated by a stereotyped oral facial response following intraoral administration of sucrose (Berridge and Kringelbach, 2008). Importantly, the hedonic component ("liking") of

sucrose is independent of the motivation to obtain it ("wanting") (Berridge et al., 2009). The two are deeply interrelated, as unconditioned stimuli that produce a hedonic response are often motivating. However, there are discrete neuronal pathways that mediate the hedonic response and motivational aspects of rewards (Berridge et al., 2009). Broadly, the hedonic component of sucrose is mediated through opioid signaling in the nucleus accumbens (Pecina and Berridge, 2005), while the motivational component is mediated through dopaminergic signaling (Berridge, 2007).

The dopaminergic system is a critical mediator of sucrose motivation and seeking. Motivation for sucrose is under the control of dopamine signaling, as reducing dopamine signaling leads to decreased progressive-ratio responding (Cheeta et al., 1995; Olarte-Sanchez et al., 2013). Seeking for sucrose is also under the control of dopamine signaling, as enhancing dopamine signaling increases sucrose seeking (Wyvell and Berridge, 2000) and reducing dopamine signaling decreases sucrose seeking (Grimm et al., 2011). Sub-second recording of dopamine concentrations in the nucleus accumbens also suggest that dopamine regulates sucrose motivation and seeking. Dopamine concentrations rise during responding for sucrose, and also increase following presentation of sucrose associated cues (Roitman et al., 2004). Rodents show similar seeking extinction and reinstatement behavior with sucrose reward as they do with drug reward, which implies that there is general underlying mechanisms that mediate both behaviors.

1.2.6 Neural Mechanisms Underlying Intracranial Self-Stimulation

From the earliest studies of Olds and Milner, it was clear that a diverse set of brain structures throughout the limbic system, and especially along the medial forebrain bundle, support ICSS (Olds and Milner, 1954; Olds and Olds, 1963). The medial forebrain bundle is a bidirectional white matter fiber track that contains axons originating from brain regions

along the bundle spanning from the midbrain to the prefrontal cortex (Nieuwenhuys et al., 1982). This bundle contains midbrain catecholamine projections that terminate throughout the limbic system. Importantly, the medial forebrain bundle courses through a diverse set of structures, so stimulating the medial forebrain bundle will also stimulate collateral brain regions. Stimulation of the medial forebrain bundle is rewarding in rats, cats, rabbits, monkeys, and humans (Bishop et al., 1963; Olds and Fobes, 1981). Although the medial forebrain bundle contains a diverse set of axons, the dopaminergic component was believed to be of special importance for the support of ICSS.

Early indications that dopamine may underlie ICSS reinforcement came from studies that measured the synergy between drugs of abuse and ICSS thresholds. Researchers found that administering drugs that enhanced dopamine levels led to lower levels current necessary to sustain ICSS (Wise, 1996). Later studies found that ablating dopamine neurons that project to the nucleus accumbens and blocking dopamine receptors in the nucleus accumbens substantially reduced medial forebrain bundle ICSS (Stellar and Corbett, 1989). Early efforts to determine the identity of neurons that support ICSS were undermined by the lack of specificity in stimulation. Electrical stimulation cannot differentiate between stimulation of cell bodies and fibers of passage, nor can it differentiate between different neuronal subtypes within brain regions or fiber bundles. However, the research outlined below clearly indicated that electrical ICSS reinforces responding through release of dopamine. Stimulating the medial forebrain bundle drives dopamine release (Rodeberg et al., 2016). Electrical ICSS of the VTA is diminished following lesions of dopamine projections to the nucleus accumbens (Fibiger et al., 1987). ICSS of the medial forebrain bundle is reduced by blocking dopamine transmission through systemic application of dopamine antagonists (Fenton and Liebman, 1982; Flagstad et al., 2006; Negus and Miller, 2014).

The advent of optogenetics allowed researchers to overcome the lack of specificity that electrical stimulation entailed. Using this technique, researchers have identified numerous subpopulations of cells that support ICSS without the risk of stimulating fibers of passage. A critical finding from these modern techniques is that the brain regions along the medial forebrain bundle contain interspersed neuronal populations whose activity can support ICSS or drive negative reinforcement. Optogenetically stimulating $VTA_{Dopamine}$ neurons supports ICSS (Witten et al., 2011; Steinberg et al., 2014; Jing et al., 2019), confirming previous experiments utilizing electrical stimulation. Optogenetic stimulation of $VTA_{Dopamine}$ mediates reinforcement through dopamine release in particular, as dopamine receptor antagonists decrease optogenetic ICSS of $VTA_{Dopamine}$ neurons (Steinberg et al., 2014; Jing et al., 2019). Stimulation of nucleus accumbens medium spiny neurons, a primary target of $VTA_{Dopamine}$ neurons, also supports ICSS (Britt et al., 2012; Cole et al., 2018). In addition to $VTA_{Dopamine}$ neurons, several other limbic brain systems support optogenetic ICSS including glutamate neurons of the VTA (Yoo et al., 2016), lateral hypothalamus GABA projections to the VTA (Barbano et al., 2016; Nieh et al., 2016), bed nucleus of the stria terminalis projection to the lateral hypothalamus (Jennings et al., 2013a), and glutamate projections from ventral hippocampus to the nucleus accumbens (Britt et al., 2012). The literature suggests that the brain regions along the medial forebrain bundle support ICSS behavior through potentiating dopamine release in the nucleus accumbens or directly stimulating nucleus accumbens neurons.

1.2.7 Neural Mechanisms Underlying Valence

The mesolimbic system is capable of producing positive and negative valence states. These states are measured online using the RTPT procedure. If the subject spends more time in the side paired online with a neuronal manipulation, that neuronal

manipulation is inferred to be rewarding, and if the subject spends less time in the paired side the manipulation is inferred to be aversive. This procedure has allowed researchers to determine the online valence of a large range of neural systems, and this research has suggested that the mesolimbic system can generate these states. Direct manipulations of medium spiny neurons of the striatum, one of the primary outputs of the mesolimbic system, modulates RTPT behavior. Stimulation of D1R-expressing medium spiny neurons in the dorsal striatum (Kravitz et al., 2012) and olfactory tubercle (Murata et al., 2019) produces RTPP, while stimulation of D2R-expressing medium spiny neurons in the same regions produces RTPA. However, there remains contention around the role of D1R-expressing and D2R-expressing medium spiny neurons in reward and aversion (Soares-Cunha et al., 2019). Many inputs to the striatum have been shown to modulate RTPT behavior including glutamate, GABA, and dopamine inputs. Glutamatergic inputs to the striatum can produce either RTPP or RTPA. Inputs from the prefrontal cortex, ventral hippocampus, and amygdala (Britt et al., 2012) all produce RTPP while glutamatergic projections from the PVT (Zhu et al., 2016) and VTA produce RTPA (Qi et al., 2016; Yoo et al., 2016), possibly though stimulating parvalbumin interneurons (Qi et al., 2016; Zhu et al., 2016). GABAergic inputs to the striatum from the PFC produce RTPA (Lee et al., 2014). Finally, dopaminergic inputs to the striatum from the VTA produce RTPP (Jeong et al., 2015).

A large body of work has implicated subpopulations of the VTA in RTPT. In the case of $VTA_{Dopamine}$ neurons, stimulation produces RTPP (Jeong et al., 2015; Yoo et al., 2016), whereas inhibition produces RTPA (Tan et al., 2012; Danjo et al., 2014). In the case of VTA_{GABA} neurons, stimulation produces RTPA (Tan et al., 2012), whereas inhibition produces RTPP (Jennings et al., 2013b). Finally, in the case of $VTA_{Glutamate}$ neurons, stimulation in a non-projection specific manner produces RTPP (Wang et al., 2015). The

role of subpopulations of VTA neurons in RTPT behavior is complicated by the interconnectivity of these subpopulations including local connections between VTA_{GABA} and glutamate populations with $VTA_{Dopamine}$ neurons (Wang et al., 2015). Within the VTA, the literature suggests that $VTA_{Dopamine}$ neurons and the regulation of $VTA_{Dopamine}$ neurons underlies the majority of effects in RTPT. Stimulation of dopamine release, whether through direct stimulation of $VTA_{Dopamine}$ neurons or indirect stimulation via inhibition of VTA_{GABA} neurons onto $VTA_{Dopamine}$ neurons or stimulation of $VTA_{Glutamate}$ neurons onto $VTA_{Dopamine}$ neurons, produces RTPP.

Projections into the VTA regulate RTPT behavior through connectivity with different subpopulations of VTA neurons. Multiple brain regions send glutamatergic input to the VTA and produce RTPA, including the lateral hypothalamus (Nieh et al., 2016; de Jong et al., 2019), bed nucleus of the stria terminalis (Jennings et al., 2013b), and lateral habenula (Lammel et al., 2012), presumably through regulating VTA_{GABA} interneurons or activation of $VTA_{Dopamine}$ neurons projecting to the prefrontal cortex (Lammel et al., 2012). Other brain regions send glutamatergic inputs to the VTA and produce RTPP, including the dorsal raphe (Qi et al., 2014), and lateral dorsal tegmentum (Lammel et al., 2012). On the other hand, multiple brain regions send GABAergic input to the VTA and produce RTPP, including both the lateral hypothalamus (Barbano et al., 2016; Nieh et al., 2016), and the bed nucleus of the stria terminalis (Jennings et al., 2013b), presumably through regulating VTA_{GABA} interneurons. From these data it is clear that many brain regions are able to modulate RTPT behavior through regulating VTA subpopulations. Interestingly, projections that modulate $VTA_{Dopamine}$ through VTA_{GABA} neurons usually make direction connections with $VTA_{Dopamine}$ neurons as well (Omelchenko et al., 2009; Jennings et al., 2013b; Nieh et al., 2016). The literature outlines a complex web of interconnected populations (Figure 1.1), which precludes accurate prediction of the valence of neuronal

inputs to the VTA. A notable exception is projections to the lateral habenula. All glutamate projections to the lateral habenula are aversive (Root et al., 2014a; Yoo et al., 2016; Barker et al., 2017; Lazaridis et al., 2019), and all GABAergic projections to the lateral habenula are rewarding (Stamatakis et al., 2013; Barker et al., 2017). The relation between VTA neuron activity and RTPT behavior becomes substantially more complex when looking at projection specific effects (Lammel et al., 2012; de Jong et al., 2019), the discussion of which is beyond the scope of this dissertation.

Figure 1.1: Overview of circuits underlying real-time place testing behavior

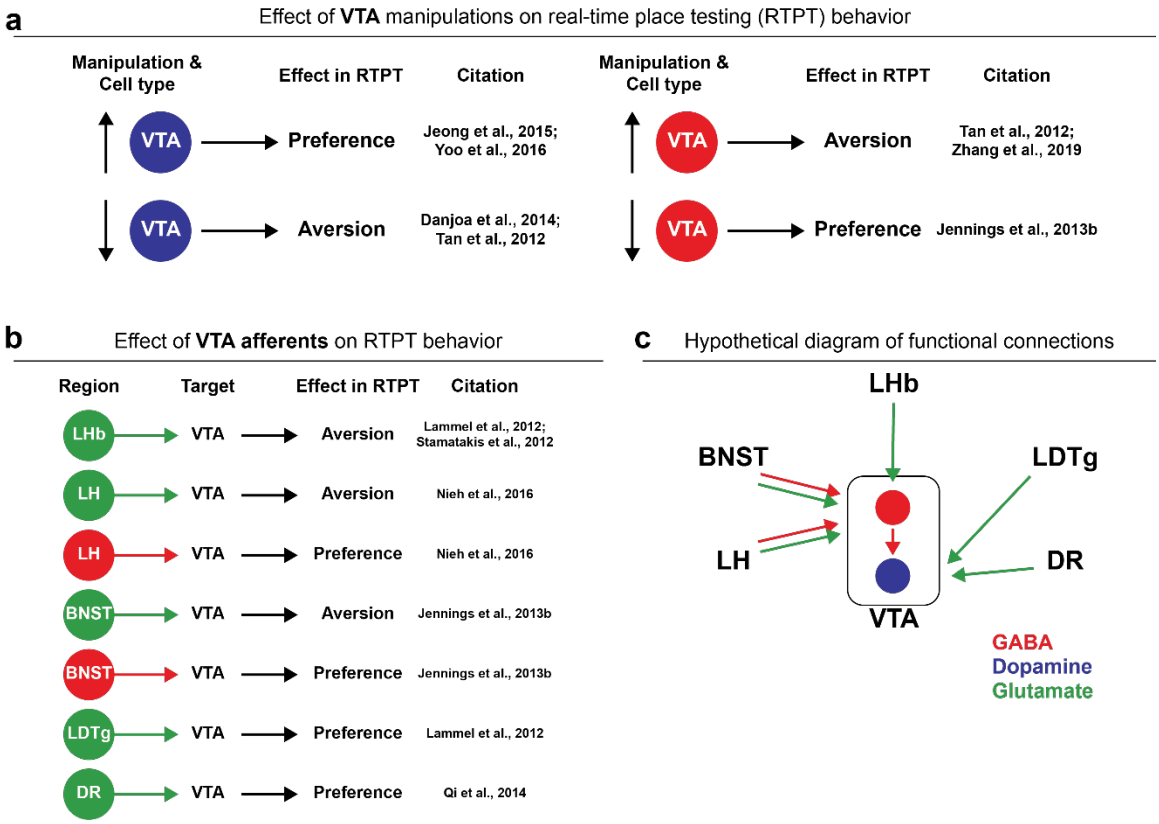

(a) Table of the effects of different manipulations within the VTA on RTPT behavior. Stimulation of $VTA_{dopamine}$ drives preference while inhibition drives aversion. Stimulation of VTA_{GABA} drives aversion while inhibition drives preference. **(b)** Table of the effects of selected projections to the VTA. Note that stimulation of glutamate inputs to the VTA from different structures can produce both preference and aversion. **(c)** Hypothetical circuit diagram that can explain the diversity in effects. There may be biased functional connectivity in different pathways projecting to the VTA that results in either direct modulation of $VTA_{dopamine}$ neurons or disynaptic modulation of $VTA_{dopamine}$ neurons via VTA_{GABA} neurons. Abbreviations: VTA: ventral tegmental area; LHb: lateral habenula; LH: lateral hypothalamus; BNST: bed nucleus of the stria terminalis; LDTg: lateral dorsal tegmental nucleus; DR: dorsal raphe. Colors: red: GABA; blue: dopamine; green: glutamate. Colors: dark blue: dopamine; red: GABA; green: glutamate

1.3 The Lateral Preoptic Area

The literature prior to this dissertation indicates that the lateral preoptic area (LPO) could be a possible overlooked member of the brain motivation and valence circuit. Through projections from the LPO to the VTA and intermediary structures, the LPO is positioned to modulate the activity of VTA neurons and the reward behaviors the VTA underlies. Furthermore, correlational and causal experiments suggest that the LPO modulate motivation and valence. In the next few sections, I will review the literature about the LPO with a focus on its potential role in modulating motivation and valence.

1.3.1 Anatomy of the Lateral Preoptic Area

The LPO contains primarily GABAergic and glutamatergic neurons, but also other neurotransmitter and neuropeptide populations. The LPO contains a large number of neurotensin neurons that project to the VTA (Zahm et al., 2001; Woodworth et al., 2018). The neurotensin population within the LPO is continuous with neurotensin populations in the medial preoptic area and lateral hypothalamus. The ventral lateral preoptic area contains galanin neurons which project to the tuberomammillary nucleus and promote sleep (Kroeger et al., 2018). The galanin population tapers off from high concentrations ventrally in ventral LPO to low concentrations dorsally in the LPO.

The position of the LPO is typically determined based on the absence of neurochemical identifiers found in neighboring regions. The lateral border of the LPO with the ventral pallidum is defined based on the expression of substance P (Root et al., 2015) and relatively higher level of parvalbumin (Zahm et al., 2014). The dorsal border of the LPO with the bed nucleus of the stria terminalis is defined based on high levels of nitric oxide synthase expression in the bed nucleus but only an intermediate level in the LPO (Zahm et al., 2014). Importantly, most neuronal subpopulations within the basal forebrain

have a transitionary drop off rather than strict delineations (Zahm et al., 2013). For example, the ventral lateral preoptic area is defined based on the presence of galanin, but there is a high concentration near the base of the brain that tapers off into neighboring structures. In practice, the position of the LPO is typically determined based on mapping to a reference atlas based on the location of histological landmarks such as white matter fiber tracks.

1.3.2 Connectivity of the Lateral Preoptic Area

The LPO receives inputs from a diverse set of limbic brain regions (Wayner et al., 1983). The LPO contains neurons with large dendritic fields that intersect the medial forebrain bundle (McMullen and Almli, 1981), which allows coursing fibers to synapse onto LPO neurons. The medial forebrain bundle travels along the rostral-caudal axis from the midbrain to the ventral medial prefrontal cortex, and contains many reward critical fiber pathways. Midbrain structures including the dorsal raphe, VTA, and locus coeruleus, project caudal to rostral through the medial forebrain bundle, while rostral structures including the nucleus accumbens and lateral septum project in the opposite direction. Brain regions along the medial forebrain bundle including the LPO and lateral hypothalamus receive input from coursing fibers. As result, the LPO receives a large input from the lateral septum and nucleus accumbens (Conrad and Pfaff, 1976; Mogenson et al., 1983; Wayner et al., 1983; Risold and Swanson, 1997; Zahm et al., 2013). The LPO also receives input from the lateral habenula, periaqueductal grey, and medial preoptic area (Wayner et al., 1983). The distribution of limbic inputs indicates that the LPO could be a player in modulating the reward and aversive behaviors that the limbic system underlies.

The LPO sends projections to a diverse set of limbic brain regions. The LPO sends both glutamatergic and GABAergic input to the VTA, where it makes up one of the largest

projections to the VTA (Yetnikoff et al., 2015). Of the LPO projection to the VTA, 33% express vGlut2, a marker for glutamate neurons, and 33% express GAD65, a marker for GABA neurons (Kalló et al., 2015). Studies using monosynaptic rabies indicate that the LPO makes monosynaptic inputs to both $VTA_{Dopamine}$ neurons (Watabe-Uchida et al., 2012; Beier et al., 2015; Faget et al., 2016), VTA_{GABA} neurons (Beier et al., 2015; Faget et al., 2016), and $VTA_{Glutamate}$ neurons (Faget et al., 2016). The LPO also projects to brain regions known to be important regulators of $VTA_{Dopamine}$ neuron activity, including the lateral habenula (Kowski et al., 2008; Yetnikoff et al., 2015; Barker et al., 2017), RMTg (Yetnikoff et al., 2015), and the dorsal raphe (Gervasoni et al., 2000; Pollak Dorocic et al., 2014). Taken together, the inputs and outputs of the LPO place the LPO in a position to receive reward and aversion related information and to transmit to brain regions capable of modulating motivated behaviors.

Figure 1.2 Connectivity of the LPO

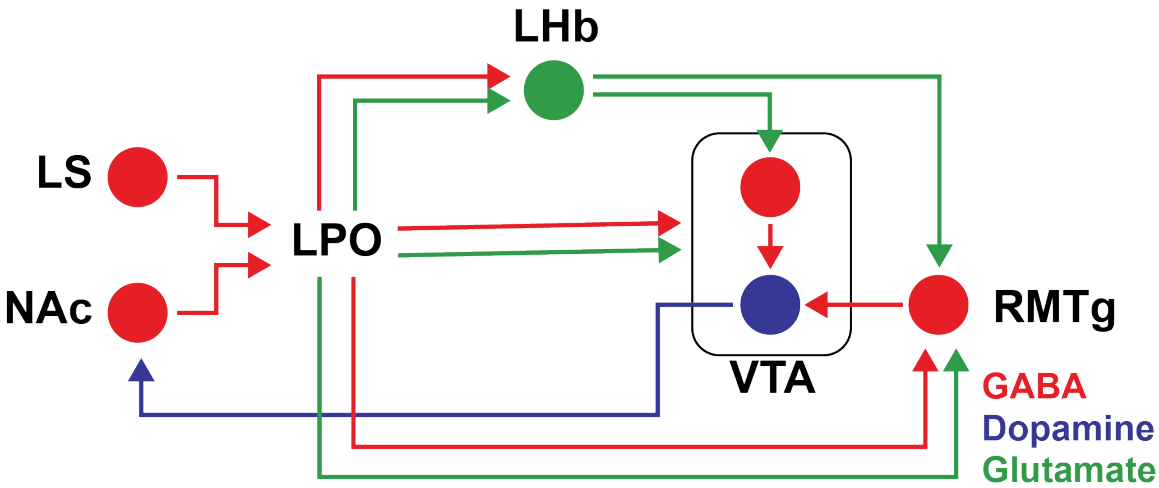

Circuit diagram of the direct and indirect connectivity between the LPO and VTA. The LPO receives a large projection from the LS and NAc. In turn, the LPO sends a direct GABA and glutamate projection to the VTA, and sends GABA and glutamate projections to brain regions that regulate the VTA including the LHb and RMTg. Abbreviations: LS: lateral septum; NAc: nucleus accumbens; LPO: lateral preoptic area; LHb: lateral habenula; VTA: ventral tegmental area; RMTg: rostromedial tegmental nucleus. Colors: red: GABA; blue: dopamine; green: glutamate.

1.3.3 Lateral Preoptic Area Neuronal Activity Correlates with Reward and Aversion

Many studies have found changes in LPO neuronal activity in response to rewarding and aversive events. Psychomotor stimulants increase c-fos, an immediate early gene that is upregulated following high levels of calcium influx, in LPO neurons that project to the VTA (Colussi-Mas et al., 2007b). The LPO also shows enhanced c-fos following a plethora of stressful stimuli including but not limited to, restraint stress (Chen and Herbert, 1995; Briski and Gillen, 2001), auditory distress (Campeau and Watson, 1997), predator exposure (Martinez et al., 2008), cold-stress (Kiyohara et al., 1995; Miyata et al., 1995), and social defeat (Martinez et al., 1998; Chung et al., 2000). The increases in LPO activity following rewarding and aversive events suggest that it could be involved in related behaviors.

The LPO also shows time-locked activity to rewarding and aversive events. During Pavlovian conditioning for sucrose, water, and aversive events, LPO neurons show a mixture of time-locked responses to the unconditioned stimuli and conditioned stimuli (Ono et al., 1986). LPO neurons show all combinations of increases and decreases to rewarding and aversive events (e.g. increase to reward, increase to aversion; increase to reward, decrease to aversion; etc.). Interestingly, the response patterns in LPO neurons differed from the response patterns in lateral hypothalamus neurons. In the lateral hypothalamus, neurons tended to show opposite effects for rewarding and aversive events (e.g. increase for reward, decrease for aversion; decrease for reward, increase for aversion). This result further underscores the difference between the LPO and LH, and argues that LPO neurons signal both rewarding and aversive events.

In addition to natural rewards, LPO neurons also show time-locked activity during drug self-administration. The majority of LPO neurons show slow-phasic patterns that correlate with cocaine self-administration behavior (Barker et al., 2015). The most common signaling pattern is a decrease progressive reversal, where firing rate drops following cocaine infusion and slowly increases until the next cocaine infusion. Interestingly, this is a similar pattern of activity seen in nucleus accumbens medium spiny neurons (Peoples et al., 1998). This is unexpected given the strong inhibitory projection from the nucleus accumbens to the LPO. The correlated activity between the LPO and rewarding and aversive events implies that the LPO may be a player in mediating reward and aversive behavior.

1.3.4 Lateral Preoptic Area's Functional Role

1.3.4.1 Lateral Preoptic Area's Role in Locomotion

So far, I have outlined the anatomy, connectivity, and correlated activity of the LPO, in this section I will review the causal role of the LPO in different behaviors. As stated above, the LPO is interconnected with brain regions that promote locomotion such as the VTA and lateral dorsal tegmental area. Another large body of work indicates that increased neuronal activity within the LPO promotes locomotion. Early researchers became interested in the LPO as a potential mediator of locomotion after finding that the LPO and neighboring structures, including the substania innominata, receive a large input from the nucleus accumbens (Conrad and Pfaff, 1976; Mogenson et al., 1983), which at the time was known to regulate locomotion through GABAergic projections to multiple brain regions. In an elegant experiment, Mogenson et al. found that application of GABA agonists to subpallidal regions, including the LPO and neighboring substantia innominata, blocked the increase in locomotion following injections of dopamine into the nucleus accumbens (Mogenson and Nielsen, 1983). For the first time, this study linked the LPO to the mesolimbic locomotion circuit. Subsequent studies further demonstrated the importance of the LPO in the mesolimbic locomotion circuit. In two manuscripts, Swerdlow et al. found that application of GABA agonists and lesioning the LPO with electricity prevented the super-sensitivity to apomorphine following dopamine denervation of the nucleus accumbens (Swerdlow and Koob, 1984; Swerdlow et al., 1984). These results indicate that there is a functional relationship between dopamine in the nucleus accumbens, activity within the LPO, and locomotion.

In another line of work, Sinnamon demonstrated that electrical and pharmacological stimulation of the LPO produces motor movements in anesthetized

animals. Sinnamon found that electrical stimulation of a wide range of sites across the rostral caudal extend of the LPO produces coordinated leg movements (Sinnamon, 1987; 1992). Interestingly, he found leg movements following stimulation of a large portion of the subpallidal region, including the LPO, medial preoptic area, the horizontal limb of the diagonal band, bed nucleus of the stria terminalis, medial portions of the substantia innominate, and medial portions of the ventral pallidum. Electrical stimulation of brain regions caudal to subpallidal regions, including the lateral hypothalamus, also drove leg movements (Sinnamon et al., 1991). Sinnamon's work indicates that a large portion of the hypothalamus is capable of driving locomotion behavior, suggesting a generalized functional output of these brain regions.

Recent work has begun to investigate the nuances of motor movements elicited by stimulation of different subpallidal regions. The Zahm's lab has performed many experiments to understand the differences in locomotion produced by stimulating the LPO and ventral pallidum. Unilateral stimulation of the LPO with GABA-A antagonists produces coordinated exploratory locomotion, while unilateral stimulation of the ventral pallidum (lateral to the LPO) does not affect locomotion (Zahm et al., 2014; Lavezzi et al., 2015; Subramanian et al., 2018; Reichard et al., 2019a). They also found that bilateral stimulation of the LPO produces only modest increases in locomotion above and beyond unilateral stimulation (Subramanian et al., 2018). On the other hand, bilateral stimulation of the ventral pallidum drives locomotion, but also drives abnormal movement behavior that does not manifest as the smooth naturalistic movement elicited by stimulation of the LPO (Subramanian et al., 2018). Furthermore, blocking dopamine receptors systemically prevents locomotion induced by LPO stimulation, indicating that the LPO enhances locomotion through regulating the dopamine system (Subramanian et al., 2018; Reichard et al., 2019a). However, even after administration of systemic dopamine receptor

antagonists, there is some movement present, suggesting that the LPO may be promoting locomotion through non-dopaminergic pathways as well.

The literature clearly demonstrates a role for the LPO in locomotion and this role in locomotion is mediated in part by the dopaminergic system. Many lines of research have found that stimulation of the LPO with electricity and pharmacology can produce both motor movements in anesthetized animals and exploratory locomotion in awake animals. The role of the LPO in locomotion is interconnected with dopaminergic signaling. Inhibiting the LPO diminishes nucleus accumbens dopamine ability to enhance locomotion, and blocking dopamine diminishes the LPO's ability to enhance locomotion.

1.3.4.2 Lateral Preoptic Area's Role in Reinforcement and Valence

Early work demonstrated that electrical stimulation of the LPO supports ICSS (Whishaw and Nikkel, 1975; Fouriezos et al., 1987). As stated before, electrical stimulation of the LPO also stimulates coursing fibers of the medial forebrain bundle, which muddles interpretations of LPO electrical stimulation. However, additional work implicates the LPO in ICSS behavior. Lesions to the LPO (Arvanitogiannis et al., 1996), but not medial preoptic area (Arvanitogiannis et al., 1999), increase brain-reward-thresholds in ICSS of the lateral hypothalamus, indicating that lesioning the LPO diminishes ICSS in the lateral hypothalamus. A series of elegant experiments conducted by Bielajew et al. also outlined the role of the LPO in ICSS behavior. They found that two thirds of stimulation sites within the LPO supported ICSS, but also found other sites that supported ICSS including the medial preoptic area and bed nucleus of the stria terminalis (Bushnik et al., 2000). In a following set of experiments, Bielajew et al. used ICSS collision studies to discern the connections of the LPO that underlie its role in ICSS. These studies revealed that ICSS reinforcement from electrical stimulation in the LPO is supported by a fiber pathway

coursing between the LPO and lateral hypothalamus (Bielajew et al., 2001), but not necessarily the LPO and VTA (Bielajew et al., 2000). The authors argue that a diffuse connection between the LPO and VTA underlies the LPO ICSS, which is likely to be the same for other brain regions that mediate ICSS behavior (Bielajew et al., 2000). The role of LPO and lateral hypothalamus projections to the VTA in ICSS behavior was conducted using optogenetic stimulation of these two pathways. The study found that stimulation of the lateral hypothalamus projection to the VTA, but not the LPO projection sustained ICSS and promoted food consumption (Gigante et al., 2016). The results expressed in this paragraph clearly indicate that the fibers that course through the LPO, but not necessarily the LPO itself, are rewarding and support ICSS responding.

In addition to ICSS, a small amount of research has indicated that LPO activity is related to reward. The clearest evidence demonstrating a role for the LPO in reward comes from Reichard et al., where they found that stimulation of the LPO not only drove enhanced locomotion but also led to conditioned place preference (Reichard et al., 2019a). Interestingly, they also found that the conditioned place preference produced by stimulation of the LPO is blocked by systemic antagonism of dopamine D1- and D2-like receptors. These results imply that the LPO is capable of driving reward behaviors and does so through regulation of the dopamine system. Further research has found bidirectional effects of LPO GABA and glutamate projections to the lateral habenula (Barker et al., 2017). Optogenetic stimulation of LPO GABA neurons that project to the lateral habenula produce RTPP, while stimulation of the glutamate projection promotes aversion. These results are expected given prior work on the effect of stimulation and inhibition of the lateral habenula on downstream $VTA_{Dopamine}$ activity and RTPT behavior (see section 1.3.7 for details). Taken together, these results argue that the LPO is capable of driving both rewarding and aversive valence.

1.3.4.3 Lateral Preoptic Area's Role in Stress and Aversion

A limited amount of research suggests that the LPO plays a role in stress response. Multiple studies show that the LPO provides inhibition to the hypothalamic-pituitary-adrenal axis following acute stressors. Inhibition of the LPO with a GABA-A agonist enhances the concentration of circulating adrenocorticotropic hormone (Zaretsky et al., 2006), implying that the LPO is providing down-stream tonic inhibition of the pituitary gland. Furthermore, blocking neuronal input to the LPO using the nonselective synaptic blocker CoCl2 leads to a heightened increase in circulating corticosterone following restraint stress. These two results suggest that the LPO inhibits the hypothalamic-pituitary-adrenal axis (Duarte et al., 2017).

In addition to a role in stress, a single study indicates that the LPO is capable of driving aversion. As outlined previously, LPO glutamate projection to the lateral habenula produces aversion, and supports negative reinforcement in the form of shuttling to avoid stimulation to this pathway (Barker et al., 2017). To my knowledge, no other studies provide support for or against the role of the LPO in aversive behavior.

1.4 GAPS IN KNOWLEDGE

1.4.1 The Functional Connectivity between the Lateral Preoptic Area and Subpopulations of Ventral Tegmental Area Neurons

Extensive work has demonstrated that the LPO is positioned to regulate neurons of the VTA, but the nature of the functional connectivity between the LPO and VTA remains undetermined. Multiple lines of research have shown that the LPO sends a direct glutamate and GABA projection to the VTA (Kalló et al., 2015), and projections to brain regions known to be potent regulators of dopaminergic activity, including the lateral habenula, lateral hypothalamus, dorsal raphe, and rostromedial tegmental nucleus (Gervasoni et al.,

2000; Pollak Dorocic et al., 2014; Yetnikoff et al., 2015). As the literature stands, it is unclear how neuronal activity within the LPO is related the activity of neurons in the VTA. The functional outcome of the direct projection from the LPO to the VTA is unknown and cannot be confidently deduced from the evidence in the literature as the LPO send a mixed projection and synapses onto both $VTA_{Dopamine}$ and VTA_{GABA} neurons (Beier et al., 2015; Faget et al., 2016), making prediction of the net effects on VTA neurons impossible. The complexity of the relation between the LPO and neuronal activity in subpopulations of the VTA is further complicated by connections between the LPO and intermediary structures (Yetnikoff et al., 2015). However, there is indirect evidence that suggests the LPO may enhance dopamine transmission, as limited set of studies found that activation of the LPO leads to behaviors which are blocked by systemic dopamine antagonists (Subramanian et al., 2018; Reichard et al., 2019a). However, $VTA_{Dopamine}$ neuron activity and dopamine release have not been measured directly following stimulation of the LPO. In this dissertation, I will show the functional connection between the LPO and VTA with both the direct pathway and the net outcome with all intermediary structures intact. These results will outline a role for the LPO in the regulation of the VTA and provide a framework for understanding how the LPO is related to the reward behaviors the VTA underlies.

1.4.2 The Role of the Lateral Preoptic Area in Reinforcement and Valence

Correlational studies indicate that the LPO is regulated by psychomotor stimulants, including amphetamine and cocaine (Colussi-Mas et al., 2007a; Barker et al., 2015), but the causal relationship between LPO activity and psychomotor stimulant behavior is unknown. Administration of amphetamine leads to an upregulation of c-fos in LPO neurons that project to the VTA (Colussi-Mas et al., 2007a), and LPO neurons track behavior during self-administration of cocaine (Barker et al., 2015). In addition to responding to drugs of

abuse, the LPO also responds to sucrose rewards (Ono et al., 1986). From the literature prior to this dissertation, it is clear that activity in the LPO fluctuates in response to drug and sucrose rewards but it is unknown if and how this activity is causally related to reward self-administration behavior.

The effect of LPO stimulation on reinforcement and valence is also poorly understood, and the effect of the LPO to VTA pathway have not been studied. Early work demonstrated that electrical stimulation of the LPO supports ICSS (Whishaw and Nikkel, 1975; Fouriezos et al., 1987), which suggests the LPO is rewarding. These results are complicated by the coursing of medial forebrain bundle fibers through the LPO, which support ICSS on its own (Bishop et al., 1963; Olds and Fobes, 1981). No one has demonstrated that LPO neurons themselves support ICSS. However, there have been two studies that tested the valence of LPO activity. One found that stimulating the LPO with bicuculline leads to conditioned place preference (Reichard et al., 2019a). On the other hand, another study found that stimulation of the LPO projection to the lateral habenula using optogenetics can produce both aversion and reward in RTPT depending on which neurotransmitter population was stimulated (Barker et al., 2017). Finally, there is only one published experiment on the LPO projection to the VTA and the results were inconclusive (Gigante et al., 2016). From these experiments it remains unclear how neuronal activity in the LPO and the LPO to VTA pathway are related to reinforcement and valence.

Finally, the relation between the LPO and rewarding and aversive behaviors is also poorly understood. Many studies have shown that both stressful and rewarding events drive increased c-fos in the LPO, but only a small number of studies have actually recorded the LPO during these events. Electrophysiological recordings of LPO neurons found both increased and decreased firing rate in response to rewarding and aversive stimuli (Ono et al., 1986; Barker et al., 2015). Calcium recordings of the LPO to lateral habenula pathway

find that the LPO increases in response to aversive events but not rewarding events (Barker et al., 2017), but it is unknown if this signal is specific to this projection. Given the minimal number of recordings of the LPO during rewarding and aversive events and the diversity in response patterns, it remains unclear how the LPO signals at the population level to these events.

In this dissertation, I will show how stimulating the LPO shapes drug and sucrose self-administration behavior along with seeking behavior. I will also demonstrate the reinforcing and valence properties of stimulation of both the LPO as a whole and the LPO projection to the VTA. The results from these experiments will allow understanding of the causal relation between neuronal activity in the LPO and reward self-administration and seeking behavior, along with the reinforcing and valence properties of stimulation of the LPO and the LPO to VTA pathway. Through this dissertation I will demonstrate that the LPO is a formerly overlooked member of the brain reward and motivation circuit.

Chapter 2: The lateral preoptic area: a novel regulator of reward seeking and of activity of neurons in the ventral tegmental area

This chapter was submitted to Frontiers in Neuroscience in 2019. Authors: Adam Gordon-Fennell, Ryan Will, Vorani Ramachandra, Lydia Gordon-Fennell, Juan M. Dominguez, Daniel S. Zahm, and Michela Marinelli

Author contributions: A.G., R.W., and M.M. designed experiments; R.W. and V.R. conducted behavioral experiments; A.G. conducted electrophysiology experiments; A.G. and M.M performed analysis for publication; A.G. prepared figures; A.G. and M.M. drafted manuscript. A.G., M.M., R.W., V.R., L.G., J.D., and D.Z., edited and revised manuscript.

2.1 ABSTRACT

The lateral preoptic area (LPO) is a hypothalamic region whose function has been largely unexplored. Its direct and indirect projections to the ventral tegmental area (VTA) suggest that the LPO could modulate the activity of the VTA and the reward-related behaviors that the VTA underlies.

We examined the role of the LPO on reward taking and seeking using operant self-administration of cocaine or sucrose. Rats were trained to self-administer cocaine or sucrose and then subjected to extinction, whereby responding was no longer reinforced. We tested if stimulating the LPO pharmacologically with bicuculline or chemogenetically with Designer Receptors Exclusively Activated by Designer Drugs (DREADDs) modifies self-administration and/or seeking. In another set of experiments, we tested if manipulating the LPO influences cocaine self-administration during and after punishment.

To examine the functional connectivity between the LPO and VTA, we used in vivo electrophysiology recordings in anesthetized rats. We tested if stimulating the LPO modifies the activity of VTA_{GABA} and $VTA_{Dopamine}$ neurons.

We found that stimulating the LPO reinstated cocaine and sucrose seeking behavior but had no effect on reward intake. Furthermore, both stimulating and inhibiting the LPO prevented the sustained reduction in cocaine intake seen after punishment. Finally, stimulating the LPO inhibited the activity of VTA_{GABA} neurons while enhancing that of $VTA_{dopamine}$ neurons.

These findings indicate that the LPO has the capacity to drive reward seeking, modulate sustained reductions in self-administration following punishment, and regulate the activity of VTA neurons. Taken together, these findings implicate the LPO as a previously overlooked player in the reward circuit.

Illustration 2.1: Visual abstract of chapter 2

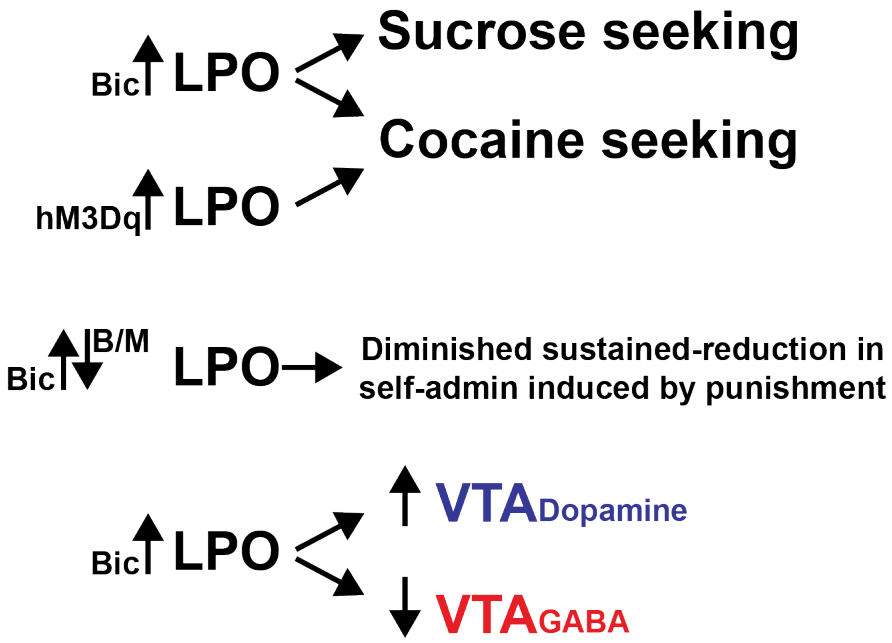

Abbreviations, and symbols: Bic: bicuculline; hM3Dq: excitatory DREADDs; B/M: baclofen + muscimol; LPO: lateral preoptic area; VTA: ventral tegmental area; up arrows: stimulation; down arrows: inhibition.

2.2 INTRODUCTION

The lateral preoptic area (LPO) is an anterior hypothalamic brain region whose function has been largely unexplored. Most studies have focused on its role in sleep and thirst (Osaka et al., 1993; Saad et al., 1996; Szymusiak et al., 2007). A small number of studies suggest that the LPO participates in reward behavior. Activating the LPO elicits locomotion (Shreve and Uretsky, 1989; 1991; Zahm et al., 2014; Lavezzi et al., 2015; Subramanian et al., 2018; Reichard et al., 2019a; Reichard et al., 2019b) and conditioned place preference (Reichard et al., 2019a). The LPO also supports intracranial electrical self-stimulation (Elder and Work, 1965; Bushnik et al., 2000), and neuronal activity in this structure is sensitive to fluctuations in cocaine levels during self-administration (Barker et al., 2015). The notion that the LPO might be important in reward is also supported by anatomical studies. The LPO sends monosynaptic projections to the ventral tegmental area (VTA) (Phillipson, 1979; Watabe-Uchida et al., 2012; Ogawa et al., 2014; Beier et al., 2015), which is a critical regulator of drug seeking and taking. Stimuli that increase the activity of $VTA_{Dopamine}$ neurons increase cocaine seeking and those that increase GABA transmission in the VTA decrease seeking (Phillips et al., 2003; Marinelli et al., 2006; Wise, 2013; Jin et al., 2018). Furthermore, the LPO projects to brain regions that influence the activity of VTA neurons, including, but not limited to, the lateral habenula (Mok and Mogenson, 1972; Kowski et al., 2008; Yetnikoff et al., 2015; Barker et al., 2017), rostromedial tegmental nucleus (Jhou et al., 2009; Yetnikoff et al., 2015), and dorsal raphe (Peyron et al., 1998; Ogawa et al., 2014). Taken together, these studies led us to postulate that the LPO modulates VTA activity and reward behavior (Zahm et al., 2001).

In this chapter, we examined the role of the LPO in reward behavior using operant self-administration of cocaine or sucrose. We measured the effects of stimulating the LPO on both self-administration and seeking behavior. Self-administration tests are a direct

measure of reward intake. In seeking tests, rats first learn to self-administer a reward, and then, they are subjected to an extinction phase, in which responding no longer delivers the reward. Seeking behavior can then be reinstated by different triggers to model "relapse" (Bossert et al., 2005). Here, we examined if stimulating the LPO produced reinstatement of seeking behavior. To increase external validity, we stimulated the LPO using two methods, pharmacologically by locally administering bicuculline (an antagonist of GABA-A receptors and calcium-activated potassium channels) and chemogenetically with excitatory Designer Receptors Exclusively Activated by Designer Drugs (DREADDs). We also examined the role of the LPO during and after punished responding for cocaine by pharmacologically stimulating the LPO with bicuculline or inhibiting it with baclofen + muscimol (agonists of GABA-B and GABA-A receptors, respectively) when the punishment was applied. Punishment involves learning the association between a response and an aversive stimulus which can lead to lasting reductions in self-administration (Ahmed, 2011; Vanderschuren et al., 2017). Finally, we investigated whether the LPO is functionally connected to the VTA by stimulating the LPO while recording neuronal activity in the VTA of anesthetized rats.

2.3 METHODS

2.3.1 Subjects

Male Sprague Dawley rats weighing 250-300g obtained from Harlan were housed by 2-3 in Plexiglas cages lined with chip bedding (P.J. Murphy, Montville, NJ, cat#: Sani-Chips) and given *ad libitum* access to water and laboratory chow (LabDiet, St. Louis, MO, cat#: 5053). Rats were maintained on a 12h reverse light-dark cycle, and all experiments began one to four hours into the dark cycle. Procedures were done in accordance with the

National Institutes of Health Guide for the Care and Use of Laboratory Animals and were approved by the Institutional Animal Care and Use Committee of The University of Texas at Austin.

2.3.2 Drugs and Viral Vectors

The following drugs were obtained from Henry Schein (Dublin, OH): isoflurane (cat#: 1169567762), meloxicam (cat#: 6451603845), flunixin meglumine (cat#: 049622), carprofen (cat#: 1311749), 0.9% saline (cat#: 002477), sodium brevital (cat#: 038431), and cefazolin (cat#: 1026761). The following drugs were obtained from Sigma-Aldrich (St. Louis, MO): phosphate buffered saline (cat#: P3813), (±)-baclofen (cat#: B5399), muscimol hydrobromide (cat#: G019), sucrose (cat#: S7903), paraformaldehyde (cat#: 158127), dimethyl sulfoxide (DMSO, cat#: D8418), and fast-green (cat#: F7252). (-)-Bicuculline Methiodide (Bic, cat#: 2503) was obtained from Tocris (Bristol, UK). Artificial cerebral spinal fluid (aCSF, cat#: 59-7316) was obtained from Harvard Apparatus (Holliston, MA). Betadine (cat#: 67618-155-32) was obtained from Purdue Products L.P. (Stamford, CT). Clozapine-n-oxide (CNO) was supplied by the NIDA Drug Supply Program.

The following adeno-associated viral vectors were obtained from UNC Viral Vector Core to use in the chemogenetics (DREADD) studies: rAAV5/hSyn-HA-hm3D(Gq)-IRES-mCitrine (hM3Dq; titer: 4e12vg/mL), rAAV5/hSyn-ChR2(E123A)-eYFP-WPRE (ChR2; titer: 3.4e12vg/mL), and rAAV5/hSyn-eGFP (GFP; titer: 3.6e12vg/mL).

Drugs injected intracranially were dissolved in aCSF. Drugs administered systemically were dissolved in sterile 0.9% saline. CNO was dissolved in DMSO before being diluted in saline (final [DMSO] 0.5%) or aCSF (final [DMSO] 0.0014%).

2.3.3 Surgical Procedures

2.3.3.1 Anesthesia

For all surgical and *in vivo* electrophysiology procedures, anesthesia was induced by placing rats into an induction chamber (E-Z Anesthesia, Palmer, PA) filled with 5% isoflurane regulated by an isoflurane vaporizer (E-Z Anesthesia). Following induction, anesthesia was maintained with 2.0-2.5% isoflurane delivered via nose cone or stereotaxic breather (E-Z Anesthesia). To ensure sufficient anesthesia, breathing rate, pinch response, and body temperature were monitored throughout procedures, and anesthesia was adjusted when necessary.

2.3.3.2 Intravenous catheterization

Areas around incisions were shaved with electric clippers (Andis Company, Sturtevant, WI, cat#: 22350), and the skin was cleaned with 10% betadine and sprayed with Lanacaine, which contains benzocaine (20%), benzethonium chloride (0.2%), and ethanol (36%). Intravenous sylastic catheters were implanted in the right external jugular vein and passed under the skin to exit in the mid-scapular region. The catheters were accessible through a backport pedestal mount that was secured under the skin with surgical staples (Braintree Scientific, Inc, Braintree, MA, cat#: ACS APL, EZC CS).

2.3.3.3 Intracranial implantation of guide-cannulas and viral injection

Surgery sites were shaved the rat's head was mounted in a stereotaxic apparatus (David Kopf Instruments, Tujunga, CA, cat#: 902) with the upper body resting on a heating pad set at ~37°C (Kent Scientific, Torrington, CT). The local anesthetic mepivacaine (2%) was injected beneath the incision site, and the site was cleaned with 10% betadine. A scalpel incision was made, the tissue overlying the skull was removed, and a burr hole was

drilled over the LPO. For experiments involving microinjections, a guide cannula (23gauge thin-wall hypodermic tubing, 15mm length Plastics One, Roanoke, VA) was lowered at 18° to a site 2mm above the LPO [final coordinate: AP: -0.12mm, ML: -1.4mm, DV: -8.6mm from bregma, according to the Paxinos and Watson atlas (Paxinos and Watson, 2007)]. The cannula was then fixed to the skull with skull screws and dental cement (Coltène/Whaledent Inc., Cuyahoga Falls, OH, cat#: H00325). For experiments involving viral injections, a custom-made stainless steel injection cannula (30gauge, BD Precisionglide, Franklin Lakes, NJ, cat#: 305128) coupled to a gas-tight 5uL Hamilton syringe and micropump (Harvard Apparatus, Holliston, MA, cat#: Pump11) was lowered at 18° into the LPO (final coordinate: AP, -0.12mm, ML -1.4mm, DV -8.6mm from bregma). A total of 500nL was injected unilaterally at a rate of 100nL/min over 5min, and the cannula was left in place for 5min before slowly retracting. At the conclusion of the surgery, the scalp was closed using surgical staples (Braintree Scientific, Inc). For both experiments, catheterization and intracranial implantation or injection was performed serially.

2.3.3.4 Surgical recovery

At the conclusion of each surgery, wounds were covered with topical antibiotic ointment (Medique Products, Fort Myers, FL, cat#: 22373). Systemic NSAID analgesics, either Meloxicam (2.5mg/kg/2mL, s.c.), Carprofen (5mg/kg/mL, s.c.), or Flunixin meglumine (2.5mg/kg/0.5mL, s.c.), were administered the day of surgery and one day following. Systemic antibiotic Cefazolin (50mg/kg/0.5mL, i.v.) was administered the day of surgery and 2-6 days following (except for 3 rats in experiment 1, which did not receive antibiotic).

Following implantations of guide-cannulae, rats were allowed to recover for at least 10 days prior to starting self-administration. Following surgeries involving viral injections, rats were allowed to recover for at least 6 days before starting self-administration. To ensure adequate expression of DREADDs, we allowed at least 6 weeks of incubation prior to activating the DREADDs with CNO.

2.3.4 Self-administration

2.3.4.1 Acquisition of self-administration

All self-administration procedures took place in Med Associates chambers (Med Associates, Fairfax, VT, cat#: CT-ENV-007-VP-X) outfitted with three horizontal photo-beam sensors to track locomotion (Med Associates, Fairfax, cat#: ENV-253SD) and two nose-holes (Med Associates, cat#: ENV-114BM) to track responding (nose-poking). Nose-poking into one hole ('active hole') concomitantly delivered a reinforcer and a 10s light cue within the hole. The onset of reinforcement coincided with the onset of time-out. Nose-poking into the other hole ('inactive hole') had no consequences and was used to track non-goal-directed nose-poking. We recorded number of nose pokes, beam breaks, and reinforcements delivered using MED-PC IV (Med Associates).

For cocaine self-administration, the rat's backport was connected to a Tygon tubing (Cole Parmer, Vernon Hills, IL, cat#: 06419-01) coupled to an infusion pump (Med Associates, cat#:PHM108), which allowed delivery of cocaine (600µg/kg/100µL, i.v.). For sucrose self-administration, sucrose pellets (45mg, Bioserv, Flemington, NJ, cat#: F06233) were delivered through a pellet dispenser and receptacle (Med Associates, cat#: ENV-203M-45 and ENV-200R2M, respectively), located between the nose-holes. Cocaine and sucrose self-administration sessions were 90 minutes long and were conducted daily for7-15 days, according to the experiment. Time-outs were of 10s for the first ten or twenty

reinforcers, 20s for the next ten, and 30s from then onward, to prevent overdose during cocaine self-administration. In a subset of experiments, we tested the effect of stimulating the LPO on self-administration on the last day of testing by pharmacologically stimulating the LPO immediately prior to placing rats in the operant chamber. For all rats self-administering cocaine, at the conclusion of the self-administration procedure, and prior to starting the extinction procedure, we tested catheter patency by administering the fast acting anesthetic sodium brevital (5mg/kg/0.5ml, i.v.). Rats not immediately anesthetized were eliminated from the study.

2.3.4.2 Extinction

Following self-administration, responding was extinguished by running rats through identical conditions as the self-administration procedure but without delivering the primary reinforcer (cocaine or sucrose). The cue light in the active hole continued to be delivered with the same schedule as self-administration. Following extinction, we tested the effect of stimulating the LPO on cocaine or sucrose seeking by stimulating the LPO immediately prior to (pharmacological stimulation) or immediately upon (chemogenetic stimulation) placing rats in the operant chamber. Extinction test conditions were identical to extinction conditions.

2.3.4.3 Punishment

During punishment, every reinforcer was punished with a coincident electric footshock (800ms, 0.32-0.44mA, mean = 0.36mA) produced by a shock generator and administered through the operant chamber floor (Med Associates, cat#: ENV-414 and CT-ENV-OO5D+T, respectively). Shock amplitude was determined for each rat individually such that the shock produced flinching without producing freezing. To determine this

amplitude, on the day prior to punishment, each rat received 3-4 test shocks starting with 0.3mA and then of higher or lower intensities to titrate to their personal "flinching" response. During punishment, we tested the effect of manipulating the LPO on punished responding by pharmacologically stimulating or inhibiting the LPO immediately prior to placing rats in the operant chamber.

2.3.5 Intracranial Microinjections

On the day prior to microinjections, we lowered a custom-made stainless steel dummy injection cannula (30gauge) into the LPO (2mm below the injector guide) for 30s while loosely holding the rat. Microinjections were performed via custom-made stainless steel injection cannulae (30gauge), connected to a micropump (Harvard Apparatus, cat#: Pump11) via PE10 tubing. On the day of the microinjections, we lowered the injection cannula into the LPO, waited 30s, injected 300nL of drug over 60s, and then waited 60s to allow for diffusion, before removing the injector. Drugs were administered at the following concentrations, unilaterally into the LPO: Bicuculline (80.4ng base/300nL) and Baclofen + Muscimol (64.1ng/300nL and 5.85ng/300nL, respectively). These doses were based on previous studies (Yetnikoff et al., 2015). Rats received the microinjections immediately before being placed into the operant chambers for self-administration or extinction tests.

2.3.6 Extracellular Recordings of VTA Neurons

Rats were mounted in a stereotaxic apparatus (David Kopf Instruments, cat#: 902) and a local anesthetic (2% Mepivacaine) was injected subcutaneously at the incision site before an incision was made. Burr holes were drilled in the skull at sites overlaying the LPO and VTA. A microinjection pipette was lowered into the LPO at a lateralward angle of 18° from vertical (to reach a final coordinate: AP: -0.12mm, ML: -1.4mm, DV: -8.6mm

from bregma). VTA recordings were performed with a glass pipette (WPI, Sarasota, FL, cat# 1B150F-4) that was pulled with a vertical puller (Narishige, Amityville, NY, cat#:PE-2), broken under a microscope to a tip diameter of 1–2µm, and filled with 2% fast-green in a 2M saline solution. The impedance of the glass pipette was 1.5–2.1MOhms measured at 135Hz (Winston Electronics, St. Louis, MO, cat#:BL1000-B). The pipette was slowly lowered to the VTA (final coordinate: AP: -5.4mm, ML: -0.6mm, DV: -8.3mm from bregma) with a hydraulic microdrive (David Kopf Instruments, cat#: 640). Extracellular voltage was amplified (Fintronics Inc., Orange, CT), passed through a Hum Bug 50/60 Hz Noise Eliminator (Quest Scientific, North Vancouver, BC), and monitored on an oscilloscope (EZ Digital, Gwang-Ju City, South Korea, cat#: OS-5020A) and audio monitor (Grass Technologies, West Warwick, RI, cat#: AM10). Signals were also digitized and recorded using AxoScope software (Molecular Devices, San Jose, CA, cat#: Digidata 1440A (digitizer) and version: 10.7 (software)) running on a Windows 7 computer (Microsoft, Redmond, WA). Neurons were classified as putative $VTA_{Dopamine}$ neurons based on established extracellular recording criteria: wide (>2.4ms, measured from start to end when recorded with 400-500Hz filters (Einhorn et al., 1988) and >1.1ms, measured from start to trough when recorded with 50-800Hz filters (Ungless and Grace, 2012; Marinelli and McCutcheon, 2014)), triphasic (+/-/+) waveform, and firing rate between 1 and 10Hz. These criteria are ~90% accurate at detecting neurons containing tyrosine hydroxylase (Ungless and Grace, 2012). We analyzed firing rate (spikes over time) and firing pattern. $VTA_{Dopamine}$ neurons exhibit intermittent bursts, which are clusters of high-frequency spikes that start with an interspike interval of 80ms and terminate with an interspike interval greater than 160ms (Grace and Bunney, 1983). The amount of bursting activity was calculated as the percentage of spikes emitted in bursts over the total number of spikes. We also calculated the frequency of burst events and the properties of the bursts

(burst duration in ms). To determine the weight of bursting vs. non-bursting activity on overall firing rate, we analyzed "non-bursting activity" by subtracting burst events from the firing trace and by analyzing non-burst events separately. For this analysis, the spikes preceding and following each burst event were removed because their timing could be influenced by factors initiating and terminating burst events. Neurons were classified as putative VTA_{GABA} if they failed to meet the dopaminergic criteria. These neurons often have biphasic waveforms and comparatively high firing rates. We recorded baseline activity over a 3 minute period, microinjected bicuculline (80.4ng base/300nL/3min) or aCSF (300nL/3min) into the LPO over 3min, and recorded for an additional 3min after the end of microinjection. Only 1 neuron was recorded per rat to eliminate confounds stemming from multiple injections. At the conclusion of the recording, rats were euthanized and fast-green was ejected from the recording pipette into the end location by passing 28.6mA cathodal current through the electrode with a current generator (Fintronics Inc., cat#: VL-1200 D). Neurons were excluded if any of the following criteria were met: 1) they were lost before 3 minutes post microinjection; 2) the microinjector placement was outside the LPO; 3) the fast-green location was outside the VTA; 4) neuronal activity had >12% baseline firing variability.

2.3.7 Validation of hM3Dq mediated stimulation

To validate that activation of the excitatory DREADD hM3Dq stimulated LPO neurons, we used a modified version of the recording procedures described above, in rats receiving a 5:3 cocktail of hM3Dq and ChR2 vectors. A burr hole was drilled over the LPO, and a triple barrel probe was lowered at an 18° angle to the LPO (final coordinate: AP: -0.12mm, ML: -1.4mm, DV: -8.6mm from bregma). Neurons were recorded across multiple tracks in and around the LPO. The triple barrel was modeled based on previous

studies (Mahler et al., 2014) and consisted of a recording pipette, as outline above, an injection pipette (ringcaps, Hirchmann, location) pulled and broken-back at a ~20µm tip and positioned ~100µm behind the recording tip, and a 200µm 0.39NA optic fiber (Thorlabs, Newton, NJ, cat#: FT200UMT) positioned ~600µm behind the recording tip (Figure 2.3a). This approach allowed us to identify ChR2 expressing neurons that have a high likelihood of co-expressing hM3Dq. For optic identification, we applied 473nm laser stimulation (Laser Glow, Toronto, ON, cat#: LD-WL206) driven by a pulse train generator (Prizmatix, Israel, cat#: Pulser) at 0.2Hz, 5ms pulses, 2-20mW. Neurons were classified as expressing ChR2 if they were excited upon laser stimulation (Cohen et al., 2012), with an average spike latency of <5ms from pulse onset and an average jitter (standard deviation of spike latency) of <2ms across 20 repeated stimulations. In a subset of neurons, we further verified ChR2 expression by also measuring fidelity (# spikes / # light pulses) at high frequency stimulation by delivering six 1s trains, 40Hz, 5ms pulses, 2-10mW, 9s inter train interval. Once a neuron was identified as expressing ChR2, we measured the effect of hM3Dq activation by locally injecting 30-60nL of 10µM CNO via pneumatic pulses (8-12psi, 50-100ms) delivered by a Picospritzer III (Parker, Cleveland, OH) over 1-2min. 1-2 neurons were recorded for each rat, with >30min and >300µm in-between injection sites, to minimize effects of CNO diffusion. At the conclusion of each experiment, fast-green was deposited and located as outlined below.

2.3.8 Histology

The locations of recording sites, intracranial microinjection sites, and the distributions of the DREADD expression were determined at the conclusion of behavioral experiments. For electrophysiology experiments, rats were euthanized with isoflurane at the end of the recording. Brains were removed and fixed in 10% formalin for >24h. For

experiments involving microinjections, rats were euthanized with CO_2 and brains were removed and stored in formalin for >24h. For experiments involving DREADDs, rats were deeply anesthetized with isoflurane and transcardially perfused with Sorensen's buffer (0.01 M PB, 2.5% sucrose, 0.9% NaCl) followed by 4% paraformaldehyde in phosphate buffer solution (0.1 M PB, 2.5% sucrose, 4% paraformaldehyde). Brains were then removed and post fixed in 4% paraformaldehyde in phosphate buffer solution for 24h then transferred to 25% sucrose solution for ~3 days until they were fully sunk. For all experiments, coronal brain sections were collected at 40µm on a cryostat (Thermo Fisher Scientific, Waltham, MA, cat# HM550) and then imaged with a microscope (Carl Zeiss, Oberkochen, Germany, cat#: Axio Zoom.V16). The recording site for electrophysiology was determined by locating and imaging the fast-green spot and then mapping it onto the corresponding section of the Paxinos and Watson atlas (Paxinos and Watson, 2007) and a house made atlas that localized the VTA following immunohistochemistry for tyrosine hydroxylase. Following fast-green localization, the relative position of recorded neurons was back-calculated. The location of the microinjection sites was determined by imaging the ventral-most position of the injector track and then mapping it onto the corresponding section of the Paxinos and Watson atlas. The distribution of the chemogenetic constructs was determined by imaging brain sections with fluorescent microscopy and then mapping the distribution of the fluorescence on the corresponding section of the Paxinos and Watson atlas.

2.3.9 Experimental Specific Procedures

2.3.9.1 Experiment 1: Effects of Pharmacological Stimulation of the LPO on Cocaine Self-Administration and Seeking

Rats were allowed to self-administer cocaine for 90 minutes every day, for 7-8 days. The fixed-ratio requirement to obtain cocaine was 1 for all days (i.e. 1 nose poke: 1 infusion). Prior to the last day of self-administration, rats were assigned to the bicuculline (n = 6) or aCSF control (n = 9) groups in a way that minimized differences in infusions between groups. To measure the effect of stimulating the LPO on cocaine taking, rats received an intra-LPO microinjection of bicuculline or aCSF on the final day of self-administration. Following cocaine self-administration, rats underwent extinction sessions for 90 minutes every day, for 19-20 days. To measure the effect of stimulating the LPO on extinguished seeking behavior, rats received an intra-LPO microinjection of bicuculline or aCSF control on the final day of extinction (day 20 or 21).

2.3.9.2 Experiment 2: Effects of Chemogenetic Stimulation of the LPO on Cocaine Seeking

Rats expressing hM3Dq (n = 7) or GFP control (n = 9) in the LPO were allowed to self-administer cocaine for 90 minutes every day, for 10 days. The fixed-ratio requirement to obtain cocaine was 1 for days 1-3, 3 for days 4-6, and 5 for day 7 onward. Fixed ratios >1 were used to enhance discrimination between the active and inactive holes. Following cocaine self-administration, rats underwent extinction sessions for 90 minutes every day, for 21 days. To measure the effect of stimulating the LPO on extinguished seeking behavior, rats received an intravenous injection of CNO (0.3mg/kg/0.5mL) on the final day of extinction.

2.3.9.3 Experiment 3: Effects of Pharmacological Stimulation of the LPO on Sucrose Self-Administration and Seeking

Rats were allowed to self-administer sucrose for 90 minutes every day, for 14-15 days. The fixed-ratio requirement and pellets per delivery (FR ratio–pellets per delivery) was FR1-1 for days 1 to 4, FR3-1 for day 5, FR5-1 for day 6, FR5-3 for days 7 and 8, and FR5-5 for days 9 and onward. One group of rats (n = 11) was started on FR1-5 for two days prior to FR1-1, but was changed to FR1-1 because rats were only eating a small proportion of the delivered pellets. There was no significant difference in behavior over the remaining self-administration days between rats started on FR1-5 and those that started on FR1-1, so the data were pooled and the first two days were excluded from analysis. Prior to the last day of self-administration, rats were assigned to bicuculline (n = 10) or aCSF control (n = 8) groups in a way that minimized differences in deliveries between groups. To measure the effect of stimulating the LPO on sucrose taking, rats received the intra-LPO microinjection of bicuculline or aCSF on the final day of self-administration. Following sucrose self-administration, rats underwent extinction sessions for 90 minutes every day, for 26 days. To measure the effect of stimulating the LPO on extinguished seeking behavior, rats received an intra-LPO microinjection of bicuculline or aCSF control on the final day of extinction.

2.3.9.4 Experiment 4: Effects of Pharmacological Manipulation of the LPO on Cocaine Self-Administration after Punishment

Rats were allowed to self-administer cocaine for 90 minutes every day, for 7 days. The fixed-ratio requirement for reward was 1 for days 1 to 4 and 3 for days 5 onward. Prior to undergoing punishment, rats were assigned to bicuculline (n = 6), baclofen + muscimol (n = 7), or aCSF control (n = 8) groups in a way that minimized differences in infusions between groups. To measure the effects of LPO manipulation during and after punishment,

rats received an intra-LPO microinjection of bicuculline, baclofen + muscimol, or aCSF on the day of punishment (day 8). We determined if punishment led to sustained changes in behavior by testing self-administration for one day of post-punishment (day 9).

2.3.9.5 Experiment 5: Effects of Pharmacological Stimulation of the LPO on the Activity of VTA Neurons

We recorded the activity of putative VTA_{GABA} and putative $VTA_{Dopamine}$ neurons in the VTA and measured their response to an intra-LPO microinjection of bicuculline (VTA_{GABA}: n = 8, $VTA_{Dopamine}$: n = 9) or aCSF control (VTA_{GABA}: n = 6, $VTA_{Dopamine}$: n = 7).

2.3.10 Statistical Analysis and Data Visualization

In behavioral experiments, operant conditioning variables were analyzed using analysis of variance (ANOVA). Each variable was analyzed independently with group as a between-subject factor and experimental day as a within-subject factor. Additionally, responding was also analyzed using active hole and inactive hole as a within-subject factor. Tukey honest significant difference (HSD) was used for post-hoc tests.

In electrophysiology experiments, the characteristics of neuron firing were expressed as delta from baseline (average of three minutes prior to the microinjection) and were analyzed with ANOVA. Each variable was analyzed independently with group and neuron type as between-subjects factors and time relative to microinjection (binned in one minute intervals) as within-subjects factor, when relevant. HSD was used for post-hoc tests.

For all experiments, $P < 0.05$ was used as a threshold for significance across statistical tests. All data are expressed as mean ± SEM. Sample sizes were calculated based on variance obtained from previous or preliminary experiments and on effect size (partial

eta squared = 0.01-0.25 for repeated measures or main effects ANOVA). Power was set at 0.80.

All statistical analysis was completed in R (version 3.5.0). ANOVA was computed using the 'afex' package (version 0.21-2), HSD was computed using the `emmeans` package (version 1.2.3), and paired t-tests were computed using base R.

Data were visualized for publication using Graph Pad Prism (version 8.2.0). Images of brain placements (cannulae or viral expressions) were created in Adobe Illustrator CC (version 22.1) using the Paxinos and Watson digital atlas (Paxinos and Watson, 2007). All other figure aspects were created in Adobe Illustrator CC.

2.4 RESULTS

2.4.1 Experiment 1: Pharmacological Stimulation of the LPO Promotes Cocaine Seeking, but Does Not Change Self-Administration

We determined if pharmacological stimulation of the LPO modulates cocaine self-administration or extinguished cocaine seeking behavior using operant conditioning (Figure 2.1).

2.4.1.1 Acquisition of Self-Administration

All rats acquired self-administration of cocaine (Figure 2.1c), as indicated by significant discrimination between the active hole and inactive hole (hole effect: $F_{1,13}$ = 67.65, P < 0.001), and this occurred similarly across groups that would later would later receive intra-LPO microinjections of bicuculline or aCSF (group x hole interaction: $F_{1,13}$ = 8.04, P = 0.14). These groups also showed similar inactive hole responding, locomotion, and infusion counts (group effect: $F_{1,13}$ = 0.25, 0.50, 0.77, P = 0.63, 0.49, 0.40, respectively) (Figure 2.2 1st row). There was slightly more responding in the active hole in rats that would later receive bicuculline compared with those that would later receive aCSF (group

effect: $F_{1,13}$ = 7.21, P = 0.019). However, during the last three days of self-administration that preceded the self-administration test, groups did not differ in active hole responding, inactive hole responding, infusions counts, or locomotion (group effect: $F_{1,13}$ = 3.33, 0.12, 4.11, 0.81, P = 0.09, 0.73, 0.64, 0.38 respectively).

2.4.1.2 Self-Administration Test

During the self-administration test (Figure 2.1 d), intra-LPO microinjections did not differentially modify responding relative to the last three days of self-administration (group x hole x day interaction: $F_{1,13}$ = 2.02, P = 0.18) nor did they differentially modify infusion counts or locomotion (group x day interaction: $F_{1,13}$ = 0.34, 0.21, P = 0.57, 0.65, respectively) (Figure 2.2 2nd row).

2.4.1.3 Extinction

Seeking, as measured by responding in the previously active hole, declined over the course of extinction sessions (Figure 2.1 e), and this occurred similarly across groups (day effect: $F_{18,198}$ = 9.2, P < 0.001; group x day interaction: $F_{18,198}$ = 1.07, P = 0.39).

Groups did not differ over the last three days of extinction that preceded the extinction test, for active hole responding, inactive hole responding, or locomotion (group effect: $F_{1,13}$ = 0.97, 1.07, 0.23, P = 0.34, 0.32, 0.64, respectively) (Figure 2.2 3rd row).

2.4.1.4 Extinction Test (Reinstatement)

During the extinction test, intra-LPO microinjections differentially modified responding (group x hole x day interaction: $F_{1,13}$ = 12.62, P = 0.0035) (Figure 2.1 f). Specifically, relative to the average of the last three days of extinction, bicuculline increased active hole responding (HSD, P = 0.0026), but aCSF did not (HSD, P = 0.63), and neither bicuculline nor aCSF modified inactive hole responding (HSD, Bic: P = 0.48;

aCSF: P=0.96). Additionally, there was a trend for bicuculline to increase locomotion (group x day interaction: $F_{1,13} = 4.58$, P = 0.052) (Figure 2.2 4th row).

2.4.2 Experiment 2: Chemogenetic Stimulation of the LPO Promotes Cocaine Seeking

We determined if chemogenetic stimulation of the LPO using hM3Dq modulates extinguished cocaine seeking behavior using operant conditioning (Figure 2.3).

2.4.2.1 Validation of hM3Dq Stimulation

Neurons in the LPO were classified as co-expressing ChR2 and hM3Dq based on responses to optical stimulation. Low frequency stimulation (0.5Hz, 10ms pulses) of LPO neurons that co-expressed ChR2 and hM3Dq excited the neurons with short latency, low jitter, and high fidelity (Figure 2.3 b-c).

Local intra-LPO application of CNO to optically identified neurons increased firing in 4 out of 6 LPO neurons (Figure 2.3 d), indicating that CNO stimulated neurons as intended.

2.4.2.2 Acquisition of Self-Administration

All rats acquired self-administration of cocaine (Figure 2.4 c), as indicated by a significant discrimination between the active hole and inactive hole (hole effect: $F_{1,14} = 5.36$, P = 0.036), and this occurred similarly across rats in the hM3Dq and GFP groups (group x hole interaction: $F_{1,14} = 2.14$, P = 0.17). These groups also showed similar active hole responding, inactive hole responding, infusion counts, and locomotion (group: $F_{1,14} = 0.07, 2.00, 1.12, 0.17$, P = 0.80, 0.18, 0.31, 0.68, respectively) (Figure 2.5 1st row).

2.4.2.3 Extinction

Seeking, as measured by responding in the previously active hole, declined over the course of extinction sessions (Figure 2.4 d), and this occurred similarly across groups (day effect: $F_{23,332} = 18.28$, $P < 0.001$; group x day interaction: $F_{23,332} = 0.56$, $P = 0.95$) (Figure 2.5 2nd row).

Groups did not differ over the last three days of extinction that preceded the extinction test, for active hole responding, inactive hole responding, or locomotion (group effect: $F_{1,14} = 0.40, 0.00, 0.60$, $P = 0.54, 0.99, 0.45$, respectively).

2.4.2.4 Extinction Test (Reinstatement)

During the extinction test, administration of CNO differentially modified responding in the hM3Dq and GFP control groups (group x hole x day interaction: $F_{1,14} = 15.21$, $P = 0.0016$) (Figure 2.4 e). Specifically, relative to the average of last three days of extinction, CNO increased active hole responding in the hM3Dq group (HSD, $P < 0.001$), but not in the GFP group (HSD, $P = 0.35$), and it did not modify inactive hole responding in either the hM3Dq or GFP groups (HSD, Bic: $P = 0.99$; aCSF: $P = 1.00$). Additionally, CNO had no differential effects on locomotion (group x day interaction: $F_{1,14} = 2.46$, $P = 0.14$) (Figure 2.5 4th row).

2.4.3 Experiment 3: Pharmacological Stimulation of the LPO Promotes Sucrose Seeking, but Does Not Change Sucrose Self-Administration

In order to ascertain whether stimulation of the LPO has a general effect across rewards or is specific for cocaine, we repeated experiments with sucrose in place of cocaine. We determined if pharmacological stimulation of the LPO modulates sucrose self-administration or extinguished sucrose seeking behavior using operant conditioning (Figure 2.6).

2.4.3.1 Acquisition of Self-Administration

All rats acquired self-administration of sucrose (Figure 2.6 c), as indicated by significant discrimination between the active hole and inactive hole (hole effect: $F_{1,16}$ = 194.9, P < 0.001), and this occurred similarly in rats that would later receive intra-LPO microinjections of bicuculline or aCSF(group x hole interaction: $F_{1,16}$ = 0.28, P = 0.60). These groups also showed similar active hole responding, inactive hole responding, number of pellets delivered, number of pellets eaten, and locomotion (group effect: $F_{1,16}$ = 0.20, 0.42, 0.22, 0.20, 0.0040, P = 0.66, 0.53, 0.22, 0.66, 0.95, respectively) (Figure 2.7 1st row).

During the last three days of self-administration that preceded the self-administration test, groups did not differ in active hole responding, inactive hole responding, number of pellets delivered, number of pellets eaten, nor locomotion (group effect: $F_{1,16}$ = 0.73, 0.01, 1.25, 0.86, 0.0056, P = 0.41, 0.94, 0.28, 0.37, 0.52, respectively).

2.4.3.2 Self-Administration Test

During the self-administration test (Figure 2.6 d), intra-LPO microinjections did not differentially modify responding relative to the last three days of self-administration (group x hole x day interaction: $F_{1,16}$ = 1.31, P = 0.27) nor did they differentially modify number of pellets delivered, number of pellets eaten, nor locomotion (group x day interaction: $F_{1,16}$ = 0.82, 0.89, 3.32, P =0.38, 0.36, 0.087) (Figure 2.7 2nd row).

2.4.3.3 Extinction

Seeking, as measured by responding in the previously active hole, declined over the course of extinction sessions (Figure 2.6 e), and this occurred similarly across groups (day effect: $F_{25,400}$ = 12.85, P < 0.001; group x day interaction: $F_{25,400}$ = 0.71, P = 0.85).

Groups did not differ over the last three days of extinction that preceded the extinction test, for active hole responding, inactive hole responding, or locomotion (group effect: $F_{1,16}$ = 0.030, 2.73, 1.17, P = 0.87, 0.12, 0.30, respectively) (Figure 2.7 3rd row).

2.4.3.4 Extinction Test (Reinstatement)

During the extinction test, intra-LPO microinjections produced a trend of differentially altered responding (group x hole x day interaction: $F_{1,16}$ = 4.12, P = 0.059) (Figure 2.6 f). Specifically, relative to the average of last three days of extinction, bicuculline increased active hole responding (HSD, P = 0.0080), but aCSF did not (HSD, P = 0.92), and neither bicuculline nor aCSF modified inactive hole responding (HSD, Bic: P = 0.99; aCSF: P = 1.00). Additionally, bicuculline and aCSF had a differential effect on locomotion (group x day interaction: $F_{1,1F16}$ = 6.81, P = 0.019) (Figure 2.7 4th row). Specifically, relative to the average of last three days of extinction, bicuculline increased locomotion (HSD, P = 0.0024), but aCSF did not (HSD, P = 0.98).

2.4.4 Experiment 4: Pharmacological Manipulation of the LPO Disrupts Reduction in Self-Administration of Cocaine After Punishment

We determined if pharmacological stimulation or inhibition of the LPO during punishment reduces cocaine self-administration during and after punishment, using operant conditioning (Figure 2.8).

2.4.4.1 Acquisition of Self-Administration

All rats acquired self-administration of cocaine, as indicated by a significant discrimination between the active hole and inactive hole (hole effect: $F_{1,18}$ = 27.57, P < 0.001) (Figure 2.9 a, b). This occurred similarly in groups that would later receive intra-LPO microinjection of aCSF, bicuculline, or baclofen + muscimol (group x hole

interaction: $F_{2,18}$ = 0.44, P = 0.65). These groups also showed similar active hole responding, inactive hole responding, infusion counts, and locomotion (group effect: $F_{2,18}$ = 0.46, 0.07, 0.15, 1.96, P = 0.64, 0.93, 0.86, 0.17, respectively) (Figure 2.9 a-d).

Groups did not differ over the last three days of self-administration that preceded the punishment test, for active hole responding, or inactive hole responding, infusion counts, and locomotion (group effect: $F_{2,18}$ = 0.029, 0.86, 0.0087, 0.015, P = 0.97, 0.44, 0.99, 0.98, respectively).

2.4.4.2 Punishment

There was a significant difference in cocaine infusion counts across groups during the three phases of the procedure: average of the last three days of self-administration, electric footshock punishment, and post punishment (Figure 2.8 d) (group x day interaction: $F_{4,36}$ = 3.76, P = 0.012). Footshock punishment suppressed intake in all groups (all groups: HSD, Ps < 0.001). However, rats that received aCSF showed a sustained decrease in cocaine infusions on the day following the punishment (SA Pre vs. SA Post: HSD, P < 0.001), whereas rats that received bicuculline or baclofen + muscimol did not (SA Pre vs. SA Post: HSD, P = 0.20, 0.99, respectively). Additionally, across the different phases of the procedure, groups did not differentially change active hole responding, inactive hole responding, or locomotion (group x day interaction, $F_{4,36}$ = 2.04, 0.65, 1.84, P = 0.11, 0.63, 0.14) (Figure 2.9 f-g).

2.4.5 Experiment 5: Pharmacological Stimulation of the LPO Modulates Firing of VTA Neurons

We determined if pharmacological stimulation of the LPO modulates the activity of VTA neurons using in vivo anesthetized extracellular recordings (Figure 2.10).

Relative to aCSF control, stimulating the LPO with bicuculline had differential effects on putative VTA_{GABA} and $VTA_{Dopamine}$ neurons (neuron type x group x time interaction: $F_{8,208} = 4.62$, $P < 0.001$) (Figure 2.10).

2.4.5.1 Pharmacological Stimulation of the LPO Inhibits VTA_{GABA} Neurons

In the case of putative VTA_{GABA} neurons, the average baseline firing rate (three minutes preceding the microinjection) was 10.48 ± 1.48Hz, and activity was similar in groups that would later receive intra-LPO microinjection of aCSF or bicuculline (group effect: $F_{1,12} = 0.50$, $P = 0.49$). Intra-LPO microinjection of bicuculline decreased firing relative to aCSF control and to baseline (group effect: $F_{1,12} = 4.81$, $P = 0.049$; group x time interaction: $F_{8,96} = 3.29$, $P = 0.0023$) (Figure 2.10 c). The decrease in firing rate produced by bicuculline was significant during minutes 3, 4, and 5 after the start of the microinjection, compared with baseline (minutes -3, -2, and -1) (all comparisons: HSD, Ps < 0.05). There were no significant changes in firing rate after aCSF at any time (all comparisons: HSD, Ps > 0.98).

2.4.5.2 Pharmacological Stimulation of the LPO Stimulates $VTA_{dopamine}$ Neurons

In the case of putative $VTA_{dopamine}$ neurons, the average baseline firing rate (three minutes preceding the microinjection) was 4.69 ± 0.69Hz, and activity was similar in groups that would later receive intra-LPO microinjection of aCSF or bicuculline (group effect: $F_{1,14} = 0.24$, $P = 0.63$). Intra-LPO microinjection of bicuculline increased firing rate relative to aCSF control and to baseline (group effect: $F_{1,14} = 5.82$, $P = 0.030$; group x time interaction: $F_{8,112} = 2.87$, $P = 0.0060$) (Figure 2.10 f). The increase in firing rate produced by bicuculline was significant during minutes 2, 3, 4, and 5 after the microinjection, compared with baseline (minutes -3, -2, and -1) (all comparisons: HSD, Ps < 0.05). There

were no significant changes in firing rate after aCSF at any time (all comparisons: HSD, Ps > 0.98).

We also examined the firing pattern of $VTA_{Dopamine}$ neurons (Figure 2.10 i). Relative to aCSF control, bicuculline increased non-burst firing rate (group x time interaction: $F_{8,112} = 2.46$, P = 0.017). This increase was significant during minutes 2 and 4 compared with baseline (minutes -3, -2, -1) (all comparisons: HSD, P < 0.05). Bicuculline increased the amount of bursting measured as percent of spikes in bursts (group x time interaction: $F_{8,112} = 3.06$, P = 0.0037) and burst event frequency (group x time interaction: $F_{8,112} = 3.12$, P = 0.0032). The increase was significant during minutes 2, 4, and 5 for percent of spikes in bursts and minutes 4 and 5 for burst event frequency (all comparisons: HSD, P < 0.05). In those neurons that exhibited bursting activity (14/16), stimulation of the LPO produced a slight increase in burst duration (group x time interaction: $F_{8,96} = 2.14$, P = 0.039) that was significant during minute 2. There were no changes in intra-burst frequency (group x time interaction: $F_{8,96} = 0.72$, P = 0.67).

2.5 DISCUSSION

Our results indicate that stimulating the LPO precipitates reinstatement of reward seeking behavior for both cocaine and sucrose, but it does not alter cocaine or sucrose self-administration. Manipulating the LPO also prevents the reduction in cocaine self-administration after punishment. Finally, stimulating the LPO inhibits the activity of putative VTA_{GABA} neurons and increases the activity of putative $VTA_{Dopamine}$ neurons.

2.5.1 Stimulating the LPO Modulates Reward-Behaviors

Previous studies showed that stimulating the LPO elicits conditioned place preference and locomotor activity. We therefore hypothesized that the LPO might play a

role in reward (Reichard et al., 2019a). Here we studied it directly by measuring reward self-administration and seeking. Self-administration is a direct measure of reward intake. Seeking is represented by responding in the absence of the reward, and stimulus-induced increases in seeking (i.e. reinstatement of seeking behavior) are thought to model relapse (Bossert et al., 2005). Reinstatement of seeking behavior was observed after stimulating the LPO using two independent methods: pharmacology and chemogenetics. Pharmacological stimulation was achieved with bicuculline, an antagonist of GABA-A receptors and calcium-activated potassium channels, while chemogenetic stimulation was achieved with hM3Dq, a receptor that is coupled to an excitatory g-protein and stimulated by CNO. These convergent results provide higher confidence that stimulating the LPO precipitates reinstatement of cocaine seeking than either result alone. Pharmacological stimulation of the LPO precipitated reinstatement of seeking of both sucrose and cocaine. These results suggest that the LPO serves a general function for reward seeking, rather than a specific function for cocaine seeking. In all cases, reinstatement of seeking led to selectively higher responding on the active compared with the inactive hole, indicating a specific enhancement of goal-directed seeking behavior, rather than simply a generalized increase in arousal or activity.

In contrast to findings that pharmacological stimulation of LPO increased seeking behavior, pharmacological stimulation of the LPO did not substantially increase sucrose or cocaine intake during self-administration. It is unlikely that this was due to a ceiling effect because on the day of LPO stimulation, intake and responding were lower than they were during the earlier phases of the self-administration procedure. Results showing that the LPO does not impact the consummatory aspect of rewards is consistent with previous findings showing that stimulation of the LPO does not modify consumption of food (Reichard et al., 2019a).

Drug intake during and after punishment have been used in self-administration studies to test the ability of punishment to act as a deterrent to future drug taking. Punishment, in the form of electric footshock, suppressed cocaine intake in all groups. Similar to what is reported in the literature, punishment was a deterrent for future drug intake in control rats, illustrated by intake levels remaining suppressed the day following punishment (Ahmed, 2011). However, this was not the case for rats that received either stimulation or inhibition of the LPO pharmacologically. These rats returned to baseline intake of cocaine the day after punishment, indicating that punishment was not a deterrent in these rats. These results suggest that normal activity patterns within the LPO during punishment are necessary to consolidate lasting changes in behavior following punishment. This effect was not explained by differences in the number of punishments received or the degree of suppression in cocaine intake, as all groups suppressed intake on the day of the punishment, and there were no differences in the number of punishments delivered. These results imply that the LPO is not only involved in reward seeking behaviors but also in long-term reductions in cocaine self-administration following punishment, without altering the acute effects of punishment. Previous studies showed that electric footshock, which is the punishment stimulus used here, enhances the activity of neurons within the LPO (Ono et al., 1986; Campeau and Watson, 1997; Martinez et al., 1998; Snowball et al., 2000; Briski and Gillen, 2001), but ours is the first to link activity in the LPO to sustained effects following punishment.

In our studies, we did not consistently observe an increase in locomotor activity after stimulating the LPO with bicuculline. This is in contrast to previous studies, which have consistently shown increases in locomotor activity in an open field (Shreve and Uretsky, 1989; 1991; Zahm et al., 2014; Lavezzi et al., 2015; Subramanian et al., 2018; Reichard et al., 2019a; Reichard et al., 2019b). One possible caveat is the method we used

to measured locomotion in our studies. Our self-administration chambers allow changes in motor activity to be measured (Marinelli et al., 2003), but they might not be sensitive enough to detect the changes in locomotion that were observed with larger chambers equipped with more photo-beams. Another possibility is that in a passive context, such as an open field, stimulating the LPO may heighten exploration behavior, which manifests as an increase in locomotion. Instead, in an engaging context, such as self-administration, increased responding may compete with locomotion, wherein rats spent their time seeking reward, rather than moving throughout the chamber. The fact that stimulating the LPO triggered seeking is in line with the idea that stimulating the LPO could be driving fixed action patterns (Reichard et al., 2019a). In our case, stimulating the LPO after self-administration training and extinction may reengage fixed action patterns involved in self-administration.

Reinstatement of drug and food seeking behavior occurs after both rewarding and stressful stimuli (Venniro et al., 2016). Our data do not make clear if stimulating the LPO is mimicking rewarding or stressful stimuli to produce a reinstatement of seeking behavior. Reichard et al. (2019a) found that stimulating the LPO produces conditioned place preference. This suggests that stimulating the LPO may precipitate reinstatement by mimicking reward. However, additional studies will be needed to directly determine the valence of stimulating the LPO.

While our studies indicate that stimulating the LPO is sufficient to precipitate reinstatement of seeking, they do not indicate that neuronal activity within the LPO is necessary for reinstatement of seeking. Such studies would require inhibiting the LPO during drug, stress, or cue-precipitated reinstatement. Nevertheless, even if the activity in the LPO is not necessary for precipitated reinstatement, our results still indicate that the LPO is capable of driving the behavior.

2.5.2 Stimulating the LPO Modulates VTA Neurons

The LPO projection to the VTA had long been described (Zahm et al., 2001; Colussi-Mas et al., 2007a; Geisler et al., 2007; Watabe-Uchida et al., 2012; Beier et al., 2015; Kalló et al., 2015; Yetnikoff et al., 2015; Faget et al., 2016), but its functional connectivity had never been experimentally determined. Our results show that stimulating the LPO with bicuculline inhibits putative VTA_{GABA} neurons and stimulates putative $VTA_{Dopamine}$ neurons. The inhibition of putative VTA_{GABA} neurons was strong, some neurons completely stopped firing, only to slowly return to firing, while the excitation of putative $VTA_{Dopamine}$ neurons was more modest. This excitation coincided with an increase in both non-bursting activity (the spikes emitted outside of burst events) and the amount of bursting (the percentage of spikes emitted in bursts, and frequency of burst events). The size of the bursts was slightly increased, but the frequency of the spikes within the bursts was not. This increase in neuronal activity is consistent with changes in synaptic input, specifically, an increase in glutamatergic input and a decrease in GABAergic input onto $VTA_{Dopamine}$ neurons (Paladini and Tepper, 1999; Lobb et al., 2010; Morikawa and Paladini, 2011).

While our study clearly indicates there is a functional connection between the LPO and subpopulations within the VTA, it does not reveal the mechanism by which the LPO regulates these subpopulations. One possibility is that LPO inhibition of VTA_{GABA} neurons disinhibits $VTA_{Dopamine}$ neurons. Our observation that stimulating the LPO leads to major suppression of VTA_{GABA} neurons and a slight enhancement of $VTA_{Dopamine}$ neurons is in line with this idea (Subramanian et al., 2018). However, the LPO also contains a mixture of glutamate and GABA neurons (Kalló et al., 2015; Barker et al., 2017) that project to the VTA (Kalló et al., 2015). If both GABA and glutamate projections are functionally connected to both GABA and $VTA_{dopamine}$ neurons in the VTA, then our results suggest

that this functional connectivity is biased toward inhibition on VTA_{GABA} neurons and excitation on $VTA_{Dopamine}$ neurons, akin to what is observed in the lateral hypothalamus (Nieh et al., 2015). A final possibility is that our results reflect LPO connectivity with other intermediary structures. Indeed, the LPO sends projections to several other brain structures known to regulate the activity of VTA neurons (e.g. the lateral habenula, or rostromedial tegmental nucleus). Regardless of mechanism, detailed monosynaptic and poly-synaptic electrophysiological experiments will be necessary to definitively determine the nature of the functional connectivity.

We identified VTA neurons as putative VTA_{GABA} or $VTA_{Dopamine}$ based on established extracellular waveform and firing rate criteria (Ungless and Grace, 2012). We refer to these neuron populations as "putative" because we recognize the controversy around using extracellular criteria for identifying dopamine neurons. However, using the extracellular identification technique we employed, there is high likelihood (88-93%) that neurons classified as dopamine would also be classified as such using immunohistochemistry (Ungless and Grace, 2012). VTA neurons that did not reach the criteria for classification as a dopamine neuron were classified as putative GABA neurons based on research indicating that GABA neurons are the second largest population of VTA neurons (~35%) behind dopamine neurons (Nair-Roberts et al., 2008). We acknowledge that there may be glutamate neurons within the sample we identified as putative VTA_{GABA} neurons; however, glutamate neurons are a small portion of VTA neurons (~2-3%) in the regions in which we recorded (Nair-Roberts et al., 2008).

2.5.3 Connections between the VTA and Reward-Behaviors

Stimuli that increase the activity of $VTA_{Dopamine}$ neurons trigger reinstatement of seeking behavior (Marinelli et al., 2006). Similarly, $VTA_{Dopamine}$ receptor activation or

increases in dopamine in VTA-projection areas such as the nucleus accumbens also precipitate reinstatement of cocaine seeking (De Vries et al., 1999; Schmidt et al., 2006). In addition, reducing the activity of $VTA_{Dopamine}$ neurons or blocking dopamine receptors in the nucleus accumbens reduce cocaine seeking (Anderson et al., 2003; Bachtell et al., 2005; Anderson et al., 2006; Marinelli et al., 2006; Xue et al., 2011) . Therefore, the increase in activity of $VTA_{Dopamine}$ neurons we observed after LPO stimulation is a plausible mechanism underlying our findings, as shown for other behaviors (Zahm et al., 2014; Subramanian et al., 2018; Reichard et al., 2019a).

The role of VTA_{GABA} neurons in reinstatement of drug seeking behaviors has not been extensively studied, but recent findings suggest that VTA_{GABA} neurons also play a role. Increasing GABA transmission in the VTA reduces dopamine levels in the nucleus accumbens and suppresses seeking behavior (Jin et al., 2018); it also attenuates the ability of cues to trigger reward seeking (Wakabayashi et al., 2019). Therefore, together, the decrease in activity of VTA_{GABA} neurons and the increase in the activity of $VTA_{Dopamine}$ neurons could work to drive the reinstatement of seeking we observed. A similar regulation of behavior has been described in the lateral hypothalamus. Stimulation of lateral hypothalamus GABA neurons promotes behavioral activation (Barbano et al., 2016; Nieh et al., 2016; Tyree and de Lecea, 2017) through disinhibition of $VTA_{dopamine}$ (Nieh et al., 2016). This suggests that a functional connection from hypothalamic GABA neurons to VTA_{GABA} neurons generalizes across the hypothalamus.

Changes in the activity of VTA neurons after manipulating the LPO could also be responsible for the observed effects on cocaine taking after punishment. The VTA exhibits heterogeneous responses after aversive stimuli (Volman et al., 2013). In a reward context, $VTA_{Dopamine}$ neurons can pause briefly in response to an aversive stimulus, such as the footshock punishment used here (McCutcheon et al., 2012; Holly and Miczek, 2016;

Matsumoto et al., 2016), whereas VTA_{GABA} neurons increase activity (Tan et al., 2012). These temporally-precise responses in the VTA have been proposed to be a "teaching signal" that allows making associations with stimuli (Schultz, 2007; Mileykovskiy and Morales, 2011; Tan et al., 2012; Creed et al., 2014; Stelly et al., 2019). Both stimulating and inhibiting VTA activity disrupts these temporally-precise responses, and thereby prevents making associations with stimuli (Salinas-Hernandez et al., 2018). In our studies, both stimulating and inhibiting the LPO was capable of disrupting sustained effects of punishment. Probably, these manipulations, by disrupting the activity of VTA neurons, prevent the temporal changes in VTA activity and thus association with punishment. At this point, this mechanism remains speculative.

In conclusion, our results indicate that the LPO has the capacity to drive reward seeking, modulate sustained reductions in self-administration following punishment, and regulate the activity of VTA neurons. Taken together, the LPO may be a previously overlooked player of the reward circuit that could represent an additional component of the brain reward system.

2.6 Figures and Figure Legends

Figure 2.1 Pharmacological Stimulation of the LPO Precipitates Reinstatement of Cocaine Seeking, but Does Not Modulate Cocaine Taking

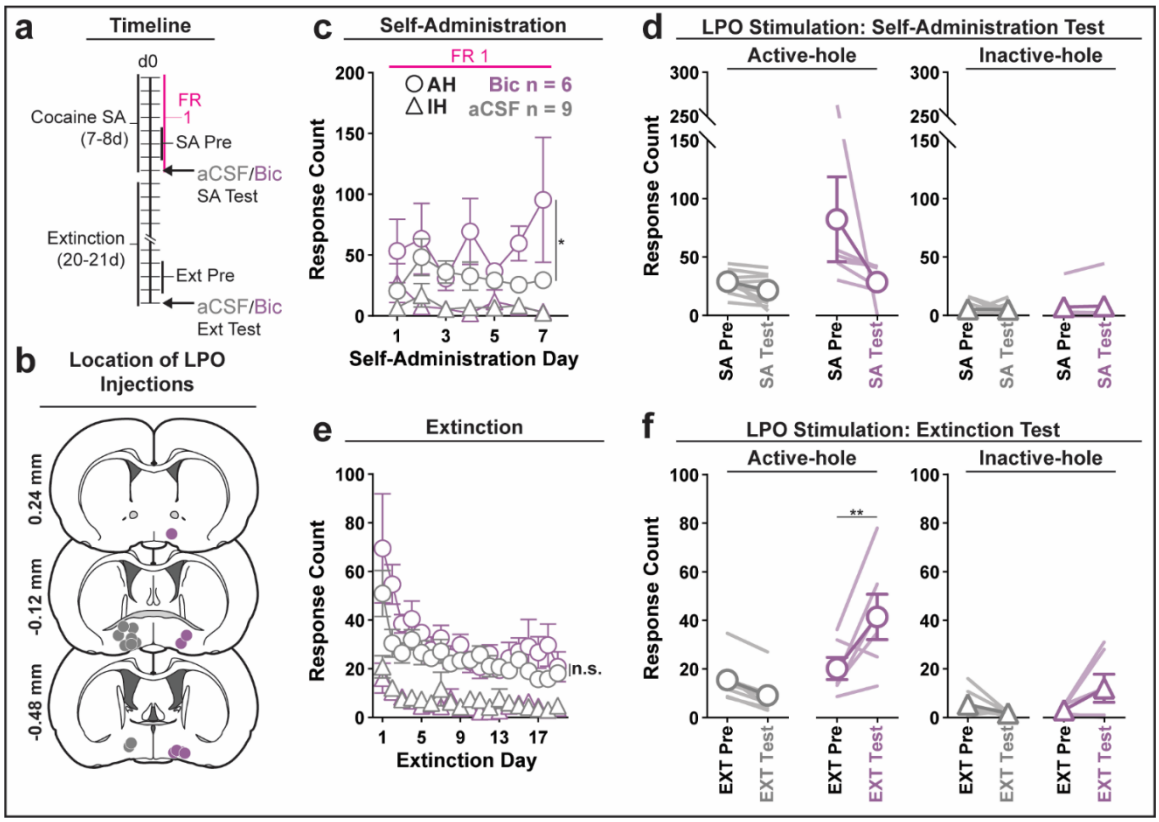

(a) Timeline of behavioral procedures (SA: self-administration); FR: fixed ratio (number of responses required to obtain one cocaine infusion, depicted with pink line). **(b)** Location of LPO injections for aCSF (grey) and bicuculline (Bic, purple). **(c)** Cocaine self-administration behavior. There was slightly more responding in the active hole in rats that would later receive bicuculline compared with those that would later receive aCSF; however, during the last three days of self-administration that preceded the self-administration test, groups did not differ. **(d)** Self-administration test (SA Test). Stimulating the LPO with bicuculline did not change active hole or inactive hole responding relative to aCSF or the average of the last three days of self-administration (SA Pre). **(e)** Extinction behavior. Both groups extinguished responding on the previously active hole. There was no difference between groups across extinction nor over the last three days of extinction (Ext Pre). **(f)** Extinction test (Ext Test). Stimulating the LPO with bicuculline reinstated cocaine seeking behavior, observed as increased responding on the previously active hole (HSD, $^{**}P < 0.01$) but not inactive hole (HSD, $P = 0.47$). Symbols are means ± SEM for each group; lines are individual subjects. See main text for detailed statistics.

Figure 2.2 Pharmacological Stimulation of the LPO Promotes Cocaine Seeking, but does not Change Cocaine Self-Administration (Details)

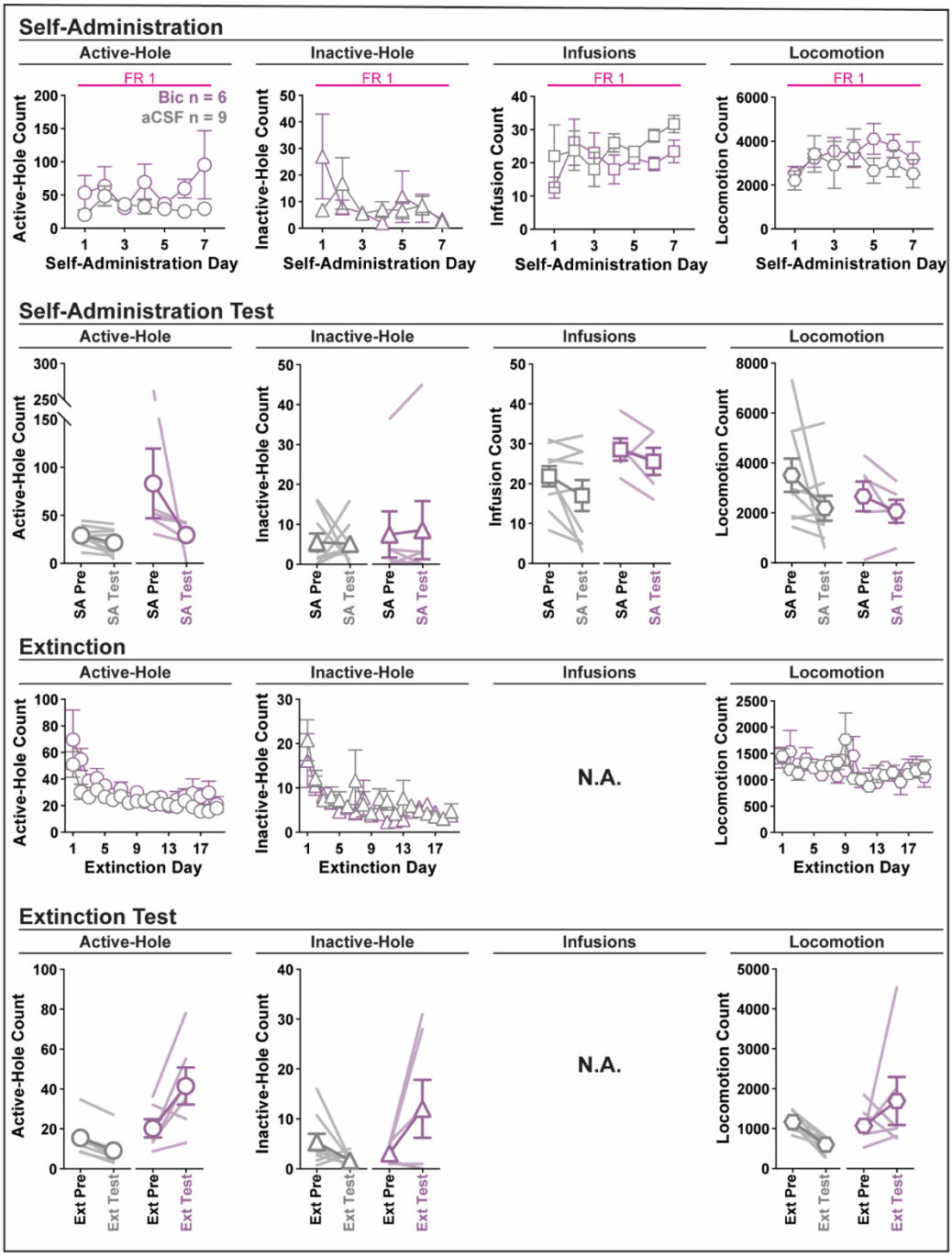

(1st row) Behavior during cocaine self-administration (SA). From left to right, active hole responding, inactive hole responding, infusions, and locomotion. **(2nd row)** Behavior during the self-administration test (SA Test). From left to right, active hole responding, inactive hole responding, infusions, and locomotion. Stimulating the LPO with bicuculline

did not change active hole responding, inactive hole responding, infusions, or locomotion (group x day interaction: $F_{1,13}$, $P > 0.19$ for all comparisons) relative to aCSF or the average of the three last days of self-administration (SA Pre). **(3rd row)** Behavior during the extinction phase. From left to right: active hole responding, inactive hole responding, and locomotion. **(4th row)** Behavior during the extinction test (Ext Test). Stimulating the LPO with bicuculline increased active hole and inactive hole responding (group x day interaction: $F_{1,13} = 18.86, 7.14$, $P < 0.001$, $P = 0.019$, respectively) relative to aCSF control and the average of the last three days of extinction (Ext Pre). There was trend for an increase in locomotion (group x day interaction $F_{1,13} = 4.58$, $P = 0.052$). Symbols are mean ± SEM for each group; lines are individual subjects. See main text for more detailed statistics.

Figure 2.3 Validation of hM3Dq Stimulation

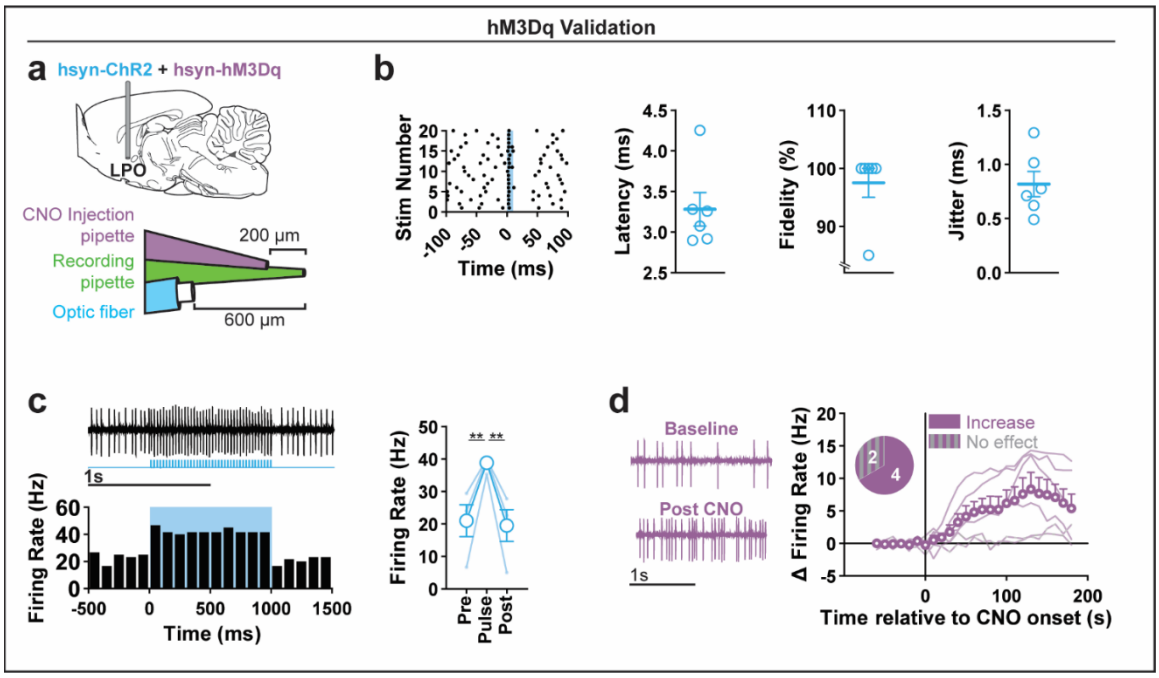

(a) Recording preparation (top), and diagram of the triple barrel pipette used for these experiments (bottom). **(b)** From left to right: peri-stimulus raster of firing in response to single pulse stimulations (0.2Hz, 10ms, 20 pulses), and latency, fidelity, and jitter to pulse stimulation. Horizontal lines are mean ± SEM and circles are individual neurons. **(c)** Representative trace of an LPO neuron (top) and average firing rate (bottom) in response to high-frequency stimulation (1s, 40Hz, 5ms pulse, 9s ITI, 6 trains, blue bars). Firing rate in responses to high frequency stimulation (right) (**HSD, P<0.01). Circles are mean ± SEM and lines are individual neurons. **(d)** Representative trace of an LPO neuron before (baseline) and after CNO application (Post CNO) (left) and firing rate relative to intra-LPO application of CNO (CNO onset) (right). Inset shows a pie chart of the number of neurons showing a change in firing or no change in firing. Circles are mean ± SEM and lines are individual neurons.

Figure 2.4 Chemogenetic Stimulation of the LPO Promotes Cocaine Seeking

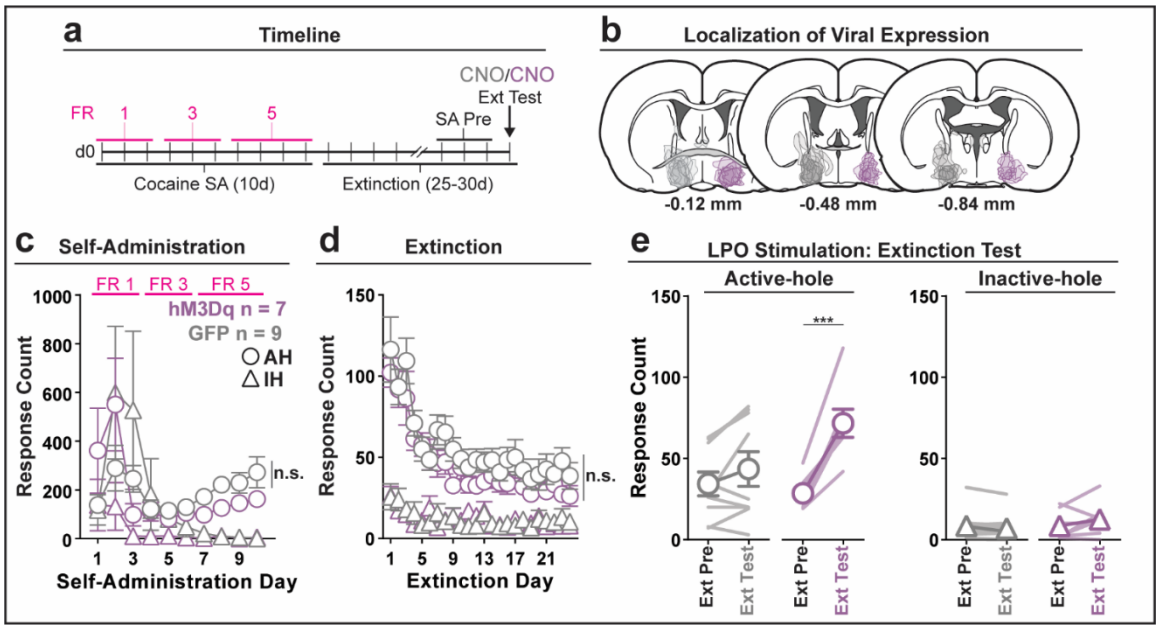

(a) Timeline of behavioral procedures.SA: self-administration; FR: fixed ratio (number of responses required to obtain one cocaine infusion, depicted by pink lines). **(b)** Localization of viral expression for GFP (grey) and hM3Dq (purple). **(c)** Cocaine self-administration behavior. Both groups acquired cocaine self-administration and there was no difference between groups across self-administration or over the last three days of self-administration (SA Pre). **(d)** Extinction behavior. Both groups extinguished responding on the previously active hole. There was no difference between groups across extinction or over the last 3 days of extinction (Ext Pre). **(e)** Extinction test (Ext Test). Stimulating the LPO with bicuculline reinstated cocaine seeking behavior, observed as increased responding on the previously active hole (HSD, ***$P < 0.001$) but not inactive hole (HSD, $P = 0.99$). Symbols are means ± SEM for each group; lines are individual subjects. See main text for detailed statistics.

Figure 2.5 Chemogenetic Stimulation of the LPO Promotes Cocaine Seeking (Details)

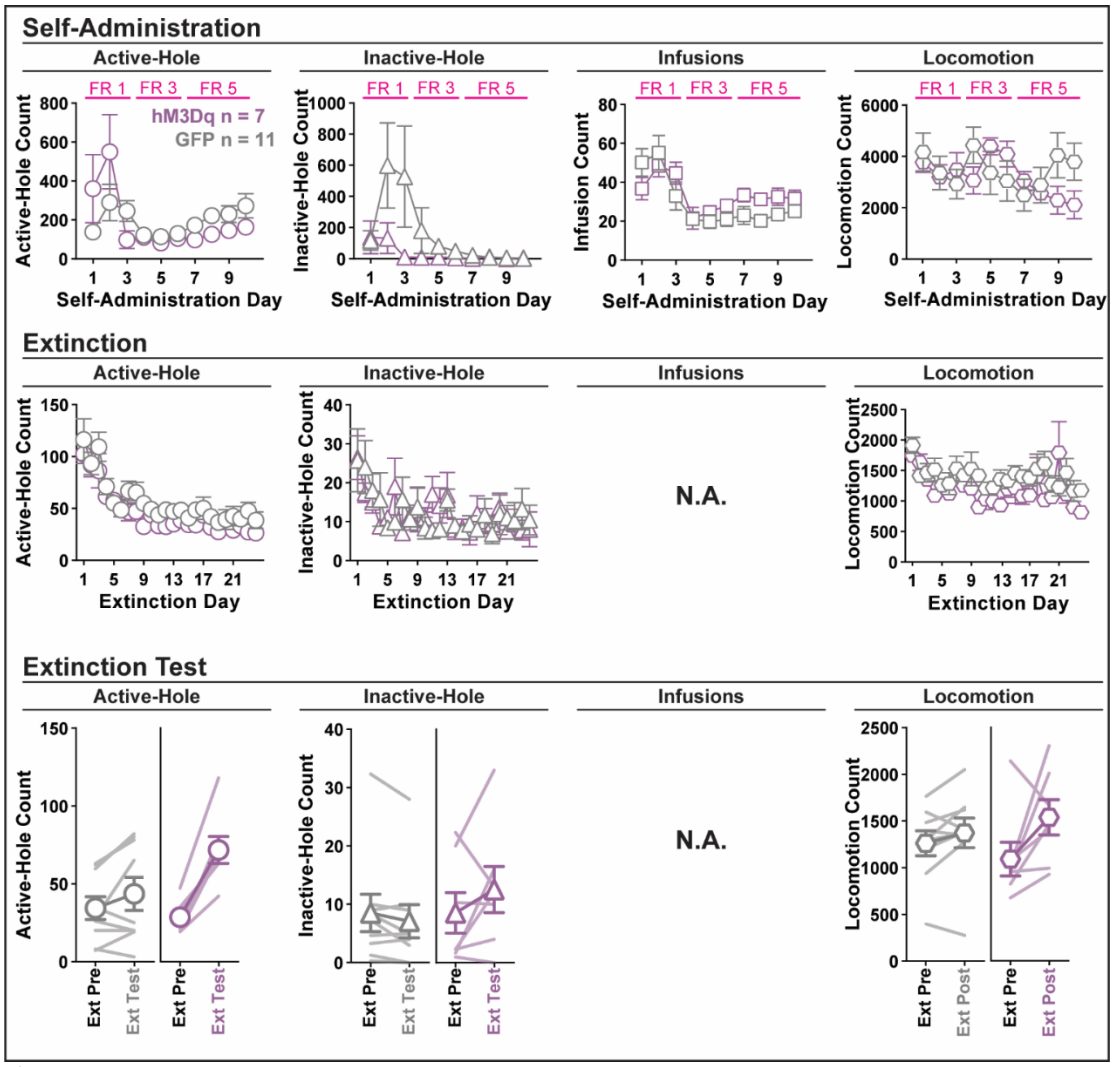

(1st row) Behavior during cocaine self-administration (SA); FR: fixed ratio (number of responses required to obtain one infusion of cocaine, depicted with pink lines). From left to right, active hole responding, inactive hole responding, infusions, and locomotion. **(2nd row).** Behavior during the extinction phase. From left to right: active hole responding, inactive hole responding, and locomotion. **(3rd row)** Behavior during the extinction test (Ext Test). Stimulating the LPO with hM3dq and CNO increased active hole, but not inactive hole responding (group x day interaction: $F_{1,14} = 17.05$, 3.34, $P < 0.001$, $P = 0.089$, respectively) relative to aCSF control and the average of the last three days of extinction (Ext Pre). There was no effect on locomotion ($F_{1,14} = 2.46$, $P = 0.14$). Symbols are mean ± SEM for each group; lines are individual subjects. See main text for more detailed statistics.

Figure 2.6 Pharmacological Stimulation of the LPO Promotes Sucrose Seeking, but Does Not Modulate Sucrose Taking

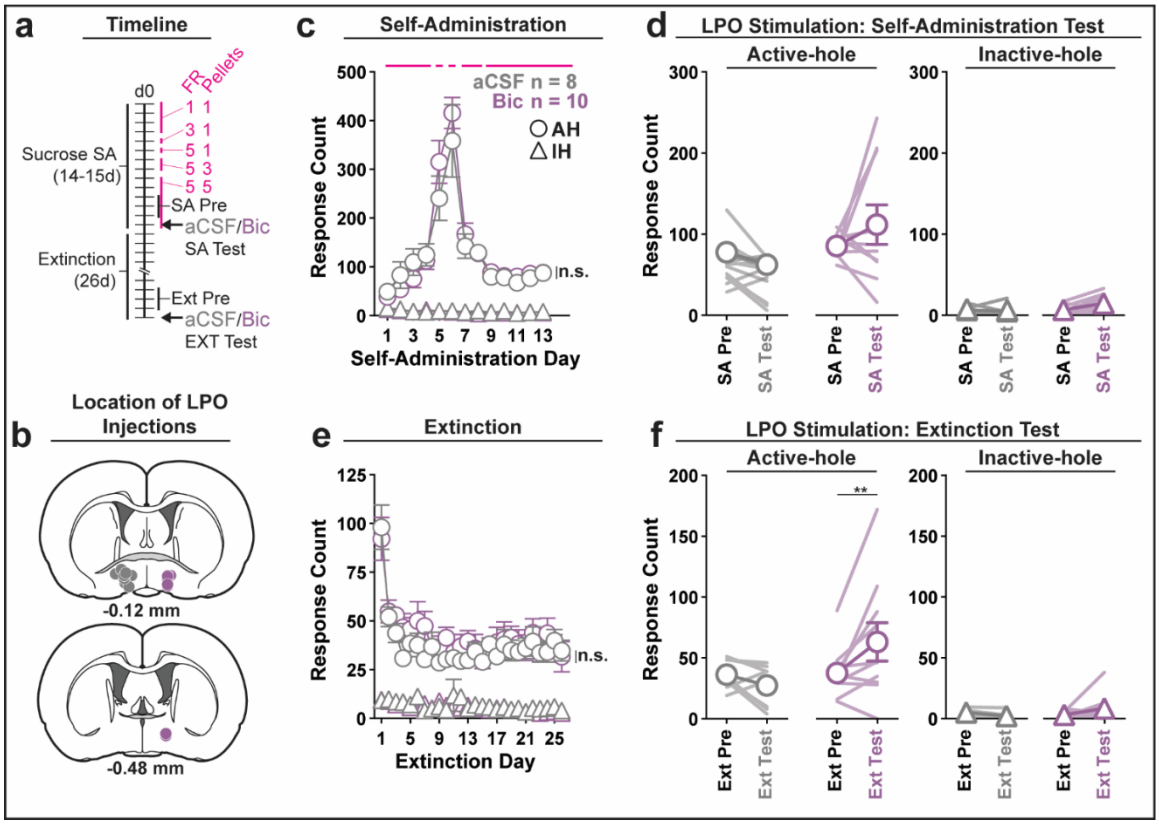

(a) Timeline of behavioral procedures. SA: self-administration; FR: fixed ratio (number of responses required to obtain one reward delivery, depicted with pink lines). Pellets: number of pellets obtained per reward delivery, depicted with pink lines. **(b)** Location of LPO injections for aCSF (grey) and bicuculline (Bic, purple). **(c)** Sucrose self-administration behavior. Both groups acquired sucrose self-administration and there was no difference between groups across self-administration or over the last three days of self-administration (SA Pre). Rats updated responding with changes in FR schedule and number of rewards per delivery. **(d)** Self-administration test (SA Test). Stimulating the LPO with bicuculline did not change active hole or inactive hole responding relative to aCSF controls. **(e)** Extinction behavior. Both groups extinguished responding on the previously active hole. There was no difference between groups across extinction or over the last 3 days of extinction (Ext Pre). **(f)** Extinction test (Ext Test). Stimulating the LPO with bicuculline reinstated sucrose seeking behavior, observed as increased responding on the previously active hole (HSD, $^{**}P < 0.01$) but not the inactive hole (HSD, $P = 1.00$). Symbols are mean ± SEM for each group; lines are individual subjects. See main text for detailed statistics.

Figure 2.7 Pharmacological Stimulation of the LPO Promotes Sucrose Seeking, but Does Not Modulate Sucrose Taking (Details)

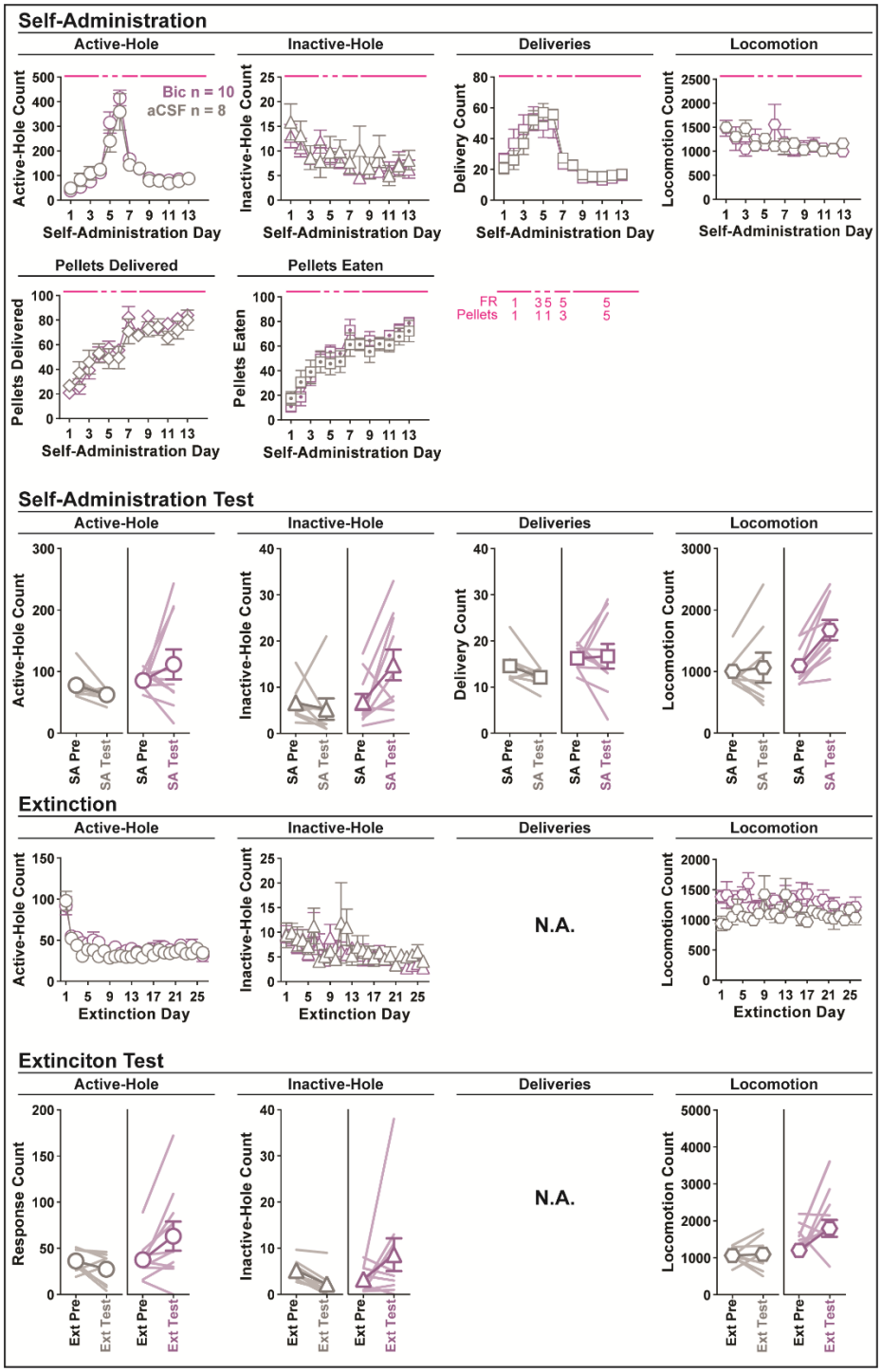

(1st row) Behavior during sucrose self-administration (SA); FR: fixed ratio (number of responses required to obtain reward, depicted with pink lines); Pellets: number of pellets

obtained per reward delivery, (also depicted with pink lines). From left to right, active hole responding, inactive hole responding, delivery counts, pellets delivered, and pellets eaten. **(2nd row)** Behavior during the self-administration test (SA Test). Stimulating the LPO with bicuculline did not change active hole responding, delivery counts, or locomotion (group x day interaction: $F_{1,16}$, $P > 0.087$ for all comparisons) relative to aCSF control and the last three days of self-administration (SA Pre). Stimulating the LPO with bicuculline increased inactive hole responding ($F_{1,16} = 5.55$, $P = 0.032$).
(3rd row) Behavior during the extinction phase. From left to right: active hole responding, inactive hole responding, and locomotion. **(4th row)** Behavior during the extinction test (Ext Test). Stimulating the LPO with bicuculline increased active hole, inactive hole responding, and locomotion (group x day interaction: $F_{1,16} = 6.91, 4.57, 6.81$, $P = 0.018, 0.048, 0.019$ respectively) relative to aCSF control and the average of the last three days of extinction (Ext Pre). Symbols are mean ± SEM for each group; lines are individual subjects. See main text for detailed statistics.

Figure 2.8 Pharmacological Manipulation of the LPO Disrupts the Reduction in Self-Administration After Punishment

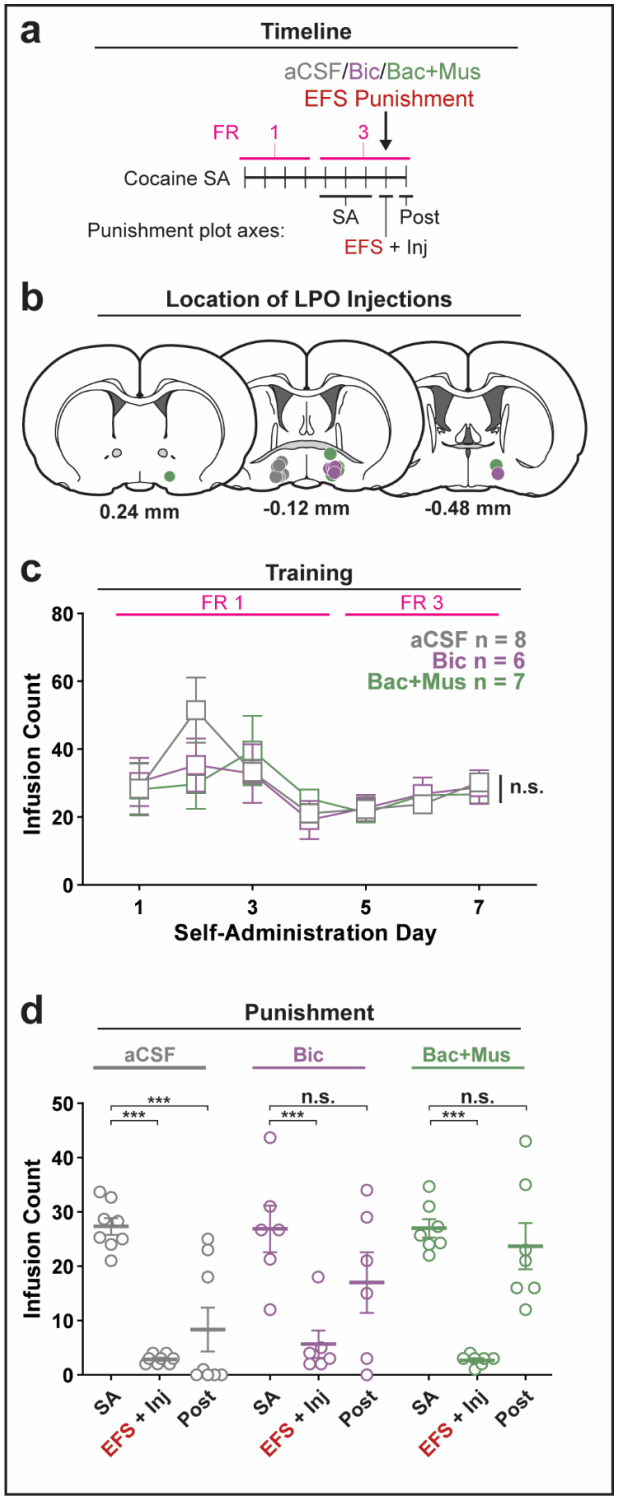

(a) Timeline of behavioral procedures (SA: self-administration); FR: fixed ratio (number of responses required to obtain one cocaine infusion, depicted with pink line). **(b)** Location of LPO injections for aCSF (grey), bicuculline (Bic, purple), and baclofen + muscimol (Bac+Mus, green). **(c)** Cocaine self-administration behavior, data are mean ± SEM of each group. There was no difference between groups across self-administration or over the last three days of self-administration (SA). **(d)** Behavior during punishment. Circles are individual subjects; horizontal lines are means ± SEM of each group. During footshock (EFS) punishment, all groups decreased the number of infusions relative to pre punishment (SA) (all HSD comparisons, Ps < 0.001), and this occurred to a similar extent in animals receiving aCSF, bicuculline or baclofen + muscimol. On the day following punishment (Post), only the aCSF group remained significantly below baseline intake (HSD, aCSF: ***P < 0.001), whereas the other groups returned to pre-baseline intake (HSD, Bic: P = 0.20; Bac+Mus: P = 0.99).

Figure 2.9 Pharmacological Manipulation of the LPO Disrupts the Reduction in Self-Administration After Punishment (Details)

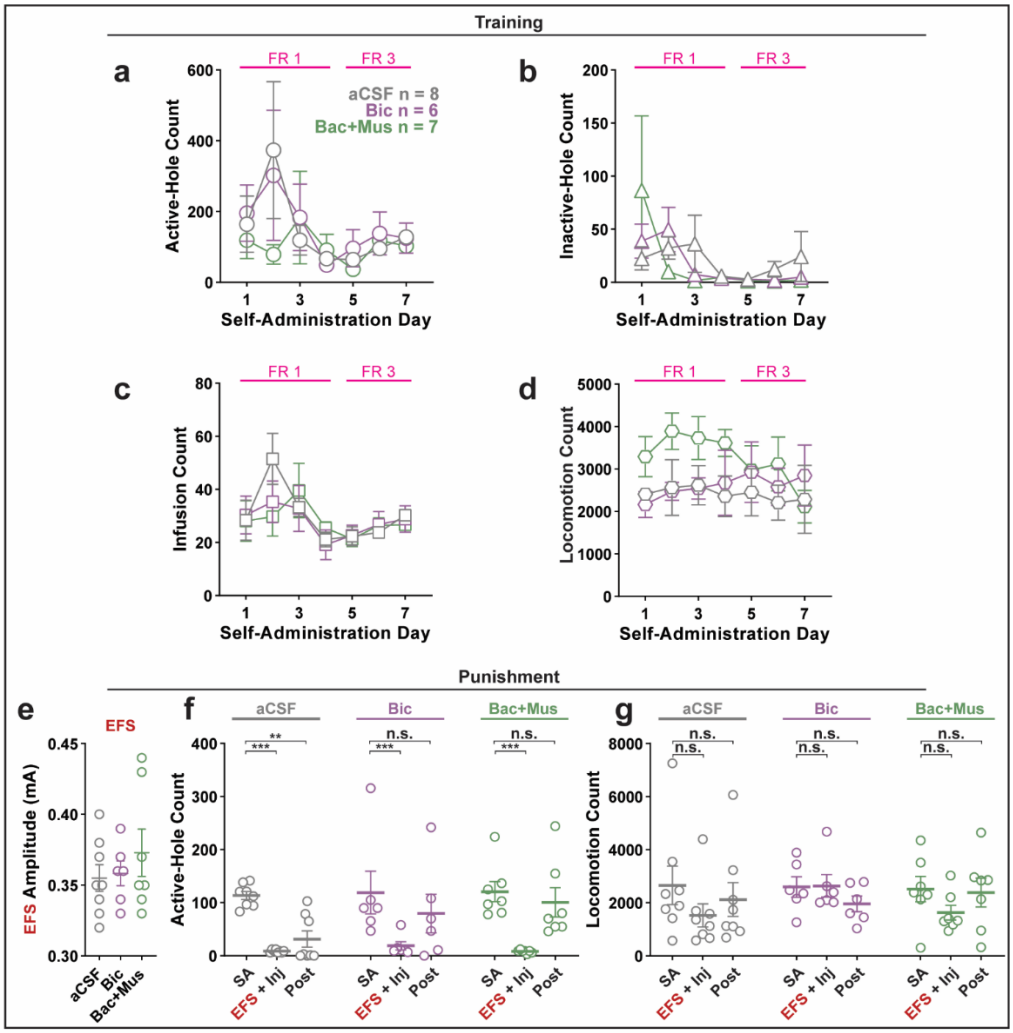

(a-d) Behavior during cocaine self-administration (SA); FR: fixed ratio (number of responses required to obtain one cocaine infusion). **(a)** active-hole responding, **(b)** inactive-hole responding, **(c)** infusions, and **(d)** locomotion. **(e)** Amplitudes of electric footshock (mA) given to each rat and group averages. **(f-g)** Behavior before punishment (SA), during punishment (EFS + Inj) and after punishment (Post). **(f)** Active hole responding. Punishment suppressed responding in all groups; after punishment, only animals microinjected with aCSF remained below baseline responding whereas those receiving bicuculline or baclofen + muscimol returned to pre-punishment levels (HSD, *** $P < 0.001$, **$P < 0.01$). **(g)** Locomotion: there were no effects of microinjections or punishment on locomotion. For a-d, symbols are mean ± SEM for each group; for e-g horizontal lines mean ± SEM for each group and circles are individual subjects. See main text for detailed statistics.

Figure 2.10 Pharmacological Stimulation of the LPO Modulates Firing of VTA Neurons

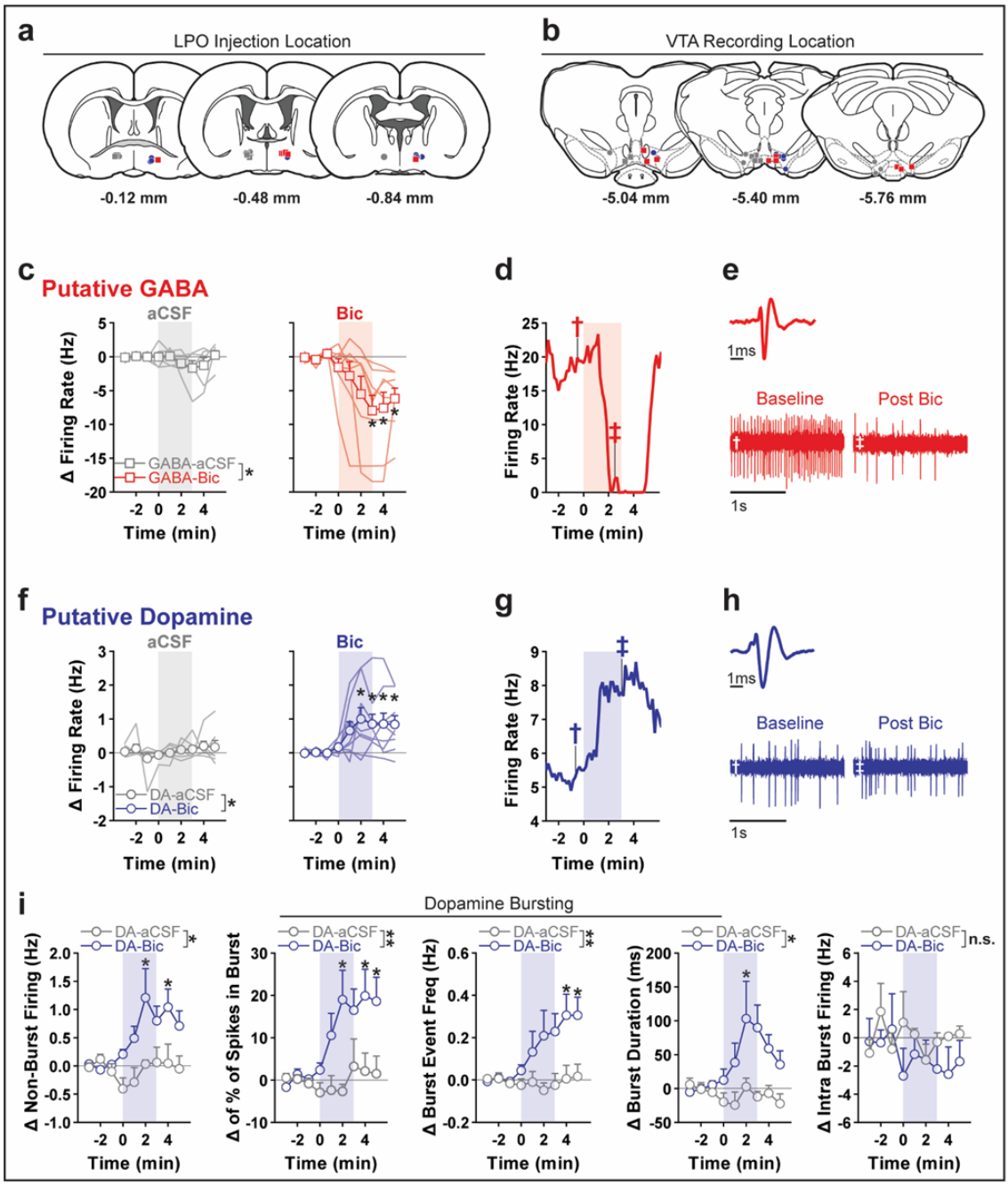

(a) Location of LPO injections: aCSF (grey), bicuculline (Bic, red for VTA_{GABA} and blue for $VTA_{Dopamine}$), during recordings of VTA_{GABA} neurons (squares) or dopamine neurons (circles). **(b)** Locations of $VTA_{Dopamine}$ (circles) and VTA_{GABA} (squares) neurons within the VTA. Color indicates corresponding intra-LPO injection: aCSF (grey), bicuculline (Bic, red for VTA_{GABA} and blue for $VTA_{Dopamine}$ neurons). **(c)** Firing in VTA_{GABA} neurons (delta from baseline) before and after the administration of aCSF (grey) or bicuculline (Bic, red).

Time is relative to onset of 3-minute microinjection; each point represents the mean ± SEM values of each group. Stimulating the LPO with bicuculline decreased firing in VTA_{GABA} neurons relative to aCSF control and baseline (pre-injection) activity (group x time interaction: $F_{8,96} = 3.29$, P = 0.0023, HSD, *P<0.05 compared with all pre-injection time-points). **(d)** Representative firing rate in a VTA_{GABA} neuron. There was substantial decrease in firing rate throughout injection and following. **(e)** Average waveform and recording traces for the neuron shown in (d). Symbols denote the time period from which each trace was obtained. **(f)** Firing in $VTA_{Dopamine}$ neuron (delta from baseline) before and after the administration of aCSF (grey) or bicuculline (Bic, blue). Time is relative to onset of the 3-minute microinjection; each point represents the mean ± SEM values of each group. Stimulating the LPO with bicuculline increased the firing rate of $VTA_{Dopamine}$ neurons, relative to aCSF control and baseline (pre-injection) activity (group x time interaction: $F_{8,122} = 2.87$, P = 0.0060, HSD, *P<0.05 compared with all pre-injection time-points). **(g)** Representative firing rate in a $VTA_{Dopamine}$ neuron. There was an increase in firing rate throughout the injection and following. **(h)** Average waveform and recording traces for the neuron shown in in (g). Symbols denote the time period from which each trace was obtained. **(i)** Burst characteristics of $VTA_{Dopamine}$ neurons before and after the administration of aCSF or Bic (delta from baseline) for non-burst frequency (Hz), (% of spikes emitted in bursts, burst event frequency (Hz), burst duration (ms), and intra burst frequency (Hz); (HSD, *P < 0.05 compared with all pre injection time-bins). Symbols are mean ± SEM for each group; lines are individual subjects. See main text for detailed statistics.

Chapter 3: The Lateral Preoptic Area and the LPO Projection to the VTA Regulates VTA Neuron Activity and Drives Paradoxical Reward Behaviors

This chapter is a draft of a manuscript to be submitted in December 2019. Authors: Adam Gordon-Fennell, Lydia Gordon-Fennell, and Michela Marinelli.

Author contributions: A.G., and M.M. designed experiments; A.G. conducted behavioral and electrophysiological experiments; L.G. performed *in-situ* hybridization, confocal imaging, and histological mapping; A.G. and M.M performed analysis for publication; A.G. prepared figures; A.G. and M.M. drafted manuscript. A.G., M.M., and L.G., edited and revised manuscript.

3.1 ABSTRACT

The ventral tegmental area (VTA) underlies motivation and reinforcement of natural rewards. The lateral preoptic area (LPO) is an anterior hypothalamic brain region that sends direct glutamate and GABA projections to the VTA and to other brain structures known to regulate VTA activity. This positions the LPO to regulate the activity of VTA neurons and the motivational behaviors the VTA underlies. Here we investigated the functional connection between the LPO and subpopulations of VTA neurons and explored the reinforcing and valence qualities of the LPO in rats. Using in-situ hybridization and retrograde tracing, we found that the LPO projection to the VTA contains a greater proportion of GABA than glutamate. We measured the effect of stimulating the LPO cell bodies and the LPO→VTA pathway *in-vivo* and found that both inhibited VTA_{GABA} neurons and had a mixed effect on $VTA_{dopamine}$ neurons. We next assessed the reinforcing and valence qualities of the LPO and LPO→VTA pathway using optogenetics and found that stimulating the LPO supports operant responding under both fixed-ratio and progressive-ratio schedules. The same rats also displayed avoidance of LPO stimulation

during a real-time place preference assay but also displayed heightened reinforcement to enter the paired compartment. Finally, we recorded the LPO using fiber photometry, and found that the LPO signals to aversive events but not rewarding events. These results demonstrate that the LPO modulates the activity of the VTA and drives motivated behavior and indicates that the LPO may drive the reinstatement observed in chapter 2 through enhancing reinforcement.

Illustration 3.1: Visual abstract of chapter 3

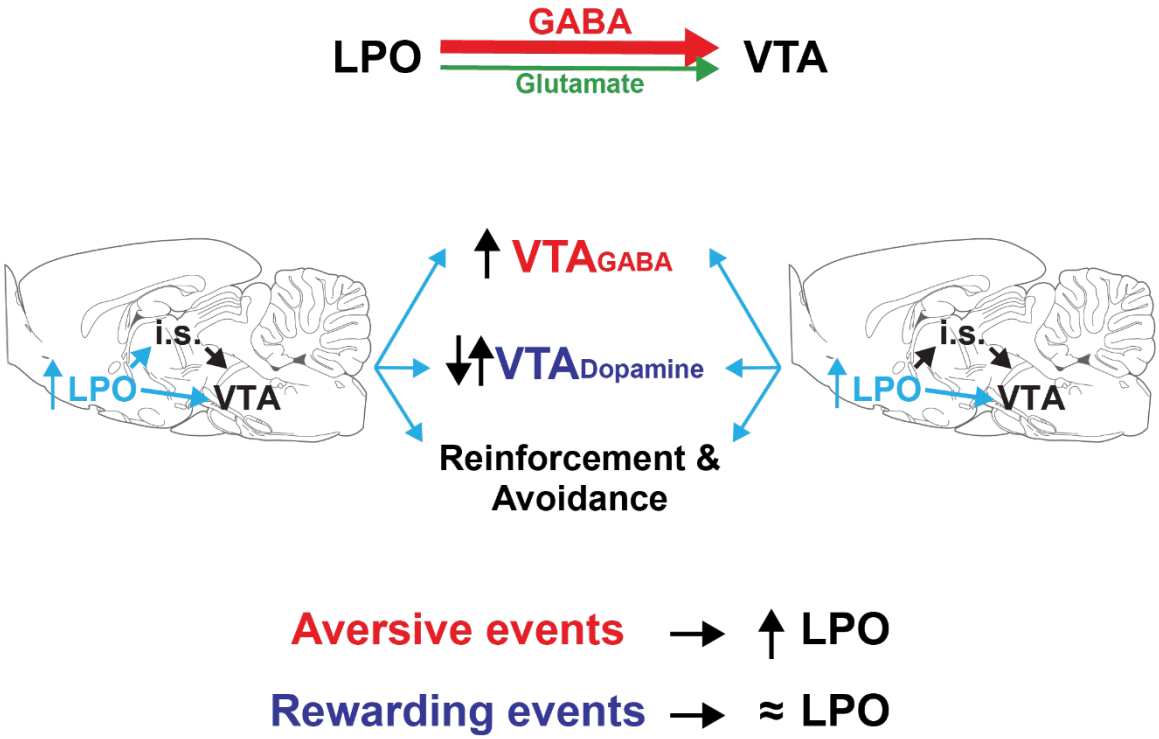

Abbreviations, symbols, and colors: LPO: lateral preoptic area; VTA: ventral tegmental area; i.s.: intermediary brain structures; dark blue: dopamine; red: GABA; green: glutamate; light blue: stimulation

3.2 INTRODUCTION

The lateral preoptic area (LPO) is an understudied region of the hypothalamus that is deeply interconnected with the brain reward system. The LPO contains GABA and glutamate neurons that project to numerous brain regions known to be important regulators of reward, including projections to the lateral habenula, rostromedial tegmental nucleus, and a direct projection to the ventral tegmental area (VTA) (Phillipson, 1979; Kalló et al., 2015; Yetnikoff et al., 2015). The VTA contains dopamine, GABA, glutamate, and dual-expressing populations (Barker et al., 2016; Root et al., 2016; Barker et al., 2017), and sends a broad output throughout the limbic forebrain (Matsuda et al., 2009; Russo and Nestler, 2013; Aransay et al., 2015; Barker et al., 2016). $VTA_{Dopamine}$ neurons are important mediators of motivated behaviors (Ikemoto and Panksepp, 1999), thus it is possible that through connections with the VTA, the LPO may to regulate reward.

Activity within the LPO fluctuates with rewarding and aversive events and manipulating the LPO drives can drive both reward and aversion. For example, LPO neurons show a mixture of no effects, including increased and decreased firing rates in response to both rewarding and aversive events (Ono et al., 1986). Furthermore, LPO neurons exhibit increased cfos expression following several aversive events including but not limited to restraint stress (Chen and Herbert, 1995; Briski and Gillen, 2001), auditory distress (Campeau and Watson, 1997), and social defeat (Martinez et al., 1998; Chung et al., 2000). Studies also determined that the LPO can contribute to affective valence: stimulating the LPO with bicuculine leads to conditioned place preference (Reichard et al., 2019a), and stimulating the GABAergic projection from the LPO to the lateral habenula produces real-time place preference, whereas stimulating the glutamatergic projection produces real-time place aversion (Barker et al., 2017). Other work has found that blocking synaptic inputs to the LPO exacerbates the increase in plasma corticostrone produced by

restraint stress (Duarte et al., 2017). Finally, work from our lab indicates that stimulating the LPO with bicuculine precipitates reinstatement of reward seeking behaviors. Altogether, the literature indicates that the LPO is interconnected with reward systems, regulated by reward and aversive events, and plays a causal role in reward and stress responses.

Given the complexity of mixed connections between the LPO and reward structures, it is unclear how activity in the LPO is related to activity in the VTA. Our previous study (chapter 2 of this dissertation) found that stimulating the LPO with bicuculline enhances the activity of $VTA_{Dopamine}$ neurons and inhibits the activity of VTA_{GABA} neurons. However, it is unclear if the direct connection between the LPO and or if connections with intermediary structures underlie these effects. Furthermore, the diversity of behavioral responses produced by stimulating the LPO, including both rewarding and aversive responses (Barker et al., 2017; Reichard et al., 2019a), makes it unclear how activity within the LPO is causally related to reward and aversion behavior. Finally, the mixture of the single cell firing responses of LPO neurons to rewarding and aversive events makes it unclear how the LPO signals in response to these events at the population level. To answer these questions, we used in vivo optogenetics to measure the functional connectivity between the LPO and subpopulations of neurons in the VTA. We then used optogenetic stimulation to study the reinforcing properties of stimulating the LPO using intracranial self-stimulation (ICSS); we also measured the valence properties of stimulating the LPO using real-time place testing (RTPT) procedures. Finally, in order to determine if the LPO naturally signals in response to rewarding or aversive events at the population level, we recorded calcium signals of the LPO using fiber photometry during rewarding and aversive Pavlovian conditioning.

3.3 METHODS

3.3.1 Subjects

Male Sprague Dawley rats were acquired from Harlan and housed 2-3 per cage and were housed on a reverse 12h dark-light cycle with *ad libitum* access to water and laboratory chow (LabDiet, St. Louis, MO, cat#: 5053). Rats weighed between 250-300g upon arrival. All experiments were completed during the rat's dark cycle. Procedures were done in accordance with The National Institutes of Health Guide for the Care and Use of Laboratory Animals and were approved by the Institutional Animal Care and Use Committee of The University of Texas at Austin.

3.3.2 Drugs and Viral Vectors

The following drugs were obtained from Henry Schein (Dublin, OH): isoflurane (cat#: 1169567762), 0.9% saline (cat#: 002477), flunixin meglumine (cat#: 049622), and cefazolin (cat#: 1026761). The following drugs were obtained from Sigma-Aldrich (St. Louis, MO): phosphate buffered saline (PBS, cat#: P3813), sucrose (cat#: S7903), paraformaldehyde (cat#: 158127), and fast green (cat#: F7252). From Purdue Products L.P (Stamford, CT), we obtained Betadine (cat#: 67618-155-32). From Thermo Fisher Scientific (Waltham, MA), we obtained Magnesium- and calcium-free PBS (cat#: 10010023).

The following panneuronal adeno-associated viral vectors were obtained from UNC Viral Vector Core: AAV5/hsyn-ChR2(E123A)-eYFP (titer: 3.7e12 or 5.3e12); AAV5/hsyn-eNpHR3.0-eYFP (titer: 5e12); rAAV5_hSyn-GCaMP6f (titer: 5.43e12); AAV5/hsyn-mCherry (titer: 4.8e12, or 2.5e12). From the same location, we obtained the cre-dependent vector, rAAV5/EF1a-DIO-hChR2/(H134R)-eYFP (titer: 5e12). All vectors were aliquoted and stored at -80°C upon arrival. Prior to injections, aliquots were removed

from the freezer, stored at 4°C, and used within 1 week of thawing. For the AAV5/hsyn-eNpHR3.0-eYFP behavioral experiment, the vector was diluted to 1:4 in aCSF prior to use.

From Institut de Génétique Moléculaire de Montpellier, we obtained the retrograde vector, CAV-2 Cre (promoter: CMV + SV40 polyA tail; titer: 1.25e13) and it was diluted 1:10 in magnesium- and calcium-free PBS (final titer: 1.25e12), aliquoted at 5μL, and refrozen at -80°C. On the day of injection surgeries, aliquots were removed from the freezer and were used within 12h of thawing.

3.3.3 Surgical Procedures

For all electrophysiology recordings and surgical procedures, anesthesia was induced by placing rats in an induction chamber (E-Z Anesthesia, Palmer, PA) filled with 5% isoflurane. Following induction, rats were transferred to a stereotaxic apparatus (David Kopf Instruments, Tujunga, CA, cat#: 902) and connected to a stereotaxic breather (E-Z Anesthesia, Palmer, PA) that delivered 2-2.5% isoflurane regulated by a vaporizer (E-Z Anesthesia, Palmer, PA). Throughout surgery, we monitored breathing rate and pinch reflex, and adjusted the level of isoflurane anesthesia when necessary. For electrophysiology experiments, body temperature was recorded with a rectal probe and maintained by a heating pad (Kent Scientific, Torrington, CT, or Fintronics Inc., Orange, CT).

During surgery and the day following surgery, rat received an injection of analgesic (flunixin meglumine, 5mg/kg/mL, s.c.) and antibiotic (cefazolin, 100mg/kg/mL, s.c.). In a small number of cases, on the day following surgery, no antibiotic was provided (16 out of 145 rats) and/or lower dose of analgesic was provided (28 out of 145 rats; flunixin meglumine, 2.5mg/kg/mL, s.c.).

3.3.3.1 General Surgical Procedures

For all electrophysiology recordings and surgical procedures, anesthesia was induced by placing rats in an induction chamber (E-Z Anesthesia, Palmer, PA) filled with 5% isoflurane. Following induction, rats were transferred to a stereotaxic apparatus (David Kopf Instruments, Tujunga, CA, cat#: 902) and connected to a stereotaxic breather (E-Z Anesthesia, Palmer, PA) that delivered 2-2.5% isoflurane regulated by a vaporizer (E-Z Anesthesia, Palmer, PA). Throughout surgery, we monitored breathing rate and pinch reflex, and adjusted the level of isoflurane anesthesia when necessary. For electrophysiology experiments, body temperature was recorded with a rectal probe and maintained by a heating pad (Kent Scientific, Torrington, CT, or Fintronics Inc., Orange, CT).

During surgery and the day following surgery, rat received an injection of analgesic (flunixin meglumine, 5mg/kg/mL, s.c.) and antibiotic (cefazolin, 100mg/kg/mL, s.c.). In a small number of cases, on the day following surgery, no antibiotic was provided (16 out of 145 rats) and/or lower dose of analgesic was provided (28 out of 145 rats; flunixin meglumine, 2.5mg/kg/mL, s.c.).

3.3.3.2 Viral Injection

Rat heads were shaved with clippers (#) and cleaned with 10% betadine. The scalp was injected with local anesthetic (2% mepivicain), a scalpel incision was made, the tissue was gently removed, and the skull was leveled by adjusting the incisor bar. A small bur hole was made overlaying the injection target and the dura at the site was removed. The stereotaxic arm was angled at 18° for targeting the LPO (final coordinate in mm: AP: -0.12, ML: -1.4, DV: -8.6, relative to bregma) and 10° for targeting the VTA (final coordinate in mm: AP: -5.4, ML: -0.6, DV: -8.3, relative to bregma). At the conclusion of

viral injection surgeries, the incision was closed with surgical staples (Braintree Scientific, Inc, Braintree, MA, cat#: ACS APL, EZC CS) and covered in antibiotic ointment (Medique Products, Fort Myers, FL, cat#: 22373).

For behavioral experiments, viral constructs were injected using, a pulled glass pipette (~30μm inner tip diameter) coupled to a Nanoject II (cat#, manufacture, location) that was lowered into the target brain region and allowed to rest in place for a 1-5min pre-injection wait period. A total of 165.6-179.4nL of viral construct was injected over the course of 5-10min, which was then followed by a 5-10min post-injection wait period to allow for diffusion before slowly retracting the injection pipette.

For the combinatorial LPO→VTA optogenetic electrophysiology experiment, we used the protocol above to inject the VTA with 500nL of CAV-2 Cre over 10min and the LPO with 303.6nL of DIO-ChR2 over 11min. Injections were performed serially over a single surgery session. Using this procedure, all neurons that project to the VTA will express cre, and only LPO neurons that project to the VTA will express ChR2.

For LPO optogenetic electrophysiology experiments, we either injected using the protocol above or, in a small number of cases (16 out of 145 rats), using a 30G injection cannula coupled to a 5uL syringe (Hamilton) driven by a microinjection pump (Harvard Apparatus, Holliston, MA). In these cases, there was no pre-infusion wait period, only a 300-500nL injection over 4-6m and a post infusion wait period of 5-7min. Later, we employed a Nanoject in order to improve accuracy of targeting and reduce viral spread. In a small subset of LPO ChR2 VTA recording experiments, we injected rats with a 1:1 cocktail of ChR2 and hM3Dq. The data from these recordings did not differ from data collected with ChR2 expression alone, therefore they were pooled. Importantly, no neurons were included post hM3Dq activation via clozapine-n-oxide (CNO, NIDA Drug Supply Program). For experiments validating ChR2 mediated stimulation in the LPO, rats received

an intra-LPO injection with a vector cocktail of 3:5 ChR2 and hM3Dq. This cocktail of ChR2 and hM3Dq was used to validate hM3Dq-mediated excitation for another project (chapter 2 of this dissertation); however, all illumination-driven responses reported in this chapter were recorded prior to local CNO administration, and all neurons were at >30min after and >300µm away from local injection of 30-60nL CNO.

3.3.3.3 Fiber Implantation

For rats undergoing optogenetic behavioral experiments, immediately following the viral injection, we implanted an ~8mm 200µm 0.39NA fiber (Thorlabs, Newton, NJ, cat#: FT200UMT) attached to a 1.25mm stainless steel ferrule (Thorlabs, cat#: SF440, or Senko, cat#: ZRS-25-114) 0.3-0.6mm above the viral injection site. For rats undergoing calcium recording, we implanted an 8mm 400µm 0.48NA fiber attached to a 2.5mm stainless steel ferrule (Doric Lenses Inc, Québec, Canada, cat#: MFC_400/430-0.48_8mm_FLT) 0.3mm above the viral injection site. Fibers were fixed to skull screws with a metabond epoxy layer (Parkell Inc., Edgewood, NY, cat#: S380) covered with a dental cement epoxy layer (Coltène/Whaledent Inc., Cuyahoga Falls, OH, cat#: H00325). Fibers were covered with custom-made ferrule covers composed of melted pipette tips or 3D-printed caps fixed to ceramic ferrule sleeves. Transmission rates were recorded for all fibers prior to implantation and values were used to accurately set light power for each rat to achieve desired power at the fiber tip.

3.3.4 Optogenetic Stimulation and Inhibition

For behavioral experiments, rats were attached to a metal sheathed 200µm patch cord via a stainless steel 1.25mm ferrule (Thorlabs, Newton, NJ, cat#: FT200UMT-Custom) that was coupled to a fiber optic rotary joint (Doric Lenses Inc., Québec, Canada,

cat#: FRJ_1x1_FC-FC or FRJ_1x2i_FC-FC). Experiments involving ChR2 stimulation, the rotary joint was coupled to a 450nm laser diode (Doric Lenses Inc., Québec, Canada, cat#: LDFLS_450/075_450/075_450/075_450/075) that was under TTL control; light pulses were driven by Doric Neuroscience Studio (Doric Lenses Inc., Québec, Canada, version 5.2.2.3) and were delivered at 15-20mW (measured at the fiber tip), 5ms duration, and at 20-40 Hz, with variable train durations. For experiments involving HR inhibition, the rotary joint was coupled to a 520nm laser diode (Doric Lenses Inc., Québec, Canada, cat#: LDFLS_520/060_520/060_520/060_520/060) that was under TTL control; continuous illumination, 10-12mW (measured at the fiber tip) was driven by Doric Neuroscience Studio (Doric Lenses Inc., Québec, Canada, version 5.2.2.3).

For electrophysiology experiments, optrodes composed of a recording pipette (details below) and 200μm fiber (Thorlabs, Newton, NJ, cat#: FT200UMT) were coupled to either a 450nm or 520nm laser diode (details above) or a 473nm diode-pumped solid state laser (DPSS) (Laser Glow, Toronto, ON, cat#: LD-WL206). For laser diodes and DPSS, we used Doric Neuroscience Studio and a pulse train generator (Prizmatix, Israel, cat#: Pulser), respectively, to control pulse parameters and timing.

3.3.5 Behavioral Procedures

3.3.5.1 Intracranial self-stimulation (ICSS)

To determine the reinforcement properties of stimulation of the LPO and LPO→VTA pathway, rats were tested with ICSS procedures. Rats were placed in an operant chamber (Med Associates, Fairfax, VT, cat#: CT-ENV-007-VP-X) outfitted with two nose-holes (Med Associates, Fairfax, VT, cat#: ENV-114BM) and three locomotion infrared beam detectors (Med Associates, Fairfax, VT, cat#: ENV-253SD). Nose pokes into the “active-hole” triggered a delivery of 15mW, 40Hz, 5ms pulses into the LPO, along

with a simultaneous light cue inside the active-hole. The duration of the stimulation/cue differed depending on the experiment. Responses during stimulation periods were tracked but did not count towards earning an additional stimulation. Nose pokes into the "inactive-hole" had no consequences and served as a measure of non-goal-directed behavior. Throughout the session, the number and timing of active-hole, inactive-hole, and locomotion beam break events were recorded via MED-PC IV (Med Associates, Fairfax, VT, cat#:ENV-114BM). Prior to ICSS, rats were habituated to optic fiber coupling for at least 2 days.

To determine if LPO stimulation or inhibition is reinforcing, rats were tested for ICSS in 60min daily sessions, on a fixed-ratio 1 schedule (1 reward / 1 response) with 1s illumination per reward. The number of sessions differed based on the experiment. To determine if rats are highly motivated to obtain LPO stimulation, a subset of rats moved from a fixed-ratio schedule to a within-session progressive-ratio procedure, where the cost for each reward increased in a semilogorithmic fashion (Figure 3.7g). Progressive-ratio sessions lasted for 6h or until subjects did not earn a stimulation for over 1h. To determine if there is a duration at which LPO stimulation becomes aversive, the duration of the stimulation was progressively increased from 1s to 300s every other day (e.g. day 1: 1s, day 2: 1s, day 3: 3s, etc.). During progressive-ratio sessions we tracked the break point (last cost subjects paid for reward), in addition to the variables listed above.

3.3.5.2 Real-time Place Testing (RTPT)

To determine the valence of stimulating or inhibiting the LPO and LPO→VTA pathway, we tested rats in a RTPT task where rats could freely control the inter-stimulation-interval and the stimulation-interval. Prior to RTPT, rats were habituated to optic fiber coupling for at least 2 days. RTPT procedures were conducted in a custom made 2-chamber

opaque Plexiglas apparatus (dimensions: 24in x 12in x 12in), where rats were tracked online using Ethovision XT (Noldus Information Technology, Wageningen, Netherlands, version 10.0.828), enabling a closed-loop stimulation protocol based on the rat's position in the apparatus. On day 1 (habituation (Hab)), rats were placed for 10 min into the apparatus that had identical textured floors on each side of the apparatus. This session served as a habituation day to acclimate the rats to handling and connecting them to the patch chord. On day 2 (preference test (PT)), rats were placed into the same apparatus but with a novel floor texture that was maintained throughout the remainder of the experiment. The preference test and all subsequent sessions were 20min in duration. Aside from receiving laser stimulation, both sides of the chamber were identical. On days 3-5 or 3-6 (initial pairing (Int)), one side of the box was assigned to be the *initially paired side*. Assignments were made for each rat individually to minimize the baseline bias of each group towards the initially paired side. During the initial pairing, rats received laser stimulation any time their center point was detected in the initially paired side; stimulation ceased the moment the center point was detected in the initially unpaired side. On days 6-8 or 7-10 (inverted paring (Inv)), laser pairing was inverted from the initial pairing, so that the initially unpaired side now triggered stimulation and the initially paired side no longer did. This allowed us to observe a change in side preference with the change in laser-pairing contingency. To quantify the amount of preference or aversion associated with stimulation, we calculated an RTPT score by subtracting the mean time spent in the initially paired side during the initial pairing and inverted pairing conditions, and dividing by the session duration (RTPT score = (mean (initially paired side Int) – mean (initially paired side Inv)) / session duration. This produces a score between -1 and 1, where -1 is maximal aversion, 1 is maximal preference, and 0 is no valence. Stimulation parameters varied across experiments, see main text for details.

3.3.5.3 RTPT with progressive adversity

To determine the reinforcing properties of stimulating the LPO and LPO→VTA pathway within the RTPT procedure, we tested rats in a modified RTPT procedure in which the optically paired side was also paired with adversity (electricity). Rats were tested as outlined above (habituation, preference test, and 4 days of initial laser pairing) but in a med associates chamber (cat#: CT-ENV-007-VP-X, dimensions: 11.625in x 9.78in x 7.35in) where one side of the apparatus had a floor consisting of metal bars and the other had a floor consisting of Plexiglas. In this experiment, initial pairing was assigned to the side of the chamber with metal bars for all subjects regardless of baseline preference. The laser illumination pattern was 40Hz, 5ms pulses, 15mW, 3s trains, and 3s ITI. After initial pairing, subjects were tested for 13 additional days where we applied electricity to side of the chamber with metal bars, which continued to be paired with optical stimulation. The electric footshock amplitude was progressively increased across the first three days (0.05mA, 0.10mA, 0.15mA), maintained at 0.15mA for the next eight days, and then stepped back down for the last three days (0.13 mA, 0.10 mA, 0.08 mA) (Figure 3.24b). To quantify the reinforcing properties of laser stimulation, we measured the amount of time spent in both sides of the chamber, the number of crossings into the paired side that resulted in a visit of greater than 3s. We used a minimum visit of 3s because this ensure that rats received illumination within the illumination pattern (3s train, 3s ITI).

3.3.5.4 Pavlovian Conditioning for Sucrose

To determine if the LPO has time-locked signals to rewarding events and predictive cues, rats were ran through Pavlovian conditioning for sucrose. Prior to training, rats went through 4 days of food port habituation in which 5 sucrose pellets (45mg, Bioserv, Flemington, NJ, cat#: F06233) were provided in the port before rats were placed into a

conditioning chamber (Med Associates, Fairfax, VT, cat#: CT-ENV-007-VP-X). Food port training sessions were 20 minutes, all subsequent sessions were 60 minutes. The first procedure rats underwent was concurrent magazine training and presentation of a tone cue over 6 days (Preconditioning). During this phase 30 pellets were delivered by magazine and 30 tone cues (10s, 3 kHz, 76 dB) were presented on independent 60-120s pseudorandom inter-trial intervals (Figure 3.29b). The latency from magazine delivery to port entry was tracked and analyzed to determine when rats learned the association between the sound of the magazine delivering the pellet and the presence of a pellet in the port. After magazine and tone cue preconditioning, rats were tested in one session for the response to pellet delivery in the absence of the tone cues (Magazine test) (Figure 3.29c). The following day, rats were tested in one session for the response to the tone cue in the absence of pellet delivery (Tone test) (Figure 3.29d). Next, rats were trained over 15 days of Pavlovian reward conditioning, where 30 10s tone cues were paired with pellets delivered at the tone offset (trace conditioning), that were presented on 70-110s pseudorandom inter-trial intervals (Figure 3.29e). Learning was monitored by measuring the number of food-port entries during the tone cue and the 10s period immediately prior to cue onset. Finally, rats went through three days of Pavlovian conditioning where 80% of trails occurred as normal (expected), 10% of trails occurred without tone delivery (unexpected) and 10% of trails occurred without pellet delivery (omission) (Figure 3.29f). Calcium signals in the LPO were recorded during the following sessions: first day of preconditioning; cue test; magazine test; first day and last 3 days of Pavlovian conditioning; 3 days of Pavlovian conditioning with expected, unexpected, and omission conditions (Figure 3.29a).

3.3.5.5 Pavlovian Conditioning for Footshock

Following Pavlovian conditioning for sucrose, rats were tested in a novel, fear conditioning chamber (Noldus Information Technology, Wageningen, Netherlands), where a 20s tone (5kHz, 74db) was paired with a 2s, coterminating electric footshock (0.7mA, scrambled) in a 20 minute session (Figure 3.29g). Rats were ran though one session per day for 3 days. Each session started with a 5min baseline period to allow rats to acclimate and to allow for baseline photo bleaching, followed by 5 tone/footshock pairings separated by a 100-140s random interval. Sessions were recorded using an analog camera and were digitized using Ethovision XT (Noldus Information Technology, Wageningen, Netherlands, version 10.0.828). On rare occurrences, the shock delivery malfunctioned and there was no indication that the subject received a shock; these trials were removed from the analysis. Calcium signals in the LPO were recorded during all 3 days of fear conditioning.

3.3.6 Extracellular Recording Procedures

3.3.6.1 General Procedures

Rats were anesthetized with isoflurane and mounted in a stereotaxic apparatus (David Kopf Instruments, Tujunga, CA, cat#: 902). Local anesthetic (2% Mepivicaine) was injected in the scalp, an incision was made, the tissue was removed, and the skull was leveled. A small bur hole was made overlaying the recording target, and the dura at the site was removed. The stereotaxic arm was angled at 18° for targeting the LPO (final coordinate: AP: -0.12, ML: -1.4, DV: -8.6, relative to bregma), and 0° for targeting the VTA (final coordinate: AP: -5.4, ML: -0.6, DV: -8.3, relative to bregma). Extracellular recordings were made using a glass pipette (WPI, Sarasota, FL, cat# 1B150F-4) pulled with a vertical puller (Narishige, Amityville, NY, cat#:PE-2) and broken back to an inner

diameter of 1-2µm and 1.5–2.1MOhms impedance, measured at 135Hz (Winston Electronics, St. Louis, MO, cat#:BL1000-B). The recording solution consisted of 2% fastgreen in 2M saline. Optrodes were built by fixing recording pipettes to 200µm optic fibers (Thorlabs, Newton, NJ, cat#: FT200UMT) using light curing epoxy (3M, Maplewood, MN, cat#: 35266 & 3920A1B). Optrodes were lowered slowly into the recording region using a hydrolic Microdrive (David Kopf Instruments, Tujunga, CA, cat#: 640). Extracellular voltage was amplified and band pass filtered (Fintronics Inc., Orange, CT), passed through a 50/60Hz noise filter (Quest Scientific, North Vancouver, BC), and then digitized and recorded using AxoScope (Molecular Devices, San Jose, CA, cat#: Digidata 1440A (digitizer) and version: 10.7 (software)) running on a PC. Voltage was also monitored on an oscilloscope (EZ Digital, Gwang-Ju City, South Korea, cat#: OS-5020A) and audio monitor (Grass Technologies, West Warwick, RI, cat#: AM10). The timing of optogenetic stimulation pulses was recorded via a TTL output that was fed from the laser into the digitizer. VTA neurons were classified as putative $VTA_{Dopamine}$ neurons based on established extracellular recording criteria: 1) firing rate between 1 and 10Hz; 2) triphasic (+/-/+) waveform ; 3) wide extra cellular waveforms (>2.4ms, measured from start to end of spike when using a 400-500Hz band-pass filter (Einhorn et al., 1988) and >1.1ms, from start to trough when using a 50-800Hz band-pass filter (Ungless and Grace, 2012; Marinelli and McCutcheon, 2014)). Using these criteria, are ~90% accurate at detecting neurons containing tyrosine hydroxylase (Ungless and Grace, 2012). VTA neurons were classified as putative VTA_{GABA} neurons when they failed to reach dopaminergic criteria. These neurons were often biphasic and exhibited high firing rates (>10Hz).

To measure baseline firing characteristics, all neurons were recorded for 2-3min prior to optogenetic manipulations that consisted of illumination to either the LPO or VTA. For ChR2, illuminations consisted of six 1s-long trains (40Hz, 5ms pulses) with a 9s inter

train interval (ITI). Stimulation power ranged from ~1-20mW (mean: 14.51; sd: 7.37) when delivered at the recording site, and 10-20mW (mean: 19.55; sd: 2.10) when delivered at a distant site. For stimulation at the recording site, power was decreased to minimize light artifacts. There was no effect of the stimulation power, so all data was pooled across power. For HR, illumination was a continuous 2mW pulse with varying durations (50ms, 1s, 10s, 60s). For all electrophysiology experiments with 1s manipulations, the effect of illumination was determined by binning the data into a 2s prior to illumination (Pre), 1s during illumination (Pulse), and 2s post illumination (Post) and expressing firing rate in Hz. For HR illumination of 10s and 60s, the Pre and Post bin durations equaled the length of the illumination. Binned firing rates were then expressed relative to baseline (the 10s preceding the first bin) in order to determine relative changes. Neurons were classified as having an effect using a paired *t*-Test of Pre vs Pulse firing over the six trains.

At the conclusion of recording, fast-green was deposited at the final pipette position using 28.6mA cathodal current (Fintronics Inc., Orange, CT, cat#: VL-1200 D) in order to back calculate the position of recorded cells (see histology section below for details).

3.3.6.2 LPO Functional Connectivity with the VTA

Rats received an injection of AAV5/hsyn-ChR2(E123A)-eYFP into the LPO, that was followed by an incubation period of >9wks to allow for adequate presynaptic ChR2 expression within the VTA. Neurons were recorded in the VTA during stimulation of the LPO cell bodies and LPO→VTA presynaptic terminals. In a separate experiment, the LPO→VTA pathway was isolated by injecting rAAV5/EF1a-DIO-hChR2(H134R)-eYFP into the LPO and CAV-2 Cre into the VTA. This was followed by an incubation period of >20wks to allow for adequate ChR2 expression. This combinatorial approach produced

expression of ChR2 only in LPO neurons that have presynaptic terminals within the VTA. Neurons were recorded in the VTA during LPO→VTA cell body stimulation.

3.3.6.3 Validation of ChR2 stimulation and HR inhibition

To validate ChR2-mediated excitation, rats received an injection of AAV5/hsyn-ChR2(E123A)-eYFP into the LPO that was followed by an incubation period of >8wks. Neurons were recorded in the LPO during LPO cell body illumination. Multiple illumination parameters were used to determine if LPO neurons are excited across parameters. First, 10ms pulses were delivered at 0.2-0.5Hz for 20 pulses. Neurons were classified as expressing ChR2 if they had <5ms average latency to spike, <2ms latency jitter (latency standard deviation), and >80% fidelity (number of spikes / number of pulses). To determine if trains of illumination drove excitation, neurons were also stimulated at high frequency trains (20 and 40Hz, 5ms pulses, 1s train, 9s inter-train interval).

To validate HR-mediated inhibition, rats received an injection of AAV5/hsyn-eNpHR3.0-EYFP into the LPO that was followed by an incubation period of >9wks. Neurons were recorded in the LPO during LPO cell body illumination. To ensure that illumination inhibited neurons across parameters, we delivered 2mW illumination over multiple durations (50ms, 1s, 10s, 60s). To determine if illumination inhibited firing rate and if the offset of illumination drove rebound stimulation, we analyzed the firing rate both during and after illumination.

3.3.7 Calcium Recording and Analysis

Calcium signals in the LPO were recorded using fiber photometry as adapted from Guaydin et. al. (Gunaydin et al., 2014). Rats were attached to a 1m metal sheathed 400µm 0.48NA patch chord coupled directly to a filter cube (Doric Lenses Inc., cat#: B340-1149).

GCaMP signals were monitored using a blue 465nm LED (Doric Lenses Inc., cat#: LEDC1-B_FC) sinusodially modulated at 208.62Hz with a mean fiber power of 30-50μw. Autofluorescent signals were monitored using a violet 405nm LED (Doric Lenses Inc., cat#: LEDC1-405_FC) modulated at 530.48Hz with a mean fiber power of 30-50μw. Fluorescence of both channels were detected on modified Newport femtowat detectors (Doric Lenses Inc., cat#: D490-1003) and demodulated using a fiber photometry console (Doric Lenses Inc., cat#: D460-2002). Signals were filtered with a low pass (12Hz) and were digitized at 1200 ksps.

The calcium and autofluorescent channels were processed post hoc using custom MATLAB and R scripts by taking 1s moving median on both channels, computing z-scores ($(x - \mu) / \sigma$), and then down-sampling to 20Hz. Peri-event histograms were created by subtracting the median baseline zscore from each sample and then averaging across trials. We did not perform subtraction of a fitted autofluorescent channel because we found changes in power time-locked to behavior channel both the calcium and autofluoresent channels, expect the changes in the autofluorecent channel were on a smaller scale, resulting in poor fitting and ineffectual subtraction. Instead of performing a fitted subtraction, we assessed effects in the z-score of the calcium channel by analyzing within-subject comparisons with the z-score of the autofluorescent channel.

3.3.8 Fluorescent *In-Situ* Hybridization

After 2 months of incubation to allow for adequate viral expression, rats were deeply anesthetized with isoflurane, decapitated, and their brains were removed and frozen in 2-methylbutane (Sigma-Aldrich, Cat#: M32631) on dry ice. After 5-10 seconds in 2-methylbutane, the brains were blocked into brain molds using optimal cutting temperature compound (OCT; Fisher Healthcare, Scigen Scientific, Cat#: 23-730-571) wrapped in

aluminum foil and placed on dry ice. All utensils used during brain removal were cleaned with RNaseZap (Fisher scientific, cat#: AM9780) between rats. Brains were stored in an air-tight plastic container filled with desiccant at -80°C for no longer than 2 weeks, until slicing,. Brains were serially sectioned at 14µm on a cryostat set at -14°C and collected onto Superfrost Plus slides (Fisher Scientific, Cat#: 12-550-15). Slides were stored in a slide box containing desiccant and covered in aluminum foil at -80°C, for no longer than 2 weeks, until hybridization. We pretreated the samples following the guidelines provided by the manufacturer for fresh frozen tissue (procedure Cat No 320513), using paraformaldehyde as our fixative. We performed the in situ hybridization assay using the RNAscope Fluorescent Multiplex Detection Reagents (ACD, Cat No 320851), according to the guidelines provided by the manufacturer (procedure Cat No 320293) with a few adjustments: Simport Scientific EasyDip Slide Staining Jars were used in place of Tissue-Tek Staining Dishes; 75µL of probe mixture (mixed the day of the assay) was applied to each full rat section instead of the suggested 120µL; for all amplifiers, we used approximately 2 drops instead of the suggested 4 drops; and DAPI Fluoromount-G (SouthernBiotech, Fisher Scientific, cat# 0100-20) was used in place of the combination of DAPI and fluorescent mounting medium. We used the following target probes: EGFP (cat#: 400281) for eYFP, Rn-Slc17a6-C2 (cat#: 317011-C2) for VGlut2, and Rn-Gad1-C3 (cat#: 316401-C3) for GAD1. Amp-4 Alt A was used to fluorescently label the probes: eGFP (Alexa488), VGlut2 (Atto550), and GAD1 (Atto647). After coverslipping, the slides were kept covered in a fume-hood overnight in order for slides to air-dry before being stored in a slide box covered in aluminum foil and stored at 4°C. Slides were imaged with a confocal microscope (Nikon A1R confocal microscope). Large images were taken at 20X with 10 z-steps of 1um and stitched together with 25% overlap. The maximum intensity projection was produced using NIS-Elements to be used for further analysis. Location of

the target region was determined manually by mapping on the appropriate Paxinos and Watson rat brain atlas image onto the fluorescent image using the Big Warp plugin in ImageJ. Neuron counting was performed manually using the Cell Counter plugin in ImageJ. A neurons was determined to be expressing a target gene if it contained 5 or more fluorescent dots in or surrounding a DAPI-stained nucleus.

3.3.9 Histology

The location of optic fibers and viral expressions were determined at the conclusion of each experiment. Rats were deeply anesthetized with isoflurane and transcardialy perfused with PBS followed by 4% PFA. For experiments with optic fiber implants, rats were decapitated and their skulls were post-fixed for 24h with fibers intact, after which, the fibers were extracted by first using a Dremel to remove the implant surrounding the fiber and then using a hemostat to remove the optic fiber. Brains were then removed and post-fixed for an additional 24h. For experiments without optic fiber implants, brains were removed and post fixed for 24h. For all experiments, after post fixing, brains were transferred to 20% sucrose until they sunk. Brains were serially sectioned at 40µm on a cryostat (Thermo Fisher Scientific, Waltham, MA, cat# HM550) and collected into wellplates filled with a cryoprotectant (24% glycerol and 29% ethylene glycol in PBS). Sections were imaged in wellplates with a fluorescent stereomicroscope (Carl Zeiss, Oberkochen, Germany, cat#: Axio Zoom.V16) using a consistent exposure for each subject to allow for fluorescent intensity comparisons across sections.

The fastgreen spot and/or optic fiber tip locations were located and imaged, and then mapped onto a reference atlas. For electrophysiology experiments, the position of other recorded neurons was back-calculated relative to the fastgreen location.

3.3.10 Statistical Analysis and Data Visualization

We analyzed results using repeated measures ANOVA followed by post-hoc using Tukeys honest significant differences test (HSD), or Pearson product-moment correlation followed by an extra-sum-of-squares F test against hypothetical slopes and/or x intercepts. In cases where the data was not normally distributed, as determined by the Shapiro-Wilk normality test, a paired Wilcoxon rank sum test was used in place of a student *t*-test. Across all statistical tests, $P < 0.05$ was used as a threshold for significance. Sample sizes were determined based on preliminary experiments or on on effect size (partial eta squared = 0.01-0.25 for repeated measures or main effects ANOVA). In all plots, error bars indicate the standard error of the mean (SEM).

All statistical analysis was conducted in R. We used the 'afex' package (version 0.21-2) to compute ANOVAs, the 'emmeans' package to compute HSD, and base R to compute *t*-tests and Wilcox tests, and 'Smatr' (version 3.5.2) and correlations. In cases where the data was not normally distributed, as determined by the Shapiro-Wilk normality test, a paired Wilcoxon rank sum test was used in place of a student *t*-test. For some data analysis, initial processing steps prior to statistical analysis and visualization, were conducted using MATLAB (version R2018a).

We created graphs using Graph Pad Prism (version 8.2.0) or R using 'ggplot2' (version 3.0.0). Color scales were created using the 'viridis' package. Atlas images were adapted from Paxinos and Watson digital atlas (Paxinos and Watson, 2007) using Adobe Illustrator CC (version 22.1). All other figure aspects were created in Adobe Illustrator CC.

3.4 RESULTS

3.4.1 The LPO sends GABA and glutamate projections to the VTA

We determined the relative proportions of GABA and glutamate of the LPO projection to the VTA. To selectively express eYFP in LPO neurons that project to the VTA, we injected CAV-Cre in the VTA and a Cre-dependent vector, rAAV5/EF1a-DIO-hChR2/(H134R)-eYFP in the LPO (Figure 3.1a). We then performed fluorescent in-situ hybridization for GFP (which effectively probes for eYFP) to identify LPO neurons that project to the VTA, VGlut2 to identify glutamate neurons, and GAD1 (GAD-67) to identify GABA neurons (Figure 3.1b, c). In LPO to VTA neurons, we found that ~60% expressed GAD1 alone, ~30% expressed vGlut2 alone, ~3% coexpresed both GAD1 and vGlut2, and ~7% did not express neither GAD1 nor vGlut2 (Figure 3.1d). Furthermore, we found differences in the proportion of expression across the anterior to posterior axis for both GABA and glutamate populations: expression of GAD1 was higher rostrally than caudally, and expression of vGlut2 was lower rostrally than caudally (Figure 3.1e). These results indicate that the LPO sends direct GABAergic and glutamatergic projections to the VTA, and that GABA makes up a larger proportion of this projection in rostral portions of the LPO, while glutamate makes up a larger proportion in caudal portions of the LPO.

3.4.2 The LPO and LPO→VTA pathway modulates VTA subpopulations

To validate that channel rhodopsin (ChR2) can stimulate LPO neurons, we measured the effect of optogenetic stimulation of LPO neurons in rats that received an intra-LPO injection of a viral vector encoding rAAV5/hsyn-ChR2(E123A)-EYFP. We recorded the activity of LPO neurons under anesthesia, while delivering local laser illumination (450nm, 1-10mW) (Figure 3.2a). Delivering single 10ms light pulses at 0.2-0.5Hz produced responses with low latency and low jitter responses (Figure 3.2c, e);

delivering 1s trains of 5ms light pulses at 20Hz and 40Hz stimulated LPO neurons with high fidelity (Figure 3.2e, f).

We measured the functional connectivity between the LPO and VTA in rats that received an intra-LPO injection of a viral vector encoding rAAV5/hsyn-ChR2(E123A)-EYFP. We recorded the activity of VTA neurons under anesthesia, while delivering laser illumination either to the LPO or to the VTA (to stimulate the LPO→VTA pathway). VTA neurons were classified as putative dopamine and putative GABA based on established extracellular recording criteria (Ungless and Grace, 2012); these neurons will be referred to as $VTA_{Dopamine}$ and VTA_{GABA} neurons from this point onwards.

Stimulation of the LPO had differential effects on $VTA_{Dopamine}$ and VTA_{GABA} neurons (Figure 3.3). (neuron type x time interaction: $F_{2,64} = 3.68$, $P = 0.031$). In the case of VTA_{GABA} neurons, stimulation of the LPO produced a strong decrease in firing rate that returned to baseline after the stimulation ended (time effect: $F_{2,30} = 17.87$, $P < 0.001$; HSD pre vs pulse: $P < 0.001$; HSD pre vs post: $P = 0.13$) (Figure 3.3c). In the case of $VTA_{Dopamine}$ neurons, stimulation of the LPO produced a mixture of effects that did not lead to a group effect (time effect: $F_{2,34} = 0.84$, $P = 0.44$) (Figure 3.3d). However, LPO stimulation led to an increase in firing in 4 out of 18 neurons, a decrease in firing in 9 out of 18 neurons, and no effects in 5 out of 18 neurons. We found that the position of the cell within the VTA and position of the optic fiber in the LPO did not correlate with the effect of stimulation of the LPO (Figure 3.4, Figure 3.5).

Stimulation of the LPO→VTA pathway had differential effects on $VTA_{Dopamine}$ and VTA_{GABA} neurons (cell type x time interaction: $F_{2,166} = 6.57$, $P = 0.0020$). In the case of VTA_{GABA} neurons, stimulation of the LPO produced a strong decrease in firing rate that returned to baseline after the stimulation ended (time effect: $F_{2,38} = 20.40$, $P < 0.001$; HSD pre vs pulse: $P < 0.001$; HSD pre vs post: $P = 0.27$) (Figure 3.3e). In the case of $VTA_{Dopamine}$

neurons, stimulation of the LPO produced a mixture of effects that did not lead to a group effect (time effect: $F_{2,78} = 0.42$, $P = 0.66$) (Figure 3.3f). However, LPO stimulation led to an increase in firing in 8 out of 40 neurons, a decrease in firing in 13 out of 40 neurons, and no effects in 19 out of 40 neurons. We found that the position of the cell within the VTA did not correlate with the effect of stimulation of the LPO→VTA pathway (Figure 3.4).

We further validated the effect of stimulating the LPO→VTA pathway, we used a combinatorial approach. Rats received an intra-VTA injection of the retrograde vector CAV-2 Cre, and an intra-LPO injection of the viral vector encoding Cre-dependent ChR2 (DIO-ChR2). This approach results in selective expression of ChR2 in LPO neurons that have project to the VTA (Junyent and Kremer, 2015). Stimulation of the cell bodies of the LPO→VTA pathway did not have differential effects on $VTA_{Dopamine}$ and VTA_{GABA} neurons but trended in that direction (time effect: $F_{2,60} = 2.57$, $P = 0.085$) (Figure 3.3g). In the case of VTA_{GABA} neurons, stimulation of the cell bodies of the LPO→VTA pathway produced a strong decrease in firing rate that returned to baseline after the stimulation ended (time effect: $F_{2,48} = 14.69$, $P < 0.001$; HSD pre vs pulse: $P < 0.001$; HSD pre vs post: $P = 0.62$) (Figure 3.3h). In the case of $VTA_{Dopamine}$ neurons, stimulation of the LPO produced a mixture of effects that did not lead to a group effect (time effect: $F_{2,12} = 0.0027$, $P = 0.66$). However, LPO stimulation led to an increase in firing in 2 out of 7 neurons, a decrease in firing in 1 out of 7 neurons, and no effects in 4 out of 7 neurons.

In a subset of VTA neurons we were able to compare the effect of stimulating the LPO and stimulating LPO→VTA pathway (Figure 3.3i, j). We found that stimulating the LPO and LPO→VTA pathway led to a trend towards different effects in both $VTA_{Dopamine}$ and VTA_{GABA} neurons (stim region x time interaction: $VTA_{Dopamine}$, $F_{2,28} = 3.12$, $P = 0.060$; VTA_{GABA}, $F_{2,18} = 3.47$, $p = 0.053$). To analyze the relationship between the effect of

stimulating the LPO and LPO→VTA pathway we assessed the correlation of their effects. Stimulation of the LPO and LPO→VTA pathway produces similar effects on VTA_{GABA} and $VTA_{Dopamine}$ neurons, as indicated by a significant correlation between the two stimulations (VTA_{GABA}: $r = 0.89$, $P < 0.001$; $VTA_{Dopamine}$: $r = 0.59$, $P = 0.021$) (Figure 3.3i). However, for both neuron types there was a lower magnitude of effect for stimulation of the LPO→VTA pathway compared to stimulation of the LPO, as indicated by an intercept not different from 0 and a slope less than 1 (intercept vs intercept of 0, VTA_{GABA}: $F_{1,8} = 0.71$, $P = 0.43$; $VTA_{Dopamine}$: $F_{1,13} = 0.16$, $P = 0.69$; slope vs. slope of 1, VTA_{GABA}: $F_{1,8} = 6.20$, $P = 0.038$; $VTA_{Dopamine}$: $F_{1,13} = 14.96$, $P = 0.0019$) (Figure 3.3j). Taken together, stimulating the LPO modulates the firing of VTA neurons, and stimulation of the LPO→VTA pathway produces similar modulation but to a lower magnitude.

We also determined if stimulations of long and short duration produce similar effects in a subset of neurons (Figure 3.6). We stimulated the LPO and LPO→VTA pathway for 1s and 60s (450nm, 5ms pulses, 40Hz) and recorded the change in firing in VTA neurons. In the case of VTA_{GABA} neurons, for both the LPO and LPO→VTA pathway, 1s and 60s stimulation produced similar effects (paired *t*-test, LPO: $P = 0.61$; LPO→VTA: $P = 0.46$). This was also indicated by a strong correlation between effects produced by 1s and 60s for both stimulation regions (LPO: $r = 0.96$, $P = 0.0024$; LPO→VTA: $r = 0.99$, $P < 0.001$). Comparing 60s with 1s stimulation, there was a slightly diminished effect of 60s stimulation for LPO stimulation but no difference for LPO→VTA pathway stimulations (intercept vs intercept of 0, LPO: $F_{1,4} = 2.51$, $P = 0.19$, LPO→VTA: $F_{1,4} = 0.0041$, $P = 0.95$; slope vs. slope of 1, LPO: $F_{1,4} = 11.22$, $P = 0.029$; LPO→VTA: $F_{1,4} = 0.65$, $P = 0.67$) (Figure 3.6c, e). In the case of $VTA_{Dopamine}$, comparing 60s with 1s stimulation, there was a lower magnitude of effect of 60s stimulation for both LPO and LPO→VTA pathway as indicated by an intercept no different from 0 and a slope less than

1 (intercept vs intercept of 0, LPO: $F_{1,9} = 0.27$, $P = 0.62$, LPO→VTA: $F_{1,8} = 2.37$, $P = 0.16$; slope vs. slope of 1, LPO: $F_{1,9} = 61.65$, $P < 0.001$; LPO→VTA: $F_{1,8} = 9.48$, $P = 0.015$) (Figure 3.6d, f). Taken together, these data indicate that stimulating the LPO produces effects even with long stimulation (60s). However, the effect on $VTA_{Dopamine}$ neurons is smaller with long stimulation (60s) compared with short stimulation (1s).

3.4.3 Stimulation of the LPO supports intracranial self-stimulation responding

3.4.3.1 Intracranial self-stimulation (ICSS): fixed ratio schedule

In order to determine if increases in neuronal activity within the LPO is rewarding, we investigated the reinforcing properties of stimulating the LPO using ICSS. We injected viral vectors encoding either AAV5/hsyn-mCherry (mC) or rAAV5/hSyn-ChR2(E123A)-EYFP-WPRE (ChR2) into the LPO and implanted an optical fibers above the injection site (Figure 3.7a).

In a first cohort of rats (Cohort 1), rats were tested for ICSS over 5 days (Figure 3.7b). Rats were placed in a side with an active-hole and inactive-hole (Figure 3.7c). We used a fixed ratio schedule of 1: one nose-pokes into the active-hole triggered a 1s train of intra-LPO laser illumination (40Hz, 5ms pulses, 15mW, 450nm) and a simultaneous light cue in the active-hole. Nose pokes during illumination were recorded but did not trigger a subsequent illumination. Nose-pokes into the inactive-hole had no consequence and served as a measure for non-goal-directed behaviors. In order to normalize variation across groups and nose-pokes, response counts were transformed logarithmically (before transformation all response counts were increased by one to avoid undefined values resulting from log of zero).

Optogenetic stimulation of the LPO supported ICSS, as indicated by differential discrimination for the active hole and inactive hole in the mC and ChR2 groups (group x

hole interaction: $F_{1,14}$ = 51.57, P < 0.001). Furthermore, the ChR2 group had higher responding on the active-hole compared with the mC group (group effect: $F_{1,14}$ = 68.74, P < 0.001) (Figure 3.7d).

To determine if response rates are sensitive to the duration of the stimulation per reward, after 6 days of ICSS with a reward duration of 1s, we increased to the reward duration to 10s. Increasing the reward duration led to differential effects in the mC and ChR2 groups, where the ChR2 group decreased active hole responding and the mC group showed no change (group x reward duration, $F_{1,14}$ = 17.79, P < 0.001, ChR2: HSD, df = 14, P < 0.001; mC: HSD, df = 14, P = 0.99). For both stimulation durations, the ChR2 group maintained higher responses rates compared to the mC group (1s: HSD, df = 18.76, P < 0.001; 10s: HSD, df = 18.76, P < 0.001) (Figure 3.7e, left). In contrast, increasing the reward duration led to increased total stimulation duration in both groups, but with a greater increase in the mC group compared to ChR2 (reward duration main effect, $F_{1,14}$ = 380.89, P < 0.001; group x stimulation reward duration interaction, $F_{1,14}$ = 21.38, P < 0.001; ChR2: HSD, df = 14, P < 0.001; mC: HSD, df = 14, P < 0.001) (Figure 3.7e, right). This result stems from the fact that the mC group maintained low response rates under both stimulation durations, which led to a linear increase in the total stimulation duration when the duration of the reward was increased. Even with the differential change in total stimulation duration, the ChR2 group earned a greater total stimulation duration for both reward durations than the mC group (1s: HSD, df = 17.60, P < 0.001; 10s: HSD, df = 17.61, P < 0.001). These results indicate that stimulating the LPO is reinforcing and that rats flexibly adjust response rates in correspondence to reward duration; the ChR2 group reduced the number of responses to compensate for the increase in reward duration. This experiment was also conducted in cohort 2 using 40Hz and cohort 3 using 20Hz stimulation, and in both cohorts stimulation of the LPO supported ICSS (Figure 3.8b, c).

To determine if variation in ICSS response rates was caused by the location of stimulation (Figure 3.9), we compared the optic fiber location to the mean number of responses over the last 3 days of ICSS combined across all cohorts. We found no correlation between the position of the optic fiber and mean number of responses over the last 3 days of ICSS (Figure 3.10). These results indicate that the variance observed in ICSS is not the product of variations in fiber placement.

3.4.3.2 ICSS: Progressive-ratio

In order to determine the extent of the reinforcing properties of LPO stimulation and to determine the relative value of different stimulation durations, we tested a second cohort of rats (cohort 2) with a progressive-ratio schedule. A ChR2 group was first trained with fixed-ratio 1 ICSS for 1s stimulation over 5 days, as outlined above, and then tested over 12 days of progressive-ratio (Figure 3.7f). For all progressive-ratio days, the cost of the reward increased semi-logarithmically during the session (e.g. 1, 2, 4, 6, 9, etc.) (Figure 3.7g). Every other day, the stimulation duration per reward was increased such that that the rats were tested on two consecutive days for each stimulation duration (e.g. 1s, 1s, 3s, 3s, etc.) (Figure 3.7f). A mean was calculated across days with the same stimulation duration. The purpose of progressively increasing stimulation duration was to determine if there was a duration at which LPO stimulation transitioned from being rewarding to being aversive which would manifest as a decrease in response rates.

The group of ChR2 rats acquired ICSS, as indicated by discrimination between the active hole and inactive hole (hole effect: $F_{1,6} = 164.07$, $P < 0.001$) (Figure 3.7h), and rats continued to discriminate throughout the progressive-ratio test (hole effect: $F_{1,6} = 165.93$, $P < 0.001$). Increasing the stimulation duration per reward led to an increase in active-hole responding (reward duration effect: $F_{5,30} = 4.93$, $P = 0.0021$; HSD, 1s vs 10s $P = 0.0019$,

1s vs 60s P = 0.0074) (Figure 3.7i), and break point (reward duration effect: $F_{5,30} = 2.83$, P = 0.031) (Figure 3.7i, middle). Additionally, increasing the stimulation duration per reward led to a dramatic increase in the total stimulation duration (reward duration effect: $F_{5,30} = 975.20$, $P < 0.001$; HSD, 1s vs all other durations $P < 0.001$) (Figure 3.7i, right). For stimulation durations of 300s, rats earned a mean total of 48.21 min of stimulation (SEM: 5.94min) during the 6 hours of testing. Critically, there was no stimulation duration that led to a suppression in responding that was lower than responding for 1s stimulation. These results using a progressive-ratio schedule were replicated in cohort 1, even though cohort 1 went through multiple pilot experiments in between ICSS testing at FR1 and using the progressive-ratio schedule (Figure 3.8e). Altogether, the progressive-ratio experiment reveals that LPO stimulation is reinforcing under high motivational requirements even up to extreme stimulation durations and there is no point at which stimulation transitions to being aversive.

3.4.4 Optogenetically Stimulating the LPO promotes real-time place aversion in the majority of rats

In order to further determine the valence of stimulating the LPO with optogenetics, we measured the online valence of optogenetic stimulation with real-time place testing (RTPT) (Figure 3.11). We injected viral vectors encoding either AAV5/hsyn-mCherry (mC) or rAAV5/hSyn-ChR2(E123A)-EYFP-WPRE (ChR2) into the LPO and implanted optical fibers above the injection site (Figure 3.11a). Rats were then subjected to RTPT over 9 days (Figure 3.11b). On the first day of RTPT subjects were placed in an apparatus and we measured the baseline preference for each side (Preference test, PT). On subsequent days, rats were placed in the same apparatus and detection of the rat's center point in one side of the led to laser illumination (40Hz, 5ms pulses, 15mW) and detection in the other

side had no effect (Figure 3.11c). To determine if rats updated their place preference based on laser pairing, we paired the same side of the apparatus for 4 consecutive days and then paired the opposite side of the apparatus for 4 additional days. To quantify the valance of laser illumination we computed a RTPT score by taking the mean time in the initially paired side during initial pairing and subtracting the mean time in the initially paired side during inverted pairing and dividing by the session time: high RTPT scores are indicative of reward, while low RTPT scores are indicative of aversion. Finally, we also classified the effect of illumination in subjects as aversive, rewarding, or no valence based on a paired *t*-test on time spent in the initially paired side during initial and inverted pairing and the direction of the RTPT score. In cohort 2, laser illumination had a different effects on the mC and ChR2 groups (group x day interaction: $P < 0.001$, $F_{8,96} = 5.56$, $P < 0.001$) (Figure 3.11d) and drove different proportions of rats showing aversion, reward, and no valence (fisher exact: $P = 0.029$) (Figure 3.11e). Laser illumination of the LPO in the mC group had minimal effects on place preference across laser pairing; six out of seven showed no place effects (no change in time spent on the initially paired side) and one rats showed place preference (increase in time spent in the initially paired side). Laser illumination of the LPO in the ChR2 group drove bidirectional effects; 5 out of 7 rats showed place aversion (increase in time spent in the initially paired side), 1 out of 7 rats showed place preference (decrease in time spent in the initially paired side), and 1 out of 7 rats showed no place effects (no change in time spent on the initially paired side). Importantly, real-time place avoidance behavior was observed in the same subjects that exhibited ICSS responding (see Figure 3.12a-d for an exemplar rat). To determine if groups exhibited a difference in the number of times they crossed into the laser paired side, we examined the number of crossing and found that the mC and ChR2 groups crossed at similar rates ($F_{1,12} = 3.08$, $P = 0.10$) (Figure 3.13b).

This experiment was also conducted in cohort 1 using 40Hz continuous train illumination. On the group level, illumination did not have differential effects on the mC and ChR2 groups (group x day interaction: $F_{8,104} = 1.59$, $P = 0.14$) (Figure 3.11f), however illumination drove different proportions of rats showing aversion, reward, and no valence (fisher exact: $P = 0.011$) (Figure 3.11g). Laser illumination of the LPO in the mC group had minimal effects on place preference across laser pairing; five out of seven rats showed no place effects, one showed place preference and one place aversion. Laser illumination of the LPO in the ChR2 group drove bidirectional effects, where 2 out of 9 rats showed place preference, 6 out of 9 subjects showed place aversion, and 0 out of 9 subjects showed no place effects. Interestingly, the ChR2 group made more crossings compared to the mC group ($F_{1,13} = 20.02$, $P < 0.001$) (Figure 3.13a). All together, the results in cohort 1 largely replicated the effects in cohort 2 except subjects crossed more frequently than cohort 2.

Finally, we conducted the same experiment a 3rd time in cohort 3 (naïve) using 20Hz continuous train illumination and biased assignment where laser pairing was assigned to the side least preferred in during the preference test to enhance the likelihood of measuring place preference. Despite biased assignment, rats still did not display preference for the laser paired side. On the group level, illumination pairing did not have differential effects on mC and The ChR2 group (group x day interaction: $F_{6,60} = 2.05$, $P = 0.072$) (Figure 3.14a), illumination did not drive differential proportions of rats showing aversion, reward, and no valence (fisher exact: $P = 0.15$) (Figure 3.14b). Laser illumination of the LPO in the mC group had minimal effects on place preference across laser pairing. Laser illumination of the LPO in The ChR2 group drove primarily aversion, where 2 out of 5 subjects showed place aversion (increase in time in the initially paired side), 0 out of 5 subjects showed place preference (decrease in time in the initially paired side), and 3 out of 5 subjects showed no place effects (no change in time spent on the initially paired side).

Finally, the mC and ChR2 groups made a similar number of crossings ($F_{1,10} = 0.18$, $P = 0.67$) (Figure 3.13c). This cohort indicates that optogenetic stimulation of the LPO with lower frequencies still produces effects, however the effects are smaller compared to stimulation with high frequency.

To determine if diversity in effects within RTPT was caused by the location of stimulation, we compared the optic fiber location to the RTPT score combined across all cohorts. We found no correlation between the position of the optic fiber and the RTPT score (Figure 3.15). These results indicate that the reward and aversion observed within RTPT are not the product of variations in optic fiber placement.

3.4.5 Optogenetically inhibiting the LPO does not promote ICSS responding or real-time place testing behavior

To validate that halorhodopsin (HR) can inhibit LPO neurons, we measured the effect of optogenetic inhibition of LPO neurons in rats that received an intra-LPO injection of a viral vector encoding AAV5/hsyn-eNpHR3.0-eYFP (HR). We then recorded the activity of LPO neurons while delivering laser illumination (520nm, 2mW) into the LPO (Figure 3.16a, b). Delivering 50ms light pulses at 0.2Hz produced low rapid inhibition of activity that quickly recovered; delivering 1s, 10s, and 60s light pulses produced total, sustained inhibition of activity without producing rebound excitation (Figure 3.16c-e).

To determine if the LPO provides a tonic regulation of valence, we injected viral vectors encoding either AAV5/hsyn-mCherry (mC) or AAV5/hsyn-eNpHR3.0-eYFP (HR) and implanted optical fibers above the injection site (Figure 3.17a, fiber placements shown in Figure 3.18). Rats were then subjected to RTPT and ICSS, sequentially (Figure 3.17b). Interestingly, laser illumination in the LPO in mC and HR groups drove a slight preference for laser illumination seen in both groups (day effect: $F_{8,120} = 4.80$, $P < 0.001$) (Figure

3.17c). However, laser illumination did not drive differential real-time place testing behavior across groups (group x day interaction: $F_{8,120} = 0.74$, $P = 0.65$) (Figure 3.17c) and did not drive differences in the proportion of rats showing aversion, reward, or no valence (Fisher exact: $P = 0.40$) (Figure 3.17d). Laser illumination also did not drive differences in crossings between the mC and HR groups ($F_{1,15} = 0.20$, $P = 0.66$) (Figure 3.13d). In the ICSS procedure, the mC and HR groups did not exhibit differential discrimination between the active and inactive holes (group x hole interaction: $F_{1,14} = 0.011$, $P = 0.92$) (Figure 3.17e, left), or differences in active-hole responses (group effect: $F_{1,14} < 0.001$, $P = 1.00$) (Figure 3.17e, right), indicating that inhibition of the LPO was neither reinforcing or aversive. Together, the RTPT and ICSS results indicate that the LPO does not provide tonic regulation of valance or reinforcement.

3.4.6 Optogenetically stimulating the LPO→VTA pathway replicates effects of stimulating the LPO

To determine if the effects of optogenetically stimulating the LPO is mediated in part by the LPO→VTA pathway, we injected viral vectors encoding either AAV5/hsyn-mCherry (mC) or rAAV5/hSyn-ChR2(E123A)-EYFP-WPRE (ChR2) into the LPO and implanted optical fibers above the injection site in the LPO and above the VTA (Figure 3.19a, fiber placements shown in Figure 3.20). Rats were then subjected to RTPT and ICSS. During RTPT, laser illumination of the LPO→VTA pathway had differential effects on the mC and ChR2 groups (group x day interaction: $P < 0.001$, $F_{8,96} = 4.34$, $P < 0.001$) (Figure 3.19c), and drove differential proportions of rats showing aversion, reward, and no valence (fisher exact: $P = 0.0057$) (Figure 3.19d). Laser illumination of the LPO→VTA pathway in the mC group had minimal effects on place preference; seven out of eight rats showed no place effects and one rat showed place aversion. Laser illumination of the

LPO→VTA pathway in the ChR2 group drove bidirectional effects, where 4 out of 6 subjects showed place aversion, 1 out of 6 subjects showed place preference, and 1 out of 6 subjects showed no place effects. Finally, the mC and ChR2 groups made similar numbers of crossings ($F_{1,12}$ = 0.0014, P = 0.97) (Figure 3.13e). These results largely replicated RTPT results obtained with stimulation of LPO cell bodies as outlined above.

In addition to measuring valence with RTPT, we measures the reinforcing qualities of optogenetically stimulating the LPO and the LPO→VTA pathway with a modified version of the ICSS described above, where rats received access to illumination of the LPO→VTA pathway for 9 days, followed by illumination of LPO cell bodies for 3 days, and finally illumination of the LPO→VTA pathway for 3 additional days. Over the course of ICSS, the ChR2 group, but not the mC group acquired ICSS responding, as indicated by differential discrimination between the active-hole and inactive-hole for the mC and ChR2 groups (group x hole interaction: F1,12 = 15.21, P = 0.0021) (Figure 3.19e, left). To determine a difference in reinforcement between stimulation of LPO cell bodies and stimulation of the LPO→VTA pathway, we took the mean responding over the last 3 days of illumination of the LPO→VTA pathway, the 3 days of illumination of LPO cell bodies, and the 3 days of illumination of the LPO→VTA pathway following illumination of LPO cell bodies. Across illumination regions, the mC and ChR2 groups differentially responded on the active hole and inactive hole (group x hole interaction: $F_{1,12}$ = 22.42, P < 0.001). Over all three epochs, the ChR2 group responded more often on the active-hole than the mC group but showed no difference in responding on the inactive-hole (HSD, active hole: P < 0.001, inactive hole: P > 0.05 for all epochs) (Figure 3.19e, right). Relative to the LPO→VTA pathway, stimulating LPO cell bodies led to higher raw responding (data not shown) (group x hole x fiber interaction: $F_{2,24}$ = 6.30, P = 0.0063; HSD, active hole: VTA-LPO vs LPO, P < 0.01 for both comparisons) (data not shown), but not log transformed

responding (group x hole x fiber interaction: $F_{2,24}$ = 2.74, P = 0.085; HSD, active hole: VTA-LPO vs LPO, P > 0.05 for both comparisons) (Figure 3.19e, right). Together, the RTPT and ICSS data indicate that stimulation of the LPO→VTA pathway is both reinforcing and aversive, which mirrors the effect of stimulating LPO cell bodies.

3.4.7 ICSS and RTPT measures of reward are correlated

To understand the apparent contradiction stemming from the ICSS (reinforcement) and RTPT (aversion) results outlined above, we analyzed the relationship between ICSS and RTPT behavior in rats that were tested with both procedures.

We chose to analyze ChR2 rats of cohort 2, which displayed the strongest real time place aversion with 3s train, 3s ITI stimulation but also displayed both fixed-ratio and progressive-ratio responding. In order to compare the two tasks, we analyzed the relationship between RTPT and fixed-ratio 1 ICSS because both tasks enable rats to administer as much stimulation as desired. To compare these two assays we compared last three days of initial training within each task (ICSS: last 3 days of FR1; RTPT: last 3 days of initial paring) over the same time period (20 minutes) (Figure 3.21a). There was a strong correlation between the total stimulation duration received in RTPT and fixed-ratio 1 ICSS (r = 0.91, P = 0.0039) (Figure 3.21c), but rats received more stimulation during RTPT compared with ICSS (Wilcoxon, W = 26, P = 0.031) (Figure 3.21b), which was also indicated by a correlation slope below 1 (slope different than 1, F = 373.29, P < 0.001) (Figure 3.21c).

The relationship between ICSS and RTPT was similar across experiments. Combing across cohorts 1, 2, and 3, and the LPO→VTA pathway stimulation group, rats received more stimulation in RTPT compared to ICSS over the same 20 minute time period (Wilcoxon, W = 350, P < 0.001) (Figure 3.22a). Furthermore, the total stimulation duration

received within these two assays was correlated ($r = 0.48$, $P = 0.012$) (Figure 3.22b), even when normalizing within each experiment ($r = 0.50$, $P = 0.0091$) (Figure 3.22c); these results indicate that despite the large difference in total stimulation duration, the assays are measuring a related effect. Altogether, these results demonstrate that rats received significantly more stimulation in the RTPT procedure than the ICSS procedure, despite the fact that the RTPT results would lead us to believe stimulation is aversive and the ICSS results would lead us to believe stimulation in rewarding.

3.4.8 Stimulation-intervals contribute more to RTPT results than inter-stimulation-intervals

After finding that rats received substantially more optogenetic stimulation in the RTPT test than the ICSS test, we next analyzed specific components of the behavior to determine what underlies the ICSS and RTPT aggregate scores. Using the first 20 minutes of both procedures, we broke down the task into two independent components: 1) the stimulation-interval (duration of each stimulation received) and 2) the inter-stimulation-interval (duration of periods in between each stimulation). In the case of ICSS, the rats can only control the inter-stimulation-interval, as the stimulation-interval is fixed at 1s by the experimenter (Figure 3.21d, right). In the case of RTPT, the rats can control both the inter-stimulation-interval and stimulation-interval, both of which could underlie the final RTPT score (Figure 3.21d, left). For example, the variance in RTPT scores could be the result of consistent inter-stimulation-intervals with variable stimulation-intervals, where high stimulation-intervals would lead to high RTPT scores, or could be the result of consistent stimulation-intervals with variable inter-stimulation-intervals, where low inter-stimulation-intervals would lead to higher RTPT scores.

During fixed-ratio 1 ICSS, rats with shorter inter-stimulation-intervals received a greater total stimulation duration, suggested by the cumulative distribution functions of inter-stimulation-intervals for each rat (Figure 3.21e, left). This was further demonstrated by analyzing the correlation between the inter-stimulation-interval at each percentile against the total stimulation duration earned where we observed clear correlations between the two across a large portion of percentiles (Figure 3.21e, right, Figure 3.21f). These results indicate that rats with a high total stimulation durations had a greater proportion of short inter-stimulation-intervals.

During RTPT, there was a limited relationship between the inter-stimulation-interval and RTPT score, suggested by the cumulative distribution functions of inter-stimulation-intervals for each rat (Figure 3.21g, left). This was further demonstrated by analyzing the correlation between the inter-stimulation-interval at each percentile against the RTPT score where we observed poor correlations between the two across percentiles (Figure 3.21g, right, Figure 3.21h). These results indicate that there is a limited relationship between the inter-stimulation-interval (the rates at which rats re-enter the stimulation paired side), and the RTPT score. On the other hand, there was a strong relationship between the stimulation-interval and RTPT score, suggested by the cumulative distribution functions of stimulation-intervals for each rat (Figure 3.21i, left). This was further demonstrated by analyzing the correlation between the stimulation-interval at each percentile against the RTPT score where we observed poor correlations between the two across percentiles (Figure 3.21i, right, j). Over the entire interval distribution, the stimulation-interval had a greater correlation with the RTPT score compared with the inter-stimulation-interval, as indicated by a larger area under the percentile vs. R^2 curve.

The relationships between the RTPT score and the inter-stimulation-intervals and stimulation durations was also seen when combining rats across experiments (Figure 3.23).

We combined rats form cohort 1, 2, and 3, along with the LPO→VTA experiment and observed similar relationships to the analysis of cohort 2 alone. Compared to the inter-stimulation-interval, the stimulation-interval correlated more strongly with the RTPT score (Figure 3.23).

Altogether these results indicate that optogenetically stimulating the LPO produces the ultimate RTPT scores primarily through differences in preferred stimulation-intervals and not through preferred inter-stimulation-durations. These results raise the possibility that stimulating the LPO with optogenetics is reinforcing despite real-time place aversion, which would manifest as continued entry into the paired compartment despite the lack of preference for the environment after entering.

3.4.9 stimulating the LPO is reinforcing in the RTPT assay

To determine if optogenetically stimulating the LPO with is reinforcing in the RTPT procedure, we injected viral vectors encoding either AAV5/hsyn-mCherry (mC) or rAAV5/hSyn-ChR2(E123A)-EYFP-WPRE (ChR2) into the LPO and implanted optical fibers above the injection site (Figure 3.24a, placements shown in Figure 3.25). Rats were then subjected to RTPT before and after pairing the laser-paired side of the side with progressively higher electricity, delivered via the floor of the side. In this procedure, rats were ran through RTPT in an apparatus where one side was covered in acrylic and the other consisted of metal bars. Throughout the entire procedure, the side of the side with metal bars was paired with illumination (40Hz, 3s train, 3s ITI). Following 4 days of pairing, the metal bars of the floor on the illumination paired side were electrified according to the schedule outlined in Figure 3.24b and c. this side of the apparatus will be referred to as the dual-paired side. Electrifying the floor of the illumination-paired side led to a decreased amount of time spent in the dual-paired side (day effect: $F_{17,255} = 30.34$, $P < 0.001$) (Figure

3.24d). However, this occurred to a greater extent in the mC and ChR2 groups (day x group interaction: $F_{17,255} = 5.55$, $P < 0.001$) (Figure 3.24d) and was present throughout the testing session (Figure 3.26a-c). To determine if the ChR2 group was willing to endure the electricity when entering the dual-paired side to receive stimulation, we analyzed the number of crossings that led to a minimum dual-paired interval of 3 seconds; this ensures that a subject will receive stimulation during each visit because the illumination pattern was a 3s train and 3s ITI. Electrifying the floor led to a decreased number of crossings into the dual-paired side that were longer than 3s (day effect: $F_{17,255} = 26.71$, $P < 0.001$) (Figure 3.24e). However, this occurred to a greater extent in the mC group compared with the ChR2 group (day x group interaction: $F_{17,255} = 4.06$, $P < 0.001$) (Figure 3.24e). The increased in time spent in the dual-paired compartment and increased number of crossings into the dual-paired compartment indicate that stimulation of the LPO is reinforcing, even if it does not drive increased time during standard RTPT procedures.

3.4.10 The LPO signals to aversive conditioning, but not rewarding conditioning

Given the complex effects of optogenetic stimulation of the LPO outlined above, we measured the activity of the LPO during rewarding and aversive events, using fiber photometry. To this end, we recorded the LPO during Pavlovian conditioning for sucrose and electric footshock. To record calcium signals with fiber photometry, we injected a viral vector encoding the calcium indicator, rAAV5-hSyn-GCaMP6f (GCaMP6f) into the LPO and implanted an optical fiber above the LPO. In order to measure selective increases in calcium activity, we recorded a 465nm GCaMP channel and a 405nm auto-fluorescent channel, and then looked for differential changes in these channels during behavior (Figure 3.27a-2); selective increases in the 465nm GCaMP channel will be referred to as calcium signals from this point forward. Prior to Pavlovian conditioning for sucrose, rats received

magazine training and pre-exposed to a 10s tone cue (76db, 3 kHz) that would later be paired with sucrose delivery (Figure 3.29b). Over the course of magazine training, rats acquired an association between the sound of the pellet delivery and the presence of sucrose pellets in the food port, as indicated by a progressively decreased latency from pellet delivery to port entry over training (day effect: $F_{5,25} = 17.73$, $P < 0.001$) (Figure 3.30a). For Pavlovian conditioning, rats were placed in a chamber, where they received 30 pairings of a 10s tone and sucrose pellet delivery (Figure 3.29e). Over the course of Pavlovian conditioning, rats acquired an association between the sound of the tone and the presence of sucrose pellets in the food port, as indicated by a progressively increased number of port entries during the tone compared with an equal length time prior to the tone (time period x day interaction: $F_{14,70} = 2.68$, $P = 0.0034$) (Figure 3.30b-c). After 12 days of Pavlovian conditioning, we recorded the activity of the LPO for 3 additional days of conditioning. In trained animals, the LPO did not exhibit calcium signals in response to the tone or sucrose delivery (channel x time interaction: $F_{2,10} = 2.79$, $P = 0.11$) (Figure 3.28a-b). This lack of time-locked LPO calcium signals was observed despite the presence of non-time-locked spontaneous transients (data not shown). Small reductions in both the GCaMP and auto-fluorescent channels were observed during the cue period of late Pavlovian conditioning (Figure 3.31**a**) which mirrored the time course of head entries into the food port throughout training (Figure 3.30**d**). However, there were no changes in time-locked LPO calcium signals throughout training (training stage x channel x time interaction: $F_{4,20} = 2.15$, $P = 0.11$) (Figure 3.31**a-b**). To test if the LPO may signal reward-prediction error, we ran rats through 3 more days of Pavlovian conditioning for sucrose where 10% of trials occurred without pellet delivery (omission) and 10% of trials occurred without the tone (unexpected). During this procedure, LPO calcium signals did not signal differentially based on expectancy during the post sucrose delivery bin but did show a trend towards that

effect (channel x expectancy interaction: $F_{2,10}$ = 3.89, P = 0.056) (Figure 3.31**c-d**). Importantly, there were small decreases in both channels that was time-locked to head entries into the food port which leads us to believe this trend is the consequence of movement artifact and not LPO calcium activity. Together, these results indicate that the LPO does not signal to sucrose or sucrose predicting cues.

Following Pavlovian conditioning for sucrose, rats were trained in Pavlovian conditioning for footshock over 3 days, in a different apparatus from the one used for Pavlovian conditioning for sucrose. Fear conditioning consisted of 5 pairings of a 20s tone (74 db, 5 kHz) with a co-terminating footshock (2s, 0.7 mA) (Figure 3.29g). We recorded the activity of the LPO for all 3 days of conditioning. In trained animals (day 3), LPO calcium signals increased in response to footshock predictive tones and trended towards an increase in calcium signals to footshock (channel x time interaction: $F_{2,10}$ = 11.06, P = 0.0029; HSD GCaMP channel pre vs tone: P < 0.001; HSD GCaMP channel pre vs shock: P = 0.052) (Figure 3.28c-d). When all 3 days of training were averaged, LPO calcium signals increased in response to both footshock predictive tones and footshock (channel x time interaction: $F_{2,10}$ = 11.06, P = 0.0012; HSD GCaMP channel pre vs tone: P < 0.001; HSD GCaMP channel pre vs shock: P < 0.001) (data not shown). The LPO calcium signal response to the tone developed throughout training, indicated by an increase in calcium response to the tone over days (channel x time x day interaction: $F_{4,20}$ = 4.13, P = 0.013, HSD GCaMP channel tone day 1 vs day 3: P < 0.001) (Figure 3.32c). These results indicate that the LPO signals in response to aversive events and to cues that predict the aversive events.

3.5 DISCUSSION

We found that the stimulating the LPO produces primarily inhibition on VTA_{GABA} neurons and mixed effects on $VTA_{Dopamine}$ neurons. We also found that the stimulation of the LPO cell bodies, regardless of where they project, produces similar effects as stimulation of the LPO→VTA pathway, suggesting that the LPO has the same downstream modulation of VTA neurons through both a direct projection and through intermediary structures. Our results also demonstrate that stimulation of the LPO, as well as the LPO→VTA pathway, supports ICSS responding but also produces aversion in the majority of rats within the real-time place testing assay. Importantly, we observed both ICSS responding and aversion in RTPT within the same rats. Despite the apparent contradiction, the behavior across these two assays was correlated, which suggests the two tests are measuring related behaviors. We analyzed the underpinnings of RTPT scores by assessing the correlation between the RTPT scores and the stimulation-intervals or inter-stimulation-intervals and found that the stimulation-intervals correlated more strongly with the ultimate RTPT score than do inter-stimulation-intervals. We hypothesized that stimulation of the LPO is reinforcing despite the lack of preference within RTPT and tested this by pairing the stimulation-paired side also with an aversive stimulus (electricity). We found that compared with controls, optogenetic stimulation of the LPO led to a greater amount of time spent in the dual-paired side and a greater number of crossings into the dual-paired side. Finally, we recorded the activity of the LPO during rewarding and aversive Pavlovian conditioning and found that the LPO increases activity in response to footshock and related predictive cues, but not sucrose and related predictive cues. Altogether, our results indicate that the LPO has a complex functional regulation of VTA neurons, generates a complex reward phenotype, and signals in response to aversive events.

We found that the LPO projection to the VTA is made of a higher proportion of GABA neurons compared to that of glutamate. This result contrasts with previous findings that the LPO projection to the VTA contains similar levels of GABA and glutamate neurons (Kalló et al., 2015). Relative to Kallo et al., we found similar proportions of LPO→VTA glutamate neurons but substantially more LPO→VTA_{GABA} neurons. There are several possible explanations for this discrepancy. First, it could be due to the *in-situ* probe for GABA. We used a probe for GAD-67, whereas Kallo et al. used a probe for GAD-65, and theses mRNAs have differential expression (Esclapez et al., 1993; Esclapez et al., 1994). Another explanation could be the anterior-posterior definition of the LPO. We found that there is a difference in the proportion of LPO→VTA neurons that are GABAergic and glutamatergic across the anterior-posterior extend of the LPO. Rostral to caudal there is a decrease in the proportion of GABA neurons and an increase in the proportion of glutamate neurons. Therefore, the difference between our work and Kallo et al, could be the anterior-posterior position of slices used. A final explanation could be the method used to label LPO→VTA neurons. We used a combinatorial viral approach while Kallo et al. used Choleratoxin B subunit. These methods could potentially lead to difference in labeling for glutamate and GABA neurons as CAV-2 has been shown to infect subsets of neurons in other brain systems (Li et al., 2018). Regardless of the source of the discrepancy in proportions, our results clearly support a mixed GABAergic and glutamatergic projection from the LPO to the VTA.

We determined that this mixed GABAergic and glutamatergic LPO→VTA primarily inhibits VTA_{GABA} neurons and produces mixed excitation and inhibition of $VTA_{Dopamine}$ neurons. This is in contrast with our previous finding (chapter 2 of this dissertation) that stimulation of the LPO with bicuculline leads to uniform inhibition of VTA_{GABA} neurons and uniform stimulation of $VTA_{Dopamine}$ neurons. One possible

explanation is that short term optogenetic stimulation is producing differential downstream effects when compared with longer term stimulation, produced pharmacologically. We tested this by recording VTA neurons during short term (1s) and long term (60s) stimulation. Interestingly, we found that long term stimulation led to sustained effects on VTA_{GABA} neurons but led to reduced effects in $VTA_{Dopamine}$ neurons. Importantly, we did not observe consistent reversals of effects, where neurons inhibited with short term stimulation were excited with long term stimulation. This leaves open the possibility that bicuculline stimulation and optogenetic stimulation are stimulating slightly unique populations of neurons. Bicuculline produces stimulation by disinhibiting neurons by antagonizing the GABA-A receptor, therefore it may be biased towards stimulating neurons that are under tonic inhibition, which could be a different population of neurons that are excited by ChR2. No matter what the underlying difference in the effect on $VTA_{Dopamine}$ neurons is, the results presented here indicate that the LPO is functionally connected to VTA neurons.

The LPO's ability to differentially modulate $VTA_{Dopamine}$ and VTA_{GABA} populations mirrors the functional connectivity of the lateral hypothalamus (Nieh et al., 2016). The lateral hypothalamus can regulate the activity of dopamine neurons through GABAergic interneurons of the VTA, where the lateral hypothalamus GABA projection inhibits VTA_{GABA} neurons and stimulates $VTA_{Dopamine}$ neurons, and the lateral hypothalamus glutamate projection inhibits $VTA_{Dopamine}$ neurons presumably through regulation of VTA_{GABA} neurons. Our results could be the product of a similar form of connectivity. However, the mixed effects on the activity of $VTA_{Dopamine}$ neurons and the consistent effect on $VTA_{Dopamine}$ neurons suggest that the LPO must make direct functional connections with $VTA_{Dopamine}$ neurons; if the LPO only regulated $VTA_{Dopamine}$ through VTA_{GABA} then we should have observed excitation of VTA_{GABA} in order to explain the

decrease in $VTA_{Dopamine}$ activity. Further monosynaptic electrophysiology experiments will be necessary to determine the precise circuit underlying the functional connectivity between the LPO and VTA.

In a subset of neurons, we were able to record the response to both stimulation the LPO and LPO→VTA pathway. We found that both manipulations led to similar results, indicating that the stimulation of the LPO with all projections intact and stimulation of LPO→VTA pathway produces the same downstream effect on the VTA. We further verified the effects of LPO→VTA pathway stimulation using a combinatorial viral approach which selectively manipulates LPO neurons that project to the VTA. Overall, we observed similar results across LPO, LPO→VTA pathway, and LPO cell body stimulation of the LPO→VTA pathway (combinatorial viral approach). These finding suggests that the LPO sends redundant projections to intermediary structures, possibly the LHb and RMTg (Yetnikoff et al., 2015), that produce the same net effect in the VTA. Alternatively, when stimulating the LPO, the LPO→VTA pathway may short-circuit differential effects carried out by intermediary structures. The similarity in effects observed after stimulating the LPO and LPO→VTA pathway was also replicated in our behavioral assays. Together, these results indicate that the LPO and LPO→VTA pathway modulates the activity of VTA subpopulations.

We observed that optogenetic stimulation of the LPO was reinforcing with both short and long stimulation durations. Previous research demonstrated that stimulating the LPO with electricity supports intracranial self-stimulation (Fouriezos et al., 1987). However it was not clear if LPO cell bodies or fibers of passage supported ICSS behavior, because electrical stimulation of the LPO may be contaminated by stimulation of the medial forebrain bundle that passes through the LPO; thus, we are the first to demonstrate that neurons of the LPO themselves support ICSS responding. Furthermore, we found that

animals dynamically shifted their behavior with changes in reward duration: increases in reward duration lead to a decreased responding under a fixed-ratio 1 schedule, but led to increased responding under a progressive-ratio schedule. These results mirror what is seen with drugs of abuse, where increasing the reward size can simultaneously lead to decreases in fixed-ratio responding and increases in progressive-ratio responding (Arnold and Roberts, 1997). Interestingly, we did not observe a drop in progressive-ratio responding with stimulations all the way up to 300 seconds in duration. This may indicate a lack of the prototypical "inverted-U" relationship seen with drugs of abuse (Roberts and Bennett, 1993; Rowlett et al., 1996) or it could indicate that increases in reward durations past a threshold are not perceived by the animal. One possible caveat with the progressive-ratio result is that we tested subjects through ascending stimulation durations rather than using a Latin squared design. This was done by design, in order to determine if there was a transition from reward to aversion as the duration was increased, which was not observed. However, the increase in responding for longer stimulation durations could stem from changes over the course of operant conditioning independent of changes in reward value. Indeed, rats received significantly longer total stimulation durations when the stimulation duration during progressive-ratio for 1s at the end of training then they received during 1s at the start of training. Even still, our results with fixed-ratio and progressive-ratio indicate that stimulation of the LPO and LPO→VTA pathway is reinforcing across stimulation durations up to 300s long.

We also found that stimulating the LPO→VTA pathway is less reinforcing than stimulating LPO cell bodies, because the same subjects increased responding when stimulation was switched from the LPO→VTA pathway to LPO cell bodies. A possible reason for lower stimulation rates in the LPO→VTA pathway compared with the LPO is that we are not simulating as many LPO→VTA terminals with optic fibers in the VTA as

we do with optic fibers in the LPO. Another possibility is that stimulation of LPO cell bodies leads to stronger modulation of the VTA as our electrophysiological experiments indicate. Alternatively, the LPO could produce ICSS behavior through different pathways that don't rely on $VTA_{Dopamine}$ activity (Britt et al., 2012). Our results are also the first to demonstrate that stimulation of the LPO→VTA pathway supports ICSS, which contradicts previous findings (Gigante et al., 2016). This could stem from the viral vector used for stimulation. Gigante et al. used a CaMKII promotor, while we used an h-Syn promoter. These may lead to differential targeting that could produce differential downstream regulation of $VTA_{Dopamine}$ neurons. Another more likely possibility could be that the stimulation frequency used: Gigante et al. used 20Hz stimulation while we used 40Hz stimulation. With stimulation of LPO cell bodies, we found that 20Hz stimulation produced lower ICSS responding that 40Hz stimulation (Figure 3.8a-c). Given that the LPO→VTA pathway stimulation with 40Hz was lower than LPO cell body stimulation at 40Hz, it stands to reason that LPO→VTA pathway stimulation with 20Hz could be bellow the necessary stimulation for ICSS reinforcement.

We found that stimulation of the LPO and LPO→VTA pathway produced bidirectional effects in RTPT but primarily produced aversion. Overall, stimulating the LPO and LPO→VTA pathway, on average, produced a reduction in time spent in the optically paired side without consistently changing the number of crossings. However, at the single subject level, stimulation of the LPO and LPO→VTA pathway produced mixed effects, where the majority of subjects showed clear aversion while a minority showed clear preference. The mixture valence produced by stimulating the LPO and LPO→VTA pathway in the RTPT assay could be due to differential functional connectivity of the LPO across animals. Previous research has demonstrated that stimulation of the LPO→lateral habenula glutamate pathway produces real-time place aversion, while stimulation of

GABA pathway produces real-time place preference (Barker et al., 2017). The capacity of the LPO to mediate opposite effects on valence depending on weather glutamate or GABA neurons are stimulated grants the possibility that differences in the balance of connectivity of glutamate and GABA neurons across subjects can explain differences in valence. The difference in valence we observed are unlikely to stem from regional differences in stimulation, as the location of the probe did not correlate with RTPT effects. While the underlying mechanism explaining the bidirectional effects within the RTPT assay are unclear, we have demonstrated that stimulation of the LPO is aversive in the majority of subjects.

How can stimulation be reinforcing within ICSS but aversive in RTPT? One possibility is that the behavior underlying RTPT is more nuanced than previously thought. The standard metric used to determine if a neuronal manipulation is rewarding or aversive in RTPT is the amount of time spent in the optically paired side. However, our results indicate that time spent in the paired side in the RTPT task may not be sufficient to determine if a neuronal manipulation is rewarding or aversive. Many researchers have found that different neuronal manipulations contribute to RTPT effects but not ICSS effects, or vice versa. To our knowledge, Yoo et. al. 2016 is the only published paper that found aversion in RTPT and mild reinforcement with ICSS with the same brain system (Yoo et al., 2016). In their paper, the authors found that stimulating glutamate neurons in the VTA supports mild ICSS behavior but leads to a reduction in time spent in the optically paired side in the RTPT task. They also found large increases in the number of crossings made into the optically paired side and a decrease in stimulus durations, which was interpreted as mice displaying a self-stimulation behavior for preferred short stimulations. In our study, we also observed ICSS and aversion in RTPT, however we did not observe consistent increases in crossings into the stimulation-paired side, as we only observed an

increased crossing rate in one group of animals (cohort 1). An explanation for observing both aversion in RTPT and responding in ICSS is that stimulation is reinforcing despite not producing positive valence. This hypothesis is backed up by our finding that the duration of stimulation durations, but not inter-stimulation-intervals the RTPT behavior (RTPT score): subjects showed similar re-entry latencies (poor correlation of inter-stimulation-interval with the RTPT score) but lingered in the stimulation side for different durations (strong correlation of stimulation-interval with the RTPT score). Furthermore, in the RTPT experiment where we used dual-pairing of both laser stimulation and electricity, rats continued to enter the dual-paired side despite the adversity produced by the electricity. If stimulating the LPO is reinforcing despite not being rewarding, then an aversive RTPT score could be the result of subjects being continually reinforced to enter the paired side, but exiting once stimulation transitioned to being aversive. One remaining complexity is the lack of aversion with long duration stimulation within the progressive-ratio experiment. However, in this assay the stimulation duration is set by the experimenter, not the subject, which could produce different behavior.

We found that the LPO does not provide tonic regulation of valence or reinforcement, as bilateral inhibition of the LPO with HR produced no effects in both RTPT and ICSS tests. This may indicate that the LPO's regulation of valence and reinforcement is evoked under specific contexts instead of being a consistent baseline regulator. Interestingly, in this experiment, we observed a slight preference in RTPT for both the HR group and in controls; this preference was not consistently observed in the ChR2 experiments. This could be due to effects stemming from continuous light illumination that employed in HR experiments. Recent research indicates that continuous light pulses can modulate the activity of striatal neurons (Owen et al., 2019). Regardless of the baseline

effects stemming from the general experimental procedure, inhibition of the LPO produced no further effect.

Our recording experiments revealed that the LPO had time-locked population signals to aversive events but not rewarding ones. We found that the LPO increases activity in response to footshock, and that the LPO increases in activity in response to a tone which predicts footshock. On the other hand, the LPO showed no meaningful time-locked effects in response to sucrose or sucrose predictive cues. These results largely replicate results obtained from recording the calcium activity of the LPO to lateral habenula pathway (Barker et al., 2017) which found that the LPO glutamate and GABA projection to the lateral habenula was excited by aversive events and related predictive cues but not rewarding events and related predictive cues. The lack of response to rewarding events or their predictive cues was not due to a lack of conditioning, because subjects showed behavioral conditioning. We observed small changes in fluorescence during the Pavlovian conditioning task for sucrose, however these reductions were observed in both the 465nm GCaMP channel and auto-fluorescent channel and largely mirrored head entry behavior. This leads us to believe the reductions were most likely due to movement artifacts rather than being real differences in population activity within the LPO. Together the Pavlovian conditioning results indicate that the LPO may be involved in responses to aversive events rather than rewarding events. Given the effects on reinforcement, it could be the case that activity in the LPO could reinforce behaviors necessary to avoid or escape aversive events. The finding from chapter 1 demonstrated that both inhibition and stimulation of the LPO using pharmacology during punishment blocks the ability of punishment to drive lasting reductions in responding. Our current results provide evidence that the LPO signals during aversive events, which suggests that it could naturally influence the response to these events.

One important consideration in our experiments is the possible ambiguity of precisely which neurons were stimulated in our experiments. For all the experiments we targeted the LPO using viral injections paired with fibers overlaying the LPO or VTA. Even with the small viral injections (165-180 nL), there was almost always some expression in neighboring brain regions. We used the fiber placement as the primary factor for including or excluding animals from our experiments because optogenetic ion channels are only activated when illuminated. Even though the majority of neuronal manipulations should occur under the fiber tip (Cole et al., 2018), we cannot exclude the possibility that we are also manipulating fibers of passage of other, unintended brain regions that express ChR2. In the future more precise targeting could be used to determine the exact neuronal populations that underlie our effects.

In conclusion, our results demonstrate that the LPO and the LPO→VTA pathway are functionally connected to the activity of $VTA_{Dopamine}$ and VTA_{GABA} neurons. Stimulating the LPO and LPO→VTA pathway inhibits VTA_{GABA} neurons and both stimulates and inhibits $VTA_{Dopamine}$ neurons. We also demonstrated that stimulation of the LPO and LPO→VTA pathway supports ICSS but also drives aversion, indicating that the LPO can regulate reinforcement and affective valance. Finally we demonstrated that the LPO signals in response to aversive events but not rewarding events. Altogether these results indicate that the LPO is a player within the reward circuit and warrant further research into how it regulates behavior.

3.6 Figures and Figure Legends

Figure 3.1 The LPO sends GABA and glutamate projections to the VTA

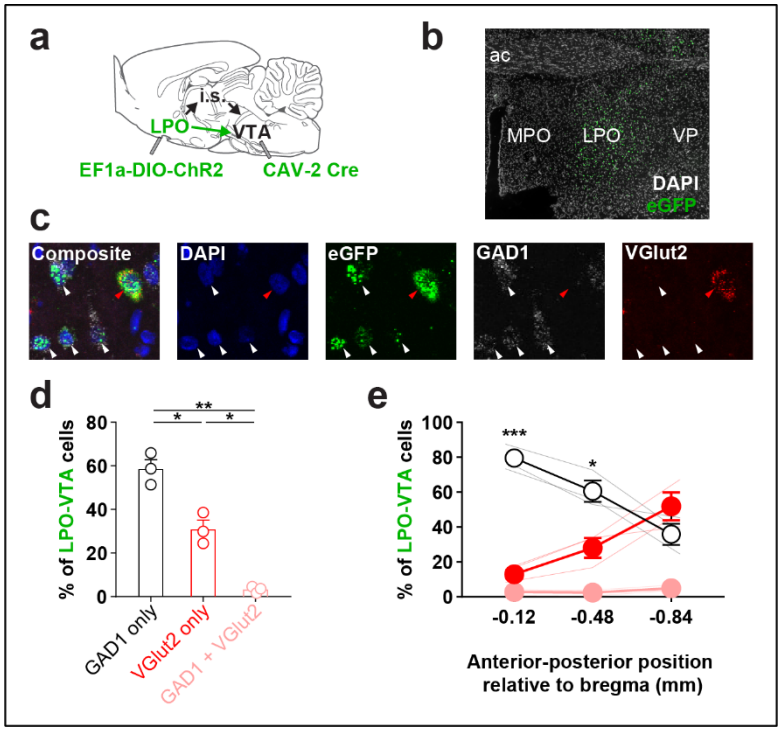

(a) Diagram of approach: to express a fluorescent marker selectively in LPO→VTA neurons we injected EF1a-DIO-ChR2 in the LPO and CAV-2 Cre in the VTA. **(b)** Representative fresh-fluorescence image of eGFP expression in the LPO. **(c)** The neurotransmitter identity of LPO→VTA neurons was determined using *in-situ* fluorescent hybridization for eGFP, GABA (GAD1), and glutamate (VGlut2). From left to right: composite image of all markers, and images of DAPI, eGFP, GAD1, and VGlut2; white arrows indicate eGFP + GAD1 only neurons, red arrow indicates eGFP + VGlut2 only neuron. **(d)** Overall, the LPO→VTA pathway contains a greater proportion of GAD1 expressing cells compared with VGlut2 expressing cells and only contains a small population of dual GAD1 + VGlut2 expressing cells (HSD, **: $P < 0.01$; *: $P < 0.05$). **(e)** The relative proportion of GAD1 and VGlut2 within the LPO→VTA pathway varies across the rostral to caudal extent of the LPO. The percent of LPO→VTA neurons expressing GAD1 was greater than the percent that expressed VGlut2 in more rostral portions of the LPO (GAD1 only vs. VGlut2 only, HSD, ***: $P < 0.001$; *: $P < 0.05$). Abbreviations for (a-b): LPO: lateral preoptic area; VTA: ventral tegmental area; i.s.: intermediary brain structures (i.e. structures that connect the LPO to the VTA); ac: anterior commissure; MPO: medial preoptic area; VP: ventral pallidum). In (d), points depict percentages of individual subjects; bars and error bars depict group mean and SEM, respectively. In (e), faded lines depict values of individual subjects; points and error bars depict mean and SEM, respectively.

Figure 3.2 Validation of ChR2 mediated stimulation of LPO neurons

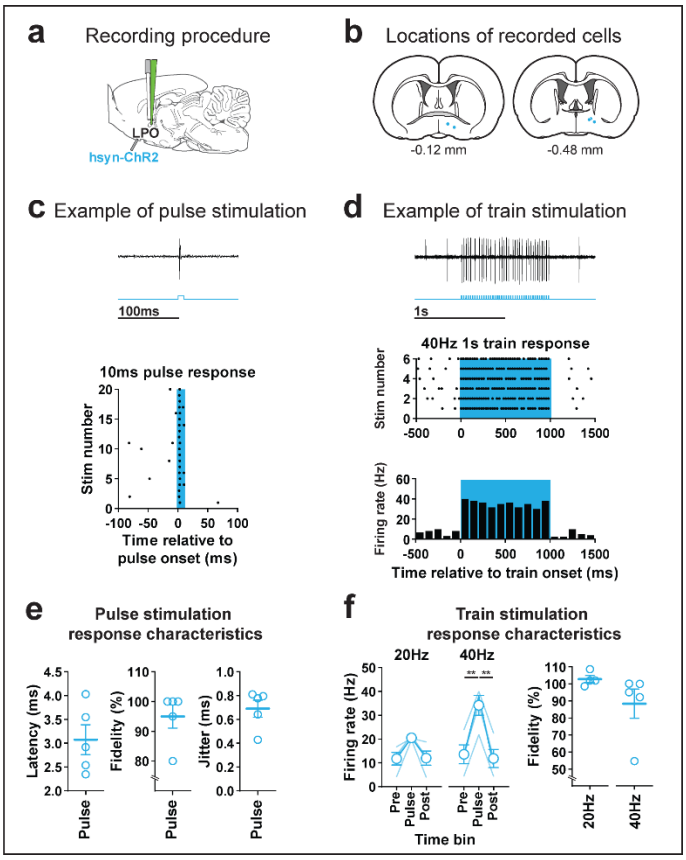

(a) Recording procedure: we injected hsyn-ChR2 in the LPO and recorded the activity of neurons in the LPO using an optrode. **(b)** Location of recorded neurons within the LPO. **(c)** Example of single neuron responding to 10ms 0.2Hz stimulation. Top: extracellular trace of the response to a single stimulation pulse; bottom: raster plot of spikes in response to 20 pulses, each dot represent a single action potential. **(d)** Single neuron example of response to 1s, 40 Hz stimulation, 5ms pulses. Top: extracellular trace of the response to a single stimulation train; middle: raster plot of spikes in response to 6 trains; bottom: peristimulus time histogram showing firing rate in each 100ms time bin for raster plot shown above. **(e)** Response characteristics for pulse stimulation including the latency from pulse onset to action potential, fidelity (percent of pulses that resulted in an action potential), and the action potential jitter (sd of action potential latency). Points depict values from individual subjects; lines and error bars depict mean and SEM, respectively. **(f)** Response characteristics for train stimulation including the firing rate in response to 20Hz and 40Hz trains (Pre: 2s prior to train onset, Pulse: 1s train, Post: 2s following train offset) and fidelity in response to 20Hz and 40Hz trains. Stimulation trains led to increased firing rate (time effect: $F_{2,4} = 498.16$, $P < 0.001$; pulse train frequency effect: $F_{1,4} = 3.93$, $P = 0.18$; interaction: $F_{2,4} = 4.22$, $P = 0.10$). (HSD, ***: $P < 0.001$; **: $P < 0.01$). Lines depict values from individual subjects; points and error bars depict mean and SEM, respectively.

Figure 3.3 The LPO and LPO→VTA pathway modulates VTA subpopulations

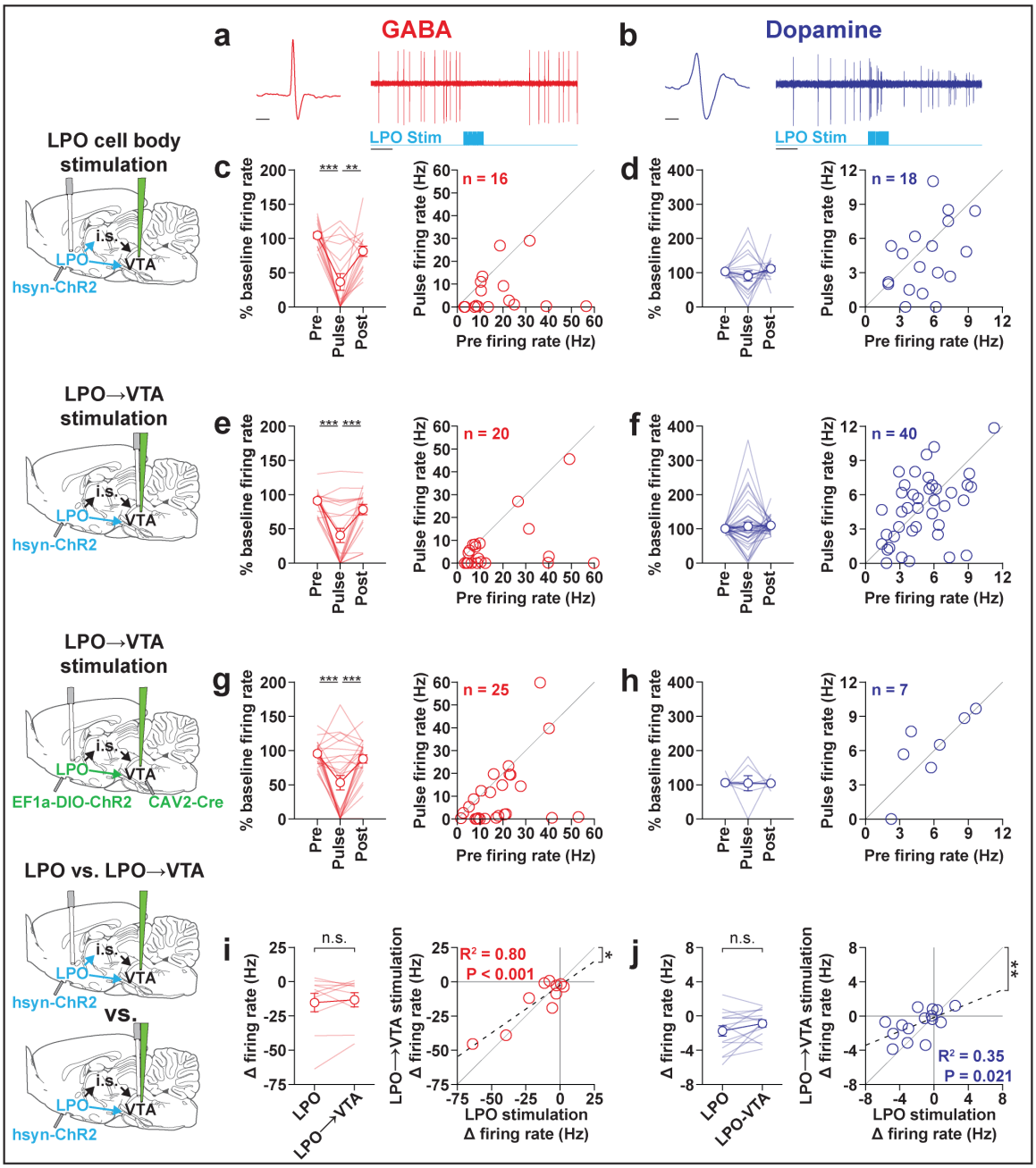

(a) Representative VTA_{GABA} neuron (red) during stimulation of the LPO showing the extracellular waveform (left) and inhibitory response to laser stimulation of the LPO (1s, 40Hz, 5ms pulses, 20mW) (right). **(b)** Representative $VTA_{Dopamine}$ neuron (blue) during stimulation of the LPO showing the extracellular waveform (left) and stimulatory response to laser stimulation of the LPO (1s, 40Hz, 5ms pulses, 20mW) (right). General format for **(c-h)**: Left plot: binned firing rate expressed as percent of baseline firing (10s prior to first

train) across peri-stimulation time bins (Pre: 2s bin prior to stimulation, Pulse: 1s bin during stimulation, Post: 2s bin following stimulation offset) (HSD, ***: $P < 0.001$; **: $P < 0.01$); Right plot: scatter plot of Pre vs. Pulse bin firing rate (Hz); the diagonal grey line is the identity line (i.e. slope = 1) and represents no change during stimulation. **(c-d)** In rats previously injected with hSyn-chR2 into the LPO, stimulating LPO cell bodies inhibited VTA_{GABA} neurons **(c)** and had mixed effects on $VTA_{dopamine}$ neurons **(d)**. **(e-f)** In rats previously injected with hSyn-chR2 into the LPO, stimulating the LPO→VTA pathway inhibited VTA_{GABA} neurons **(e)** and had mixed effects on $VTA_{dopamine}$ neurons **(f)**. **(g-h)** In rats previously injected with CAV-2 Cre into the VTA and EF1a-DIO-ChR2 into the LPO, stimulating cell bodies of the LPO→VTA pathway inhibited VTA_{GABA} neurons **(g)** and had mixed effects on $VTA_{dopamine}$ neurons **(h)**. General format for **(i-j)**: Left plot: change in firing rate (Pulse - Baseline) produced by stimulation of the LPO and LPO→VTA pathway (HSD, n.s.: $P > 0.05$). Right plot: scatter plot of change in firing rate produced by stimulation of LPO neuron bodies vs change in firing rate produced by stimulation of the LPO→VTA pathway; the diagonal grey line is the identity line and represents no difference in change in firing produced by the two stimulation configurations. **(i)** Stimulation of LPO and LPO→VTA pathway had similar effects on VTA_{GABA} neurons (left), although there was a slightly smaller magnitude of effect with stimulation of the LPO→VTA pathway (correlation slope vs slope of 1 (right): *: $P<0.05$). **(j)** Stimulation of the LPO and LPO→VTA pathway had similar effects on $VTA_{dopamine}$ neurons (left), although there was a smaller magnitude of effect with stimulation of the LPO→VTA pathway (right) (correlation slope vs slope of 1: **: $P < 0.01$). In line plots, faded lines depict values of individual subjects; points and error bars depict mean and SEM, respectively. Abbreviations for brain diagrams: LPO: lateral preoptic area; VTA: ventral tegmental area, i.s.: intermediary structures (i.e. structures that connect the LPO to the VTA).

Figure 3.4 Location of neurons within the VTA does not correlate with effect of LPO and LPO→VTA pathway stimulation

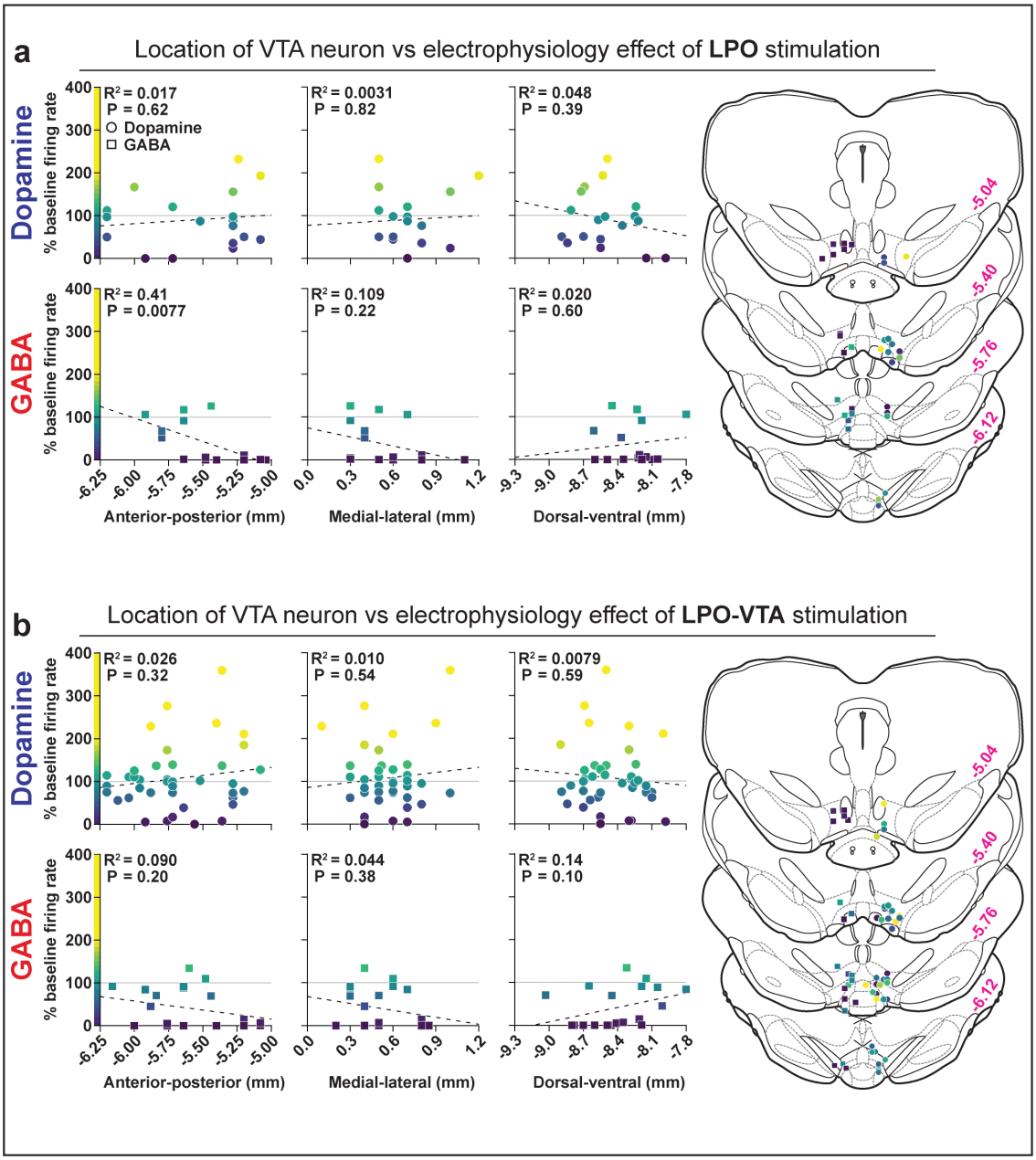

(a) Correlation between location of recorded neurons within the VTA and effects on firing rate of $VTA_{Dopamine}$ and VTA_{GABA} neurons produced by stimulating the LPO. The anterior-posterior (left), medial-lateral (middle), and dorsal-ventral (right) location of $VTA_{Dopamine}$ neurons (top row) and VTA_{GABA} neurons (bottom row) did not correlate with the change in firing rate produced by stimulating the LPO. The one exception was the anterior-posterior location of GABA neurons, which showed a greater inhibition in the rostral

portions of the VTA. Inset shows the back-calculated location of neurons within the VTA. For all plots in (a), the color of points indicates the effect of LPO stimulation (scale depicted on the left side of the scatter plots; yellow: excited, purple inhibited). **(b)** Correlation between location of recorded neurons in the VTA and effects on firing rate of $VTA_{Dopamine}$ and VTA_{GABA} neurons produced by stimulating the LPO-VTA pathway. The anterior-posterior (left), medial-lateral (middle), and dorsal-ventral (right) location of $VTA_{Dopamine}$ neurons (top) and VTA_{GABA} neurons (bottom) did not correlate with the change in firing rate produced by stimulating the LPO→VTA pathway. Inset shows the back-calculated location of neurons within the VTA. For all plots in (b), the color of points indicates the effect of LPO→VTA pathway stimulation (color scale is depicted on the left side of the scatter plots; yellow: excited, purple inhibited).

Figure 3.5 Placement of optic fibers in the LPO does not correlate with effect of LPO stimulation

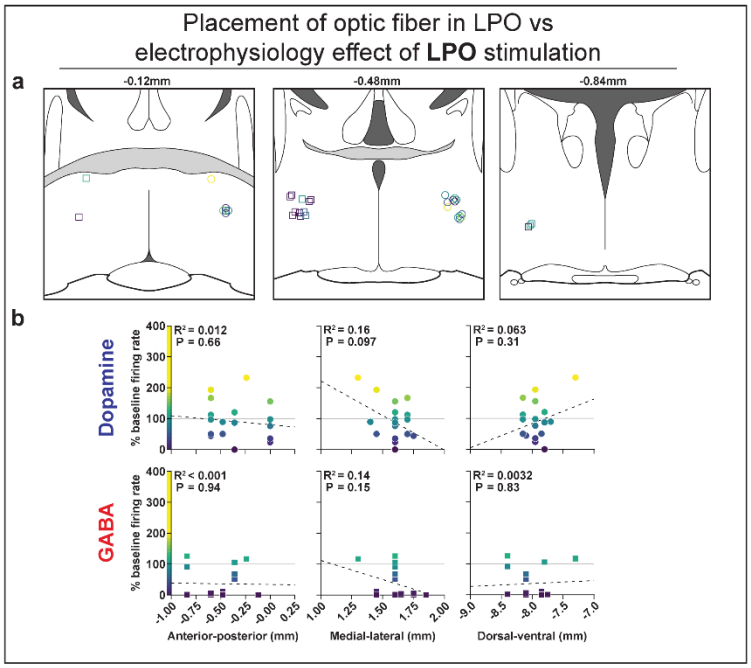

(a) Placement of the optic fibers within the LPO. Jitter was added to prevent overlap of optic fiber position when multiple cells were recorded for a single fiber position. **(b)** Correlation between placement of the optic fibers in the LPO and effects on firing rate. The anterior-posterior (left), medial-lateral (middle), and dorsal-ventral (right) placement of the optic fiber within the LPO did not correlate with effects on $VTA_{Dopamine}$ neurons (top row) and VTA_{GABA} neurons (bottom row). For all plots, the color of points indicates the effect of LPO stimulation (color scale is depicted on the left side of the scatter plots; yellow: excited, purple inhibited).

Figure 3.6 Comparison of long and short trains for optogenetic stimulation of the LPO and LPO→VTA pathway

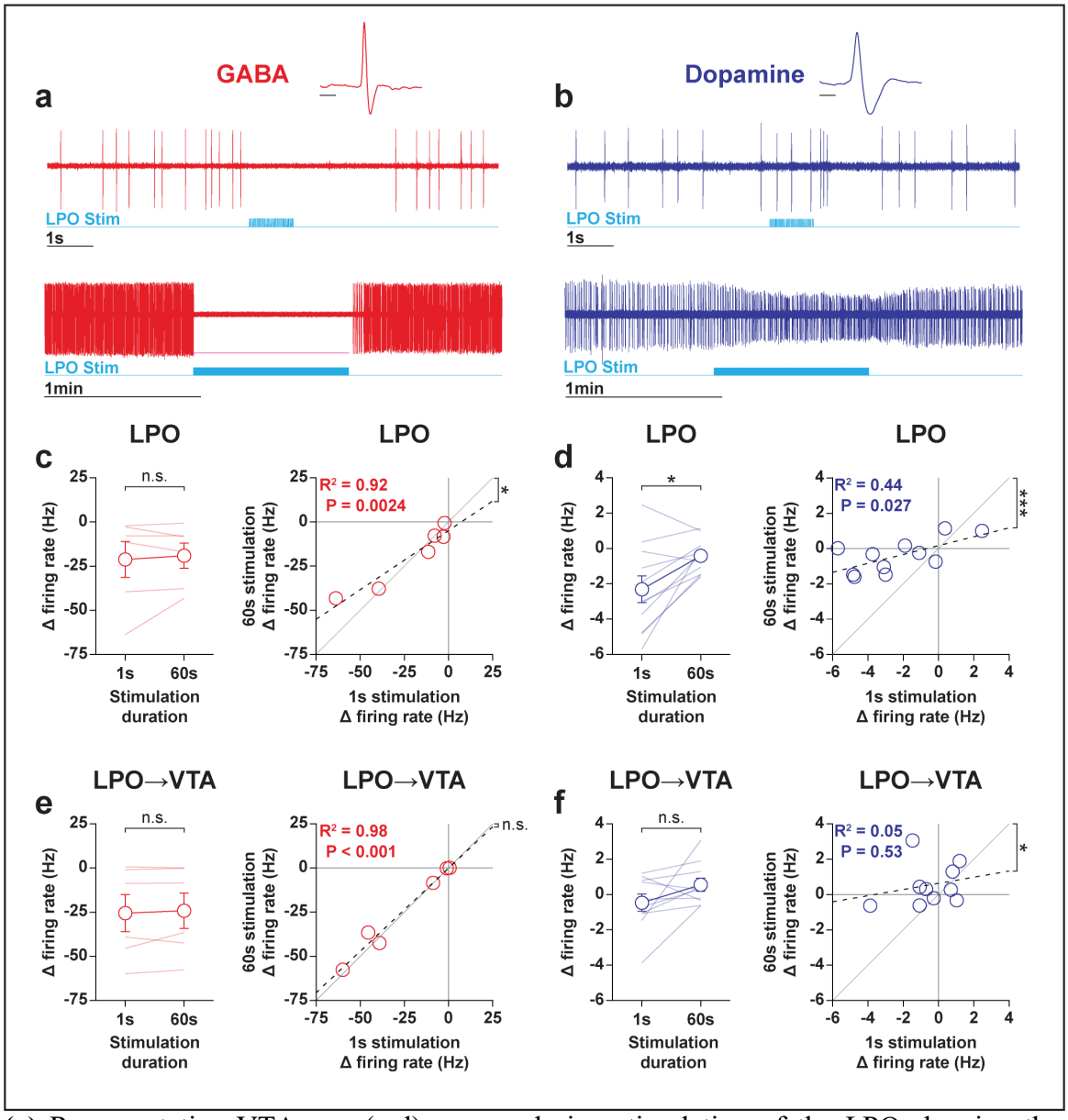

(a) Representative VTA_{GABA} (red) neuron during stimulation of the LPO showing the extracellular waveform and inhibitory response to LPO laser stimulation (40Hz, 5ms pulses, 20mW) during a 1s train (top), and 60s train (bottom). **(b)** Representative $VTA_{Dopamine}$ (blue) neuron during stimulation of the LPO showing the extracellular waveform and excitatory response to LPO laser stimulation during a 1s train (top), and 60s train (bottom). General format for **(c-f)**: left plot: line plot depicting change in firing rate during the 1s train relative to the 10s baseline prior to the first stimulation train for 1s and 60s stimulation durations (*: *t*-test, $P < 0.05$); right plot: scatter plot depicting the

relationship and correlation between the change in firing for 1s and 60s stimulation durations (slope vs. slope of 1: ***: $P < 0.001$; *: $P < 0.05$; n.s.: $P > 0.05$). **(c)** 1s and 60s stimulation of the LPO had similar effects on VTA_{GABA} neurons (left), although there was a slightly smaller magnitude of effect for 60s stimulation, as indicated by a slope less than 1 (right). **(d)** Compared with 1s stimulation, 60s stimulation of the LPO produces higher firing rates for $VTA_{Dopamine}$ neurons (left), and produced a reduced magnitude of effect as indicated by a slope less than 1 (right). **(e)** 1s and 60s stimulation of the LPO→VTA pathway had similar effects on VTA_{GABA} neurons (left), and produced a similar magnitudes of effects, as indicated by a slope not different than 1 (right). **(f)** 1s and 60s stimulation of the LPO→VTA pathway had similar effects on $VTA_{Dopamine}$ neurons (left), although there was a slightly smaller magnitude of effect for 60s stimulation, as indicated by a slope less than 1 (right). In line plots, faded lines depict values of individual subjects; points and error bars depict mean and SEM, respectively.

Figure 3.7 The LPO supports intracranial self-stimulation

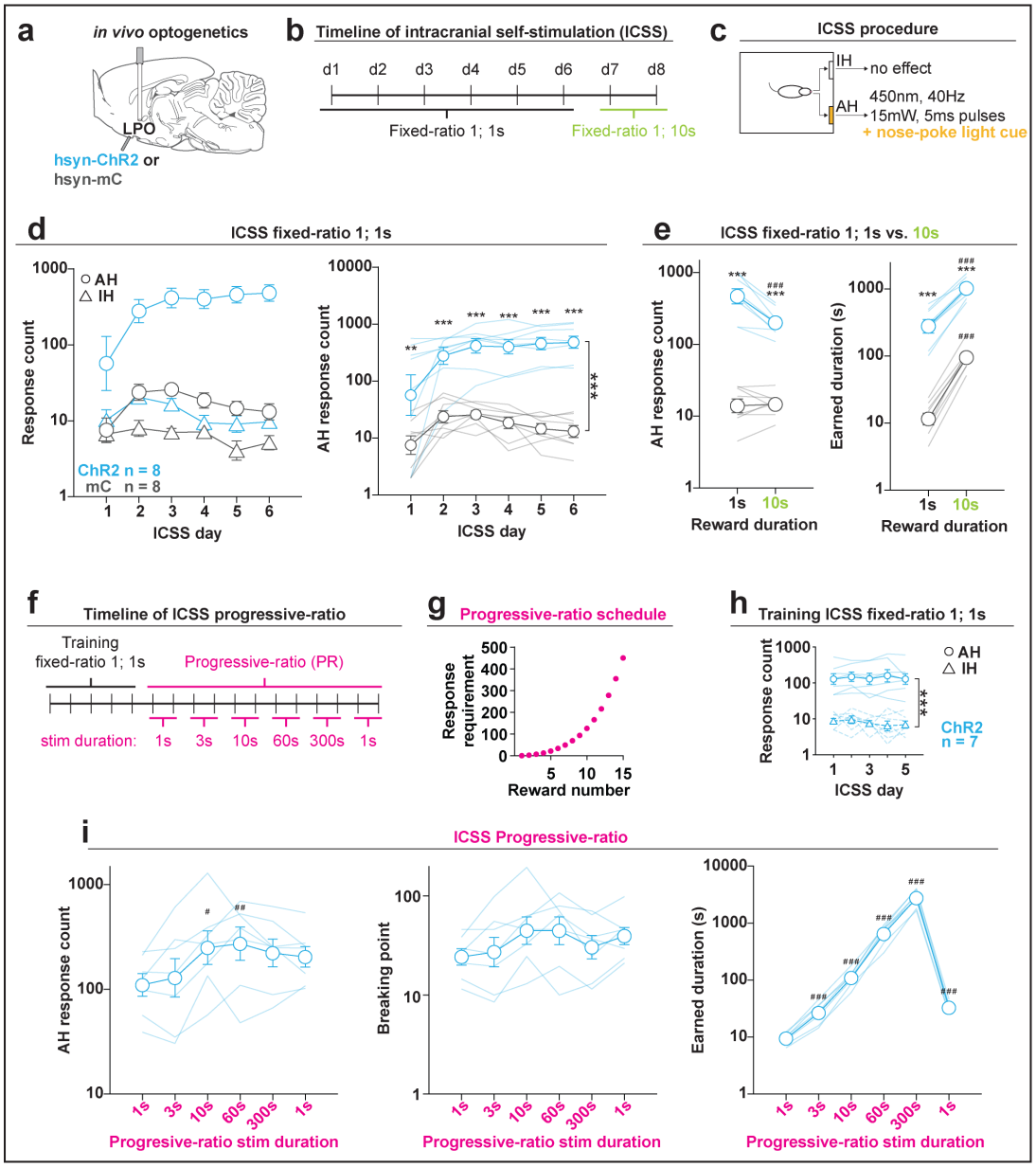

(a) *in-vivo* optogenetics setup: we injected either hsyn-ChR2 (ChR2) or hsyn-mCherry (mC) in the LPO and implanted an optic fiber overlaying the injection site. **(b)** Timeline of intracranial self-stimulation (ICSS) testing. **(c)** Illustration of the ICSS procedure. **(d)** Self-administration behavior during ICSS fixed-ratio 1, for stimulation duration of 1s. Left: ChR2 (blue) and mC (grey) rats showed differential discrimination between the active hole (circles) and inactive hole (triangles); right: the ChR2 group made more active hole responses then the mC group throughout ICSS (***: group effect: $F_{1,14} = 68.74$, $P < 0.001$). **(e)** Active hole responses over the last two days of responding for 1s stimulation and two

days of responding for 10s stimulation. The ChR2 group decreased active hole responding, while mC did not (left). Both groups increased the total earned stimulation duration, however rats in the mC group increased to a greater degree (right). **(f)** Timeline of progressive-ratio testing. **(g)** Progressive-ratio schedule: the cost for each subsequent reward was increased in a semilogarithmic fashion. **(h)** Training in ICSS fixed-ratio 1 for 1s stimulation prior to progressive-ratio. Rats discriminated between active and inactive holes (***: hole effect: $F_{1,6} = 164.07$, $P < 0.001$). **(i)** Self-administration behavior during progressive-ratio indicated that increasing the duration of the stimulation led to an increase in active hole responding (left), break point (mid), and stimulation duration (right). Throughout the figure, active hole responses, inactive hole responses, break point, and earned stimulation duration are shown on a log scale; (HSD ChR2 vs mC, **: $P < 0.01$, ***, $P < 0.001$; HSD vs. 1s, #: $P < 0.05$, ## $P < 0.01$, ### $P < 0.001$); In (d-e) and (h-i), faded lines depict values of individual subjects; points and error bars depict mean and SEM, respectively.

Figure 3.8 The LPO supports intracranial self-stimulation responding across cohorts and stimulation parameters

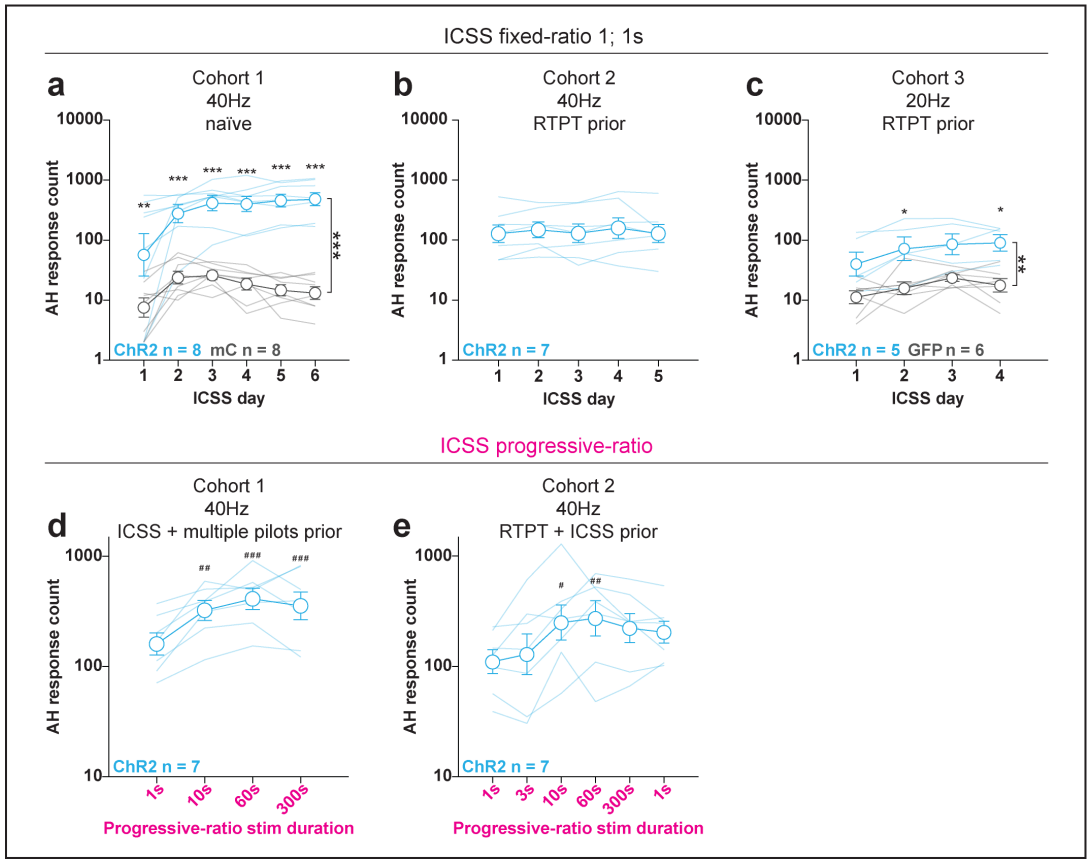

(a-c) Active hole responses during intracranial self-stimulation (ICSS) at a fixed-ratio1 for 1s stimulation in 3 separate cohorts of rats. **(a)** Prior to ICSS, Cohort 1 did not undergo any behavioral procedures. The ChR2 group made more active hole responses than the mC group throughout the ICSS procedure (group x hole interaction: $F_{1,15} = 50.28$, $P < 0.001$). **(b)** Prior to ICSS, Cohort 2 underwent RTPT with 40Hz 3s trains and 3s inter-train intervals. Data are shown for comparison to other cohorts. **(c)** Prior to ICSS, Cohort 3 underwent RTPT with 20Hz continuous stimulation. The ChR2 group made more active hole responses than the mC group throughout the ICSS procedure (group x hole interaction: $F_{1,10} = 15.71$, $P = 0.0027$). **(d-e)** Active hole responses during ICSS in a progressive ratio schedule in 2 separate cohorts. **(d)** Prior to PR, Cohort 1 underwent RTPT and multiple pilot experiments. The ChR2 group made more responses for longer stimulation durations compared with the shorter (1s) stimulation duration. **(e)** Prior to PR, Cohort 2 underwent RTPT and ICSS training. The ChR2 group made more responses for longer stimulation durations compared with the shorter (1s) stimulation duration. (HSD ChR2 vs mC, **: $P < 0.01$, ***, $P < 0.001$; HSD vs. 1s, #: $P < 0.05$, ## $P < 0.01$, ### $P < 0.001$); in (a-e), faded lines depict values of individual subjects; points and error bars depict mean and SEM, respectively.

Figure 3.9 Placement of optic fiber placements for optogenetic stimulation of LPO cell bodies

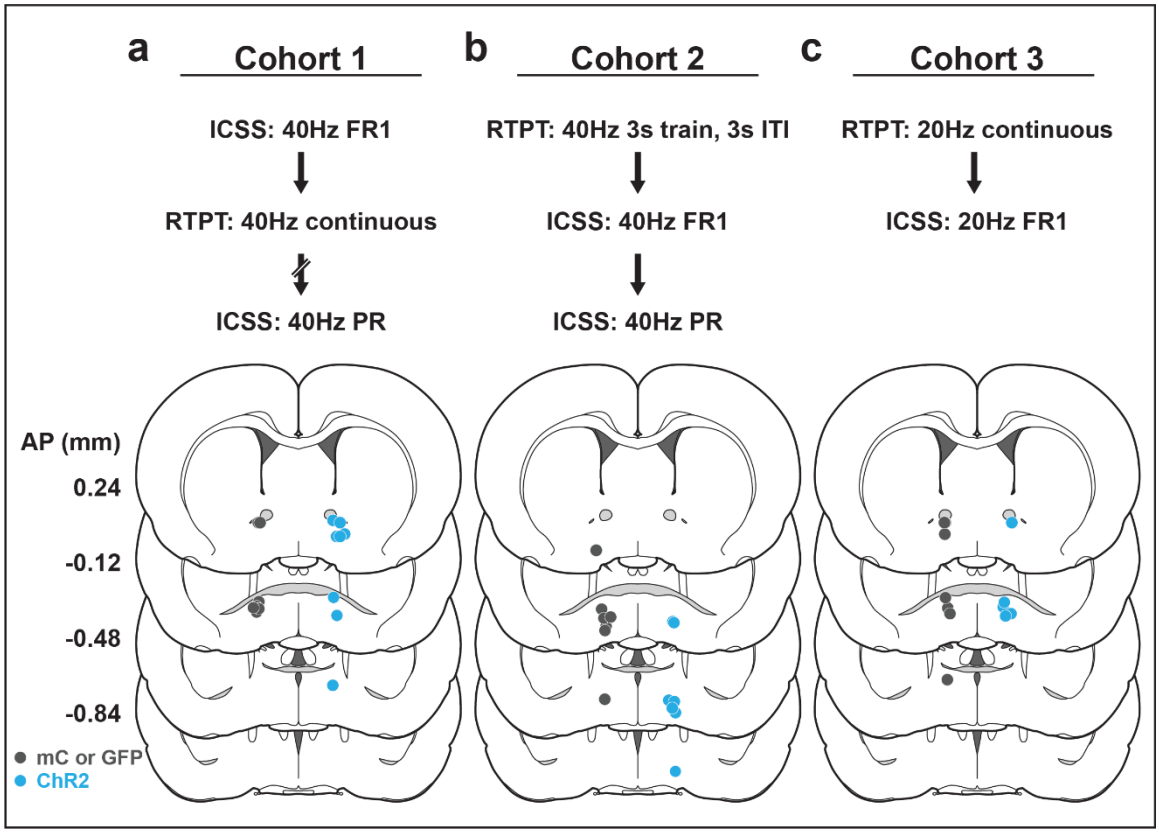

(a-c) Order of experimental procedures (top) and placement of optic fibers within the LPO (bottom) for ICSS and RTPT experiments stimulating LPO cell bodies in the mCherry or GFP group (grey) or the ChR2 group (blue). Cohort descriptions can be found the main body of the text (results and figure legends). All placements were on the right side of the brain.

Figure 3.10 Placement of optic fibers in the LPO does not correlate with ICSS responding

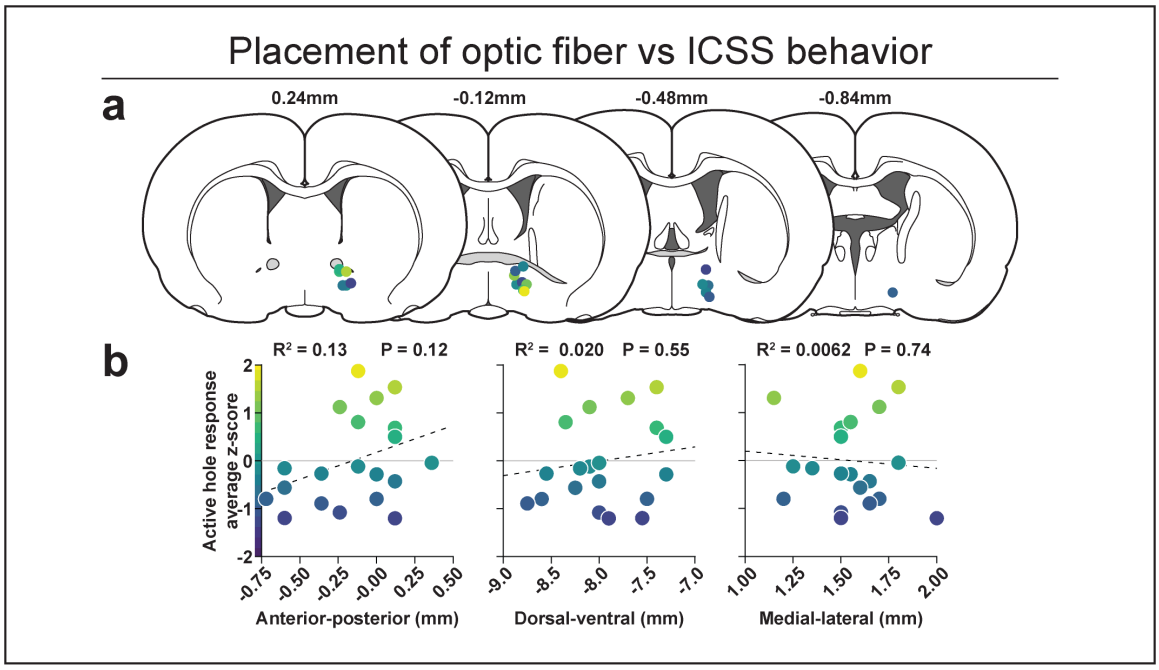

(a) Placement of optic fibers within the LPO. **(b)** Correlation between placement of the optic fibers in the LPO and response rates in ICSS. The anterior-posterior (left), medial-lateral (middle), and dorsal-ventral (right) placement of the optic fiber within the LPO did not correlate with ICSS responding (z-score of the mean response count during the last three days of ICSS). Data points are combined from cohorts 1-3 and z-scores were calculated within each experiment in order to normalize across stimulation parameters. For all plots, colors depict the magnitude of ICSS (color scale is depicted on left side of scatter plots; yellow: high responding, purple low responding).

Figure 3.11 The LPO promotes real-time place aversion in the majority of rats

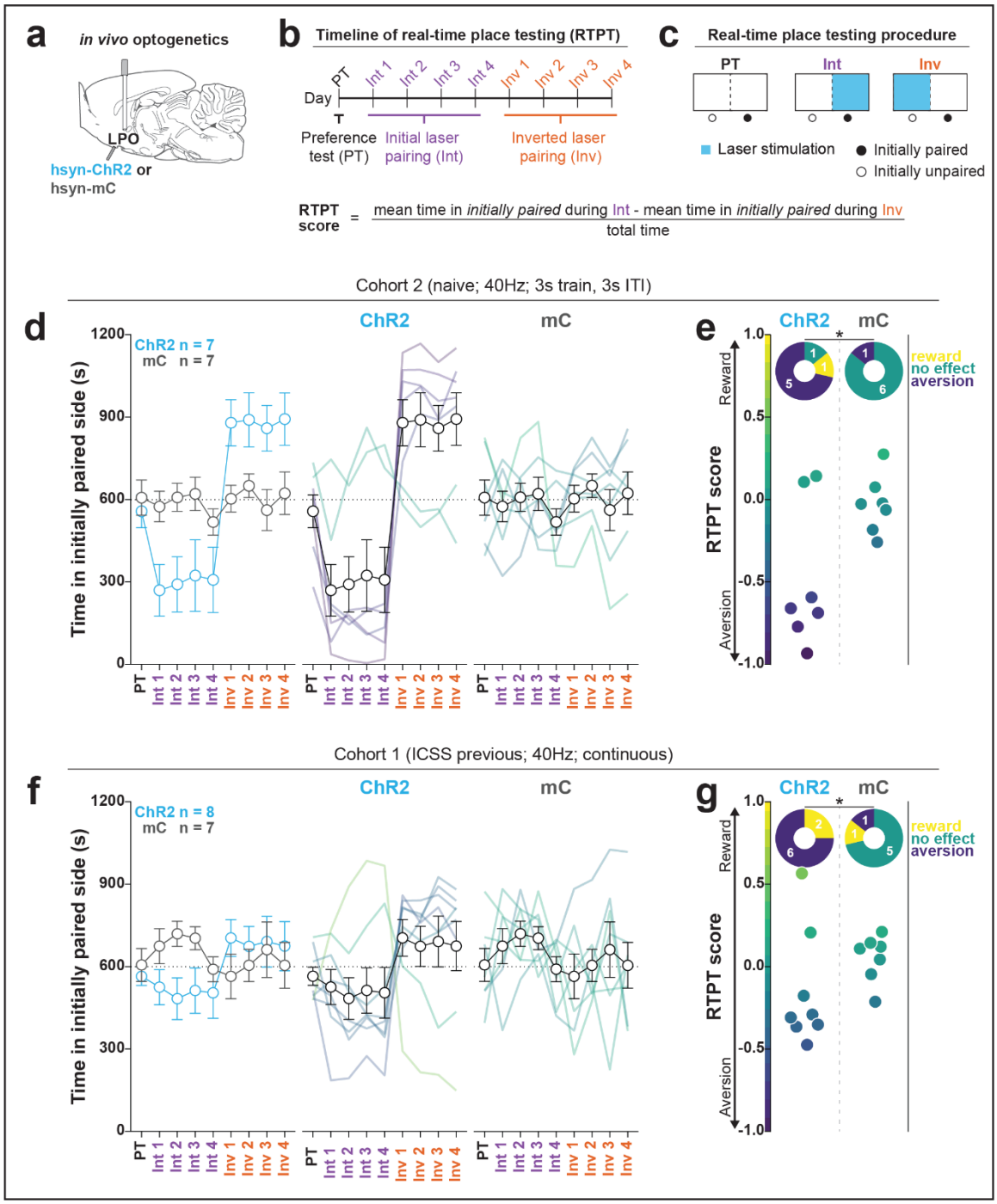

(a) *in-vivo* optogenetics setup: we injected either hsyn-ChR2 (ChR2) or hsyn-mCherry (mC) in the LPO and implanted an optic fiber overlaying the injection site. **(b)** Timeline for real-time place testing (RTPT). **(c)** RTPT procedure and equation for RTPT score is shown below **(d)** mean time in the initially paired side over days of RTPT in ChR2 (blue)

and mC (grey) groups; single subjects are color-coded based on their RTPT score. The ChR2 and the mC groups showed differential effects across days of RTPT (group x day interaction: $F_{8,96} = 5.56$, $P < 0.001$), where the majority of rats in the ChR2 group show aversion, indicated by a low amount of time in the initially paired side during initial pairing and a high amount of time during inverted pairing. **(e)** RTPT scores for rats in the ChR2 and the mC group; inset shows the number of rats within the ChR2 and the mC groups that displayed aversion, reward, and no valence across RTPT pairing. Relative to the mC group, the ChR2 group showed different proportions of subjects with RTPT effects (Fisher exact, *: $P = 0.029$). **(f-g)** same as (d-e) for cohort 1, which was tested for ICSS prior to RTPT. **(f)** On average, the ChR2 and the mC groups did now show differences in time spent in the initially paired side across days of RTPT (group x day interaction: $F_{8,112} = 0.44$, $P = 0.89$). **(g)** Relative to the mC group, the ChR2 group showed different proportions of rats that displayed aversion, reward, and no valence across RTPT pairing (Fisher exact, ***: $P < 0.001$). In (d) and (f), faded lines depict values of individual subjects; points and error bars depict mean and SEM, respectively.

Figure 3.12 Single rat example of RTPT aversion and ICSS reinforcement

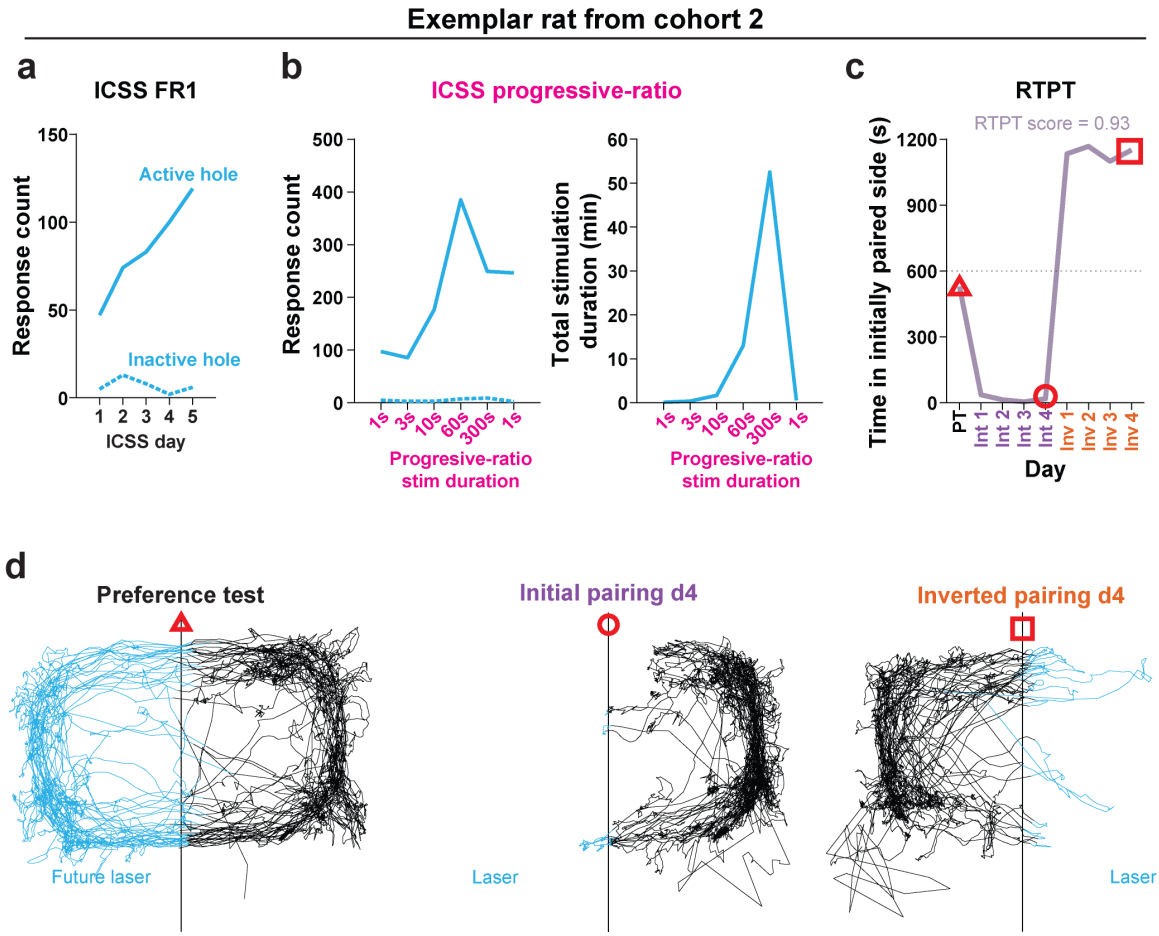

(a) Response rates in the intracranial self-stimulation (ICSS) test at fixed-ratio (FR) indicate the reinforcing properties of LPO stimulation; the solid line depicts active hole responding and the dashed line depicts inactive hole responding. **(b)** Response rates (left) in the progressive-ratio task indicate the motivating property of LPO stimulation; line types match those of (a). Total stimulation duration earned within the progressive-ratio task (right) show that the rat earns more stimulation during progressive-ratio test than the entire 20-minute duration of real-time place testing (RTPT). **(c)** RTPT behavior shows clear aversion, as indicated by avoidance of the side paired with LPO stimulation. **(d)** traces depicting the rats center point in RTPT during the preference test, last day of initial pairing, and last day of inverted pairing; blue color indicates future laser pairing side (preference test) or the laser paired side (initial pairing / inverted pairing).

Figure 3.13 Crossing events across days of RTPT

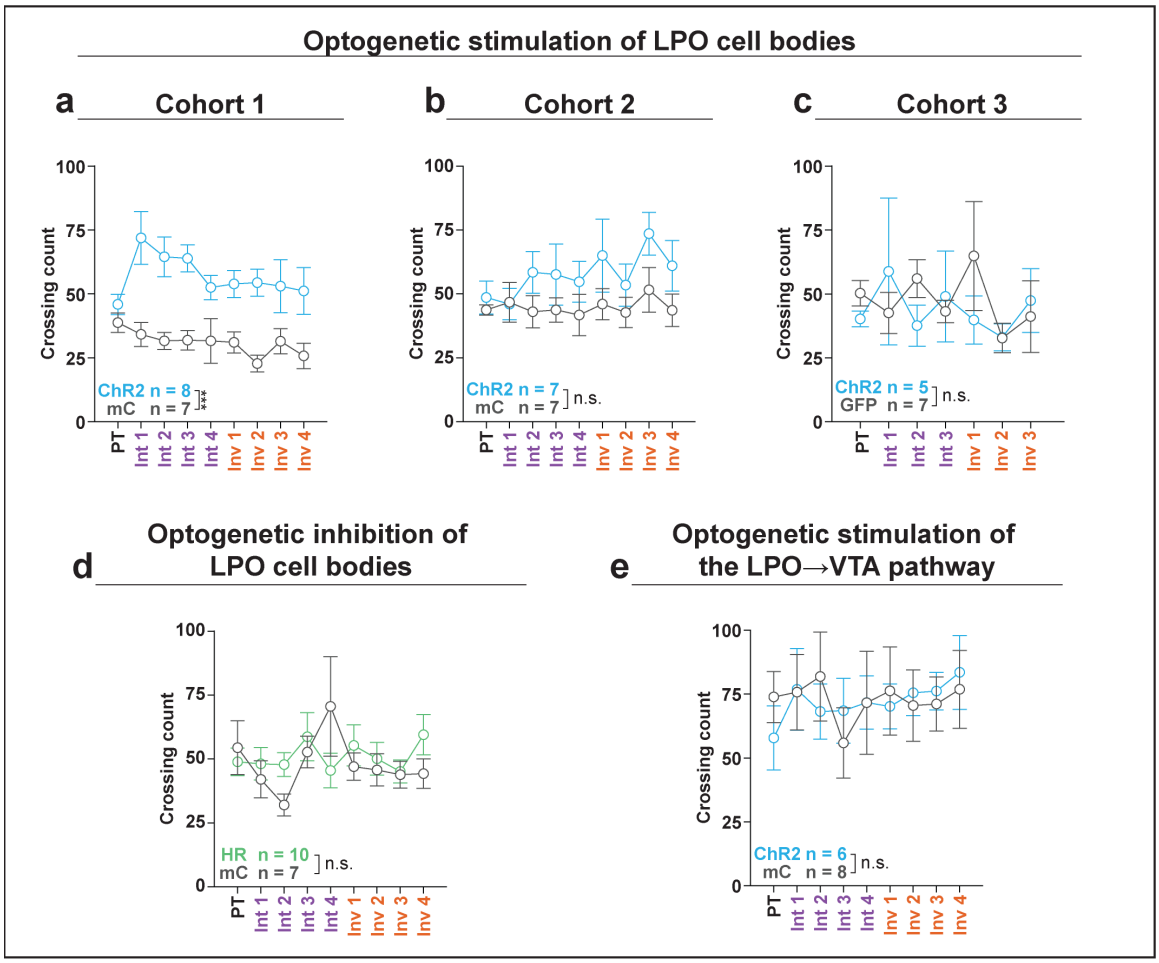

(a-e) Number of crossings across real-time place testing (RTPT). **(a)** In Cohort 1 (stimulation of LPO cell bodies, 40Hz, continuous) the ChR2 group showed an enhanced crossing between sides of the RTPT apparatus relative to the mC group (group effect: $F_{1,13} = 20.02$, $P < 0.001$). **(b)** In Cohort 2 (stimulation of LPO cell bodies, 40Hz, 3s train, 3s ITI) the ChR2 group did not show differences in crossings relative to the mC group (group effect: $F_{1,12} = 3.08$, $P = 0.10$). **(c)** In Cohort 3 (stimulation of LPO cell bodies, 20Hz, continuous) the ChR2 group did not show differences in crossings relative to the GFP group (group effect: $F_{1,10} = 0.18$, $P = 0.67$). **(d)** In the experiment testing inhibition of LPO cell bodies, the HR group did not show differences in crossings relative to the mC group (group effect: $F_{1,15} = 0.020$, $P = 0.66$). **(e)** In the experiment testing stimulation of the LPO→VTA pathway, the ChR2 group did not show differences in crossings relative to the mC group (group effect: $F_{1,12} = 0.0014$, $P = 0.97$). In (a-e), points and error bars depict mean and SEM, respectively.

Figure 3.14 Stimulation of the LPO with low frequency promotes minor real-time place aversion

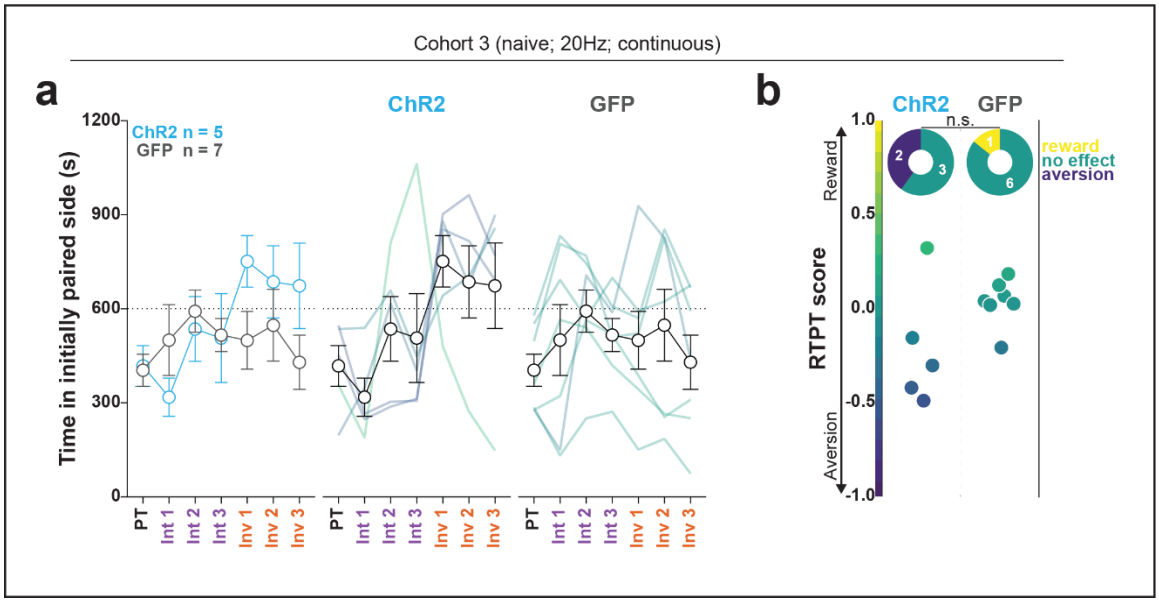

(a) Mean time in the initially paired side over RTPT, in ChR2 (blue) and GFP (grey) groups. Lines depict single subjects, which are color-coded based on RTPT score. Unlike in cohorts 1 and 2, the least preferred side during the preference test was assigned as the initially paired side, to enhance the ability to detect preference. ChR2 and the GFP groups showed similar effects across days of RTPT (group x day interaction: $F_{6,60} = 2.05$, $P = 0.072$. **(b)** RTPT scores for rats in the ChR2 and the GFP groups; inset shows the number of rats within the ChR2 and the GFP groups that displayed aversion, reward, and no valence. Relative to the GFP group, the ChR2 group did not show different proportions of rats in each category (fisher exact: $P = 0.15$). In (a), points and error bars depict mean and SEM, respectively.

Figure 3.15 Placement of optic fibers in the LPO does not correlate with RTPT behavior

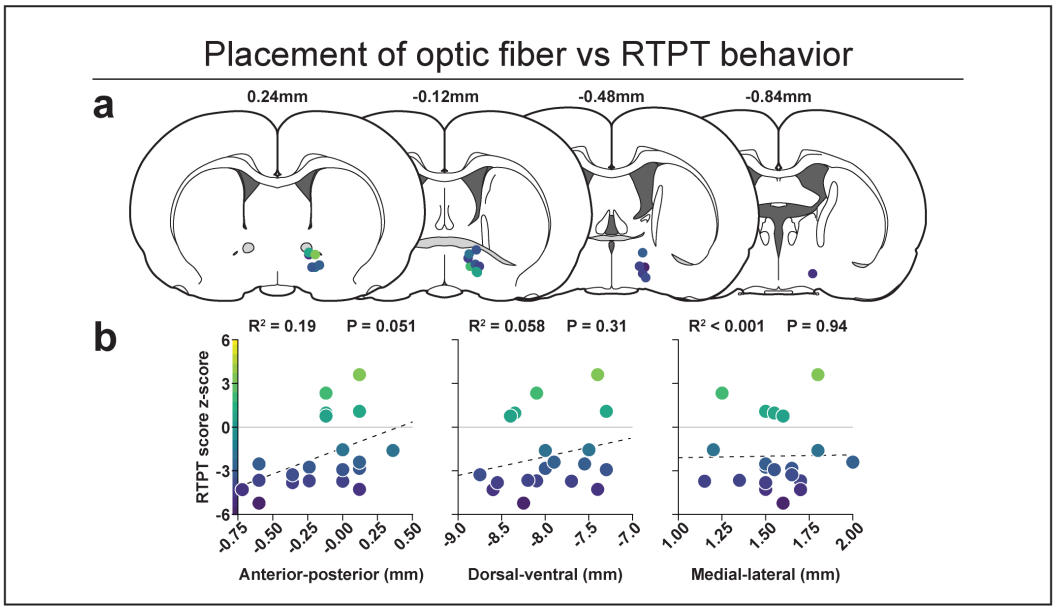

(a) Placement of optic fibers within the LPO. **(b)** Correlation between placement of the optic fibers in the LPO and real-time place testing (RTPT) behavior. The anterior-posterior (left), medial-lateral (middle), and dorsal-ventral (right) placement of the optic fiber within the LPO did not correlate with the normalized RTPT score (z-score of the RTPT score using the standard deviation of the control group). Data points are combined from cohorts 1-3. For all plots, the color of points indicates the RTPT (color scale is depicted on left side of scatter plots; yellow: high normalized responding, purple low normalized responding).

Figure 3.16 Validation of HR mediated inhibition of LPO neurons

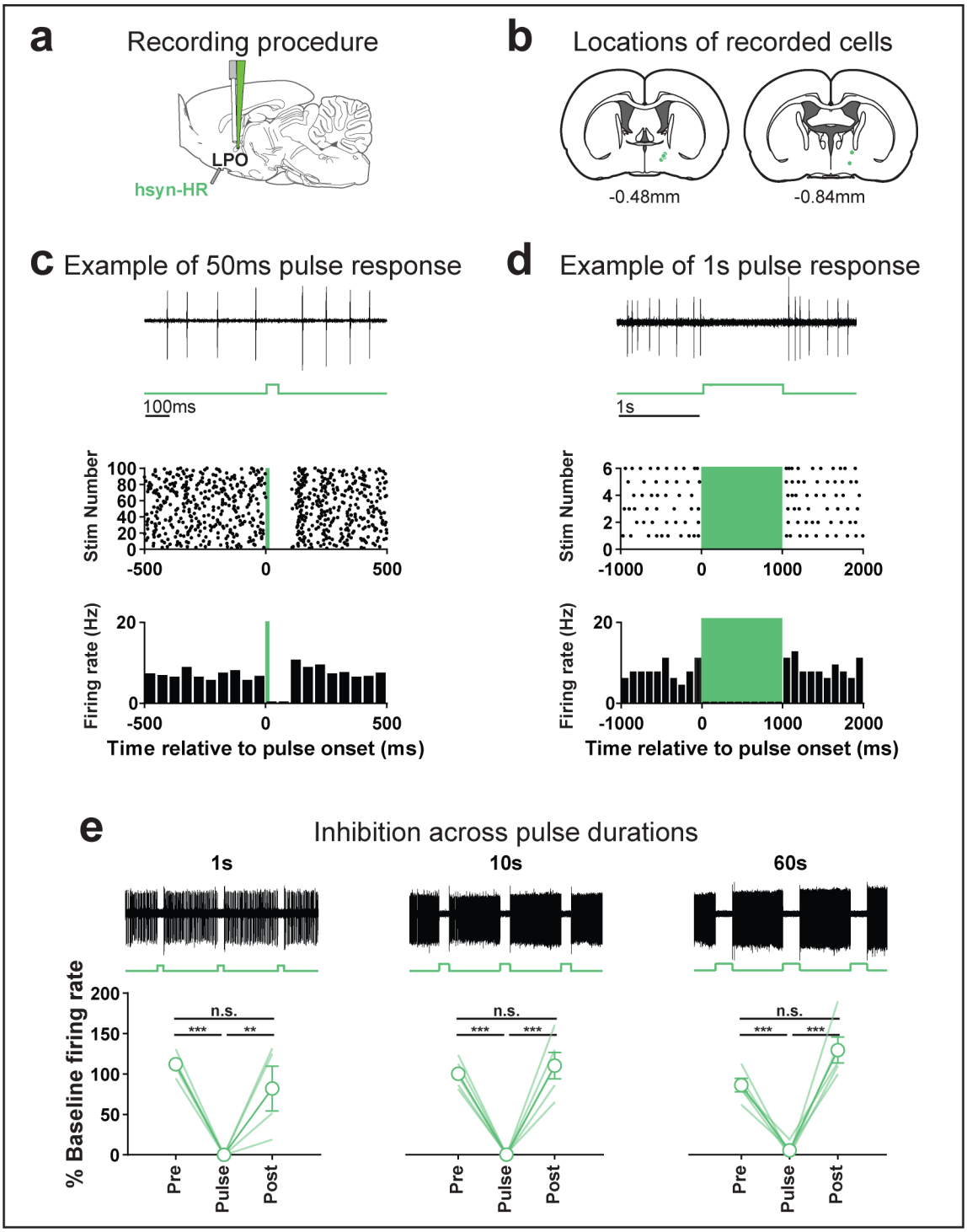

(a) Recording procedure: we injected hsyn-HR in the LPO and recorded LPO neurons with an optrode. **(b)** Location of recorded neurons. **(c)** Example of a single neuron responding

to 100ms, 0.2Hz illumination pulses. Top: extracellular trace of the response to a single illumination pulse; middle: raster plot of spikes in response to 100 pulses, each dot represents a single action potential; bottom: peristimulus time histogram showing firing rate in each 100ms bin for t raster plot shown above **(d)** single neuron example of response to 1s, 0.1Hz illumination. Top: extracellular trace of the response to a single pulse; middle: raster plot of spikes in response to 6 pulses; bottom: peristimulus time histogram showing firing rate in each 100ms bin for the raster plot shown above. **(e)** Responses to pulses of 1s, 10s, and 60s duration. Top: single neuron inhibitory responses to each pulse duration; bottom: binned firing rate divided by 10s baseline firing rate in response to each pulse duration (Pre: 2s bin prior to train onset, Pulse: 1s train, Post: 2s bin following train offset). As shown, every neuron recorded showed complete inhibition across pulse durations (time effect: $F_{2,22} = 81.79$, $P < 0.001$; pulse duration effect: $F_{2,11} = 2.75$, $P = 0.76$; interaction: $F_{4,22} = 4.22$, $P = 0.062$). (***: HSD, $P < 0.001$, **: HSD, $P < 0.01$). In (e), faded lines depict subject values; points and error bars depict mean and SEM, respectively.

Figure 3.17 Optogenetic inhibition of the LPO does not support ICSS or drive real-time place preference

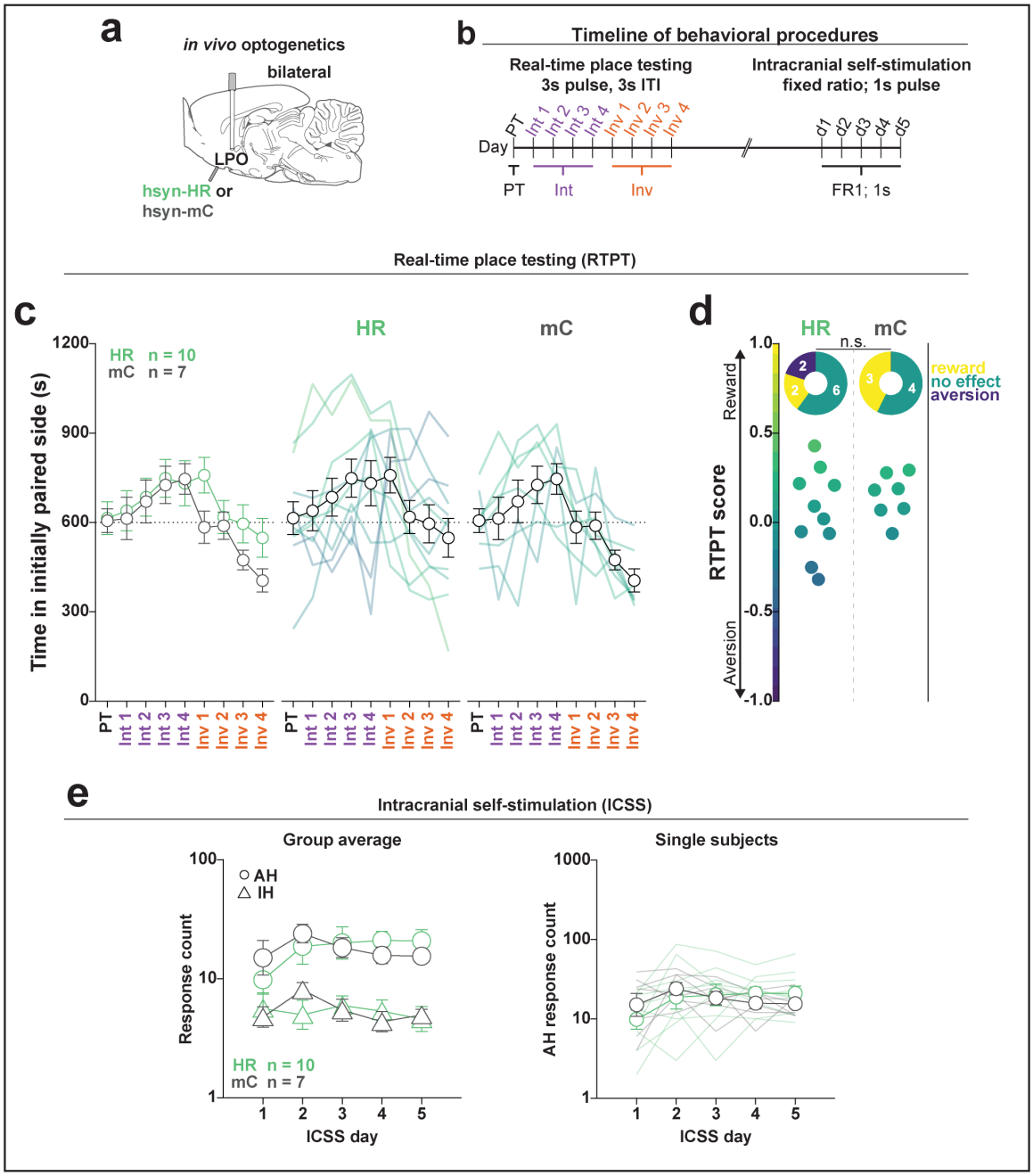

(a) *in-vivo* optogenetics setup: We injected either hsyn-HR (HR) or hsyn-mCherry (mC) bilaterally in the LPO and implanted optic fibers overlaying the injection sites. **(b)** Timeline for real-time place testing (RTPT) and intracranial self-stimulation (ICSS) (procedure details can be found in legends for Figure 3.11 and Figure 3.7, respectively). **(c)** Mean time in the initially paired side across days of RTPT in HR (green) and mC (grey) groups; single subjects are color-coded based on their RTPT score. The HR and the mC groups showed preference but did not show different behavior across days of RTPT (day effect: $F_{8,120}$ =

4.80, P < 0.001, group x day interaction: $F_{8,120}$ = 0.74, P = 0.65). **(d)** RTPT scores for rats in the HR and mC groups; inset shows the number of rats within the HR and mC groups that displayed aversion, reward, and no valence across RTPT. Relative to the mC group, the HR group did not show different proportion of subjects with RTPT effects (Fisher exact, n.s.: P = 0.40). **(e)** Self-administration behavior during ICSS at a fixed-ratio 1 for 1s illumination. Left: The HR and the mC groups did not show different discrimination between the active hole (circles) and inactive hole (triangles) (group x hole interaction: $F_{1,14}$ = 0.011, P = 0.92); right: The HR group did not make more or less active hole responses than the mC group throughout the ICSS procedure (group effect: F1,14 < 0.001, P = 1.00). Active hole and inactive hole responses are shown on a log scale. In (c) and (e), faded lines depict values from individual subjects; points and error bars depict mean and SEM, respectively.

Figure 3.18 Placement of optic fibers for optogenetic inhibition of LPO cell bodies

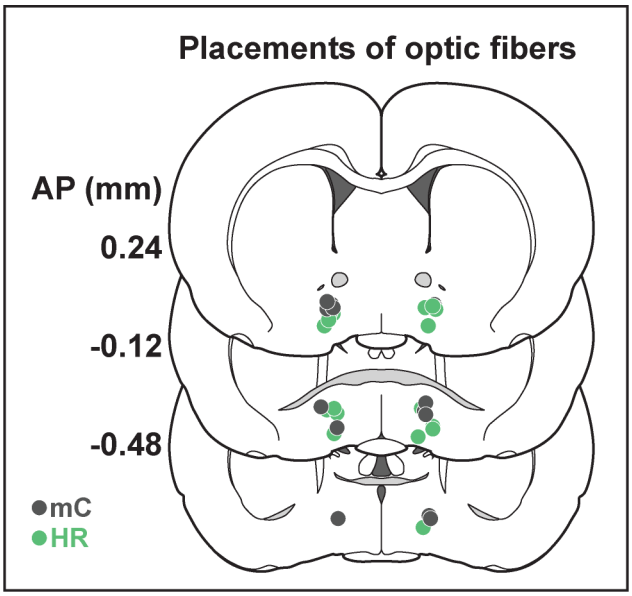

Placement of optic fibers placed bilaterally within the LPO for illumination in the halorhodopsin (green) and mCherry (grey) groups.

Figure 3.19 The LPO→VTA pathway supports ICSS and promotes real-time place aversion in the majority of rats

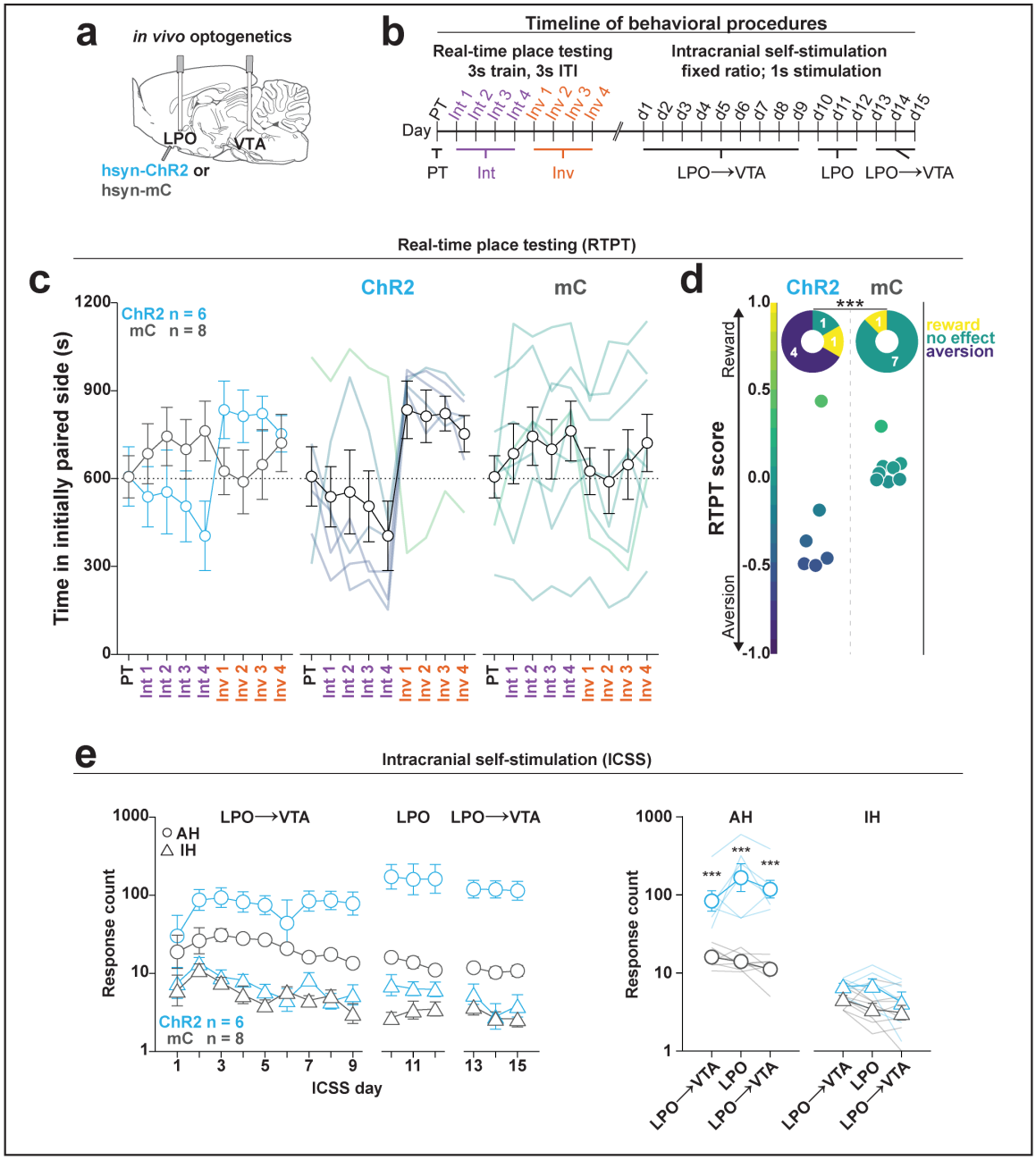

(a) *in-vivo* optogenetics setup: We injected either hsyn-ChR2 (ChR2) or hsyn-mCherry (mC) in the LPO and implanted optic fibers overlaying the injection site and VTA. **(b)** Timeline for real-time place testing (RTPT) and intracranial self-stimulation (ICSS) (procedure details can be found in legends for Figure 3.11 and Figure 3.7). **(c)** Mean time in the initially paired side across days of RTPT in the ChR2 (blue) and mC (grey) groups; single subjects are color-coded based on their RTPT score. The ChR2 and the mC groups

showed differential time spent in the initially paired side across days of RTPT (group x day interaction: $P < 0.001$, $F_{8,96} = 4.34$, $P < 0.001$), where the ChR2 group showed aversion indicated by a low amount of time spent in the initially paired side during initial pairing and a high amount of time during inverted pairing. **(d)** RTPT scores for rats in ChR2 and the mC groups; inset shows the number of rats within the ChR2 and the mC groups that displayed aversion, reward, and no valence across RTPT. Relative to the mC group, the ChR2 group showed different proportions of subjects with RTPT effects (fisher exact, **: $P = 0.0057$). **(e)** Self-administration behavior during ICSS at a fixed-ratio 1, for 1s illumination in the LPO→VTA pathway and LPO. Left: The ChR2 and the mC groups showed differential discrimination between the active hole (circles) and inactive hole (triangles) (group x hole interaction: $F_{1,12} = 15.21$, $P = 0.0021$); right: three-day mean responding on the active hole and the inactive hole. Relative to the mC group, the ChR2 group showed higher responding in the active hole for stimulation of the LPO→VTA pathway and LPO but did not show any difference in inactive hole responding (HSD, ***: $P < 0.001$). Active hole and inactive hole responses are shown on a log scale. In (c) and (e), faded lines depict value from individual subject; points and error bars depict mean and SEM, respectively.

Figure 3.20 Placement of optic fiber placements for optogenetic stimulation of LPO cell bodies and the LPO→VTA pathway

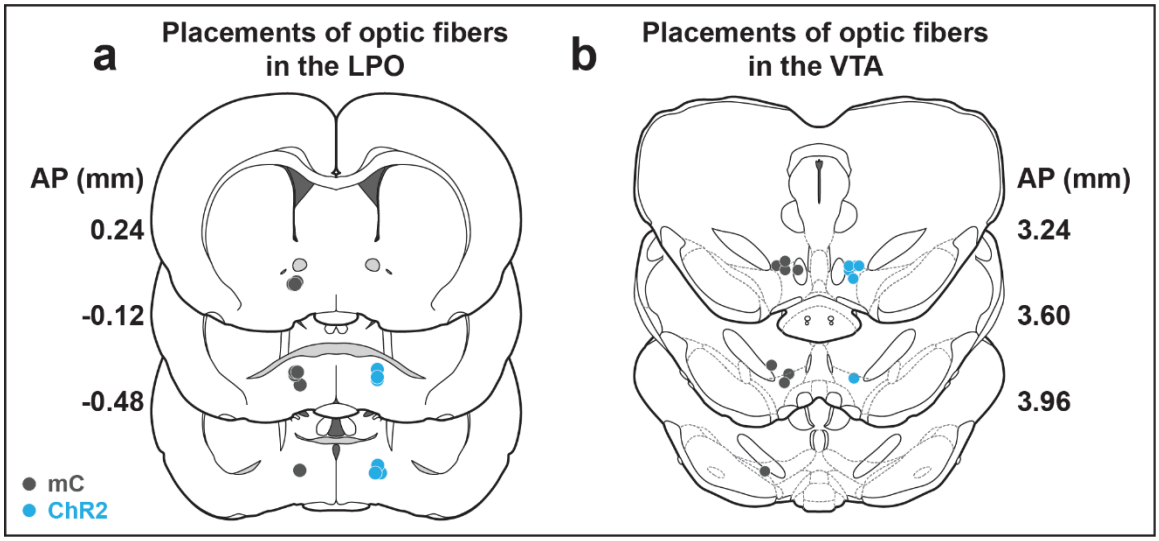

(a-b) Placement of the optic fibers placed unilaterally within the LPO (a) and LPO→VTA pathway (b) in the ChR2 (blue) and mC (grey) groups. All placements were on the right side of the brain.

Figure 3.21 ICSS and RTPT measures of reward are correlated are the product of different underlying variables

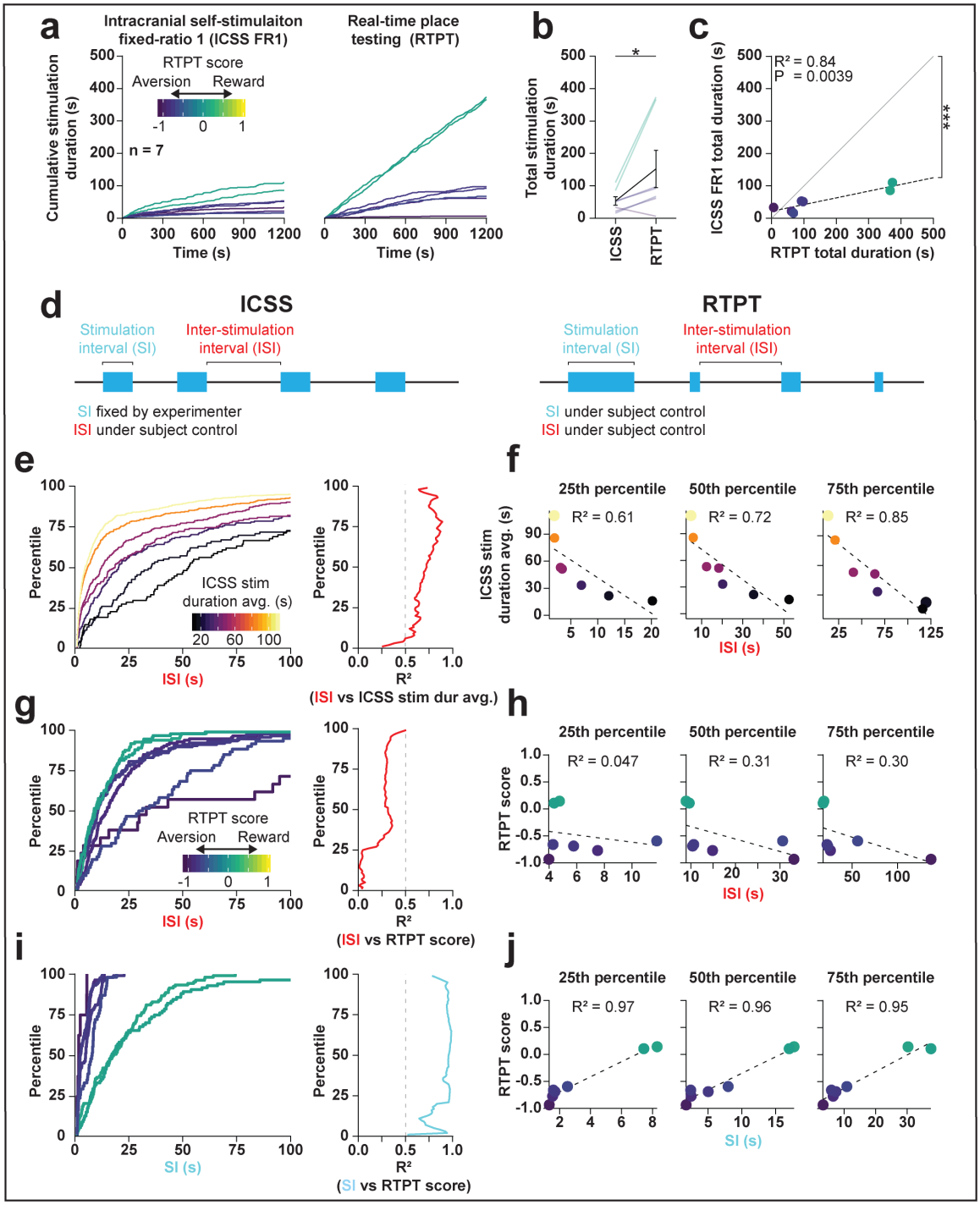

(a) mean of cumulative stimulation duration over the last 3 days of intracranial self-stimulation (ICSS) (left) or the last 3 days of real-time place testing (RTPT) (right). ICSS

data are truncated to the first 20min in order to compare them to RTPT over the same time scale. Subjects are color coded based on their RTPT score (see RTPT behavior in Figure 3.11). **(b)** The total stimulation duration earned in RTPT was higher than that in ICSS (Wilcoxon, *: $P < 0.05$). **(c)** The total stimulation duration earned within RTPT and ICSS is correlated but substantially lower for ICSS compared with RTPT, as indicated by slope below 1 (slope of 1 vs correlation slope, ***: $P < 0.001$). **(d)** Diagram depicting the behavioral components that underlie the total stimulation duration within ICSS (left) and RTPT (right). In ICSS, the stimulation-interval (SI) is defined by the experimenter, while the inter-stimulation-interval (ISI) is under the animal's control. In RTPP, both the SI and ISI are under the animal's control and can independently contribute to the stimulation duration earned within the RTPT procedure. **(e)** Cumulative distribution function (CDF) for ISI within ICSS for each subject color coded by the total ICSS duration earned (inset shows color scale). Right: Correlation of ISI vs. total ICSS duration earned from percentiles 1 to 99 indicate a clear relationship between variables across percentiles. **(f)** Correlations at each percentile indicating strong correlations. **(g)** CDF for ISI within RTPT for each subject, color coded by RTPT score (inset shows color scale). Right: Correlation of ISI vs. total ICSS duration earned from percentiles 1 to 99 indicate a relatively weak correlation between variables across percentiles. **(h)** Correlations at each percentile indicating poor correlations. **(i)** CDF for SI within RTPT for each subject, color coded by RTPT score (color scale identical to inset in (g)). Right: Correlation of ISI vs. total ICSS duration earned from percentiles 1 to 99 indicate a strong relationship between variables across percentiles. **(j)** Scatter plots showing correlations at each percentile indicating a strong correlation between variables.

Figure 3.22 Across stimulation parameters, RTPT and ICSS behavior are correlated but rats obtain more stimulation in RTPT.

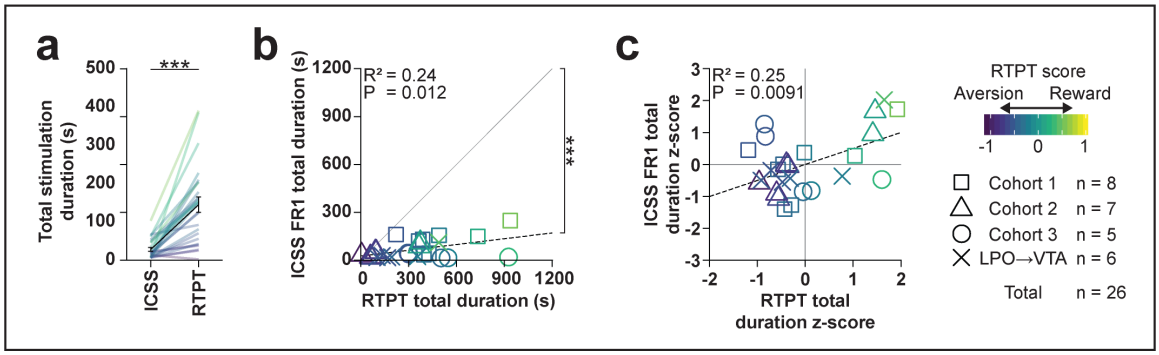

(a) Across experimental parameters, the total stimulation duration earned in RTPT was higher than in ICSS (Wilcoxon, ***: $P < 0.001$). **(b)** Across experimental parameters, the stimulation duration earned within RTPT and ICSS is correlated but substantially lower in the ICSS compared with RTPT indicated by slope below 1 (slope of 1 vs correlation slope, ***: $P < 0.001$); shapes indicate the experimental group of each data point **(c)** Normalizing the amount of stimulation obtained by taking the z-score of the ChR2 animals within each experimental group reveals a correlation between the amount of stimulation obtained in ICSS and RTPT; shapes indicate the experimental group of each data point.

Figure 3.23 Across stimulation parameters, the stimulation-interval underlies the RTPT behavior to a greater degree than the inter-stimulation-interval

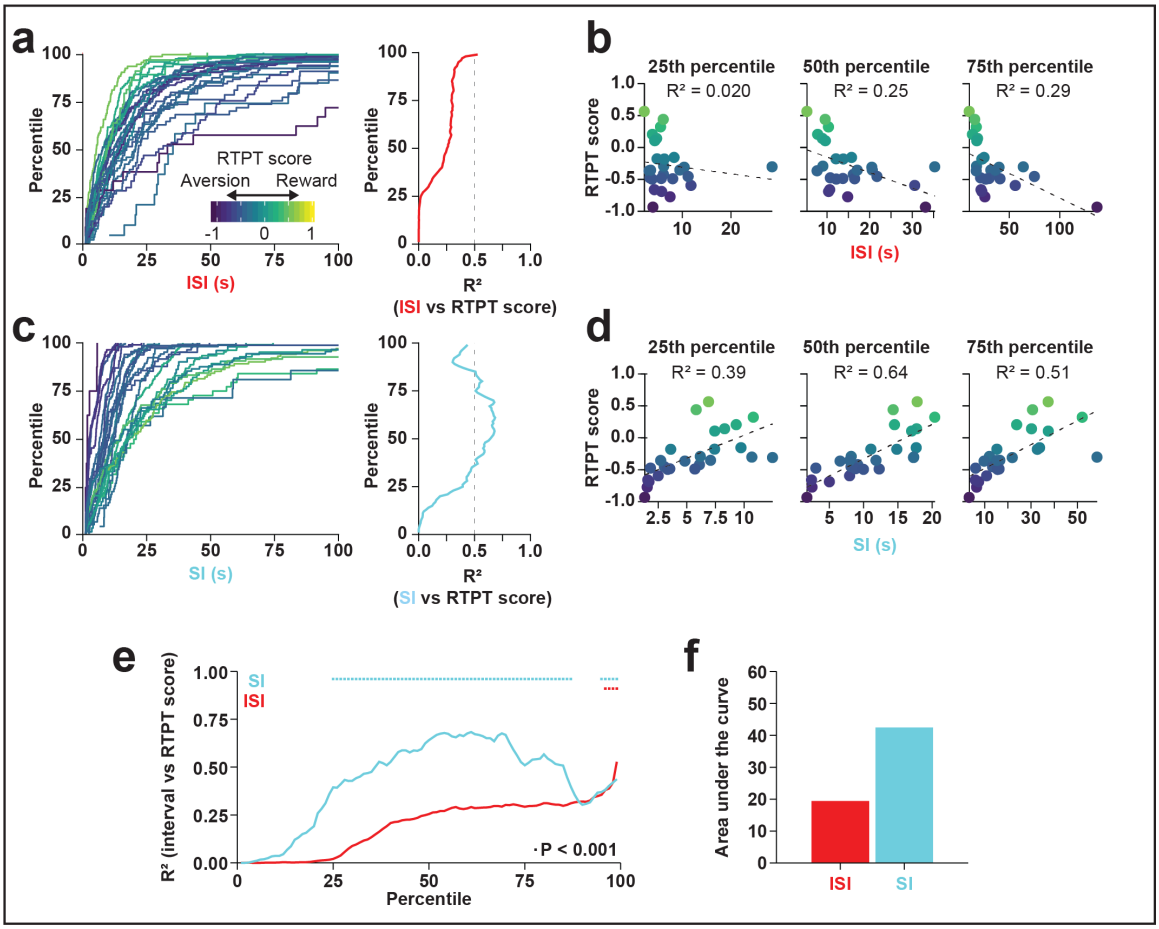

(a) Left: Cumulative distribution function (CDF) for inter-stimulation-interval (ISI) within real-time place testing (RTPT) for each subject, color coded by RTPT score (inset indicates scale) Right: Correlation of ISI vs. total ICSS duration earned from percentiles 1 to 99 indicate a relatively weak relationship between variables across percentiles. **(b)** Correlations at each percentile indicate poor correlations between the inter-stimulation-interval and RTPT score. **(c)** CDF for SI within RTPT for each subject, color coded by RTPT score. Right: Correlation of ISI vs. total ICSS duration earned from percentiles 1 to 99 indicate a strong correlation between variables across percentiles. **(d)** Correlations at each percentile indicate strong correlations between the stimulus-interval and RTPT score. **(e)** Overlay of the curves shown in the left side of (a) and (c) demonstrate substantially greater correlation of the stimulation-interval compared with inter-stimulation-interval; dots indicate interval percentiles that show a correlation with $P < 0.001$. **(f)** Area under the curve for (e) further indicates that the stimulation-interval correlates more strongly with the RTPT score compared with the inter-stimulation-interval.

Figure 3.24 Stimulating the LPO is reinforcing in the RTPT assay

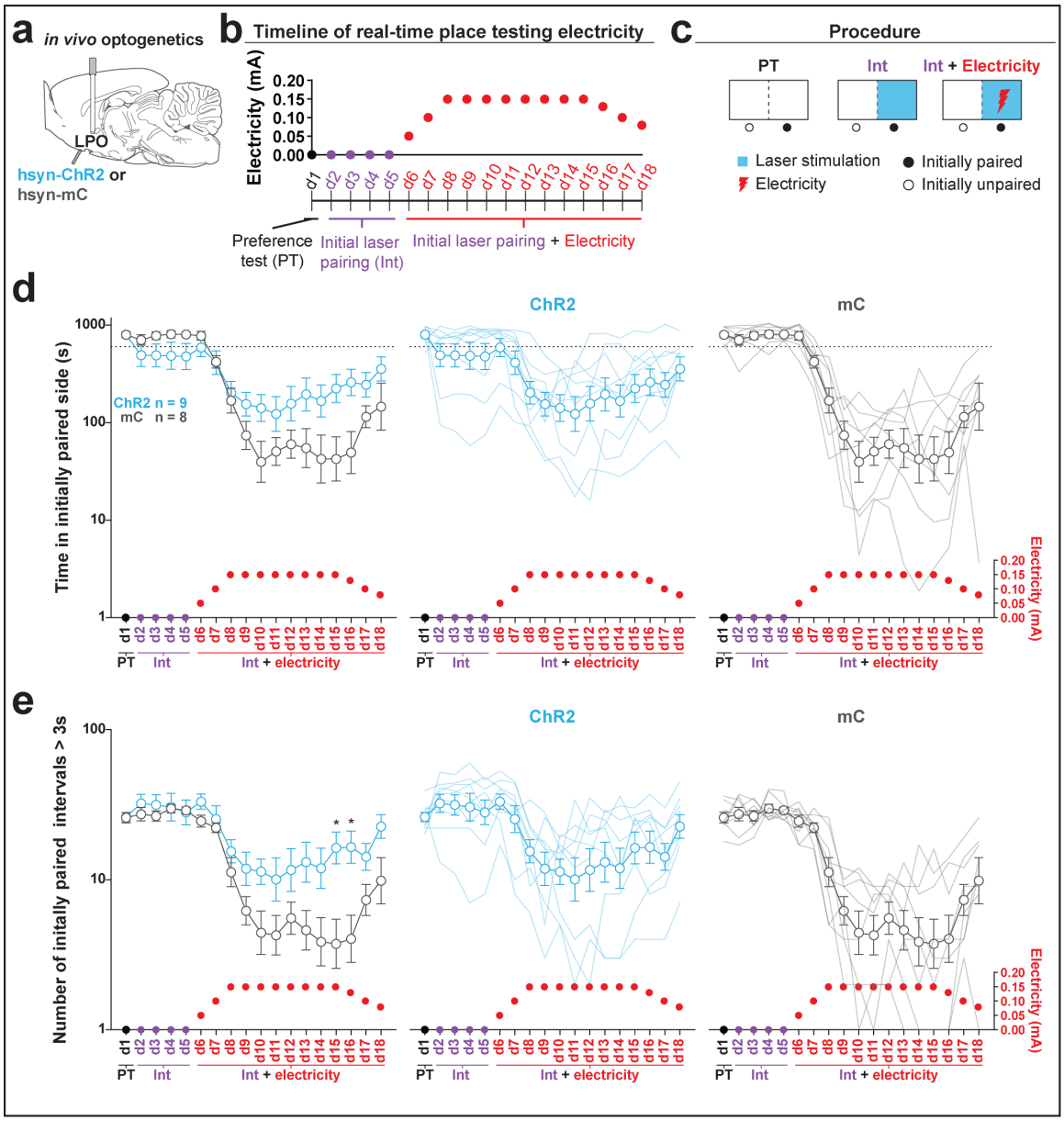

(a) *in-vivo* optogenetics setup: We injected either hsyn-ChR2 (ChR2) or hsyn-mCherry (mC) in the LPO and implanted a fiber overlaying the injection site. **(b)** RTPT electricity procedure **(c)** Timeline for real-time place testing. Note that pairing remains consistent across training and the optically paired side becomes dual-paired with electricity. **(d)** Time spent in the initially paired side across RTPT decreased across days as the initially paired side was paired with electricity (day effect: $F_{17,255} = 30.34$, $P < 0.001$). The mC group decreased to a greater degree than the ChR2 group (day x group interaction: $F_{17,255} = 5.55$, $P < 0.001$). **(e)** The number of initially paired intervals greater than 3s across RTPT decreased across days as the initially paired side was paired with electric electricity (day

effect: F17,255 = 26.71, P < 0.001). The mC group decreased to a greater degree than the ChR2 group (day x group interaction: $F_{17,255} = 4.06$, P < 0.001). In (d-e), faded lines depict subject values; points and error bars depict mean and SEM, respectively.

Figure 3.25 Placement of optic fibers for optogenetic stimulation of LPO cell bodies in the RTPT electricity procedure

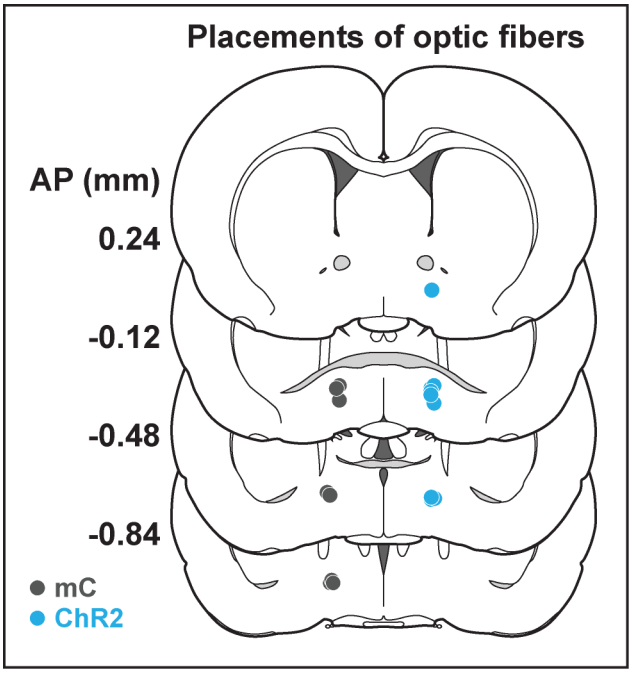

Placement of the optic fibers placed unilaterally within the LPO illumination in the mC (grey) and ChR2 (blue) groups. All placements were on the right side of the brain.

Figure 3.26 Binned preference during the RTPT shock procedure

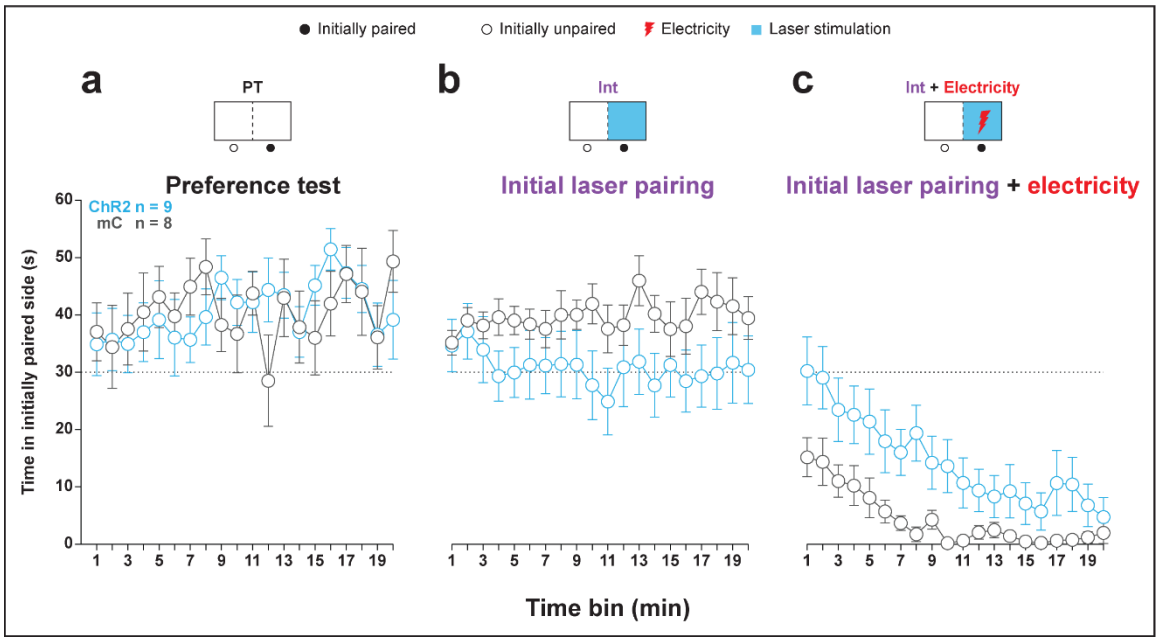

(a-b) Time spent in the initially paired side across training stages. **(a)** Mean behavior during the preference test. **(b)** Mean behavior across all 4 days of initial pairing (average across days). **(c)** Mean behavior during the last 4 days of initial pairing + 0.15mA electricity (average across days). Results indicate differential behavior between the mC and ChR2 groups depending on training stage (group x stage interaction: $F_{2,30} = 4.09$, $P = 0.027$). During the dual laser + electricity pairing, the ChR2 group spent a greater amount of time in the dual-paired side compared with the mC group and this occurred similarly throughout the session (group effect: $F_{1,15} = 5.17$, $P = 0.038$; group x time interaction: $F_{19,285} = 1.77$, $P = 0.026$). In (a-c), points and error bars depict mean and SEM, respectively.

Figure 3.27 Fiber photometry analysis and placements of optic fibers

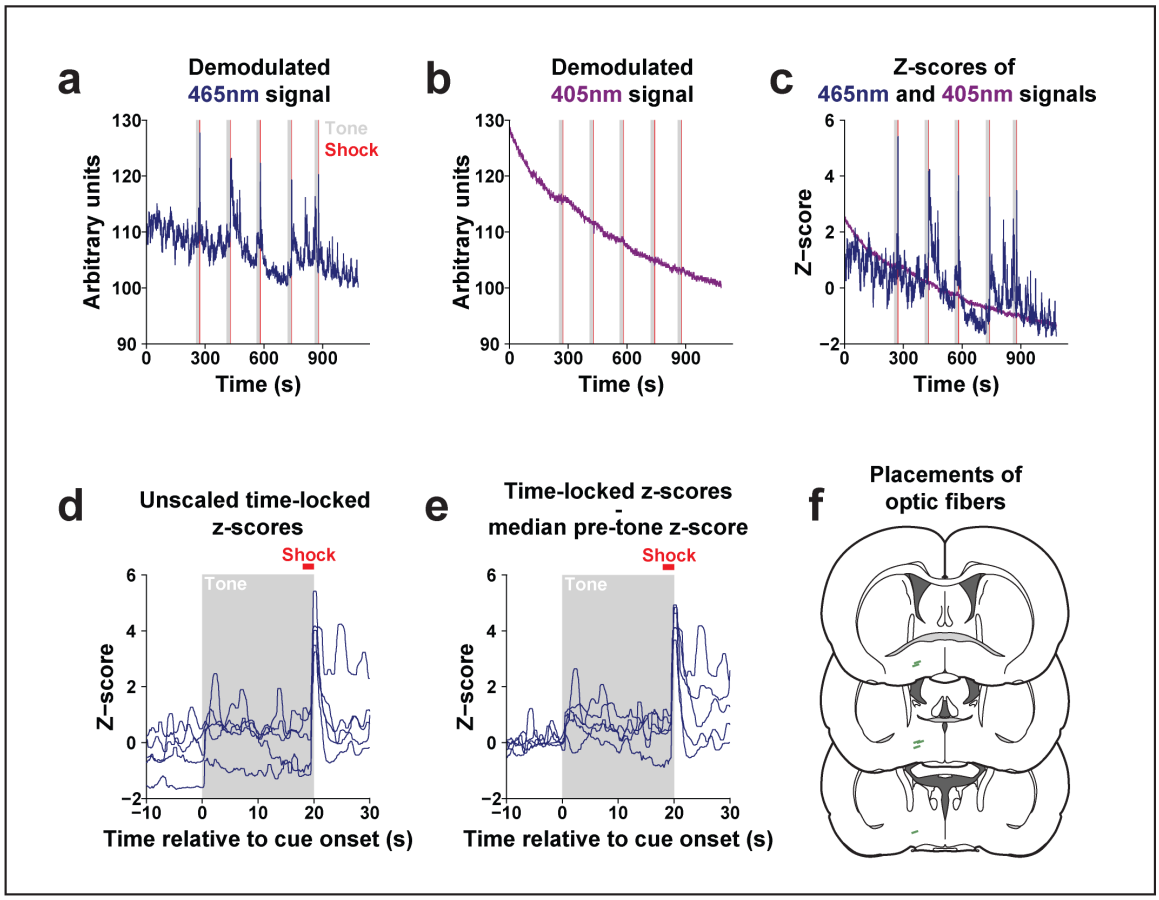

(a) Raw 465nm GCaMP and **(b)** raw 405nm auto-fluorescent channel recording during Pavlovian conditioning for footshock. **(c)** The z-score was taken for both channels for the entire session duration. **(d)** Single trial perievent signals of the z-score of the 465nm GCaMP channel. **(e)** To reduce the effect of downward baseline drift, perievent signals of both channels were subtracted by the median baseline **(b)** Raw 405nm auto-fluoresenct (10s prior to event). Group mean and SEM of perievent signals were created by calculating the mean of all recorded signals (n = number of subject x trials). Mean area under the curve was calculated for each subject independently, and then these means were used to calculate group mean and SEM. **(f)** Fiber photometry placements of fibers in the LPO. All placements were on the right side of the brain.

Figure 3.28 The LPO signals to aversive conditioning, but not rewarding conditioning

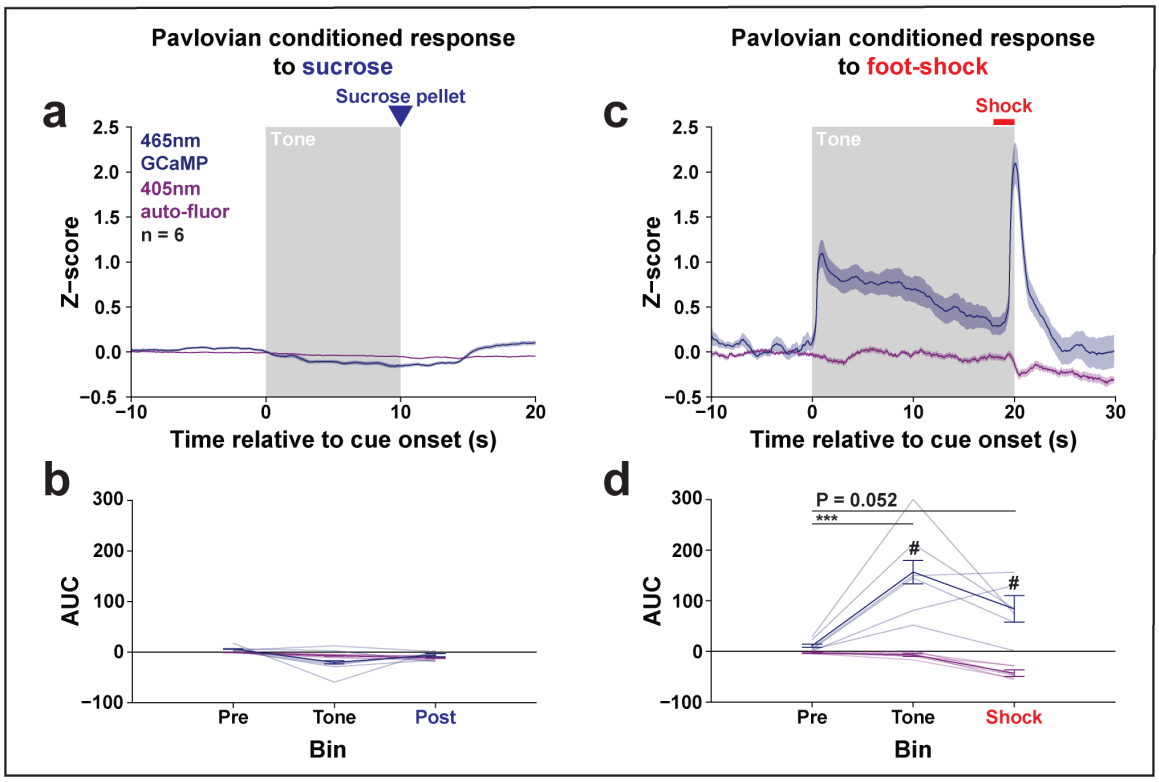

(a) Mean fiber photometry signals across days 25-27 of Pavlovian conditioning for sucrose. The predictive tone and sucrose delivery did not change signals in either channel (6 subjects x 90 trials). **(b)** Area under the curve (AUC) for data shown in (a). The LPO does not show changes in activity during the tone and post sucrose periods. **(c)** Mean fiber photometry signals on day 3 of Pavlovian conditioning for footshock. The predictive tone and electric footshock (EFS) led to an increase in z-score within the GCaMP channel (blue) but not the auto-fluorescent channel (purple) (6 subjects x 5 trials) **(d)** Area under the curve (AUC) for z-scores shown in (c). The LPO shows enhanced activity during the tone and shock periods (HSD, vs. Pre bin, ***: $P < 0.01$; vs. 405 auto-fluorescent channel, #: $P < 0.05$). In (a) and (c), the thick link depicts group mean and shaded ribbon depicts SEM; colors indicate the recording channel (465nm GCaMP channel: blue; 405nm auto-fluorescent channel: purple). In (b) and (d), faded lines depict subject mean AUC and dark lines depict group mean and SEM; the bin size for all AUC data was 10s in duration, the pre bin started 10s prior to tone onset (-10s), the tone bin began at tone onset (0s), the shock bin started at shock onset (18s), and the post sucrose bin began at sucrose delivery (10s).

Figure 3.29 Conditioning timeline and procedures

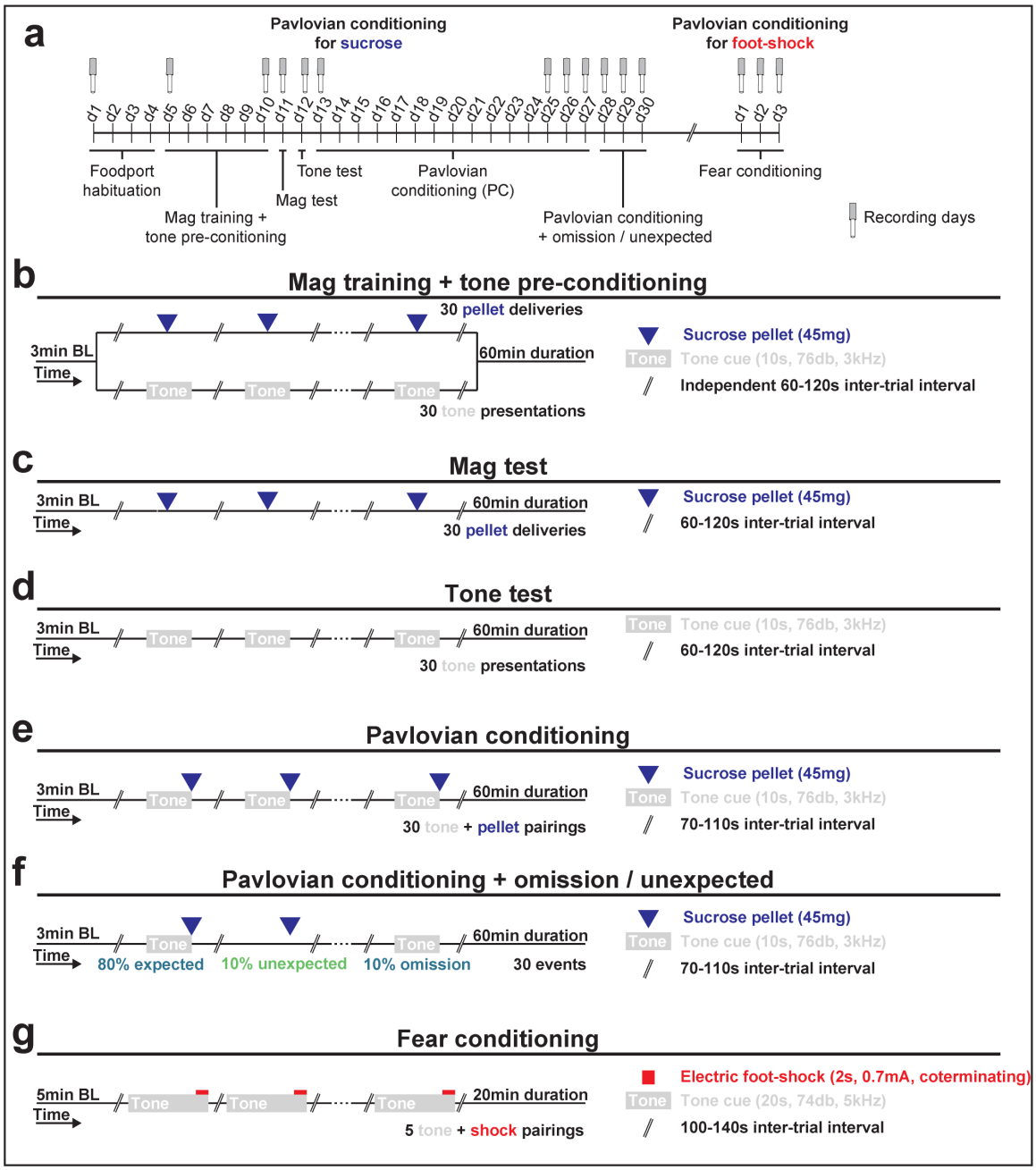

(a) Full behavioral timeline for fiber photometry experiments. Fiber icon indicates recording days. **(b-g)** individual behavioral procedures for each procedure within the experiment.

Figure 3.30 Behavior during Pavlovian conditioning to sucrose

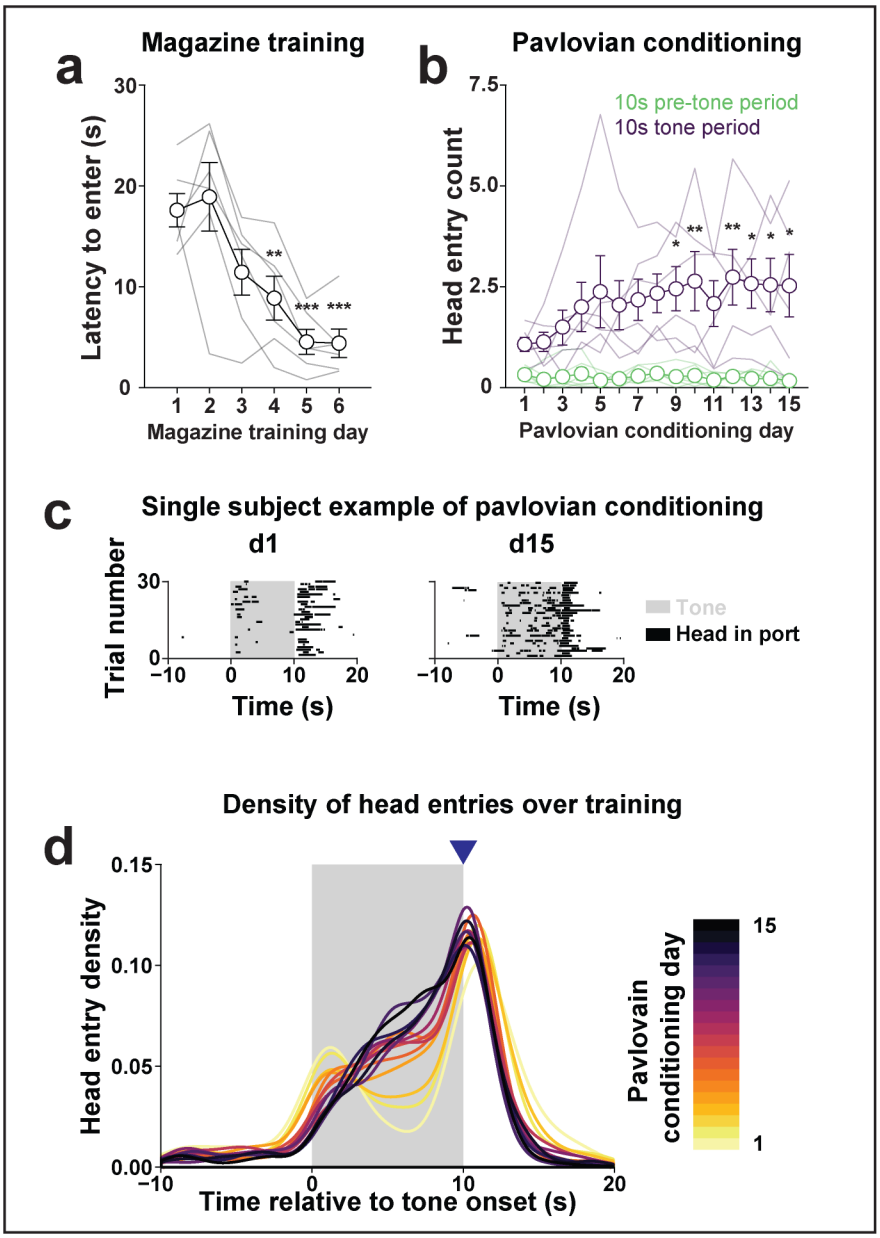

(a) Rats showed a decrease in latency from pellet delivery to head entry over the course of magazine training, indicating that rats learned the association between magazine delivery and the presence of sucrose pellets within the food port, indicated by a (day effect: $F_{5,25}$ = 17.73, P < 0.001; HSD, vs. day 1, *: P < 0.05, **: P < 0.01, ***: P < 0.001). **(b)** Rats increase the number of head entries during the tone period but not the pre-tone period, indicating rats developed a conditioned response to the predictive tone (time period x day interaction: $F_{14,70}$ = 2.68, P = 0.0034; HSD, vs. day 1, *: P < 0.05, **: P < 0.01, ***: P < 0.001). **(c)** Example of a conditioned response for a single subject. The rat increased the

number of head entries during the predictive done from the first day to the day prior to the first fiber photometry recording. **(d)** Group density of head entry across training reveals a progressive shift in head entry time relative to the tone. Early in training rats tended to near the start of the tone, but as training progressed, they began to enter during the middle of the tone more often. Note that the apparent increase prior to time 0 is the result of the smoothing function used to calculate the density and not due to head entries prior to 0. In (a) and (b), faded lines depict subject values; points and error bars depict group mean and SEM.

Figure 3.31 LPO calcium signaling across Pavlovian conditioning for sucrose and reward expectation

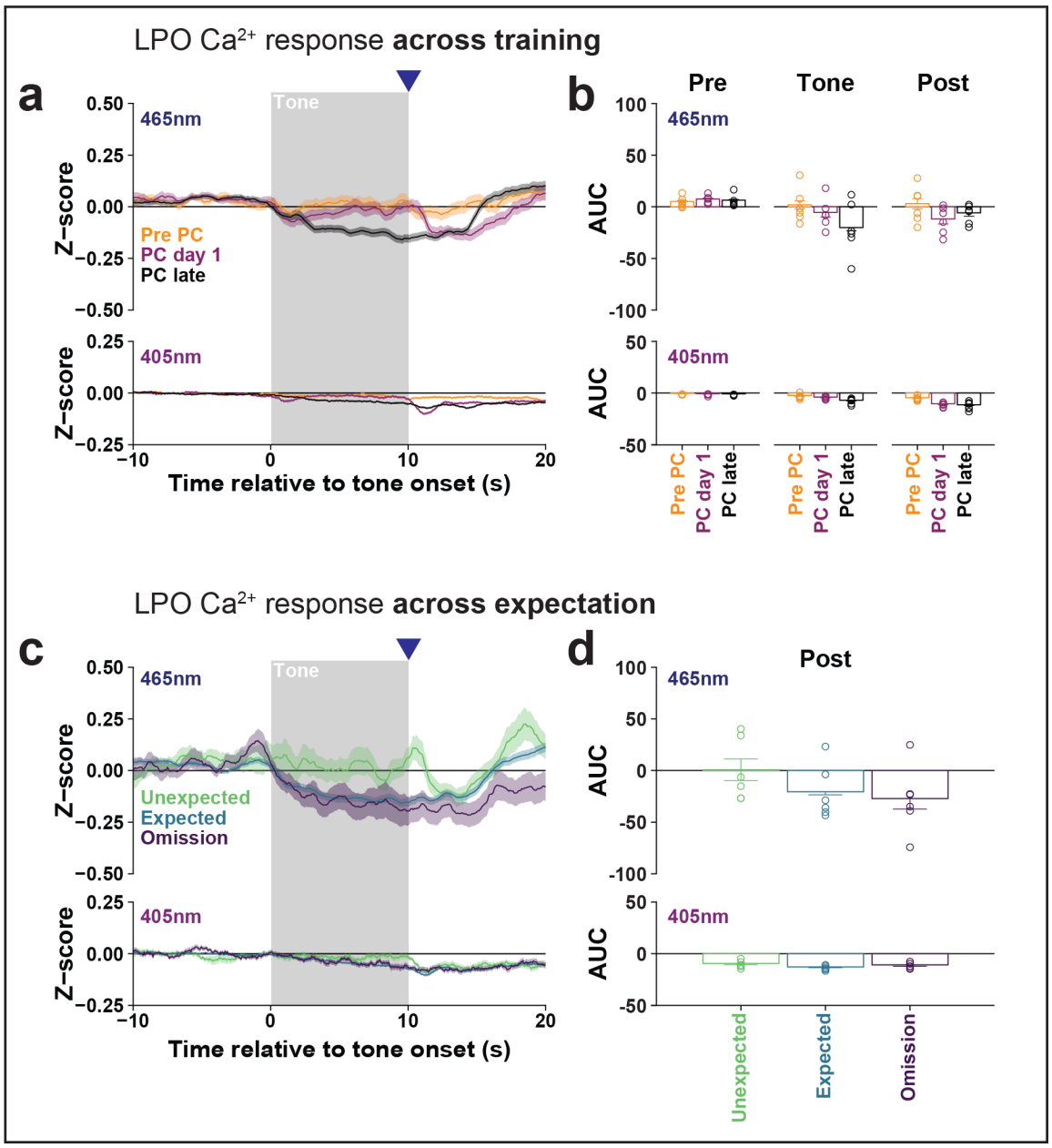

(a) LPO 465nm GCaMP (top) and 405nm auto-fluorescence (bottom) over the course of training indicates minimal responses in both channels to the tone. On the last day of magazine training + cue preconditioning ("Pre PC") there were no time-locked changes in either channel. In the case of Pavlovian conditioning for sucrose on the first day (PC day 1) and the last 3 days (PC late), there were minor time-locked decreases in both channels. However, note the similarity between the timing of signal decreases with port entries shown in (Figures 3.30); early in training, rats entered at the start and end of the tone, while later in training rats entered throughout the tone period. **(b)** Area under the curve (AUC) for data shown in (a) indicates no selective changes in the 465nm GCaMP channel in any

epoch over training. **(c)** LPO 465nm GCaMP (top) and 405nm auto-fluorescence (bottom) over the across expectation indicates minimal reward prediction error encoding. **(d)** AUC during the 10s post pellet period for data shown in (c) indicates no selective changes in the 465nm GCaMP channel across expectation. In (a) and (b), the thick link depicts group mean and shaded ribbon depicts SEM; colors indicate the training stage (a) or expectancy (c) as outlined in the inset. In (b) and (d), points depict subject mean AUC and bars with error bars depict group mean and SEM.

Figure 3.32 LPO calcium signaling across Pavlovian conditioning for footshock

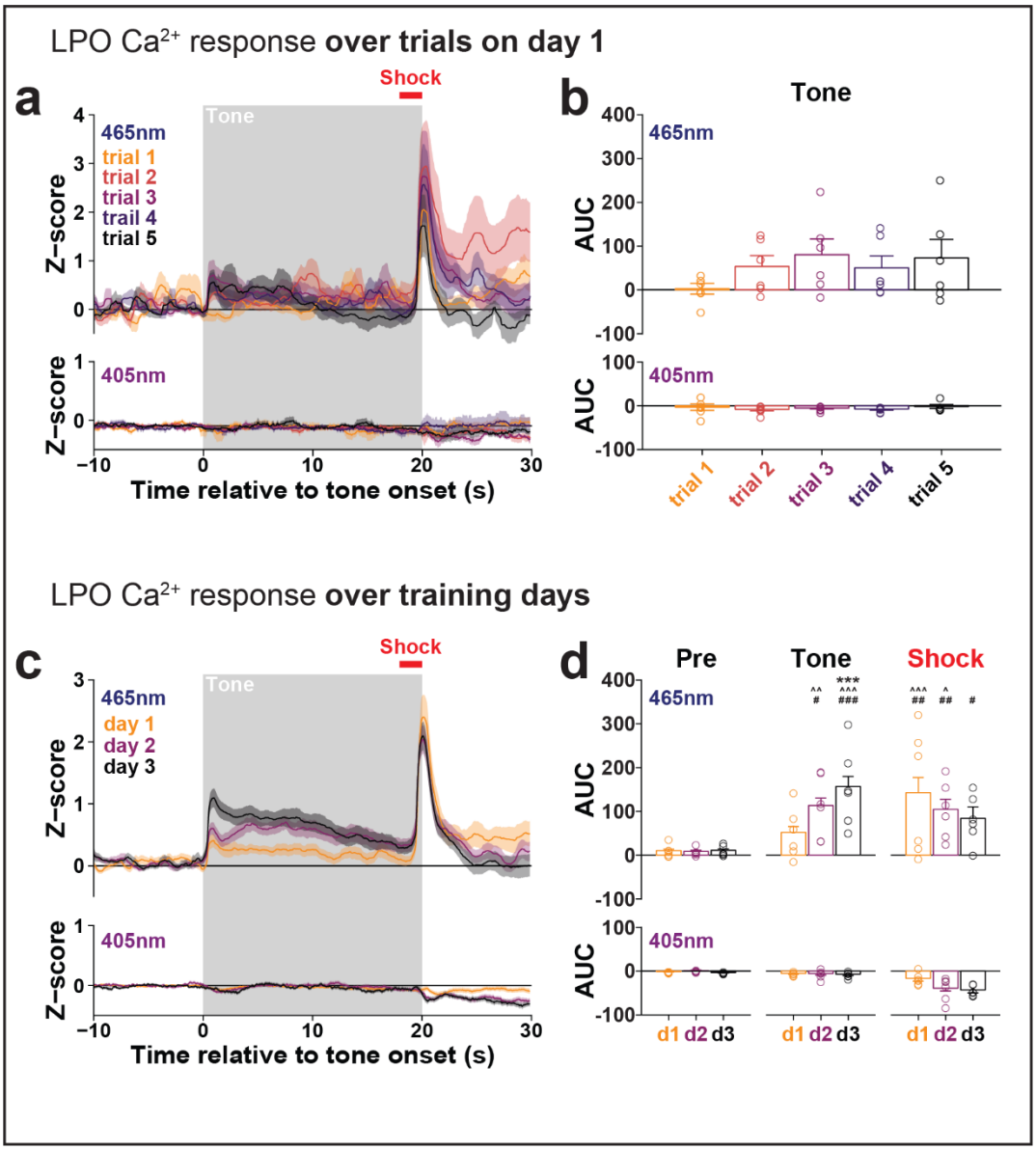

(a) LPO 465nm GCaMP (top) and 405nm auto-fluorescence (bottom) over the course of footshock conditioning trails on day 1 indicates a trend towards increase in calcium signaling to the tone and an obvious increase in calcium during footshock. **(b)** Area under the curve (AUC) for data shown in (a) over the first 10s of the tone indicates no selective changes in the 465nm GCaMP channel in any epoch over training. However, note the lack of tone response on trial 1. **(c)** Over the course of footshock conditioning training indicates a clear increase in calcium signaling to the tone. **(d)** AUC for data shown in (c) indicates an increase in calcium in response to the tone and footshock on multiple days. Furthermore, there was an increase in the tone response over training days (HSD, vs. d1 ***: $P < 0.001$; vs. Pre: ^: $P < 0.05$, ^^: $P < 0.01$, ^^^: $P < 0.001$; vs. 405nm: #: $P < 0.05$, ##: $P < 0.01$, ###:

$P < 0.001$). In (a) and (b), the thick link depicts group mean and shaded ribbon depicts SEM; colors indicate the trial (a) or day (c) as outlined in the inset. In (b) and (d), points depict subject mean AUC and bars with error bars depict group mean and SEM.

3.7 ACKNOWLEDGEMENTS

In addition to the author contributions listed at the beginning of this chapter, I would like to acknowledge and thank the people below for their contributions to the experiments in this chapter. Adrian Gunawan for assisting with and performing multiple behavioral experiments. Kevin Sattler for capturing images and performing histology for many experiments. Stève Desaivre and Vorani Ramachandra assisting with and performing many behavioral experiments. Jacklyn Nguyen for sectioning brains for multiple experiments. Finally, Robert Twining for his early pilot experiments exploring the functional connection from the LPO to the VTA using electrophysiology.

I also acknowledge and thank the people below who were important consultants during the setup of the techniques used in this chapter. Giordano de Guglielmo (Olivier George lab), and Anthony Lacagnina (Michael Drew lab) for consulting during the initial stages of setting up optogenetics for behavior. Finally, Johannes 'Han' de Jong (Stephan Lammel lab), David Barker (Marisela Morales lab), and Tom Davidson (Karl Deisseroth lab) for consulting during the initial stages of setting up fiber photometry hardware and analysis.

Chapter 4: General Discussion

The goal of this dissertation was to determine if and how the LPO is functionally connected to the VTA and to determine the role of the LPO in reinforcement and valence. Throughout this dissertation I have demonstrated the functional connectivity between the LPO and subpopulations of VTA neurons. Previous work indicated that the LPO is connected to the VTA through direct projections (Watabe-Uchida et al., 2012; Beier et al., 2015; Kalló et al., 2015), and indirect projections through the lateral habenula and RMTg (Yetnikoff et al., 2015), but a functional connection between activity in the LPO and subpopulations of neurons in the VTA had not been shown. Using pharmacological and optogenetic stimulation of the LPO, I was able to determine that the LPO inhibits the activity of VTA_{GABA} neurons and produces mixed effects on the activity of $VTA_{Dopamine}$ neurons. Throughout this dissertation I have also demonstrated that the LPO plays a causal role in reinforcement and valence. First, I demonstrated that stimulation of the LPO reinstates seeking behavior, but does not alter self-administration behavior. These results were the first to determine that an increase in LPO activity is casually related to operant behavior. Because both stressful events and rewarding events precipitate reinstatement (Venniro et al., 2016), we next conducted a series of experiments to determine if stimulation of the LPO produces reward or aversion. These experiments found that stimulation of the LPO was reinforcing but also produced avoidance. Furthermore, we recorded the activity of the LPO during rewarding and aversive conditioning and found that the LPO signals in response to aversive events, but not rewarding events. Together, the studies in this dissertation indicate that the LPO is a previously overlooked member of the brain reward and aversion circuit.

4.1 The Functional Connectivity Between the LPO and VTA

Indirect research preceding this dissertation implied that the LPO may modulate activity of $VTA_{Dopamine}$ neurons. The LPO sends monosynaptic projections to $VTA_{Dopamine}$ and VTA_{GABA} neurons (Beier et al., 2015), and also sends dense projections to brain regions known to be powerful regulators of dopamine neuron activity (Yetnikoff et al., 2015). Furthermore, electrical stimulation of the LPO supports ICSS behavior (Whishaw and Nikkel, 1975; Fouriezos et al., 1987) and ICSS is typically supported through enhanced dopamine signaling (Fenton and Liebman, 1982; Flagstad et al., 2006; Negus and Miller, 2014). Together these results indirectly imply that electrical stimulation of the LPO may enhance the activity of $VTA_{Dopamine}$ neurons. More recently, it was found that stimulation of the LPO with bicuculline promotes locomotion and conditioned place preference in a dopamine dependent manner (Subramanian et al., 2018; Reichard et al., 2019a). These results, along with a speculation that the LPO project was functionally GABAergic, led to the hypothesis that the LPO may disinhibit $VTA_{Dopamine}$ neurons by inhibiting VTA_{GABA} neurons (Subramanian et al., 2018). All together, the literature suggested there was a functional connection between the LPO and VTA, but this hypothesis had not been tested directly.

Throughout my dissertation I demonstrated that activity in the LPO is functionally related to activity within the VTA and that stimulation of the LPO inhibits VTA_{GABA} neurons and has mixed effects on $VTA_{Dopamine}$ neurons. In chapter 2, I determined the functional connectivity between the LPO and VTA using pharmacological stimulation of the LPO with the GABA-A antagonist, bicuculline. These experiments were the first to measure the effects of manipulating the LPO on the firing of VTA neurons. I found that stimulation of the LPO produced a powerful inhibition of VTA_{GABA} neurons and moderate excitation of $VTA_{Dopamine}$ neurons. These results supported the previously posited

hypothesis that stimulating the LPO with bicuculline promoted locomotion by disinhibiting dopamine neurons (Subramanian et al., 2018). From these results it was clear the LPO was functionally connected to the VTA, but the pathway that mediated this functional connection was still unclear. The LPO sends direct projections to the VTA, but also projects to intermediary structures, all of which could produce the functional connectivity measured following stimulation of LPO cell bodies with bicuculline. In chapter 3, I further determined the connectivity between the LPO and VTA and determined the contribution of the LPO→VTA pathway using optogenetic stimulation of the LPO and LPO→VTA pathway with ChR2. These experiments revealed a slightly different set of results compared to stimulating the LPO with bicuculline: stimulation of the LPO with ChR2 produced inhibition on VTA_{GABA} neurons, similar to what was observed with bicuculline. However, stimulation of the LPO with ChR2 produced mixed effects of $VTA_{Dopamine}$ neurons including both excitation and inhibition. Furthermore, I recorded the functional connectivity between the LPO and VTA by isolating the LPO→VTA pathway using a combinatorial viral approach and recording the effect of stimulating LPO→VTA cells while recording VTA neurons. In the combinatorial viral approach, I injected a retrograde CAV2-Cre in the VTA and Cre-dependent DIO-ChR2 in the LPO. Stimulating LPO→VTA neurons using this approach largely reproduced the effects of stimulating the LPO→VTA pathway. All together, these results are the first to measure the functional connectivity of the LPO→VTA pathway on VTA neuron activity, and further suggest a role for the LPO in regulation of the dopaminergic system.

The difference in $VTA_{Dopamine}$ effects produced by LPO stimulation with pharmacology and LPO stimulation with optogenetics was unexpected. Stimulation of the LPO with bicuculline leads to clear excitation of dopamine neurons but very little (if any) inhibition of dopamine neurons, while stimulation of the LPO with optogenetics leads to

both excitation and inhibition of dopamine neurons, with a greater amount of inhibition compared to excitation. At first glance, these results could appear to be contradictory; however, upon closer inspection there may be important methodological reasons that explain the difference in results. For pharmacological stimulation, we used bicuculline, which is a GABA-A receptor antagonist (but also a potassium channel antagonist), which primarily stimulates neuronal activity by blocking the GABA-A receptor, thereby releasing cells from inhibition (Curtis et al., 1970). This could produce a bias towards stimulating neurons that are under tonic inhibition. The literature shows that LPO neurons are under inhibitory control by GABA inputs from the nucleus accumbens and lateral septum (Mogenson et al., 1983; Swerdlow and Koob, 1984; Swerdlow et al., 1984); thus bicuculline may be biased towards stimulating LPO neurons that receive tonic GABA inhibition from these structures. On the other hand, for optogenetic stimulation, we used ChR2, which is a light activated cation channel, which stimulates neuronal activity by directly depolarizing the cell membrane (Boyden et al., 2005). Theoretically, ChR2 under a ubiquitous promoter (like the h-Syn promotor we employed) should produce uniform excitation across cells within the light path. In practice this does not appear to be the case. ChR2 stimulation can produce paradoxical inhibition in some cells (Herman et al., 2014), though preventing action potentials via depolarization block. Additionally, ChR2 stimulation can selectively increase firing in a subset of neurons within a larger population (Carus-Cadavieco et al., 2017). The discrepancies between stimulation methods leads to the possibility that slightly different populations of cells in the LPO are mediating the different downstream effects on VTA neurons. These results are feasible because the LPO contains both GABA and glutamate populations that can produce opposite valence (Barker et al., 2017), and neighboring hypothalamic structures, such as the lateral hypothalamus, also can produce opposite behaviors and electrophysiological results depending on weather

GABA or glutamate neurons are being manipulated (Nieh et al., 2016). With the capacity to mediate opposite modulation of VTA neurons, then biased stimulation could produce opposite results by biasing regulation of glutamate or GABA populations within the LPO. This remains speculative, and further research is necessary to determine if the stimulation mediated by bicuculline and ChR2 is producing biased effects on subpopulations of the LPO. A possible approach to test this would be to first regulate GABA and glutamate neurons in isolation and determine if the LPO produces opposing effects in the VTA as found in other brain regions. Then further studies would have to record the activity of LPO subpopulations during the application of bicuculline and stimulation of ChR2 to determine if these stimulation methods are biased in one way or another. Even in light of the differential modulation of $VTA_{Dopamine}$ activity using these two methods of stimulation, the work in this dissertation clearly indicates that the LPO can modulate the activity of VTA neurons.

Which circuitry mediates the functional connectivity between the LPO and VTA subpopulations? The data presented in this dissertation suggests that the LPO regulates VTA_{GABA} neurons through direct inhibition and drives mixed effects on dopamine neurons through either a mixed direct modulation or through a combination of direct and indirect modulation plausibly mediated by VTA_{GABA} neurons. In the case of both pharmacological and optogenetic stimulation of the LPO, we observed a powerful reduction in the activity of GABA neurons within the VTA. Many neurons ceased firing all together during stimulation, only to slowly resume firing. This powerful inhibition is likely mediated through direct inhibition, as the projection from the LPO to VTA is made up of a greater proportion of GABA compared to glutamate (chapter 3). In the case of $VTA_{Dopamine}$ neurons, the circuitry is more complicated and less clear. If we only observed excitation of $VTA_{Dopamine}$ neurons, then we could conclude that the LPO could be regulating VTA_{GABA}

neurons through disinhibition of VTA_{GABA} neurons and potentially though additional direct excitation of $VTA_{Dopamine}$ neurons. However, we observed a mixture of effects on dopamine neurons, which implies that disynaptic regulation of dopamine neurons cannot be the only mechanism by which dopamine neurons are regulated, because if the LPO only regulated $VTA_{Dopamine}$ neurons through VTA_{GABA} neurons, we should have measured a mixture of effects on VTA_{GABA} neurons. These results are in line with previous findings. First, as noted above, the LPO sends a monosynaptic projection to $VTA_{Dopamine}$ neurons (Watabe-Uchida et al., 2012; Beier et al., 2015), which implies that disynaptic regulation is not necessarily the only means of regulation. Second, neighboring brain regions, including the lateral hypothalamus (Nieh et al., 2016) and bed nucleus of the stria terminalis (Jennings et al., 2013b), send both glutamate and GABA inputs onto both $VTA_{Dopamine}$ and VTA_{GABA} neurons. These results imply, but do not confirm, that the LPO may have a similar connectivity with the midbrain dopamine system as the bed nucleus of the stria terminalis and the lateral hypothalamus, and that there is a common functional connection between the limbic forebrain and the mesolimbic dopamine system. The functional connection between the LPO and VTA positions the LPO to regulate reinforcement and reward behaviors. In the coming sections I will elaborate on the role of the LPO in behavior and discuss how the functional connection could produce these behaviors.

4.2 The Role of the LPO in Reinforcement and Valence

The data presented in this dissertation outlined how neuronal activity within the LPO is related to reinforcement and valence. We found that stimulation of the LPO with multiple methods precipitated seeking behavior but did not alter self-administration behavior. We also found that stimulation the LPO with ChR2 supported ICSS and drove real-time place aversion in the same subjects. Through analysis of RTPT behavior, we

found that the ultimate RTPT score was produced through differences in stimulation-intervals and not inter-stimulation-intervals. In a subsequent experiment, we found that stimulation of the LPO is reinforcing in the RTPT assay, despite the fact it is does not drive enhanced time spent in the side paired with stimulation. Finally, we recorded the activity of the LPO using fiber photometry during Pavlovian conditioning for footshock or sucrose and found that the LPO increases activity in response to footshock and related predictive cues, but not sucrose and related predictive cues. Over the next four sections, I will outline the results above in more detail, compare them to the existing literature, and discuss the possible circuits that underlie the results.

4.2.1 The Role of the LPO in Reward Self-Administration and Seeking

Prior to the experiments reported in this dissertation, tangential evidence suggested that the LPO could play a role self-administration of cocaine and sucrose. As noted in the previous section, connectivity studies show that the LPO projects to brain regions that are important regulators of self-administration (Yetnikoff et al., 2015). Previous literature also found a relationship between psychomotor stimulant administration and LPO neuron activity: passive administration of amphetamine increases c-fos expression in LPO neurons, specifically LPO neurons that project to the VTA (Colussi-Mas et al., 2007a), and *in-vivo* recording experiments revealed that the firing of LPO neurons fluctuate with cocaine levels during self-administration (Barker et al., 2015). The literature suggested that the LPO could be related to self-administration, but the causal role of the LPO in this behavior had not been tested.

We found that the LPO is capable of regulating reward seeking behavior but does not regulate self-administration behavior. Stimulation of the LPO with bicuculline does not affect cocaine and sucrose self-administration but it precipitates reinstatement of both

cocaine and sucrose seeking. Furthermore, we found that stimulating the LPO with an independent stimulation mechanism, excitatory DREADDs, also precipitated reinstatement of cocaine seeking behavior. The effects we observed on reinstatement of seeking can be plausibly explained by our electrophysiology experiments, where stimulation of the LPO with bicuculline leads to increased dopamine activity. Dopamine receptor activation or enhanced dopamine in the striatum precipitates reinstatement of reward seeking behavior (De Vries et al., 1999; Schmidt et al., 2006), while blocking dopamine receptors in the striatum reduces reward seeking (Anderson et al., 2003; Anderson et al., 2006). The fact that we did not observe effects of stimulating the LPO on cocaine and sucrose self-administration may imply that the LPO is already disinhibited during these behaviors; if the LPO is already maximally active, then stimulation mediated by bicuculline would be occluded. Future studies could test this directly by inhibiting the LPO during self-administration to determine if the structure regulates self-administration behavior. Taken together these results indicate that the LPO is a potential mediator of reinstatement of both drug and sucrose seeking behaviors and could represent a novel target for treatment in the prevention of relapse.

4.2.2 The Role of the LPO in Reinforcement and Valence

Early studies performing ICSS experiments suggested that the LPO could play a role in reinforcement. Stimulation of the LPO with electricity supports ICSS, but these experiments could not distinguish between activation of LPO neurons versus fibers of passage, including the medial forebrain bundle which is known to support robust ICSS (Olds and Milner, 1954; Olds and Olds, 1963). The nature of the connection was further described using collision experiments, which found that a projection that passed through, or extended from, the LPO to the VTA supported ICSS (Bielajew et al., 2001). The

strongest, but still indirect, evidence for the LPO's direct role in reinforcement came from an experiment demonstrating that excitotoxic lesions of the LPO reduced medial forebrain bundle ICSS (Arvanitogiannis et al., 1996). In this dissertation I provide the first definitive evidence that neurons of the LPO can reinforce operant behavior as indicated by the fact that optogenetic stimulation of the LPO and LPO→VTA pathway supports ICSS. Our experiments indicate that the projection from the LPO to the VTA itself, and not only pathways coursing through the LPO, support ICSS. These results imply that the LPO could play a role in reinforcing behaviors.

Our electrophysiology findings provide a plausible mechanism for how the LPO supports ICSS responding. Prior experiments have determined that ICSS behavior is dependent on an increase in dopamine concentrations (Fenton and Liebman, 1982; Flagstad et al., 2006; Negus and Miller, 2014). We found that optogenetic stimulation of the LPO with the same stimulation parameters that animals will self-stimulate leads to mixed effects on $VTA_{Dopamine}$ neurons. It stands to reason that the stimulation of $VTA_{Dopamine}$ neurons produces an increase in dopamine within the striatum, which supports ICSS. The fact that LPO stimulation produces both excitation and inhibition of $VTA_{Dopamine}$ neurons may explain why self-stimulation response rates are relatively low compared with direct, optogenetic stimulation of $VTA_{Dopamine}$ neurons (Witten et al., 2011; Steinberg et al., 2014; Jing et al., 2019). LPO stimulation may produce an intermediate level of dopamine release, which would be less reinforcing than manipulations that produce higher levels of dopamine. Another plausible explanation is that the LPO may be selectively exciting and inhibiting dopamine populations that project to different targets. If the LPO excited $VTA_{Dopamine}$ neurons that project to the prefrontal cortex and inhibited $VTA_{Dopamine}$ that project to the nucleus accumbens, we may find low levels of ICSS and real-time place aversion (Lammel et al., 2012). However, this is unlikely considering the complete lack of

correlation between the effect of LPO stimulation and the position of dopamine cells in the VTA. Broadly, medial portions of the VTA project to medial limbic structures, while lateral portions of the VTA project to lateral structures (Beier et al., 2015; Yang et al., 2018). If the LPO was selectively modulating dopamine neurons based on their projection targets, we would expect to find a semblance of a medial lateral position correlation with the effect. Future studies could test the necessity of dopamine release in mediating LPO ICSS by blocking dopamine in the striatum and measuring LPO ICSS responding. While it is not definitive that the LPO produces ICSS via dopamine modulation, it is the most plausible interpretation of the data presented in this dissertation.

In addition to determining the reinforcing qualities of stimulation of the LPO, we also determined the valence of this stimulation. We found that stimulating the LPO and LPO→VTA pathway is aversive in most rats and, as indicated by avoidance in the RTPT procedure and rewarding in others, as indicated by preference in the RTPT procedure. Our results fit within a larger literature indicating that numerous brain regions in the limbic system drive aversion or reward in the RTPT procedure. Previous results showed that stimulating the LPO-lateral habenula pathway produces reward and aversion depending on which neurotransmitter population is stimulated: stimulating the glutamate population is aversive, while stimulating the GABA population is rewarding (Barker et al., 2017). These results are expected given previous evidence from numerous labs indicating that excitation of the lateral habenula inhibits $VTA_{Dopamine}$ neurons and drives real-time place aversion (Root et al., 2014a; Yoo et al., 2016; Lazaridis et al., 2019), and that inhibition of the lateral habenula excites $VTA_{Dopamine}$ neurons and drives real-time place preference (Stamatakis et al., 2013). In this context, the aversion that we observe in the RTPT procedure could stem from the glutamate component of the LPO stimulation. Connectivity with the lateral habenula could explain the effects of LPO cell body stimulation, but the effects we

observed from stimulating the LPO→VTA pathway cannot be explained by this projection, because only a small minority of LPO neurons send projections to both targets (Yetnikoff et al., 2015). Instead, it is likely that the effects from stimulating the LPO→VTA pathway produce aversion by directly modulating the activity of VTA neurons. Previous results indicate that stimulation of $VTA_{Dopamine}$ neurons drives real-time place preference (Jeong et al., 2015; Yoo et al., 2016) while inhibition of $VTA_{Dopamine}$ neurons drives real-time place aversion (Tan et al., 2012; Danjo et al., 2014). On the other hand, stimulation of VTA_{GABA} neurons drives real-time place aversion (Tan et al., 2012), and inhibition of VTA_{GABA} neurons drives real-time place preference (Jeong et al., 2015). In this context, stimulation of the LPO→VTA pathway, and possibly LPO cell bodies, would produce aversion by inhibiting $VTA_{Dopamine}$ neurons. These results are consistent with our electrophysiology data indicating that optogenetic stimulation of the LPO produces mixed effects, including inhibition, on dopamine neurons of the VTA. The ability of the LPO to drive real-time place aversion indicates that the LPO has the capacity to drive aversive states.

Our results indicate that stimulation of the LPO with ChR2 is aversive in RTPT for the majority of rats, contrasts with data from Reichard et al (Reichard et al., 2019a) showing that stimulation of the LPO with bicuculline produces conditioned place preference. This apparent discrepancy could stem from the stimulation method used or the behavior procedure itself. Reichard et al. utilized bicuculline to stimulate LPO neurons, while we utilized ChR2. As noted above, stimulating the LPO with bicuculline consistently produces stimulation of $VTA_{Dopamine}$ neurons, whereas stimulating the LPO with ChR2 produces mixed effects on $VTA_{Dopamine}$ neurons. With this in mind, stimulating the LPO with bicuculline would stimulate $VTA_{Dopamine}$ neurons, which drives preference in conditioned place preference. Alternatively, stimulating the LPO with ChR2 would drive a mixture of effects in $VTA_{Dopamine}$ neurons including inhibition, which drives aversion in the RTPT

procedure. Another explanation for the discrepancy between Richard et al. and our experiments is the procedure used to determine if stimulation of the LPO is rewarding or aversive. Richard used conditioned place preference, which by design tests the preference following conditioning with LPO stimulation but not during LPO stimulation. Overall, our results found that stimulating the LPO with ChR2 is aversive in the majority of rats but is still reinforcing, as subjects worked to obtain stimulation in ICSS and continued to obtain stimulation in RTPT even when the optically paired side was paired with adversity (chapter 3). This could mean that in the conditioned place preference task, stimulating the LPO is aversive to the subjects but still reinforces entries into the previously paired side during the subsequent conditioning test, which would manifest as a greater amount of time in the conditioned side. Further research will be necessary to determine the valance of LPO activity across stimulation methods and procedures.

The mixed effects we observed in the RTPT assay, showing aversion in most rats and preference in some rats, mirrors the mixed effects on $VTA_{Dopamine}$ neurons in our electrophysiology data, and suggests that there can be overlapping populations that mediate the bidirectional effects. As noted above, the limbic forebrain sends mixed GABA and glutamate inputs to $VTA_{Dopamine}$ and VTA_{GABA} neurons (Jennings et al., 2013b; Nieh et al., 2016). In addition to this, activation of GABA and glutamate populations of limbic forebrain regions produces opposite effects on valence. Stimulating GABA inputs to the VTA produces preference, while stimulating glutamate inputs to the VTA produces aversion for numerous limbic forebrain structures including the lateral hypothalamus (Nieh et al., 2016), bed nucleus of the stria terminalis (Jennings et al., 2013b), and ventral pallidum (Faget et al., 2018), all of which border the LPO. If the LPO possesses a similar circuit connectivity to its bordering structures, then it is likely that the effects within the RTPT assay for GABA and glutamatergic specific stimulation would also be similar to its

bordering structures. This would mean that stimulating the LPO ubiquitously would produce a mixture of reward and aversion in subjects, but in our case, aversion prevailed in the majority of subjects. Together the literature and the data presented in this dissertation suggest that there is a common capacity for regulating valence throughout the limbic forebrain.

4.2.3 LPO Population Signaling to Rewarding and Aversive Conditioning

The knowledge of a brain regions capacity to drive valence provides us with the range of behaviors the brain region may underlie, but it does not provide us with which behaviors the brain region naturally underlies. In order to determine the behavioral function a brain structure underlies one must first determine which behaviors the structure signals to. In the final experiment of the dissertation I recorded the LPO during conditioning for rewarding and aversive events.

We found that the LPO increases activity in response to aversive events and corresponding predictive cues but does not change in response to rewarding events and corresponding predictive cues. These conclusions are based on the data obtained with calcium recording data during Pavlovian conditioning for footshock, an aversive event, and sucrose, a rewarding event. We found that over 3 days of Pavlovian conditioning for footshock there was an increase in the LPO response to the tone and there was a consistent increase in response to the footshock. On the other hand, we found that there were no substantial time-locked changes in LPO activity during Pavlovian conditioning for sucrose. These results extend results from recording of the LPO to lateral habenula pathway that found the similar effects (Barker et al., 2017). Either the LPO signals to aversive events as a whole, or the effect we recorded was the product of LPO cells that project to the lateral habenula. From our data and the literature, it is unclear if LPO projections to different brain regions show

differential activity because there have been no projection specific recordings other than the projection to the lateral habenula. The fact we observe that the LPO does not respond to rewarding events, measured as a population is somewhat surprising given prior recordings of LPO during Pavlovian conditioning for rewards which found that many LPO neurons displayed time-locked response (Ono et al., 1986). One possible explanation for the lack of a population response is that there is a relatively small portion of the LPO that shows time-locked responses, which is lost when recording the entire population. Another possibility is that there is a mixture of responses in LPO neurons, which would cancel out when recording the larger population. Recordings from Ono et al. could support either possibility, as they found that only a limited percentage of LPO neurons responded to rewarding and aversive events, and that LPO neurons showed both increased and decreased responding to these events. The recording data presented in this dissertation may shed light on the behaviors that the LPO underlies.

Why would a structure that increases activity in response to an aversive event also be reinforcing? One possibility is that the structure is providing a compensatory response to the aversive event. In addition to projections to the VTA and reward related structures, the LPO also projects to paraventricular nucleus (Cullinan et al., 1996), which implies it could be involved in regulating the stress response. Indeed, inhibiting the LPO and blocking synaptic input onto LPO neurons exacerbates the increase in circulating stress hormones in response to stressful events (Zaretsky et al., 2006; Duarte et al., 2017). These data suggest that the LPO could serve as a counterbalance to the stress response during aversive events. Another possibility is that the LPO is orchestrating behavioral responses to stressful events. Even the mesolimbic dopamine system, the quintessential reinforcement brain region, shows an increased dopamine concentration following aversive events under some circumstance (Ilango et al., 2012). There is disagreement about what

this upregulation of activity is accomplishing, but it could be related to orchestrating a response to the aversive event and/or reinforcing successful escape behaviors. This is speculative, additional research is necessary to understand what the upregulation of LPO activity during stressful events is accomplishing during the response to these events.

4.3 CONCLUSION

The data throughout this dissertation demonstrate that the LPO regulates reward centers of the brain and shape behavior. I showed that the LPO is functionally connected with the activity of VTA subpopulations, where stimulation of the LPO inhibits VTA_{GABA} neurons and has mixed effects on $VTA_{Dopamine}$ neurons. This pattern of modulation of the VTA is consistent with the complex regulation found for bordering limbic forebrain structures. Furthermore, I found that stimulation of the LPO drives reward seeking behaviors across reward modalities, directly supports reinforcement, and is aversive. Together these data show that the LPO is capable of regulating motivated behaviors. Finally, I found that the LPO signals to aversive events but not rewarding events, which further suggests a role of the LPO in mediating the behavior related to reward and aversion. All together my work suggests that the LPO is a member of the brain reward circuit and warrants further research into its role in reward and aversive behaviors.

Works Cited

Ahmed, S.H. (2011). "Escalation of drug use," in *Neuromethods: Animal models of addiction,* ed. M.C. Olmstead. (New York: Humana Press), 267-292.

American Psychiatric Association., and American Psychiatric Association. Dsm-5 Task Force. (2013). *Diagnostic and statistical manual of mental disorders : DSM-5.* Washington, D.C.: American Psychiatric Association.

Anderson, S.M., Bari, A.A., and Pierce, R.C. (2003). Administration of the D1-like dopamine receptor antagonist SCH-23390 into the medial nucleus accumbens shell attenuates cocaine priming-induced reinstatement of drug-seeking behavior in rats. *Psychopharmacology (Berl)* 168**,** 132-138.

Anderson, S.M., Schmidt, H.D., and Pierce, R.C. (2006). Administration of the D2 dopamine receptor antagonist sulpiride into the shell, but not the core, of the nucleus accumbens attenuates cocaine priming-induced reinstatement of drug seeking. *Neuropsychopharmacology* 31**,** 1452-1461.

Aransay, A., Rodriguez-Lopez, C., Garcia-Amado, M., Clasca, F., and Prensa, L. (2015). Long-range projection neurons of the mouse ventral tegmental area: a single-cell axon tracing analysis. *Front Neuroanat* 9**,** 59.

Arnold, J.M., and Roberts, D.C. (1997). A critique of fixed and progressive ratio schedules used to examine the neural substrates of drug reinforcement. *Pharmacol Biochem Behav* 57**,** 441-447.

Arvanitogiannis, A., Riscaldino, L., and Shizgal, P. (1999). Effects of NMDA lesions of the medial basal forebrain on LH and VTA self-stimulation. *Physiol Behav* 65**,** 805-810.

Arvanitogiannis, A., Waraczynski, M., and Shizgal, P. (1996). Effects of excitotoxic lesions of the basal forebrain on MFB self-stimulation. *Physiol Behav* 59**,** 795-806.

Bachtell, R.K., Whisler, K., Karanian, D., and Self, D.W. (2005). Effects of intra-nucleus accumbens shell administration of dopamine agonists and antagonists on cocaine-taking and cocaine-seeking behaviors in the rat. *Psychopharmacology (Berl)* 183**,** 41-53.

Barbano, M.F., Wang, H.-L.L., Morales, M., and Wise, R.A. (2016). Feeding and Reward Are Differentially Induced by Activating GABAergic Lateral Hypothalamic Projections to VTA. *The Journal of neuroscience : the official journal of the Society for Neuroscience* 36**,** 2975-2985.

Barker, D.J., Miranda-Barrientos, J., Zhang, S., Root, D.H., Wang, H.L., Liu, B., Calipari, E.S., and Morales, M. (2017). Lateral Preoptic Control of the Lateral Habenula through Convergent Glutamate and GABA Transmission. *Cell Rep* 21**,** 1757-1769.

Barker, D.J., Root, D.H., Zhang, S., and Morales, M. (2016). Multiplexed neurochemical signaling by neurons of the ventral tegmental area. *J Chem Neuroanat* 73**,** 33-42.

Barker, D.J., Striano, B.M., Coffey, K.C., Root, D.H., Pawlak, A.P., Kim, O.A., Kulik, J., Fabbricatore, A.T., and West, M.O. (2015). Sensitivity to self-administered cocaine within the lateral preoptic-rostral lateral hypothalamic continuum. *Brain structure & function* 220**,** 1841-1854.

Beier, K.T., Steinberg, E.E., Deloach, K.E., Xie, S., Miyamichi, K., Schwarz, L., Gao, X.J., Kremer, E.J., Malenka, R.C., and Luo, L. (2015). Circuit Architecture of VTA Dopamine Neurons Revealed by Systematic Input-Output Mapping. *Cell* 162**,** 622-634.

Ben-Ari, Y. (2002). Excitatory actions of gaba during development: the nature of the nurture. *Nat Rev Neurosci* 3**,** 728-739.

Berridge, K.C. (2007). The debate over dopamine's role in reward: the case for incentive salience. *Psychopharmacology (Berl)* 191**,** 391-431.

Berridge, K.C. (2019). Affective valence in the brain: modules or modes? *Nat Rev Neurosci* 20**,** 225-234.

Berridge, K.C., and Kringelbach, M.L. (2008). Affective neuroscience of pleasure: reward in humans and animals. *Psychopharmacology (Berl)* 199**,** 457-480.

Berridge, K.C., Robinson, T.E., and Aldridge, J.W. (2009). Dissecting components of reward: 'liking', 'wanting', and learning. *Curr Opin Pharmacol* 9**,** 65-73.

Bielajew, C., Bushnik, T., Konkle, A.T., and Schindler, D. (2000). The substrate for brain-stimulation reward in the lateral preoptic area. II. Connections to the ventral tegmental area. *Brain Res* 881**,** 112-120.

Bielajew, C., Konkle, A.T., Fouriezos, G., Boucher-Thrasher, A., and Schindler, D. (2001). The substrate for brain-stimulation reward in the lateral preoptic area: III. Connections to the lateral hypothalamic area. *Behav Neurosci* 115**,** 900-909.

Bishop, M.P., Elder, S.T., and Heath, R.G. (1963). Intracranial self-stimulation in man. *Science* 140**,** 394-396.

Bocklisch, C., Pascoli, V., Wong, J.C., House, D.R., Yvon, C., De Roo, M., Tan, K.R., and Luscher, C. (2013). Cocaine disinhibits dopamine neurons by potentiation of GABA transmission in the ventral tegmental area. *Science* 341**,** 1521-1525.

Bossert, J.M., Ghitza, U.E., Lu, L., Epstein, D.H., and Shaham, Y. (2005). Neurobiology of relapse to heroin and cocaine seeking: an update and clinical implications. *European Journal of Pharmacology* 526**,** 36-50.

Bossert, J.M., Marchant, N.J., Calu, D.J., and Shaham, Y. (2013). The reinstatement model of drug relapse: recent neurobiological findings, emerging research topics, and translational research. *Psychopharmacology* 229**,** 453-476.

Bourdy, R., and Barrot, M. (2012). A new control center for dopaminergic systems: pulling the VTA by the tail. *Trends Neurosci* 35**,** 681-690.

Bourdy, R., Sanchez-Catalan, M.J., Kaufling, J., Balcita-Pedicino, J.J., Freund-Mercier, M.J., Veinante, P., Sesack, S.R., Georges, F., and Barrot, M. (2014). Control of the nigrostriatal dopamine neuron activity and motor function by the tail of the ventral tegmental area. *Neuropsychopharmacology* 39**,** 2788-2798.

Boyden, E.S., Zhang, F., Bamberg, E., Nagel, G., and Deisseroth, K. (2005). Millisecond-timescale, genetically targeted optical control of neural activity. *Nature Neuroscience* 8**,** 1263-1268.

Briski, K., and Gillen, E. (2001). Differential distribution of Fos expression within the male rat preoptic area and hypothalamus in response to physical vs. psychological stress. *Brain Res Bull* 55**,** 401-408.

Britt, J.P., Benaliouad, F., Mcdevitt, R.A., Stuber, G.D., Wise, R.A., and Bonci, A. (2012). Synaptic and behavioral profile of multiple glutamatergic inputs to the nucleus accumbens. *Neuron* 76**,** 790-803.

Broadley, K.J. (2010). The vascular effects of trace amines and amphetamines. *Pharmacol Ther* 125**,** 363-375.

Brown, P.L., Palacorolla, H., Brady, D., Riegger, K., Elmer, G.I., and Shepard, P.D. (2017). Habenula-Induced Inhibition of Midbrain Dopamine Neurons Is Diminished by Lesions of the Rostromedial Tegmental Nucleus. *J Neurosci* 37**,** 217-225.

Brown, P.L., and Shepard, P.D. (2016). Functional evidence for a direct excitatory projection from the lateral habenula to the ventral tegmental area in the rat. *J Neurophysiol* 116**,** 1161-1174.

Bushnik, T., Bielajew, C., and Konkle, A.T. (2000). The substrate for brain-stimulation reward in the lateral preoptic area. I. Anatomical mapping of its boundaries. *Brain Res* 881**,** 103-111.

Cachope, R., Mateo, Y., Mathur, B.N., Irving, J., Wang, H.L., Morales, M., Lovinger, D.M., and Cheer, J.F. (2012). Selective activation of cholinergic interneurons enhances accumbal phasic dopamine release: setting the tone for reward processing. *Cell Rep* 2**,** 33-41.

Campeau, S., and Watson, S.J. (1997). Neuroendocrine and behavioral responses and brain pattern of c-fos induction associated with audiogenic stress. *J Neuroendocrinol* 9**,** 577-588.

Carus-Cadavieco, M., Gorbati, M., Ye, L., Bender, F., Van Der Veldt, S., Kosse, C., Borgers, C., Lee, S.Y., Ramakrishnan, C., Hu, Y., Denisova, N., Ramm, F., Volitaki, E., Burdakov, D., Deisseroth, K., Ponomarenko, A., and Korotkova, T. (2017). Gamma oscillations organize top-down signalling to hypothalamus and enable food seeking. *Nature* 542**,** 232-236.

Chang, C.Y., Esber, G.R., Marrero-Garcia, Y., Yau, H.J., Bonci, A., and Schoenbaum, G. (2016). Brief optogenetic inhibition of dopamine neurons mimics endogenous negative reward prediction errors. *Nat Neurosci* 19**,** 111-116.

Cheeta, S., Brooks, S., and Willner, P. (1995). Effects of reinforcer sweetness and the D2/D3 antagonist raclopride on progressive ratio operant performance. *Behav Pharmacol* 6**,** 127-132.

Chen, X., and Herbert, J. (1995). Regional changes in c-fos expression in the basal forebrain and brainstem during adaptation to repeated stress: correlations with cardiovascular, hypothermic and endocrine responses. *Neuroscience* 64**,** 675-685.

Christoph, G.R., Leonzio, R.J., and Wilcox, K.S. (1986). Stimulation of the lateral habenula inhibits dopamine-containing neurons in the substantia nigra and ventral tegmental area of the rat. *J Neurosci* 6**,** 613-619.

Chung, K.K., Martinez, M., and Herbert, J. (2000). c-fos expression, behavioural, endocrine and autonomic responses to acute social stress in male rats after chronic restraint: modulation by serotonin. *Neuroscience* 95**,** 453-463.

Cohen, J.Y., Haesler, S., Vong, L., Lowell, B.B., and Uchida, N. (2012). Neuron-type-specific signals for reward and punishment in the ventral tegmental area. *Nature* 482**,** 85-88.

Cole, S.L., Robinson, M.J.F., and Berridge, K.C. (2018). Optogenetic self-stimulation in the nucleus accumbens: D1 reward versus D2 ambivalence. *PLoS One* 13**,** e0207694.

Colussi-Mas, J., Geisler, S., Zimmer, L., Zahm, D.S., and Berod, A. (2007a). Activation of afferents to the ventral tegmental area in response to acute amphetamine: a double-labelling study. *Eur J Neurosci* 26**,** 1011-1025.

Colussi-Mas, J., Geisler, S., Zimmer, L., Zahm, D.S., and Bérod, A. (2007b). Activation of afferents to the ventral tegmental area in response to acute amphetamine: a double-labelling study. *The European journal of neuroscience* 26**,** 1011-1025.

Comoli, E., Coizet, V., Boyes, J., Bolam, J.P., Canteras, N.S., Quirk, R.H., Overton, P.G., and Redgrave, P. (2003). A direct projection from superior colliculus to substantia nigra for detecting salient visual events. *Nat Neurosci* 6**,** 974-980.

Conrad, L.C., and Pfaff, D.W. (1976). Autoradiographic tracing of nucleus accumbens efferents in the rat. *Brain Res* 113**,** 589-596.

Creed, M.C., Ntamati, N.R., and Tan, K.R. (2014). VTA GABA neurons modulate specific learning behaviors through the control of dopamine and cholinergic systems. *Front Behav Neurosci* 8**,** 8.

Cullinan, W.E., Helmreich, D.L., and Watson, S.J. (1996). Fos expression in forebrain afferents to the hypothalamic paraventricular nucleus following swim stress. *J Comp Neurol* 368**,** 88-99.

Curtis, D.R., Duggan, A.W., Felix, D., and Johnston, G.A. (1970). GABA, bicuculline and central inhibition. *Nature* 226**,** 1222-1224.

Danaei, G., Ding, E.L., Mozaffarian, D., Taylor, B., Rehm, J., Murray, C.J., and Ezzati, M. (2009). The preventable causes of death in the United States: comparative risk assessment of dietary, lifestyle, and metabolic risk factors. *PLoS Med* 6**,** e1000058.

Danjo, T., Yoshimi, K., Funabiki, F., Yawata, S., and Nakanishi, S. (2014). Aversive behavior induced by optogenetic inactivation of ventral tegmental area dopamine neurons is mediated by dopamine D2 receptors in the nucleus accumbens. *Proceedings of the National Academy of Sciences of the United States of America* 111**,** 6455-6460.

De Jong, J.W., Afjei, S.A., Pollak Dorocic, I., Peck, J.R., Liu, C., Kim, C.K., Tian, L., Deisseroth, K., and Lammel, S. (2019). A Neural Circuit Mechanism for Encoding Aversive Stimuli in the Mesolimbic Dopamine System. *Neuron* 101**,** 133-151 e137.

De Vries, T.J., Schoffelmeer, A.N., Binnekade, R., and Vanderschuren, L.J. (1999). Dopaminergic mechanisms mediating the incentive to seek cocaine and heroin following long-term withdrawal of IV drug self-administration. *Psychopharmacology (Berl)* 143**,** 254-260.

Dobi, A., Margolis, E.B., Wang, H.L., Harvey, B.K., and Morales, M. (2010). Glutamatergic and nonglutamatergic neurons of the ventral tegmental area establish

local synaptic contacts with dopaminergic and nondopaminergic neurons. *J Neurosci* 30**,** 218-229.

Domjan, M. (2005). Pavlovian conditioning: a functional perspective. *Annu Rev Psychol* 56**,** 179-206.

Duarte, J.O., Gomes, K.S., Nunes-De-Souza, R.L., and Crestani, C.C. (2017). Role of the lateral preoptic area in cardiovascular and neuroendocrine responses to acute restraint stress in rats. *Physiol Behav* 175**,** 16-21.

Einhorn, L.C., Johansen, P.A., and White, F.J. (1988). Electrophysiological effects of cocaine in the mesoaccumbens dopamine system: studies in the ventral tegmental area. *J Neurosci* 8**,** 100-112.

Elder, S.T., and Work, M.S. (1965). Self-determined stimulus trains of ICSS delivered to preoptic and forebrain regions as a function of biphasic rectangular pulse frequency. *Psychol Rep* 17**,** 803-806.

Esclapez, M., Tillakaratne, N.J., Kaufman, D.L., Tobin, A.J., and Houser, C.R. (1994). Comparative localization of two forms of glutamic acid decarboxylase and their mRNAs in rat brain supports the concept of functional differences between the forms. *J Neurosci* 14**,** 1834-1855.

Esclapez, M., Tillakaratne, N.J., Tobin, A.J., and Houser, C.R. (1993). Comparative localization of mRNAs encoding two forms of glutamic acid decarboxylase with nonradioactive in situ hybridization methods. *J Comp Neurol* 331**,** 339-362.

Eshel, N., Bukwich, M., Rao, V., Hemmelder, V., Tian, J., and Uchida, N. (2015). Arithmetic and local circuitry underlying dopamine prediction errors. *Nature* 525**,** 243-246.

Eshel, N., Tian, J., Bukwich, M., and Uchida, N. (2016). Dopamine neurons share common response function for reward prediction error. *Nat Neurosci* 19**,** 479-486.

Faget, L., Osakada, F., Duan, J., Ressler, R., Johnson, A.B., Proudfoot, J.A., Yoo, J.H., Callaway, E.M., and Hnasko, T.S. (2016). Afferent Inputs to Neurotransmitter-Defined Cell Types in the Ventral Tegmental Area. *Cell Rep* 15**,** 2796-2808.

Faget, L., Zell, V., Souter, E., Mcpherson, A., Ressler, R., Gutierrez-Reed, N., Yoo, J.H., Dulcis, D., and Hnasko, T.S. (2018). Opponent control of behavioral reinforcement by inhibitory and excitatory projections from the ventral pallidum. *Nat Commun* 9**,** 849.

Fenton, H.M., and Liebman, J.M. (1982). Self-stimulation response decrement patterns differentiate clonidine, baclofen and dopamine antagonists from drugs causing performance deficit. *Pharmacol Biochem Behav* 17**,** 1207-1212.

Fibiger, H.C., Lepiane, F.G., Jakubovic, A., and Phillips, A.G. (1987). The role of dopamine in intracranial self-stimulation of the ventral tegmental area. *J Neurosci* 7**,** 3888-3896.

Flagstad, P., Arnt, J., and Olsen, C.K. (2006). Classical as well as novel antipsychotic drugs increase self-stimulation threshold in the rat--similar mechanism of action? *Eur J Pharmacol* 544**,** 69-76.

Fouriezos, G., Walker, S., Rick, J., and Bielajew, C. (1987). Refractoriness of neurons mediating intracranial self-stimulation in the anterior basal forebrain. *Behav Brain Res* 24**,** 73-80.

Fremeau, R.T., Jr., Voglmaier, S., Seal, R.P., and Edwards, R.H. (2004). VGLUTs define subsets of excitatory neurons and suggest novel roles for glutamate. *Trends Neurosci* 27**,** 98-103.

Friedman, A., Lax, E., Dikshtein, Y., Abraham, L., Flaumenhaft, Y., Sudai, E., Ben-Tzion, M., Ami-Ad, L., Yaka, R., and Yadid, G. (2010). Electrical stimulation of the lateral habenula produces enduring inhibitory effect on cocaine seeking behavior. *Neuropharmacology* 59**,** 452-459.

Geisler, S., Derst, C., Veh, R.W., and Zahm, D.S. (2007). Glutamatergic Afferents of the Ventral Tegmental Area in the Rat. *The Journal of Neuroscience* 27**,** 5730-5743.

Gervasoni, D., Peyron, C., Rampon, C., Barbagli, B., Chouvet, G., Urbain, N., Fort, P., and Luppi, P.H. (2000). Role and origin of the GABAergic innervation of dorsal raphe serotonergic neurons. *J Neurosci* 20**,** 4217-4225.

Gigante, E.D., Benaliouad, F., Zamora-Olivencia, V., and Wise, R.A. (2016). Optogenetic Activation of a Lateral Hypothalamic-Ventral Tegmental Drive-Reward Pathway. *PLoS One* 11**,** e0158885.

Grace, A.A. (1991). Phasic versus tonic dopamine release and the modulation of dopamine system responsivity: a hypothesis for the etiology of schizophrenia. *Neuroscience* 41**,** 1-24.

Grace, A.A., and Bunney, B.S. (1983). Intracellular and extracellular electrophysiology of nigral dopaminergic neurons--1. Identification and characterization. *Neuroscience* 10**,** 301-315.

Grimm, J.W., Harkness, J.H., Ratliff, C., Barnes, J., North, K., and Collins, S. (2011). Effects of systemic or nucleus accumbens-directed dopamine D1 receptor antagonism on sucrose seeking in rats. *Psychopharmacology (Berl)* 216**,** 219-233.

Gulledge, A.T., and Stuart, G.J. (2003). Excitatory actions of GABA in the cortex. *Neuron* 37**,** 299-309.

Gunaydin, L.A., Grosenick, L., Finkelstein, J.C., Kauvar, I.V., Fenno, L.E., Adhikari, A., Lammel, S., Mirzabekov, J.J., Airan, R.D., Zalocusky, K.A., Tye, K.M., Anikeeva, P., Malenka, R.C., and Deisseroth, K. (2014). Natural neural projection dynamics underlying social behavior. *Cell* 157**,** 1535-1551.

Hamid, A.A., Pettibone, J.R., Mabrouk, O.S., Hetrick, V.L., Schmidt, R., Weele, C.M., Kennedy, R.T., Aragona, B.J., and Berke, J.D. (2016). Mesolimbic dopamine signals the value of work. *Nature neuroscience* 19**,** 117-126.

Hammond, C. (2015). *Cellular and molecular neurophysiology.* Amsterdam ; Boston: Elsevier/AP, Academic Press is an imprint of Elsevier.

Herman, A.M., Huang, L., Murphey, D.K., Garcia, I., and Arenkiel, B.R. (2014). Cell type-specific and time-dependent light exposure contribute to silencing in neurons expressing Channelrhodopsin-2. *Elife* 3.

Hikosaka, O., Sesack, S.R., Lecourtier, L., and Shepard, P.D. (2008). Habenula: crossroad between the basal ganglia and the limbic system. *J Neurosci* 28**,** 11825-11829.

Holly, E.N., and Miczek, K.A. (2016). Ventral tegmental area dopamine revisited: effects of acute and repeated stress. *Psychopharmacology (Berl)* 233**,** 163-186.

Hubner, C.B., and Moreton, J.E. (1991). Effects of selective D1 and D2 dopamine antagonists on cocaine self-administration in the rat. *Psychopharmacology (Berl)* 105**,** 151-156.

Ikemoto, S. (2003). Involvement of the olfactory tubercle in cocaine reward: intracranial self-administration studies. *J Neurosci* 23**,** 9305-9311.

Ikemoto, S., and Panksepp, J. (1999). The role of nucleus accumbens dopamine in motivated behavior: a unifying interpretation with special reference to reward-seeking. *Brain Res Brain Res Rev* 31**,** 6-41.

Ilango, A., Shumake, J., Wetzel, W., Scheich, H., and Ohl, F.W. (2012). The role of dopamine in the context of aversive stimuli with particular reference to acoustically signaled avoidance learning. *Front Neurosci* 6**,** 132.

Iversen, L.L. (2010). *Dopamine handbook.* Oxford ; New York: Oxford University Press.

Jennings, J.H., Rizzi, G., Stamatakis, A.M., Ung, R.L., and Stuber, G.D. (2013a). The inhibitory circuit architecture of the lateral hypothalamus orchestrates feeding. *Science* 341**,** 1517-1521.

Jennings, J.H., Sparta, D.R., Stamatakis, A.M., Ung, R.L., Pleil, K.E., Kash, T.L., and Stuber, G.D. (2013b). Distinct extended amygdala circuits for divergent motivational states. *Nature* 496**,** 224-228.

Jeong, J.W., Mccall, J.G., Shin, G., Zhang, Y., Al-Hasani, R., Kim, M., Li, S., Sim, J.Y., Jang, K.I., Shi, Y., Hong, D.Y., Liu, Y., Schmitz, G.P., Xia, L., He, Z., Gamble, P., Ray, W.Z., Huang, Y., Bruchas, M.R., and Rogers, J.A. (2015). Wireless Optofluidic Systems for Programmable In Vivo Pharmacology and Optogenetics. *Cell* 162**,** 662-674.

Jhou, T.C., Geisler, S., Marinelli, M., Degarmo, B.A., and Zahm, D.S. (2009). The mesopontine rostromedial tegmental nucleus: A structure targeted by the lateral habenula that projects to the ventral tegmental area of Tsai and substantia nigra compacta. *Journal of Comparative Neurology* 513.

Ji, H., and Shepard, P.D. (2007). Lateral habenula stimulation inhibits rat midbrain dopamine neurons through a GABA(A) receptor-mediated mechanism. *J Neurosci* 27**,** 6923-6930.

Jin, W., Kim, M.S., Jang, E.Y., Lee, J.Y., Lee, J.G., Kim, H.Y., Yoon, S.S., Lee, B.H., Chang, S., Kim, J.H., Choi, K.H., Koo, H., Gwak, Y.S., Steffensen, S.C., Ryu, Y.H., Kim, H.Y., and Yang, C.H. (2018). Acupuncture reduces relapse to cocaine-seeking behavior via activation of GABA neurons in the ventral tegmental area. *Addict Biol* 23**,** 165-181.

Jing, M.Y., Han, X., Zhao, T.Y., Wang, Z.Y., Lu, G.Y., Wu, N., Song, R., and Li, J. (2019). Re-examining the role of ventral tegmental area dopaminergic neurons in motor activity and reinforcement by chemogenetic and optogenetic manipulation in mice. *Metab Brain Dis* 34**,** 1421-1430.

Junyent, F., and Kremer, E.J. (2015). CAV-2-why a canine virus is a neurobiologist's best friend. *Current opinion in pharmacology* 24**,** 86-93.

Kalivas, P.W., and Volkow, N.D. (2005). The neural basis of addiction: a pathology of motivation and choice. *Am J Psychiatry* 162**,** 1403-1413.

Kalló, I., Molnár, C.S., Szöke, S., Fekete, C., Hrabovszky, E., and Liposits, Z. (2015). Area-specific analysis of the distribution of hypothalamic neurons projecting to the rat ventral tegmental area, with special reference to the GABAergic and glutamatergic efferents. *Frontiers in Neuroanatomy* 9**,** 112.

Kandel, E.R. (2013). *Principles of neural science.* New York: McGraw-Hill.

Keller, F.S., and Schoenfeld, W.N. (1950). *Principles of psychology; a systematic text in the science of behavior.* New York,: Appleton-Century-Crofts.

Kenny, P.J. (2011a). Common cellular and molecular mechanisms in obesity and drug addiction. *Nature Reviews Neuroscience* 12**,** 638-651.

Kenny, P.J. (2011b). Reward Mechanisms in Obesity: New Insights and Future Directions. *Neuron* 69**,** 664-679.

Kiyohara, T., Miyata, S., Nakamura, T., Shido, O., Nakashima, T., and Shibata, M. (1995). Differences in Fos expression in the rat brains between cold and warm ambient exposures. *Brain Res Bull* 38**,** 193-201.

Koob, G.F., Arends, M.A., and Le Moal, M. (2014). *Drugs, addiction, and the brain.* Amsterdam ; Boston: Elsevier/AP, Academic Press is an imprint of Elsevier.

Kowski, A.B., Geisler, S., Krauss, M., and Veh, R.W. (2008). Differential projections from subfields in the lateral preoptic area to the lateral habenular complex of the rat. *The Journal of comparative neurology* 507**,** 1465-1478.

Kravitz, A.V., Tye, L.D., and Kreitzer, A.C. (2012). Distinct roles for direct and indirect pathway striatal neurons in reinforcement. *Nat Neurosci* 15**,** 816-818.

Kroeger, D., Absi, G., Gagliardi, C., Bandaru, S.S., Madara, J.C., Ferrari, L.L., Arrigoni, E., Munzberg, H., Scammell, T.E., Saper, C.B., and Vetrivelan, R. (2018). Galanin neurons in the ventrolateral preoptic area promote sleep and heat loss in mice. *Nat Commun* 9**,** 4129.

Kuhar, M.J., Ritz, M.C., and Boja, J.W. (1991). The dopamine hypothesis of the reinforcing properties of cocaine. *Trends Neurosci* 14**,** 299-302.

Lammel, S., Lim, B.K., Ran, C., Huang, K.W., Betley, M.J., Tye, K.M., Deisseroth, K., and Malenka, R.C. (2012). Input-specific control of reward and aversion in the ventral tegmental area. *Nature* 491**,** 212-217.

Lavezzi, H.N., Parsley, K.P., and Zahm, D.S. (2015). Modulation of locomotor activation by the rostromedial tegmental nucleus. *Neuropsychopharmacology* 40**,** 676-687.

Lazaridis, I., Tzortzi, O., Weglage, M., Martin, A., Xuan, Y., Parent, M., Johansson, Y., Fuzik, J., Furth, D., Fenno, L.E., Ramakrishnan, C., Silberberg, G., Deisseroth, K., Carlen, M., and Meletis, K. (2019). A hypothalamus-habenula circuit controls aversion. *Mol Psychiatry* 24**,** 1351-1368.

Lecca, S., Melis, M., Luchicchi, A., Muntoni, A.L., and Pistis, M. (2012). Inhibitory inputs from rostromedial tegmental neurons regulate spontaneous activity of midbrain dopamine cells and their responses to drugs of abuse. *Neuropsychopharmacology* 37**,** 1164-1176.

Lecca, S., Meye, F.J., and Mameli, M. (2014). The lateral habenula in addiction and depression: an anatomical, synaptic and behavioral overview. *Eur J Neurosci* 39**,** 1170-1178.

Lee, A.T., Vogt, D., Rubenstein, J.L., and Sohal, V.S. (2014). A class of GABAergic neurons in the prefrontal cortex sends long-range projections to the nucleus accumbens and elicits acute avoidance behavior. *J Neurosci* 34**,** 11519-11525.

Li, H., Pullmann, D., Cho, J.Y., Eid, M., and Jhou, T.C. (2019). Generality and opponency of rostromedial tegmental (RMTg) roles in valence processing. *Elife* 8.

Li, S.J., Vaughan, A., Sturgill, J.F., and Kepecs, A. (2018). A Viral Receptor Complementation Strategy to Overcome CAV-2 Tropism for Efficient Retrograde Targeting of Neurons. *Neuron* 98**,** 905-917 e905.

Lobb, C.J., Wilson, C.J., and Paladini, C.A. (2010). A dynamic role for GABA receptors on the firing pattern of midbrain dopaminergic neurons. *J Neurophysiol* 104**,** 403-413.

Logrip, M.L., Zorrilla, E.P., and Koob, G.F. (2012). Stress modulation of drug self-administration: implications for addiction comorbidity with post-traumatic stress disorder. *Neuropharmacology* 62**,** 552-564.

Lohani, S., Martig, A.K., Underhill, S.M., Defrancesco, A., Roberts, M.J., Rinaman, L., Amara, S., and Moghaddam, B. (2018). Burst activation of dopamine neurons produces prolonged post-burst availability of actively released dopamine. *Neuropsychopharmacology* 43**,** 2083-2092.

Louisa Degenhardt, Harvey a Whiteford, Alize J Ferrari, Amanda J Baxter, Fiona J Charlson, Wayne D Hall, Greg Freedman, Roy Burstein, Nicole Johns, Rebecca E Engell, Abraham Flaxman, Christopher Jl Murray, and Vos, T. (2013). Global burden of disease attributable to illicit drug use and dependence: findings from the Global Burden of Disease Study 2010. *The Lancet* 382**,** 1564-1574.

Mahler, S.V., Brodnik, Z.D., Cox, B.M., Buchta, W.C., Bentzley, B.S., Quintanilla, J., Cope, Z.A., Lin, E.C., Riedy, M.D., Scofield, M.D., Messinger, J., Ruiz, C.M., Riegel, A.C., Espana, R.A., and Aston-Jones, G. (2019). Chemogenetic Manipulations of Ventral Tegmental Area Dopamine Neurons Reveal Multifaceted Roles in Cocaine Abuse. *J Neurosci* 39**,** 503-518.

Mahler, S.V., Vazey, E.M., Beckley, J.T., Keistler, C.R., Mcglinchey, E.M., Kaufling, J., Wilson, S.P., Deisseroth, K., Woodward, J.J., and Aston-Jones, G. (2014). Designer receptors show role for ventral pallidum input to ventral tegmental area in cocaine seeking. *Nat Neurosci* 17**,** 577-585.

Marinelli, M., Cooper, D.C., Baker, L.K., and White, F.J. (2003). Impulse activity of midbrain dopamine neurons modulates drug-seeking behavior. *Psychopharmacology (Berl)* 168**,** 84-98.

Marinelli, M., and Mccutcheon, J.E. (2014). Heterogeneity of dopamine neuron activity across traits and states. *Neuroscience* 282**,** 176-197.

Marinelli, M., Rudick, C.N., Hu, X.T., and White, F.J. (2006). Excitability of dopamine neurons: modulation and physiological consequences. *CNS Neurol Disord Drug Targets* 5**,** 79-97.

Martinez, M., Phillips, P.J., and Herbert, J. (1998). Adaptation in patterns of c-fos expression in the brain associated with exposure to either single or repeated social stress in male rats. *Eur J Neurosci* 10**,** 20-33.

Martinez, R.C., Carvalho-Netto, E.F., Amaral, V.C., Nunes-De-Souza, R.L., and Canteras, N.S. (2008). Investigation of the hypothalamic defensive system in the mouse. *Behavioural brain research* 192**,** 185-190.

Matsuda, W., Furuta, T., Nakamura, K.C., Hioki, H., Fujiyama, F., Arai, R., and Kaneko, T. (2009). Single nigrostriatal dopaminergic neurons form widely spread and highly dense axonal arborizations in the neostriatum. *J Neurosci* 29**,** 444-453.

Matsumoto, H., Tian, J., Uchida, N., and Watabe-Uchida, M. (2016). Midbrain dopamine neurons signal aversion in a reward-context-dependent manner. *Elife* 5.

Matsumoto, M., and Hikosaka, O. (2007). Lateral habenula as a source of negative reward signals in dopamine neurons. *Nature* 447**,** 1111-1115.

Mccutcheon, J.E., Ebner, S.R., Loriaux, A.L., and Roitman, M.F. (2012). Encoding of aversion by dopamine and the nucleus accumbens. *Front Neurosci* 6**,** 137.

Mcgregor, A., and Roberts, D.C. (1993). Dopaminergic antagonism within the nucleus accumbens or the amygdala produces differential effects on intravenous cocaine self-administration under fixed and progressive ratio schedules of reinforcement. *Brain Res* 624**,** 245-252.

Mclellan, A.T., Lewis, D.C., O'brien, C.P., and Kleber, H.D. (2000). Drug dependence, a chronic medical illness: implications for treatment, insurance, and outcomes evaluation. *JAMA* 284**,** 1689-1695.

Mcmullen, N.T., and Almli, C.R. (1981). Cell types within the medial forebrain bundle: a Golgi study of preoptic and hypothalamic neurons in the rat. *Am J Anat* 161**,** 323-340.

Mileykovskiy, B., and Morales, M. (2011). Duration of inhibition of ventral tegmental area dopamine neurons encodes a level of conditioned fear. *J Neurosci* 31**,** 7471-7476.

Miyata, S., Ishiyama, M., Shido, O., Nakashima, T., Shibata, M., and Kiyohara, T. (1995). Central mechanism of neural activation with cold acclimation of rats using Fos immunohistochemistry. *Neurosci Res* 22**,** 209-218.

Mogenson, G.J., and Nielsen, M.A. (1983). Evidence that an accumbens to subpallidal GABAergic projection contributes to locomotor activity. *Brain Res Bull* 11**,** 309-314.

Mogenson, G.J., Swanson, L.W., and Wu, M. (1983). Neural projections from nucleus accumbens to globus pallidus, substantia innominata, and lateral preoptic-lateral hypothalamic area: an anatomical and electrophysiological investigation in the rat. *J Neurosci* 3**,** 189-202.

Mohebi, A., Pettibone, J.R., Hamid, A.A., Wong, J.T., Vinson, L.T., Patriarchi, T., Tian, L., Kennedy, R.T., and Berke, J.D. (2019). Dissociable dopamine dynamics for learning and motivation. *Nature* 570**,** 65-70.

Mok, A.C., and Mogenson, G.J. (1972). Effect of electrical stimulation of the septum and the lateral preoptic area on unit activity of the lateral habenular nucleus in the rat. *Brain Res* 43**,** 361-372.

Morikawa, H., and Paladini, C.A. (2011). Dynamic regulation of midbrain dopamine neuron activity: intrinsic, synaptic, and plasticity mechanisms. *Neuroscience* 198**,** 95-111.

Murata, K., Kinoshita, T., Fukazawa, Y., Kobayashi, K., Yamanaka, A., Hikida, T., Manabe, H., and Yamaguchi, M. (2019). Opposing Roles of Dopamine Receptor D1- and D2-Expressing Neurons in the Anteromedial Olfactory Tubercle in Acquisition of Place Preference in Mice. *Front Behav Neurosci* 13**,** 50.

Nair-Roberts, R.G., Chatelain-Badie, S.D., Benson, E., White-Cooper, H., Bolam, J.P., and Ungless, M.A. (2008). Stereological estimates of dopaminergic, GABAergic and glutamatergic neurons in the ventral tegmental area, substantia nigra and retrorubral field in the rat. *Neuroscience* 152**,** 1024-1031.

Negus, S.S., and Miller, L.L. (2014). Intracranial self-stimulation to evaluate abuse potential of drugs. *Pharmacol Rev* 66**,** 869-917.

Nieh, E.H., Matthews, G.A., Allsop, S.A., Presbrey, K.N., Leppla, C.A., Wichmann, R., Neve, R., Wildes, C.P., and Tye, K.M. (2015). Decoding Neural Circuits that Control Compulsive Sucrose Seeking. *Cell* 160**,** 528-541.

Nieh, E.H., Vander Weele, C.M., Matthews, G.A., Presbrey, K.N., Wichmann, R., Leppla, C.A., Izadmehr, E.M., and Tye, K.M. (2016). Inhibitory Input from the Lateral Hypothalamus to the Ventral Tegmental Area Disinhibits Dopamine Neurons and Promotes Behavioral Activation. *Neuron* 90**,** 1286-1298.

Nieuwenhuys, R., Geeraedts, L.M., and Veening, J.G. (1982). The medial forebrain bundle of the rat. I. General introduction. *J Comp Neurol* 206**,** 49-81.

Niswender, C.M., and Conn, P.J. (2010). Metabotropic glutamate receptors: physiology, pharmacology, and disease. *Annu Rev Pharmacol Toxicol* 50**,** 295-322.

O'connor, E.C., Chapman, K., Butler, P., and Mead, A.N. (2011). The predictive validity of the rat self-administration model for abuse liability. *Neurosci Biobehav Rev* 35**,** 912-938.

Ogawa, S.K., Cohen, J.Y., Hwang, D., Uchida, N., and Watabe-Uchida, M. (2014). Organization of monosynaptic inputs to the serotonin and dopamine neuromodulatory systems. *Cell reports* 8**,** 1105-1118.

Olarte-Sanchez, C.M., Valencia-Torres, L., Cassaday, H.J., Bradshaw, C.M., and Szabadi, E. (2013). Effects of SKF-83566 and haloperidol on performance on progressive ratio schedules maintained by sucrose and corn oil reinforcement: quantitative analysis using a new model derived from the Mathematical Principles of Reinforcement (MPR). *Psychopharmacology (Berl)* 230**,** 617-630.

Olds, J., and Milner, P. (1954). Positive reinforcement produced by electrical stimulation of septal area and other regions of rat brain. *J Comp Physiol Psychol* 47**,** 419-427.

Olds, M.E., and Fobes, J.L. (1981). The central basis of motivation: intracranial self-stimulation studies. *Annu Rev Psychol* 32**,** 523-574.

Olds, M.E., and Olds, J. (1963). Approach-avoidance analysis of rat diencephalon. *J Comp Neurol* 120**,** 259-295.

Omelchenko, N., Bell, R., and Sesack, S.R. (2009). Lateral habenula projections to dopamine and GABA neurons in the rat ventral tegmental area. *Eur J Neurosci* 30**,** 1239-1250.

Omelchenko, N., and Sesack, S.R. (2009). Ultrastructural analysis of local collaterals of rat ventral tegmental area neurons: GABA phenotype and synapses onto dopamine and GABA cells. *Synapse* 63**,** 895-906.

Ono, T., Nakamura, K., Nishijo, H., and Fukuda, M. (1986). Hypothalamic neuron involvement in integration of reward, aversion, and cue signals. *Journal of neurophysiology* 56**,** 63-79.

Osaka, T., Kawano, S., Ueta, Y., Inenaga, K., Kannan, H., and Yamashita, H. (1993). Lateral preoptic neurons inhibit thirst in the rat. *Brain Res Bull* 31**,** 135-144.

Owen, S.F., Liu, M.H., and Kreitzer, A.C. (2019). Thermal constraints on in vivo optogenetic manipulations. *Nat Neurosci* 22**,** 1061-1065.

Paladini, C.A., and Tepper, J.M. (1999). GABA(A) and GABA(B) antagonists differentially affect the firing pattern of substantia nigra dopaminergic neurons in vivo. *Synapse* 32**,** 165-176.

Paxinos, G., and Watson, C. (2007). *The rat brain in stereotaxic coordinates.* Amsterdam ; Boston ;: Academic Press/Elsevier.

Pecina, S., and Berridge, K.C. (2005). Hedonic hot spot in nucleus accumbens shell: where do mu-opioids cause increased hedonic impact of sweetness? *J Neurosci* 25**,** 11777-11786.

Peoples, L.L., Gee, F., Bibi, R., and West, M.O. (1998). Phasic firing time locked to cocaine self-infusion and locomotion: dissociable firing patterns of single nucleus accumbens neurons in the rat. *J Neurosci* 18**,** 7588-7598.

Perrotti, L.I., Bolanos, C.A., Choi, K.H., Russo, S.J., Edwards, S., Ulery, P.G., Wallace, D.L., Self, D.W., Nestler, E.J., and Barrot, M. (2005). DeltaFosB accumulates in a GABAergic cell population in the posterior tail of the ventral tegmental area after psychostimulant treatment. *Eur J Neurosci* 21**,** 2817-2824.

Peyron, C., Petit, J.M., Rampon, C., Jouvet, M., and Luppi, P.H. (1998). Forebrain afferents to the rat dorsal raphe nucleus demonstrated by retrograde and anterograde tracing methods. *Neuroscience* 82**,** 443-468.

Phillips, G.D., Robbins, T.W., and Everitt, B.J. (1994). Bilateral intra-accumbens self-administration of d-amphetamine: antagonism with intra-accumbens SCH-23390 and sulpiride. *Psychopharmacology (Berl)* 114**,** 477-485.

Phillips, P.E., Stuber, G.D., Heien, M.L., Wightman, R.M., and Carelli, R.M. (2003). Subsecond dopamine release promotes cocaine seeking. *Nature* 422**,** 614-618.

Phillipson, O.T. (1979). Afferent projections to the ventral tegmental area of Tsai and interfascicular nucleus: a horseradish peroxidase study in the rat. *J Comp Neurol* 187**,** 117-143.

Pollak Dorocic, I., Furth, D., Xuan, Y., Johansson, Y., Pozzi, L., Silberberg, G., Carlen, M., and Meletis, K. (2014). A whole-brain atlas of inputs to serotonergic neurons of the dorsal and median raphe nuclei. *Neuron* 83**,** 663-678.

Qi, J., Zhang, S., Wang, H.L., Barker, D.J., Miranda-Barrientos, J., and Morales, M. (2016). VTA glutamatergic inputs to nucleus accumbens drive aversion by acting on GABAergic interneurons. *Nat Neurosci* 19**,** 725-733.

Qi, J., Zhang, S., Wang, H.L., Wang, H., De Jesus Aceves Buendia, J., Hoffman, A.F., Lupica, C.R., Seal, R.P., and Morales, M. (2014). A glutamatergic reward input from the dorsal raphe to ventral tegmental area dopamine neurons. *Nat Commun* 5**,** 5390.

Ranck, J.B., Jr. (1975). Which elements are excited in electrical stimulation of mammalian central nervous system: a review. *Brain Res* 98**,** 417-440.

Reichard, R.A., Parsley, K.P., Subramanian, S., Stevenson, H.S., Schwartz, Z.M., Sura, T., and Zahm, D.S. (2019a). The lateral preoptic area and ventral pallidum embolden behavior. *Brain Struct Funct* 224**,** 1245-1265.

Reichard, R.A., Parsley, K.P., Subramanian, S., and Zahm, D.S. (2019b). Dissociable effects of dopamine D1 and D2 receptors on compulsive ingestion and pivoting movements elicited by disinhibiting the ventral pallidum. *Brain Struct Funct* 224**,** 1925-1932.

Risold, P.Y., and Swanson, L.W. (1997). Connections of the rat lateral septal complex. *Brain Res Brain Res Rev* 24**,** 115-195.

Roberts, D.C., and Bennett, S.A. (1993). Heroin self-administration in rats under a progressive ratio schedule of reinforcement. *Psychopharmacology (Berl)* 111**,** 215-218.

Rodeberg, N.T., Johnson, J.A., Bucher, E.S., and Wightman, R.M. (2016). Dopamine Dynamics during Continuous Intracranial Self-Stimulation: Effect of Waveform on Fast-Scan Cyclic Voltammetry Data. *ACS Chem Neurosci* 7**,** 1508-1518.

Roitman, M.F., Stuber, G.D., Phillips, P.E., Wightman, R.M., and Carelli, R.M. (2004). Dopamine operates as a subsecond modulator of food seeking. *J Neurosci* 24**,** 1265-1271.

Root, D.H., Mejias-Aponte, C.A., Qi, J., and Morales, M. (2014a). Role of glutamatergic projections from ventral tegmental area to lateral habenula in aversive conditioning. *J Neurosci* 34**,** 13906-13910.

Root, D.H., Mejias-Aponte, C.A., Zhang, S., Wang, H.-L., Hoffman, A.F., Lupica, C.R., and Morales, M. (2014b). Single rodent mesohabenular axons release glutamate and GABA. *Nature Neuroscience* 17**,** 1543-1551.

Root, D.H., Mejias-Aponte, C.A., Zhang, S., Wang, H.L., Hoffman, A.F., Lupica, C.R., and Morales, M. (2014c). Single rodent mesohabenular axons release glutamate and GABA. *Nat Neurosci* 17**,** 1543-1551.

Root, D.H., Melendez, R.I., Zaborszky, L., and Napier, T.C. (2015). The ventral pallidum: Subregion-specific functional anatomy and roles in motivated behaviors. *Prog Neurobiol* 130**,** 29-70.

Root, D.H., Wang, H.L., Liu, B., Barker, D.J., Mod, L., Szocsics, P., Silva, A.C., Magloczky, Z., and Morales, M. (2016). Glutamate neurons are intermixed with midbrain dopamine neurons in nonhuman primates and humans. *Sci Rep* 6**,** 30615.

Rowlett, J.K., Massey, B.W., Kleven, M.S., and Woolverton, W.L. (1996). Parametric analysis of cocaine self-administration under a progressive-ratio schedule in rhesus monkeys. *Psychopharmacology (Berl)* 125**,** 361-370.

Russo, S.J., and Nestler, E.J. (2013). The brain reward circuitry in mood disorders. *Nat Rev Neurosci* 14**,** 609-625.

Saad, W.A., Luiz, A.C., De Arruda Camargo, L.A., Renzi, A., and Manani, J.V. (1996). The lateral preoptic area plays a dual role in the regulation of thirst in the rat. *Brain Res Bull* 39**,** 171-176.

Salinas-Hernandez, X.I., Vogel, P., Betz, S., Kalisch, R., Sigurdsson, T., and Duvarci, S. (2018). Dopamine neurons drive fear extinction learning by signaling the omission of expected aversive outcomes. *Elife* 7.

Schmidt, H.D., Anderson, S.M., and Pierce, R.C. (2006). Stimulation of D1-like or D2 dopamine receptors in the shell, but not the core, of the nucleus accumbens reinstates cocaine-seeking behaviour in the rat. *Eur J Neurosci* 23**,** 219-228.

Schultz, W. (1998). Predictive Reward Signal of Dopamine Neurons. *American Psysiological Society* 80**,** 1-27.

Schultz, W. (2007). Behavioral dopamine signals. *Trends Neurosci* 30**,** 203-210.

Shreve, P.E., and Uretsky, N.J. (1989). AMPA, kainic acid, and N-methyl-D-aspartic acid stimulate locomotor activity after injection into the substantia innominata/lateral preoptic area. *Pharmacol Biochem Behav* 34**,** 101-106.

Shreve, P.E., and Uretsky, N.J. (1991). GABA and glutamate interact in the substantia innominata/lateral preoptic area to modulate locomotor activity. *Pharmacol Biochem Behav* 38**,** 385-388.

Sinnamon, H.M. (1987). Glutamate and picrotoxin injections into the preoptic basal forebrain initiate locomotion in the anesthetized rat. *Brain Res* 400**,** 270-277.

Sinnamon, H.M. (1992). Microstimulation mapping of the basal forebrain in the anesthetized rat: the "preoptic locomotor region". *Neuroscience* 50**,** 197-207.

Sinnamon, H.M., Marciello, M., and Goerner, D.W. (1991). Locomotor sites mapped with low current stimulation in intact and kainic acid damaged hypothalamus of anesthetized rats. *Behav Brain Res* 46**,** 49-61.

Snowball, R.K., Semenenko, F.M., and Lumb, B.M. (2000). Visceral inputs to neurons in the anterior hypothalamus including those that project to the periaqueductal gray: a functional anatomical and electrophysiological study. *Neuroscience* 99**,** 351-361.

Soares-Cunha, C., De Vasconcelos, N.a.P., Coimbra, B., Domingues, A.V., Silva, J.M., Loureiro-Campos, E., Gaspar, R., Sotiropoulos, I., Sousa, N., and Rodrigues, A.J. (2019). Nucleus accumbens medium spiny neurons subtypes signal both reward and aversion. *Mol Psychiatry*.

Sokolowski, J.D., Conlan, A.N., and Salamone, J.D. (1998). A microdialysis study of nucleus accumbens core and shell dopamine during operant responding in the rat. *Neuroscience* 86**,** 1001-1009.

Staddon, J.E., and Cerutti, D.T. (2003). Operant conditioning. *Annu Rev Psychol* 54**,** 115-144.

Stamatakis, A.M., Jennings, J.H., Ung, R.L., Blair, G.A., Weinberg, R.J., Neve, R.L., Boyce, F., Mattis, J., Ramakrishnan, C., Deisseroth, K., and Stuber, G.D. (2013). A unique population of ventral tegmental area neurons inhibits the lateral habenula to promote reward. *Neuron* 80**,** 1039-1053.

Stamatakis, A.M., and Stuber, G.D. (2012). Activation of lateral habenula inputs to the ventral midbrain promotes behavioral avoidance. *Nature neuroscience* 15**,** 1105-1107.

Steffensen, S.C., Taylor, S.R., Horton, M.L., Barber, E.N., Lyle, L.T., Stobbs, S.H., and Allison, D.W. (2008). Cocaine disinhibits dopamine neurons in the ventral tegmental area via use-dependent blockade of GABA neuron voltage-sensitive sodium channels. *Eur J Neurosci* 28**,** 2028-2040.

Steinberg, E.E., Boivin, J.R., Saunders, B.T., Witten, I.B., Deisseroth, K., and Janak, P.H. (2014). Positive reinforcement mediated by midbrain dopamine neurons requires D1 and D2 receptor activation in the nucleus accumbens. *PLoS One* 9**,** e94771.

Steinberg, E.E., Keiflin, R., Boivin, J.R., Witten, I.B., Deisseroth, K., and Janak, P.H. (2013). A causal link between prediction errors, dopamine neurons and learning. *Nature Neuroscience* 16**,** 966-973.

Stellar, J.R., and Corbett, D. (1989). Regional neuroleptic microinjections indicate a role for nucleus accumbens in lateral hypothalamic self-stimulation reward. *Brain Res* 477**,** 126-143.

Stelly, C.E., Haug, G.C., Fonzi, K.M., Garcia, M.A., Tritley, S.C., Magnon, A.P., Ramos, M.a.P., and Wanat, M.J. (2019). Pattern of dopamine signaling during aversive events predicts active avoidance learning. *Proc Natl Acad Sci U S A* 116**,** 13641-13650.

Subramanian, S., Reichard, R.A., Stevenson, H.S., Schwartz, Z.M., Parsley, K.P., and Zahm, D.S. (2018). Lateral preoptic and ventral pallidal roles in locomotion and other movements. *Brain Struct Funct* 223**,** 2907-2924.

Surmeier, D.J., Ding, J., Day, M., Wang, Z., and Shen, W. (2007). D1 and D2 dopamine-receptor modulation of striatal glutamatergic signaling in striatal medium spiny neurons. *Trends Neurosci* 30**,** 228-235.

Swerdlow, N.R., and Koob, G.F. (1984). The neural substrates of apomorphine-stimulated locomotor activity following denervation of the nucleus accumbens. *Life Sci* 35**,** 2537-2544.

Swerdlow, N.R., Swanson, L.W., and Koob, G.F. (1984). Electrolytic lesions of the substantia innominata and lateral preoptic area attenuate the 'supersensitive' locomotor response to apomorphine resulting from denervation of the nucleus accumbens. *Brain Res* 306**,** 141-148.

Szymusiak, R., Gvilia, I., and Mcginty, D. (2007). Hypothalamic control of sleep. *Sleep Med* 8**,** 291-301.

Tan, K.R., Yvon, C., Turiault, M., Mirzabekov, J.J., Doehner, J., Labouebe, G., Deisseroth, K., Tye, K.M., and Luscher, C. (2012). GABA neurons of the VTA drive conditioned place aversion. *Neuron* 73**,** 1173-1183.

Threlfell, S., Lalic, T., Platt, N.J., Jennings, K.A., Deisseroth, K., and Cragg, S.J. (2012). Striatal dopamine release is triggered by synchronized activity in cholinergic interneurons. *Neuron* 75**,** 58-64.

Tian, J., and Uchida, N. (2015). Habenula Lesions Reveal that Multiple Mechanisms Underlie Dopamine Prediction Errors. *Neuron* 87**,** 1304-1316.

Tye, K.M. (2018). Neural Circuit Motifs in Valence Processing. *Neuron* 100**,** 436-452.

Tyree, S.M., and De Lecea, L. (2017). Lateral Hypothalamic Control of the Ventral Tegmental Area: Reward Evaluation and the Driving of Motivated Behavior. *Front Syst Neurosci* 11**,** 50.

Tzschentke, T.M. (2007). Measuring reward with the conditioned place preference (CPP) paradigm: update of the last decade. *Addict Biol* 12**,** 227-462.

Ungless, M.A., and Grace, A.A. (2012). Are you or aren't you? Challenges associated with physiologically identifying dopamine neurons. *Trends Neurosci* 35**,** 422-430.

Vanderschuren, L.J., Minnaard, A.M., Smeets, J.a.S., and Lesscher, H.M.B. (2017). Punishment models of addictive behavior. *Current Opinion in Behavioral Sciences* 13**,** 77-84.

Venniro, M., Caprioli, D., and Shaham, Y. (2016). Animal models of drug relapse and craving: From drug priming-induced reinstatement to incubation of craving after voluntary abstinence. *Prog Brain Res* 224**,** 25-52.

Vento, P.J., Burnham, N.W., Rowley, C.S., and Jhou, T.C. (2017). Learning From One's Mistakes: A Dual Role for the Rostromedial Tegmental Nucleus in the Encoding and Expression of Punished Reward Seeking. *Biol Psychiatry* 81**,** 1041-1049.

Volkow, N.D., Wang, G.-J.J., and Baler, R.D. (2011). Reward, dopamine and the control of food intake: implications for obesity. *Trends in cognitive sciences* 15**,** 37-46.

Volkow, N.D., Wang, G.-J.J., Fowler, J.S., and Telang, F. (2008). Overlapping neuronal circuits in addiction and obesity: evidence of systems pathology. *Philosophical transactions of the Royal Society of London. Series B, Biological sciences* 363**,** 3191-3200.

Volman, S.F., Lammel, S., Margolis, E.B., Kim, Y., Richard, J.M., Roitman, M.F., and Lobo, M.K. (2013). New insights into the specificity and plasticity of reward and aversion encoding in the mesolimbic system. *J Neurosci* 33**,** 17569-17576.

Wakabayashi, K.T., Feja, M., Baindur, A.N., Bruno, M.J., Bhimani, R.V., Park, J., Hausknecht, K., Shen, R.Y., Haj-Dahmane, S., and Bass, C.E. (2019). Chemogenetic activation of ventral tegmental area GABA neurons, but not mesoaccumbal GABA terminals, disrupts responding to reward-predictive cues. *Neuropsychopharmacology* 44**,** 372-380.

Wang, H.L., Qi, J., Zhang, S., Wang, H., and Morales, M. (2015). Rewarding Effects of Optical Stimulation of Ventral Tegmental Area Glutamatergic Neurons. *J Neurosci* 35**,** 15948-15954.

Watabe-Uchida, M., Zhu, L., Ogawa, S.K., Vamanrao, A., and Uchida, N. (2012). Whole-Brain Mapping of Direct Inputs to Midbrain Dopamine Neurons. *Neuron* 74**,** 858-873.

Wayner, M.J., Barone, F.C., Scharoun, S.L., Guevara-Aguilar, R., and Aguilar-Baturoni, H.U. (1983). Limbic connections to the lateral preoptic area: a horseradish peroxidase study in the rat. *Neurosci Biobehav Rev* 7**,** 375-384.

Whishaw, I.Q., and Nikkel, R.W. (1975). Anterior hypothalamic electrical stimulation and hippocampal EEG in the rat: suppressed EEG, locomotion, self-stimulation and inhibition of shock avoidance. *Behav Biol* 13**,** 1-20.

Wise, R.A. (1996). Addictive drugs and brain stimulation reward. *Annu Rev Neurosci* 19**,** 319-340.

Wise, R.A. (2013). Dual roles of dopamine in food and drug seeking: the drive-reward paradox. *Biol Psychiatry* 73**,** 819-826.

Witten, I.B., Steinberg, E.E., Lee, S.Y., Davidson, T.J., Zalocusky, K.A., Brodsky, M., Yizhar, O., Cho, S.L., Gong, S., Ramakrishnan, C., Stuber, G.D., Tye, K.M., Janak, P.H., and Deisseroth, K. (2011). Recombinase-driver rat lines: tools, techniques, and optogenetic application to dopamine-mediated reinforcement. *Neuron* 72**,** 721-733.

Woodworth, H.L., Brown, J.A., Batchelor, H.M., Bugescu, R., and Leinninger, G.M. (2018). Determination of neurotensin projections to the ventral tegmental area in mice. *Neuropeptides* 68**,** 57-74.

Wyvell, C.L., and Berridge, K.C. (2000). Intra-accumbens amphetamine increases the conditioned incentive salience of sucrose reward: enhancement of reward "wanting" without enhanced "liking" or …. *The Journal of neuroscience*.

Xue, Y., Steketee, J.D., Rebec, G.V., and Sun, W. (2011). Activation of D(2)-like receptors in rat ventral tegmental area inhibits cocaine-reinstated drug-seeking behavior. *Eur J Neurosci* 33**,** 1291-1298.

Yamaguchi, T., Sheen, W., and Morales, M. (2007). Glutamatergic neurons are present in the rat ventral tegmental area. *Eur J Neurosci* 25**,** 106-118.

Yamaguchi, T., Wang, H.-L.L., Li, X., Ng, T.H., and Morales, M. (2011). Mesocorticolimbic glutamatergic pathway. *The Journal of neuroscience : the official journal of the Society for Neuroscience* 31**,** 8476-8490.

Yang, H., De Jong, J.W., Tak, Y., Peck, J., Bateup, H.S., and Lammel, S. (2018). Nucleus Accumbens Subnuclei Regulate Motivated Behavior via Direct Inhibition and Disinhibition of VTA Dopamine Subpopulations. *Neuron* 97**,** 434-449 e434.

Yetnikoff, L., Cheng, A.Y., Lavezzi, H.N., Parsley, K.P., and Zahm, D.S. (2015). Sources of input to the rostromedial tegmental nucleus, ventral tegmental area, and lateral habenula compared: A study in rat. *J Comp Neurol* 523**,** 2426-2456.

Yoo, J.H., Zell, V., Gutierrez-Reed, N., Wu, J., Ressler, R., Shenasa, M.A., Johnson, A.B., Fife, K.H., Faget, L., and Hnasko, T.S. (2016). Ventral tegmental area glutamate neurons co-release GABA and promote positive reinforcement. *Nat Commun* 7**,** 13697.

Zahm, D.S., Grosu, S., Williams, E.A., Qin, S., and Berod, A. (2001). Neurons of origin of the neurotensinergic plexus enmeshing the ventral tegmental area in rat: retrograde labeling and in situ hybridization combined. *Neuroscience* 104**,** 841-851.

Zahm, D.S., Parsley, K.P., Schwartz, Z.M., and Cheng, A.Y. (2013). On lateral septum-like characteristics of outputs from the accumbal hedonic "hotspot" of Pecina and Berridge with commentary on the transitional nature of basal forebrain "boundaries". *J Comp Neurol* 521**,** 50-68.

Zahm, D.S., Schwartz, Z.M., Lavezzi, H.N., Yetnikoff, L., and Parsley, K.P. (2014). Comparison of the locomotor-activating effects of bicuculline infusions into the preoptic area and ventral pallidum. *Brain Struct Funct* 219**,** 511-526.

Zaretsky, D.V., Hunt, J.L., Zaretskaia, M.V., and Dimicco, J.A. (2006). Microinjection of prostaglandin E2 and muscimol into the preoptic area in conscious rats: comparison of effects on plasma adrenocorticotrophic hormone (ACTH), body temperature, locomotor activity, and cardiovascular function. *Neurosci Lett* 397**,** 291-296.

Zhang, S., Qi, J., Li, X., Wang, H.L., Britt, J.P., Hoffman, A.F., Bonci, A., Lupica, C.R., and Morales, M. (2015). Dopaminergic and glutamatergic microdomains in a subset of rodent mesoaccumbens axons. *Nat Neurosci* 18**,** 386-392.

Zhu, Y., Wienecke, C.F., Nachtrab, G., and Chen, X. (2016). A thalamic input to the nucleus accumbens mediates opiate dependence. *Nature* 530**,** 219-222.